

# **VESTA: a Three-Dimensional Visualization System for Electronic and Structural Analysis**

**Koichi MOMMA<sup>1</sup>**

*National Museum of Nature and Science,  
4-1-1 Amakubo, Tsukuba, Ibaraki 305-0005, Japan*

**Fujio IZUMI<sup>2</sup>**

*Graduate School of Engineering, Kyoto University*

January 27, 2019

<sup>1</sup>E-mail: [vesta.dev@gmail.com](mailto:vesta.dev@gmail.com)

<sup>2</sup>E-mail: [fizumi3776@gmail.com](mailto:fizumi3776@gmail.com)

# Contents

<b>LICENSE AGREEMENT</b>	<b>xi</b>
<b>1 INTRODUCTION AND BACKGROUND</b>	<b>1</b>
1.1 Understanding Crystal and Electronic Structures in Three Dimensions . . . . .	1
1.2 Circumstances behind the Development of VESTA . . . . .	1
1.3 What's New in VESTA 3 . . . . .	2
1.4 Notes on this Manual . . . . .	3
<b>2 OVERVIEW OF THE PROGRAM</b>	<b>4</b>
2.1 General Features . . . . .	4
2.2 Visualization of Structural Models . . . . .	4
2.2.1 A variety of structural information derived on selection of objects . . . . .	9
2.3 Visualization of Volumetric Data . . . . .	9
2.4 Visualization of Crystal Morphologies . . . . .	11
2.5 Cooperation with External Programs . . . . .	13
2.6 Input and Output Files . . . . .	13
2.7 Programming Concept . . . . .	13
2.7.1 Graphical user interface . . . . .	14
2.7.2 Core libraries . . . . .	14
<b>3 GETTING STARTED</b>	<b>15</b>
3.1 Minimum requirements of hardware . . . . .	15
3.2 Windows . . . . .	15
3.3 macOS . . . . .	16
3.4 Linux . . . . .	16
3.4.1 32-bit version . . . . .	16
3.4.2 64-bit version . . . . .	17
3.5 Trouble Shooting . . . . .	18
3.6 Loading Files . . . . .	18
<b>4 MAIN WINDOW</b>	<b>19</b>
4.1 Components of the Main Window . . . . .	19
4.2 Menus . . . . .	20
4.2.1 File menu . . . . .	20
4.2.2 Edit menu . . . . .	21
4.2.3 View menu . . . . .	21
4.2.4 Objects menu . . . . .	21
4.2.5 Utilities menu . . . . .	22

4.2.6	Help menu . . . . .	23
4.3	Tools in the Horizontal Toolbar . . . . .	23
4.3.1	Alignment . . . . .	23
4.3.2	Rotation . . . . .	24
4.3.3	Translation . . . . .	24
4.3.4	Scaling . . . . .	24
4.4	Tools in the Vertical Toolbar . . . . .	25
4.5	Text Area . . . . .	25
4.5.1	Output tab . . . . .	25
4.5.2	Summary tab . . . . .	26
4.5.3	Comment tab . . . . .	26
<b>5</b>	<b>DISPLAY STYLES</b>	<b>27</b>
5.1	Structural Models . . . . .	27
5.1.1	Objects to be displayed . . . . .	27
5.1.2	Styles . . . . .	28
5.2	Volumetric Data . . . . .	29
5.3	Crystal Shapes . . . . .	30
5.3.1	Styles . . . . .	30
<b>6</b>	<b>GIVING PHASE DATA</b>	<b>32</b>
6.1	Defining Phases . . . . .	33
6.2	Symmetry and Unit Cell . . . . .	33
6.2.1	Crystal systems and space groups . . . . .	33
6.2.2	Behavior when changing a space-group setting . . . . .	36
6.2.3	Lattice parameters . . . . .	36
6.2.4	Customization of symmetry operations . . . . .	36
6.2.5	Reducing symmetry . . . . .	36
6.2.6	Transformation of the unit cell . . . . .	37
6.2.7	Magnetic Structures . . . . .	43
6.3	Structure Parameters . . . . .	44
6.3.1	Symbols and Labels . . . . .	45
6.3.2	Formal charge . . . . .	45
6.3.3	Fractional coordinates . . . . .	45
6.3.4	Occupancy . . . . .	46
6.3.5	Atomic displacement parameters . . . . .	46
6.3.6	Importing structure parameters . . . . .	47
6.3.7	Removing duplicate atoms . . . . .	48
6.4	Volumetric Data . . . . .	48
6.4.1	Volumetric data to draw isosurfaces . . . . .	49
6.4.2	Volumetric data for surface coloring . . . . .	49
6.5	Crystal Shape . . . . .	50
6.5.1	Examples . . . . .	52
<b>7</b>	<b>OVERLAYING MULTIPLE DATA</b>	<b>54</b>
7.1	Positioning of Phases . . . . .	54
7.2	Relative Orientation of Phases . . . . .	55
7.3	Examples . . . . .	55

<b>8 CREATING BONDS AND POLYHEDRA</b>	<b>57</b>
8.1 Specifications of Searching for Bonds . . . . .	58
8.1.1 Search mode . . . . .	58
8.1.2 Boundary mode . . . . .	58
8.1.3 Options . . . . .	58
8.1.4 A pair of atoms . . . . .	59
8.2 Operating Instructions . . . . .	59
8.2.1 Creating coordination polyhedra . . . . .	59
8.2.2 Searching for molecules and clusters . . . . .	60
8.2.3 Applications of the “Search molecules” mode to inorganic crystals . . . . .	60
8.2.4 Searching for hydrogen bonds . . . . .	61
8.2.5 Visualizing cage-like structures . . . . .	61
<b>9 ADDITIONAL OBJECTS</b>	<b>63</b>
9.1 Vectors on Atoms . . . . .	63
9.1.1 Creation and editing of a vector . . . . .	64
9.1.2 Attachment of vectors to crystallographic sites . . . . .	66
9.1.3 Attachment of vectors to individual atoms . . . . .	66
9.2 Lattice Planes . . . . .	66
9.2.1 Appearance of lattice planes . . . . .	67
9.2.2 Calculate the best plane for selected atoms . . . . .	68
<b>10 DEFINING DRAWING BOUNDARIES AND VIEW DIRECTIONS</b>	<b>69</b>
10.1 Drawing Boundaries . . . . .	69
10.1.1 Ranges of fractional coordinates . . . . .	70
10.1.2 Cutoff planes . . . . .	70
10.2 View Direction . . . . .	71
10.2.1 Manner of specifying directions . . . . .	71
10.2.2 Orientation matrix . . . . .	71
10.2.3 View direction . . . . .	72
10.2.4 Viewing along crystallographic axes . . . . .	72
<b>11 INTERACTIVE MANIPULATIONS</b>	<b>73</b>
11.1 Rotate . . . . .	73
11.1.1 Drag mode . . . . .	73
11.1.2 Animation mode . . . . .	73
11.2 Magnify . . . . .	74
11.3 Translate . . . . .	74
11.4 Select . . . . .	74
11.4.1 Atom . . . . .	74
11.4.2 Bond . . . . .	75
11.4.3 Coordination polyhedron . . . . .	75
11.5 Distance . . . . .	79
11.6 Bond angle . . . . .	79
11.7 Dihedral angle . . . . .	79
11.8 Interfacial angle . . . . .	81

<b>12 PROPERTIES OF OBJECTS</b>	<b>82</b>
12.1 Properties Dialog Box . . . . .	82
12.1.1 General . . . . .	82
12.1.2 Atoms . . . . .	83
12.1.3 Bonds . . . . .	86
12.1.4 Polyhedra . . . . .	87
12.1.5 Isosurfaces . . . . .	89
12.1.6 Sections . . . . .	92
12.2 Objects Tab in the Side Panel . . . . .	95
12.2.1 List of phases and objects . . . . .	95
12.2.2 Atoms . . . . .	95
12.2.3 Bonds . . . . .	95
12.2.4 Polyhedra . . . . .	95
12.2.5 Slices . . . . .	96
12.2.6 Shapes . . . . .	96
<b>13 OVERALL APPEARANCE</b>	<b>97</b>
13.1 Background . . . . .	97
13.2 Lighting . . . . .	98
13.3 Projection Mode . . . . .	98
13.4 Depth-Cueing . . . . .	99
<b>14 UTILITIES</b>	<b>101</b>
14.1 Equivalent Positions . . . . .	101
14.2 Geometrical Parameters . . . . .	102
14.3 Standardization of Crystal Data . . . . .	103
14.4 Niggli-Reduced Cell . . . . .	105
14.5 Site Potentials and Madelung Energy . . . . .	106
14.6 Powder Diffraction Pattern . . . . .	108
14.7 Structure Factors . . . . .	110
14.8 Fourier Synthesis . . . . .	112
14.9 Model Electron Densities . . . . .	112
14.10 Model Nuclear Densities . . . . .	113
14.11 Patterson Densities . . . . .	113
14.12 2D Data Display . . . . .	114
14.13 Line Profile . . . . .	114
14.14 Peak Search . . . . .	115
14.15 Conversion of Electron Densities . . . . .	115
<b>15 TWO-DIMENSIONAL DATA DISPLAY</b>	<b>117</b>
15.1 Components of the 2D Data Display Window . . . . .	117
15.2 Menus . . . . .	118
15.3 Tools in the Toolbar . . . . .	118
15.3.1 Rotation . . . . .	118
15.3.2 Translation . . . . .	119
15.3.3 Scaling . . . . .	119
15.4 Tools in the Vertical Toolbar . . . . .	119
15.5 Create and Edit a 2D Image . . . . .	119

15.5.1 (hkl) plane in the bounding box . . . . .	120
15.5.2 (hkl) plane defined by two vectors . . . . .	120
15.5.3 Project along [hkl] axis . . . . .	120
15.6 Controlling Properties of a 2D Image . . . . .	122
15.7 Exporting 2D data . . . . .	124
<b>16 PREFERENCES</b>	<b>125</b>
16.1 Settings for RIETAN . . . . .	125
16.2 Font for Text Area . . . . .	126
16.3 Open a New File in . . . . .	126
16.4 Animation . . . . .	126
16.5 Start-up Search for Bonds . . . . .	126
16.6 A Setting for Raster Image Export . . . . .	126
16.7 Default isosurface level . . . . .	127
16.8 History level . . . . .	127
<b>17 INPUT AND OUTPUT FILES</b>	<b>128</b>
17.1 File Formats of Volumetric Data . . . . .	128
17.2 Directories for User Settings . . . . .	129
17.2.1 Windows . . . . .	129
17.2.2 macOS . . . . .	129
17.2.3 Linux . . . . .	129
17.3 Files Used by VESTA . . . . .	130
17.4 Input Files . . . . .	130
17.4.1 Structural data . . . . .	130
17.4.2 Volumetric data . . . . .	135
17.4.3 Structural and volumetric data . . . . .	137
17.5 Output Files . . . . .	139
17.5.1 Data files . . . . .	139
17.5.2 Raster images . . . . .	142
17.5.3 Vector images . . . . .	143
17.5.4 Output text . . . . .	143
<b>APPENDIX</b>	<b>145</b>
<b>A Keyboard Shortcuts</b>	<b>145</b>

# List of Figures

2.1 Screenshots of VESTA running on three kinds of operating systems . . . . .	5
2.2 Crystal structure of masutomilite represented as the ball-and-stick model . . . . .	6
2.3 Crystal structure of a polymorph of vitamin B1 represented as the space-filling model . . . . .	6
2.4 Crystal structure of beryl . . . . .	7
2.5 Crystal structure of sodalite . . . . .	7
2.6 Crystal structure of the tetragonal form of melanophlogite . . . . .	8
2.7 A displacement ellipsoid model of 17-(2 <i>H</i> -indazol-2-yl)androsta-5,16-dien-3 $\beta$ -ol having an indazole substituent at the C17 position . . . . .	8
2.8 Electron-density distribution in MgB <sub>2</sub> . . . . .	10
2.9 A (001) slice illustrating electron-density distribution in MgB <sub>2</sub> . . . . .	10
2.10 Nuclear-density distribution in the paraelectric phase of KH <sub>2</sub> PO <sub>4</sub> . . . . .	11
2.11 An external morphology of an Al <sub>2</sub> O <sub>3</sub> crystal composed of {001}, {110}, and {113} faces. . . . .	12
2.12 A crystal morphology of anatase-type TiO <sub>2</sub> superimposed on its structural model, where blue and red balls represent Ti and O atoms, respectively. . . . .	12
2.13 Crystal morphologies of adularia . . . . .	13
4.1 Main window of VESTA running on Windows 10 . . . . .	19
5.1 The Structural model frame box in the <u>Style</u> tab of the Side Panel . . . . .	27
5.2 Crystal structure of quartz represented as stick model with dot surfaces . . . . .	27
5.3 The Volumetric data frame box in the <u>Style</u> tab of the Side Panel . . . . .	29
5.4 The Crystal shapes frame box in the <u>Style</u> tab of the Side Panel . . . . .	30
6.1 New Data dialog box . . . . .	32
6.2 Unit cell page in the Edit Data dialog box . . . . .	33
6.3 Equivalent Positions dialog box with editing mode . . . . .	37
6.4 Unit Cell Transformation dialog box. . . . .	37
6.5 A warning dialog box for conversion of structure handedness . . . . .	38
6.6 An example of lattice transformation between primitive and face-centered-cubic lattices . . . . .	41
6.7 A dialog box for confirmation of unit cell transformation . . . . .	42
6.8 A dialog box showing options for how to create a larger unit cell . . . . .	42
6.9 The Unit cell page in the Edit Data dialog box, with the “Magnetic structure” option checked. . . . .	43
6.10 Structure parameter page in the Edit Data dialog box . . . . .	44
6.11 Periodic Table dialog box . . . . .	45
6.12 Crystal structure of Cs <sub>6</sub> C <sub>60</sub> , with C <sub>60</sub> represented by translucent polyhedra . . . . .	46

6.13 Volumetric data page in the Edit Data dialog box . . . . .	48
6.14 A dialog box to choose operations for volumetric data . . . . .	49
6.15 Distributions of electron densities and effective spin densities in an O <sub>2</sub> molecule . . . . .	50
6.16 Crystal shape page in the Edit Data dialog box . . . . .	51
6.17 Crystal morphologies of anatase-type TiO <sub>2</sub> crystals . . . . .	51
6.18 The <u>Objects</u> tab of the Side Panel showing a list of crystallographic faces . . . . .	52
6.19 Crystal morphologies of anatase having faces that do not follow symmetry operations . . . . .	53
7.1 Phase page in the Edit Data dialog box . . . . .	54
7.2 Molecules of L-aspartic acid and 2,4,6-trichlorobenzoic acid on the (10̄14) surface of calcite . . . . .	55
7.3 A moire pattern of graphene on the (111) surface of Ir . . . . .	56
7.4 Crystal structures of Ca-olivine (Ca <sub>2</sub> SiO <sub>4</sub> ) and isostructural monticellite (CaMgSiO <sub>4</sub> ) overlapped with each other. . . . .	56
8.1 Bonds dialog . . . . .	57
8.2 Crystal structure of δ-AlOOH . . . . .	59
8.3 “Search molecules” mode with and without “Beyond the boundary” option enabled . . . . .	60
8.4 Crystal structure of tetrakis(di-4-pyridylsulfane)dinitratocopper(II) . . . . .	61
8.5 Crystal structure of the tetragonal variant of chibaite . . . . .	62
9.1 Vectors dialog box displaying a list of atoms in SrFeO <sub>2</sub> . . . . .	63
9.2 A dialog box to create or edit a vector . . . . .	64
9.3 Results of applying a mirror operation to magnetic moments $\mu$ and polarization vectors $p$ . . . . .	65
9.4 Effects of two options for vector styles . . . . .	66
9.5 Lattice Plane dialog box . . . . .	67
9.6 A section of a difference Fourier map inserted in a ball-and-stick model of δ-AlOOH . . . . .	67
9.7 The best plane calculated for an aromatic ring in anthraquinone . . . . .	68
10.1 Boundary dialog . . . . .	69
10.2 Electron density distribution in D-sorbitol . . . . .	70
10.3 Crystal structure of diamond drawn in ranges from (-8, -8, -8) to (8, 8, 8) with and without a cutoff plane 111 . . . . .	71
10.4 Orientation dialog box . . . . .	72
11.1 The <u>Tools</u> tab of the Side Panel . . . . .	73
11.2 Calculation of a dihedral angle for four carbon atoms in an aromatic ring in 3-[4-(dimethylamino)phenyl]-1-(2-hydroxyphenyl)-prop-2-en-1-one . . . . .	80
11.3 Calculation of an interfacial angle between (100) and (511) faces in quartz. . . . .	81
12.1 General page in the Properties dialog box . . . . .	83
12.2 Atoms page in the Properties dialog box . . . . .	84
12.3 Displacement ellipsoids of an atom (A) with principal ellipses and (B) without them . . . . .	85
12.4 A displacement ellipsoid model of a structure with some atoms having negative mean square displacements . . . . .	85
12.5 General-position diagrams of space group Fd̄3m with (A) light disabled and (B) light enabled . . . . .	86

12.6 Bonds page in the Properties dialog . . . . .	87
12.7 Polyhedra page in the Properties dialog . . . . .	88
12.8 Isosurfaces page in the Properties dialog box . . . . .	89
12.9 Comparison between the two modes of rendering isosurfaces . . . . .	90
12.10The 64a <sub>1g</sub> orbital for the {Cd(S <sub>4</sub> Mo <sub>3</sub> (Hnta) <sub>3</sub> ) <sub>2</sub> } <sup>4-</sup> ion with a ball-and-stick model	91
12.11Composite images of isosurfaces and a ball-and-stick model for albatrossene . . . . .	91
12.12Relations between orientation of isosurface and the two parameters for opacity setting . . . . .	92
12.13Sections page in the Properties dialog box . . . . .	93
12.14Distribution of nuclear densities obtained for KOD at 580 K by MEM from single-crystal neutron diffraction data . . . . .	94
12.15Relations among saturation levels, data values, and colors of sections . . . . .	94
12.16The <u>Objects</u> tab of the Side Panel . . . . .	95
12.17A list of bond specifications in the <u>Objects</u> tab of the Side Panel . . . . .	95
12.18A list of polyhedra in the <u>Objects</u> tab of the Side Panel . . . . .	95
12.19A list of slices in the <u>Objects</u> tab of the Side Panel . . . . .	96
12.20A list of forms and faces of crystal morphologies in the <u>Objects</u> tab of the Side Panel	96
13.1 Overall Appearance dialog box . . . . .	97
13.2 Crystal structure of milarite drawn with light effects (A) enabled and (B) disabled dialog box . . . . .	98
13.3 Crystal structure of post-perovskite, MgSiO <sub>3</sub> , rendered by parallel and perspective projections . . . . .	99
13.4 Crystal structure of mordenite rendered with and without depth-cueing . . . . .	100
14.1 Equivalent Positions dialog box . . . . .	101
14.2 The Equivalent Positions dialog box showing magnetic data . . . . .	102
14.3 Geometrical Parameters dialog box . . . . .	103
14.4 Simulation of an X-ray powder diffraction pattern of YBa <sub>2</sub> Cu <sub>4</sub> O <sub>8</sub> . . . . .	109
14.5 Structure Factors dialog box . . . . .	110
14.6 Fourier Synthesis dialog box . . . . .	113
15.1 2D Data Display window . . . . .	117
15.2 A dialog box for three different modes to draw a 2D image . . . . .	120
15.3 Three modes of creating a 2D image . . . . .	121
15.4 Schematic image of the relation between the center of the projection and the center of the slice . . . . .	122
15.5 Bird's eye view of a (001) slice of rutile-type TiO <sub>2</sub> . . . . .	123
15.6 Electron-density distribution on the (001) plane in rutile-type TiO <sub>2</sub> with and without grid edges . . . . .	123
15.7 Contours page in the Side Panel . . . . .	124
16.1 Preferences dialog box . . . . .	125
17.1 Two types of the grids for volumetric data . . . . .	128

# List of Tables

6.1	Non-standard settings in two triclinic space groups . . . . .	35
6.2	Setting numbers of monoclinic space groups . . . . .	35
6.3	Axis choices in the orthorhombic space groups . . . . .	35
14.1	Units of converted volumetric data . . . . .	116
17.1	Files used by VESTA . . . . .	130
A.1	Keyboard shortcuts. . . . .	145

# LICENSE AGREEMENT

## VESTA LICENSE

Version 3

Copyright © 2006–2019, Koichi Momma and Fujio Izumi

VESTA is currently copyrighted with its source code not open to the public; we wish to control the development and future of VESTA by ourselves. This software is distributed free of charge for academic, scientific, educational, and non-commercial users. Users belonging to commercial enterprises may also use this software at no cost until a license for business users is established.

Permission to use this software is hereby granted under the following conditions:

1. Drawings produced by VESTA may be used in any publications (original and review articles) provided that its use is explicitly acknowledged. A suitable reference for VESTA is:

[K. Momma and F. Izumi, “VESTA 3 for three-dimensional visualization of crystal, volumetric and morphology data,” \*J. Appl. Crystallogr.\*, \*\*44\*\*, 1272–1276 \(2011\).](#)

2. You should not redistribute any copy of the distributed files including MADEL and STRUCTURE TIDY unless you have a written permission from us.

Part of these terms may be changed without any prior announcement. This software is provided “as is” without any expressed or implied warranty.

# Chapter 1

## INTRODUCTION AND BACKGROUND

### 1.1 Understanding Crystal and Electronic Structures in Three Dimensions

Progress in modern structure-refinement techniques of the maximum-entropy method (MEM) [1, 2, 3, 4] and MEM-based pattern fitting (MPF) [5, 6, 7, 8, 9], has made it easier and more popular to determine three-dimensional (3D) distribution of electron densities from X-ray diffraction data and densities of coherent-scattering lengths (nuclear densities) [10],  $b_c$ , from neutron diffraction data. On the other hand, rapid developments of computer hardware and software have accelerated and facilitated electronic-structure calculations affording physical quantities including electron densities, wave functions, and electrostatic potentials.

Such technological advances in recent years bring demands for integrated 3D visualization systems to deal with both structural models and volumetric data such as electron and nuclear densities. The crystal structures and spatial distribution of various physical quantities obtained experimentally and by computer simulations should be understood three-dimensionally. Despite the availability of many structure-drawing programs, cross-platform free software capable of visualizing both crystal and electronic structures in three dimensions is very few; if any, they are not very suitable for displaying those of inorganic and metallic compounds.

To improve such a situation, we have developed a new integrated system VESTA (**V**isualization for **E**lectronic and **S**Tructural **A**nalysis) for 3D visualization of crystal structures and volumetric data on personal computers.

### 1.2 Circumstances behind the Development of VESTA

VESTA [11, 12, 13, 14] is a successor to two visualization programs, VICS and VEND, in the VENUS (**V**isualiza-tion of **E**lectron/**N**Uclear and **S**tructures) software package<sup>1</sup> [15, 16], which was developed by Dilanian, Izumi, and Kawamura with help from Ohki and Momma during 2001–2006. VENUS comprises the following six programs:

1. VICS (**VI**sualization of **C**rystal **S**tructures) for displaying and manipulating crystal structures [15, 16],
2. VEND (**V**isualization of **E**lectron/**N**uclear **D**ensities) for displaying and manipulating volumetric data [15, 16],

---

<sup>1</sup><http://fujioizumi.verse.jp/visualization/VENUS.html>

3. PRIMA (**P**Ractice **I**terative **M**EM **A**nalyses) for MEM analysis from X-ray and neutron diffraction data [5],
4. Dysnomia [7, 8, 9] which is a successor to PRIMA,
5. ALBA (**A**fter **L**e **B**ail **A**nalysis) for the maximum-entropy Patterson method [17],
6. Alchemy: A file converter to make it possible to analyze observed structure factors and their estimated standard uncertainty, which result from Rietveld analysis using GSAS [18] and FullProf [19], by MEM with Dysnomia [7, 8, 9].

VICS and VEND are programs for 3D visualization of crystal and electronic structures, respectively. They were written in the ANSI C language with the full use of the OpenGL<sup>2</sup> technology. The graphical user interfaces (GUIs) of VICS and VEND were constructed by using GLUT and GLUI libraries.

VICS and VEND saw the light of day at the end of 2002, and since then, continued their growth to be used widely in a variety of studies. However, we never get full satisfaction from their usability and performance. First, the combined use of VICS and VEND to visualize both crystal and electronic structures *via* text files is rather troublesome; on-the-fly visualization of these two kinds of images is highly desired. Second, their GUIs are not very user-friendly because they are based on the old-fashioned toolkits, GLUT and GLUI, which have been no longer upgraded. Above all things, they lack scalability and require large system resources owing to unrefined programming.

To overcome the faults described above, we at first upgraded VICS to VICS-II employing a modern C++ GUI framework wxWidgets<sup>3</sup> [20]. Later, we further integrated VICS-II and VEND into VESTA.

### 1.3 What's New in VESTA 3

Main new features implemented in VESTA 3, which is a successor to VESTA v2.1.X, are listed below:

- Visualization of crystal morphologies
- Superimposition of multiple structural models, volumetric data, and crystal faces on the same Graphic Area
- Visualization of isosurfaces with multiple levels
- An extended bond-search algorithm to allow more sophisticated search in complex molecules, cage-like structures, *etc.*
- Calculations of electron and nuclear densities from structure parameters
- Calculations of Patterson-function densities from structure parameters or volumetric data
- Integration of electron and nuclear densities by Voronoi tessellation [21]
- Significant performance improvements in rendering of isosurfaces and calculation of slices
- Output information about principal axes and mean square displacements for anisotropic atomic displacements

---

<sup>2</sup><http://www.opengl.org/>

<sup>3</sup><http://www.wxwidgets.org/>

- Determination of the best plane for selected atoms
- Displaying labels of atoms
- Customization of styles per sites or bond types
- Customization of symmetry operations
- Improvements in inputting files with various formats
- Support of undo and redo in GUI operations

## 1.4 Notes on this Manual

Throughout this document, the following symbols are used to show kinds of input data:

- [Button] : A button (dotted lines appear after clicking it).
- “Option” : A radio button and a check box (words following it may be clicked to select it).
- {Text Box} : An input item (*e.g.*, a value or a name) including spinners and list boxes.
- Tab : A page in a multiple-page user interface (an underscore is drawn below the tab name).
- <Key> : A key in the keyboard.

The text box supports four types of basic arithmetic operations: +, −, ×, and /, which means that you can input, for example, “1/3” instead of “0.333333.” Pressing the <Tab> or <Enter> key will focus a next control, *i.e.*, text box, button, ratio button, or check box, in a dialog box. Press <Shift> + <Tab> to focus the preceding control.

# Chapter 2

# OVERVIEW OF THE PROGRAM

## 2.1 General Features

VESTA [11, 12, 13, 14] is a 3D visualization system for structural models, volumetric data (“voxel” data), and crystal morphologies. A variety of physical quantities such as electron densities, densities of coherent-scattering lengths  $b_c$  (nuclear densities) [10], wave functions, and electrostatic potentials can be superimposed on atomistic structures and external morphology of crystals. Objects (atoms, bonds, coordination polyhedra, isosurfaces, *etc.*) can be rotated, scaled, and translated fast in three dimensions, particularly in the presence of graphics cards supporting the OpenGL instruction set. The scalability of VESTA is very high; it enables us to deal with a practically unlimited numbers of objects such as atoms, bonds, polyhedra, and polygons on isosurfaces so long as memory capacity is enough. Drawing boundaries are defined by ranges along  $x$ ,  $y$ , and  $z$  axes as well as lattice planes.

As [Fig. 2.1](#) illustrates, VESTA runs on Microsoft Windows (hereafter referred to as Windows), macOS, and Linux. With VESTA, we can deal with multiple data in the same window, using a “tab” user interface. VESTA further supports multiple windows, each of which may contain multiple tabs corresponding to files.

## 2.2 Visualization of Structural Models

Structural models are represented as ball-and-stick ([Fig. 2.2](#)), space-filling ([Fig. 2.3](#)), polyhedral ([Fig. 2.4](#)), wireframe ([Fig. 2.5](#)), stick ([Fig. 2.6](#)), and displacement ellipsoid ([Fig. 2.7](#)) models. Ball-and-stick, wireframe, and stick models can be overlapped with dotted surfaces to accentuate outer surfaces of atoms. Polyhedra may be made translucent so as to make inside atoms and bonds visible.

Lattice planes with variable opacity can be inserted into a structural model. Vectors (arrows) can be attached to atoms to represent magnetic moments or directions of static and dynamic displacements.

You can superimpose multiple structural models in the same Graphic area to deal with grain boundary structures, absorption of atoms, molecules, nanosheet on a surface of crystal, or absorbed molecules in porous materials and layered structures.

Bond-search algorithm in VESTA is highly sophisticated; a variant of the cell index method by Quentrec and Brot [22, 23] was adopted. This approach is widely used in programs for molecular dynamics simulation that needs to deal with a large number of atoms.

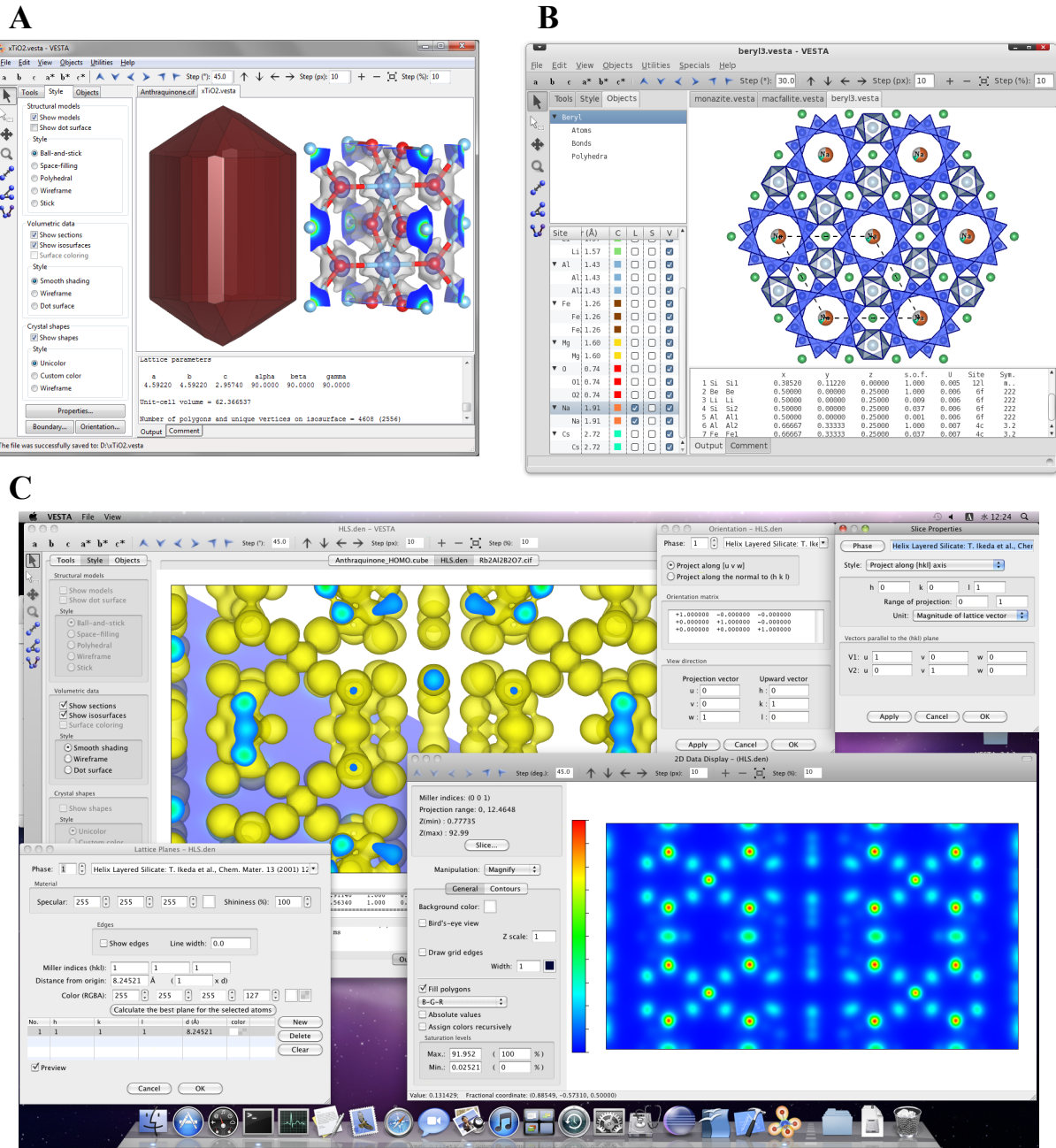


Figure 2.1: Screenshots of VESTA running on the three different operating systems: (A) Windows, (B) Linux, and (C) macOS.

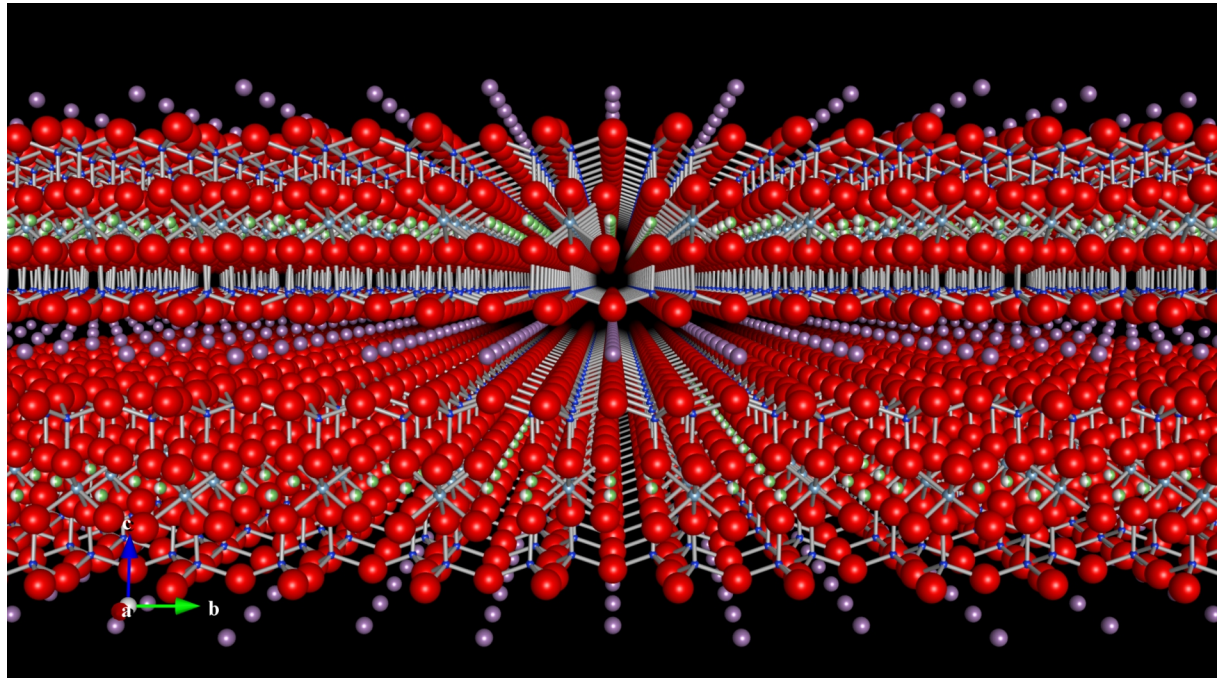


Figure 2.2: Crystal structure of a variant of mica group minerals, masutomilite  $K(Li,Al,Mn^{2+})_3[(Si,Al)_4O_{10}](F,OH)_2$  [24].

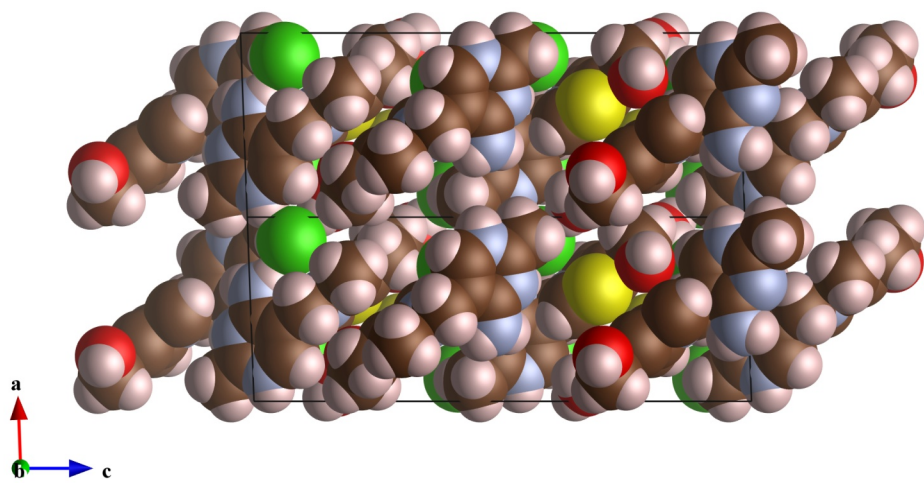


Figure 2.3: Crystal structure of a polymorph of vitamin B1 [25].

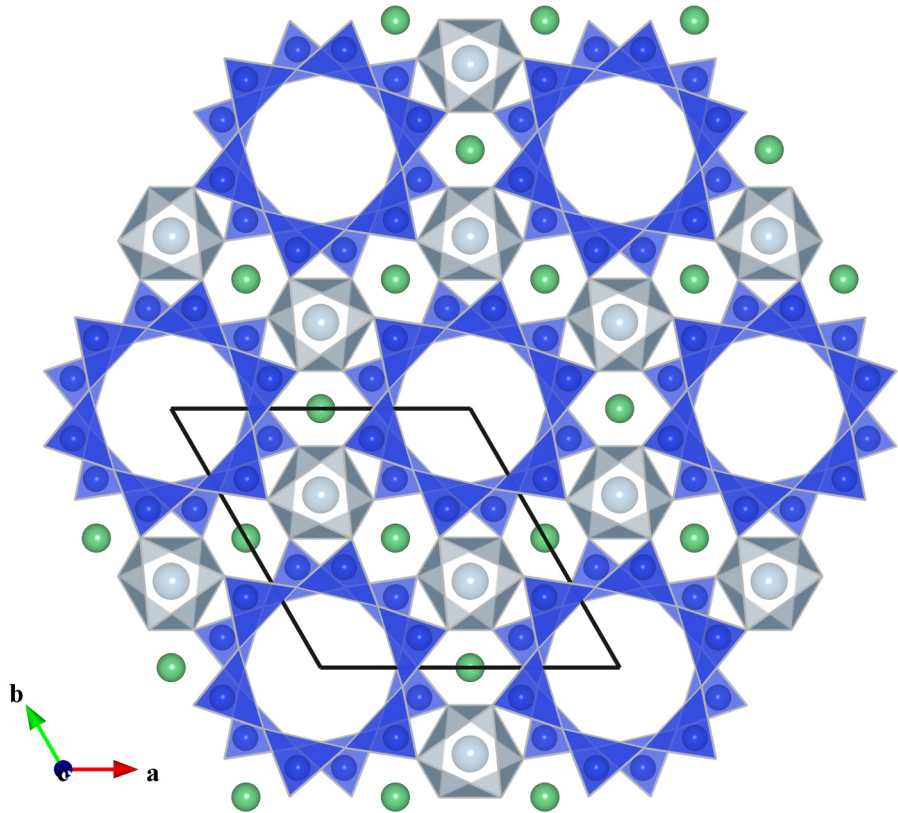


Figure 2.4: Crystal structure of beryl,  $\text{Be}_3\text{Al}_2\text{Si}_6\text{O}_{18}$  [26].

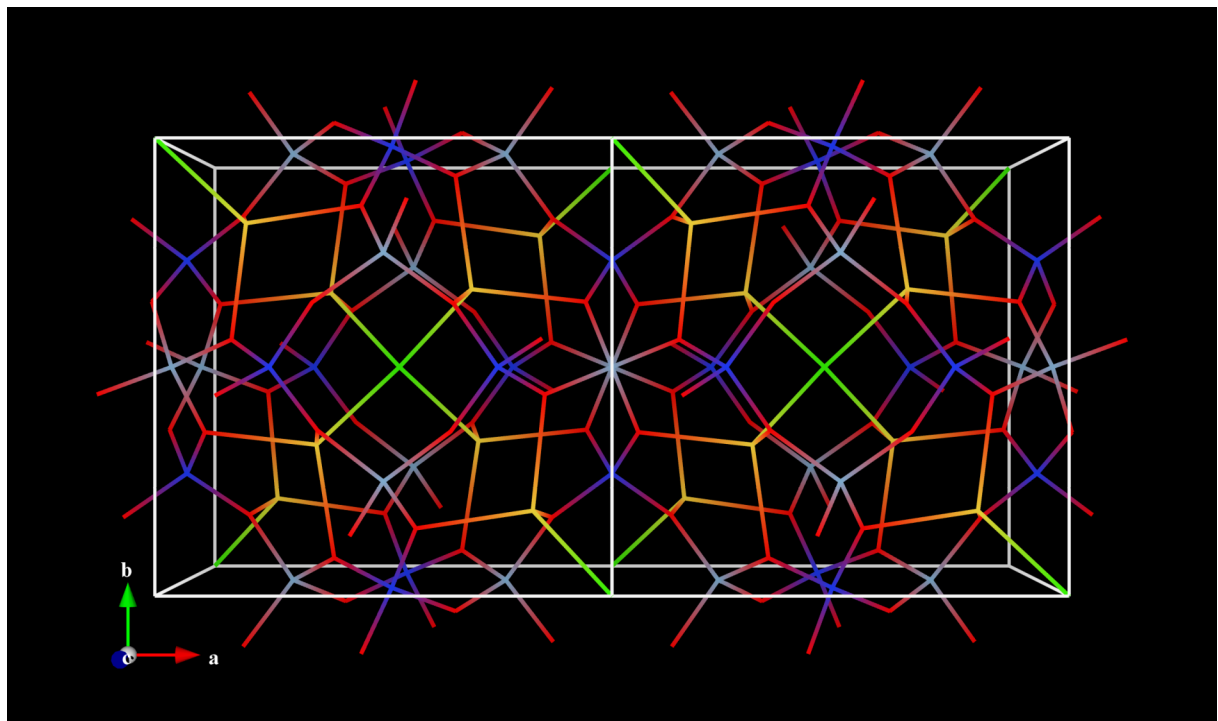


Figure 2.5: Crystal structure of sodalite,  $\text{Na}_4\text{Al}_3(\text{SiO}_4)_3\text{Cl}$  [27].

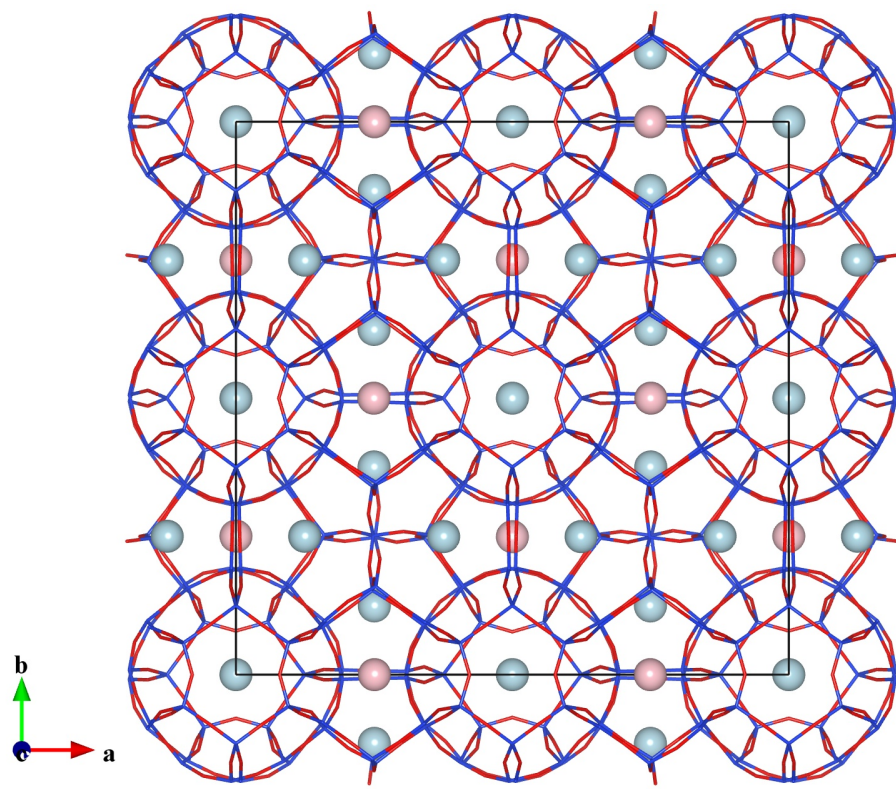


Figure 2.6: Crystal structure of the tetragonal form of melanophlogite,  $46\text{SiO}_2 \cdot 6\text{M}^{14} \cdot 2\text{M}^{12}$  ( $\text{M}^{14} = \text{N}_2, \text{CO}_2$ ;  $\text{M}^{12} = \text{CH}_4, \text{N}_2$ ) [28]. Bright-blue and pink spheres in cages of the  $\text{SiO}_4$  framework represent  $\text{M}^{14}$  and  $\text{M}^{12}$  sites for guest molecules, respectively.

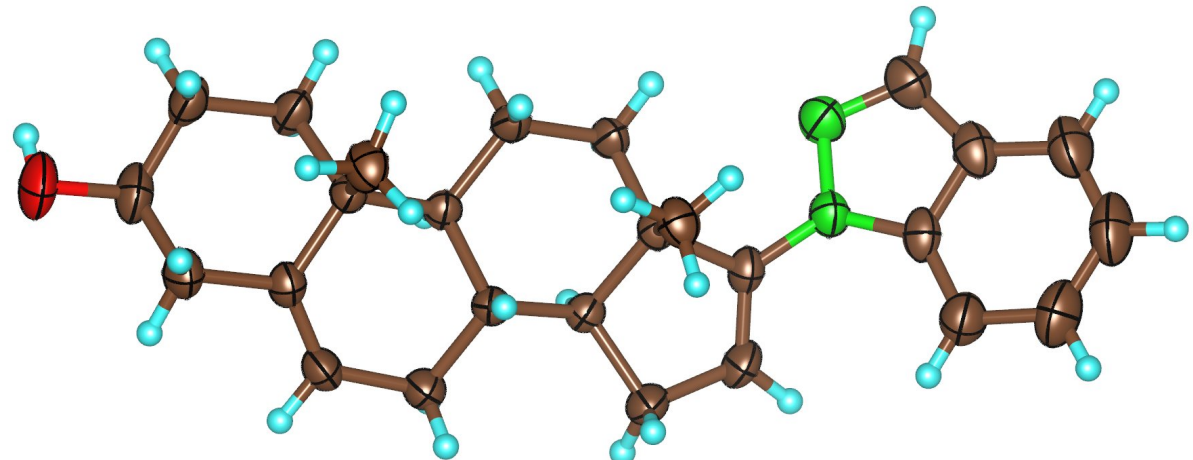


Figure 2.7: A displacement ellipsoid model of 17-(2*H*-indazol-2-yl)androsta-5,16-dien-3 $\beta$ -ol having an indazole substituent at the C17 position [29]. C: brown, N: green, O: red, H: sky-blue. The probability for atoms to be included in the ellipsoids was set at 50 % except for the small and spherical H atoms.

### 2.2.1 A variety of structural information derived on selection of objects

Selection of objects (atoms, bonds, and coordination polyhedra) by clicking with a mouse provides us with a variety of structural information:

- fractional coordinates,
- symmetry operations and translation vectors,
- site multiplicities and Wyckoff letters [30],
- site symmetries,
- principal axes and mean square displacements of anisotropic atomic displacements,
- interatomic distances, bond angles, and dihedral angles,
- information about coordination polyhedra including volumes [31], Baur's distortion indices [32], quadratic elongations [33], bond angle variances [33, 34, 35, 36], effective coordination number [34, 35, 36], charge distribution [35, 36, 37], bond valence sums of central metals [38, 39, 40], and bond lengths expected from bond valence parameters.<sup>1</sup>

## 2.3 Visualization of Volumetric Data

Electron and nuclear densities, wave functions, electrostatic potentials, Patterson functions, *etc.* are visualized as isosurfaces, bird's-eye views, and two-dimensional (2D) maps. Multiple levels of translucent isosurfaces can be overlapped with a structural model. VESTA has a feature of surface coloring to illustrate another kind of a physical quantity at each point on isosurfaces; this feature has been thoroughly redesigned to improve the quality of images [11]. In VESTA, the visibility of both outlines of isosurfaces and an internal structural model has been surprisingly improved by introducing two opacity parameters. Further, we can add 2D slices of volumetric data in their 3D image. The quality of rendering isosurfaces, boundary sections, and slices by VESTA is very high even when the resolution of data is relatively low [11]. The calculation of isosurface geometry has been appreciably accelerated in VESTA by virtue of new algorithm adopted in VESTA [11].

VESTA has a feature to calculate electron and nuclear density distributions from structure parameters and atomic scattering factors. This feature is useful for comparison of the results of MEM with model densities.

**Figure 2.8** illustrates isosurfaces of electron densities calculated with WIEN2k [41] for a superconductor MgB<sub>2</sub> [42]. A network of highly covalent B–B bonds on the  $z = 1/2$  plane and the ionic nature of bonds between Mg<sup>2+</sup> ions ( $z = 0$ ) and B atoms are clearly visualized in this figure. A (001) slice of electron densities at the  $z = 1/2$  level is depicted in **Fig. 2.9**. Such a kind of 2D maps are very useful particularly when part of atoms form 2D sheets *e.g.*, CuO<sub>2</sub> conduction sheets in high- $T_c$  superconducting oxides.

---

<sup>1</sup><http://fujioizumi.verse.jp/riean/book/book.html#BVP>

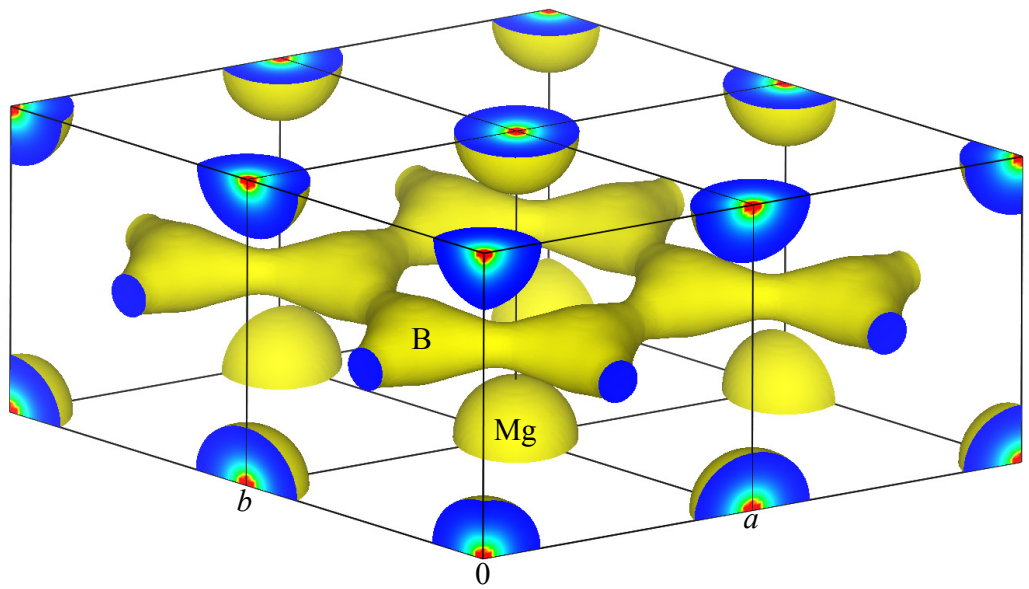


Figure 2.8: Electron-density distribution in MgB<sub>2</sub>. Four hexagonal unit cells are shown with an isosurface level of  $0.11a_0^{-3}$  ( $a_0$ : Bohr radius).

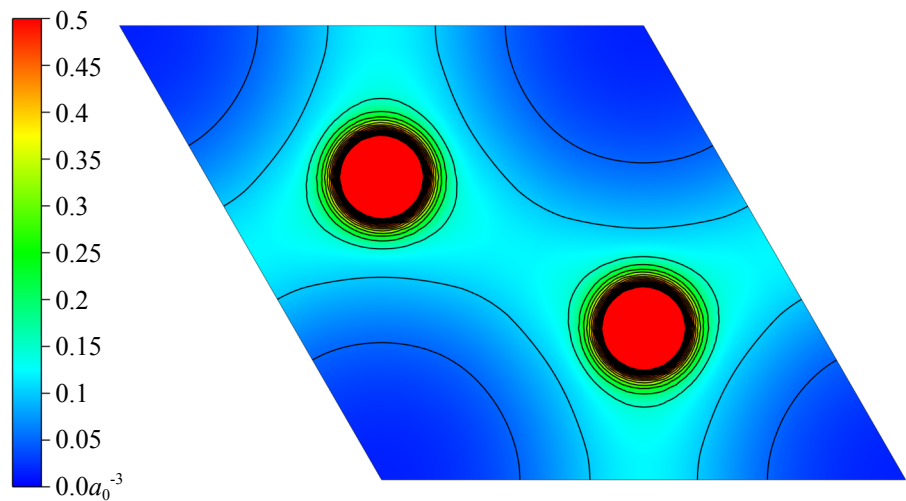


Figure 2.9: A (001) slice illustrating electron-density distribution on the  $z = 1/2$  plane in MgB<sub>2</sub>. Contours are plotted up to  $0.5a_0^{-3}$  with an interval of  $0.05a_0^{-3}$  ( $a_0$ : Bohr radius).

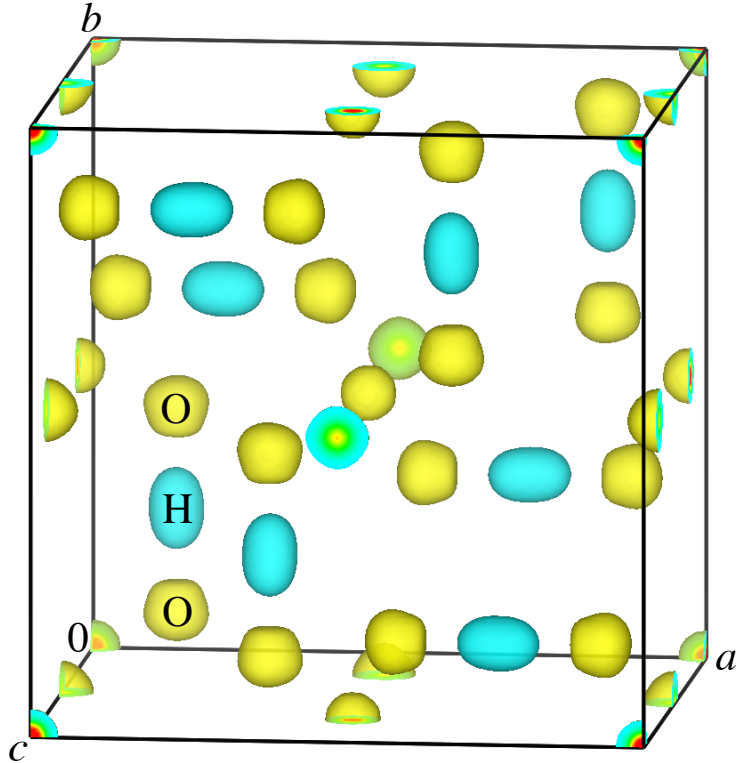


Figure 2.10: Nuclear-density distribution in the paraelectric phase of  $\text{KH}_2\text{PO}_4$ .

**Figure 2.10** shows isosurfaces of scattering-length densities determined from neutron powder diffraction data of  $\text{KH}_2\text{PO}_4$  (paraelectric phase, space group:  $I\bar{4}2d$ ) at room temperature by MEM-based pattern fitting [43]. In this way, two different colors are assigned to positive and negative isosurfaces. Blue isosurfaces (density:  $-2.5 \text{ fm}/\text{\AA}^3$ ) for H atoms are elongated toward yellow ones (density:  $2.5 \text{ fm}/\text{\AA}^3$ ) for O atoms because of double minimum potential with an H-H distance of about  $0.36 \text{ \AA}$ .

## 2.4 Visualization of Crystal Morphologies

Crystal morphologies can be drawn by inputting Miller indices of faces (see section 6.5). Crystal faces can be overlapped with structural models as well as isosurfaces of volumetric data, as exemplified by **Fig. 2.11**. Thus, VESTA facilitates understanding of the relationship between crystal morphologies and chemical bonds, for example, by application of the periodic bond chain (PBC) theory [44]. For example, **Fig. 2.12** illustrates an external morphology of anatase-type  $\text{TiO}_2$  superimposed on its ball-and-stick model. According to Hartman [44], the  $\{101\}$  face of anatase is an  $F$  face, where two PBCs are parallel to the plane. All the other  $\{h0l\}$  faces are  $S$  faces, where only one PBC is parallel to the plane. The PBC along  $[010]$  is intuitively recognized by interactive rotation of the model in three dimensions.

Morphologies of twinned crystals or epitaxial intergrowths of two or more crystals are visualized by inputting multiple crystal data (**Fig. 2.13**). After morphological data have been given, information about Miller indices, distances from the center of the crystal to faces, and the surface area of each face are output to the text area.

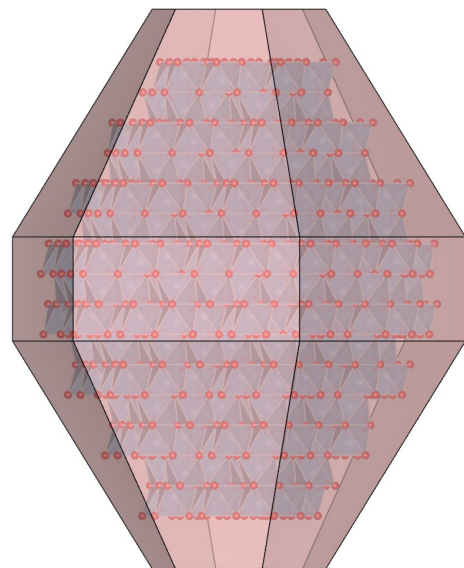


Figure 2.11: An external morphology of an Al<sub>2</sub>O<sub>3</sub> crystal composed of {001}, {110}, and {113} faces.

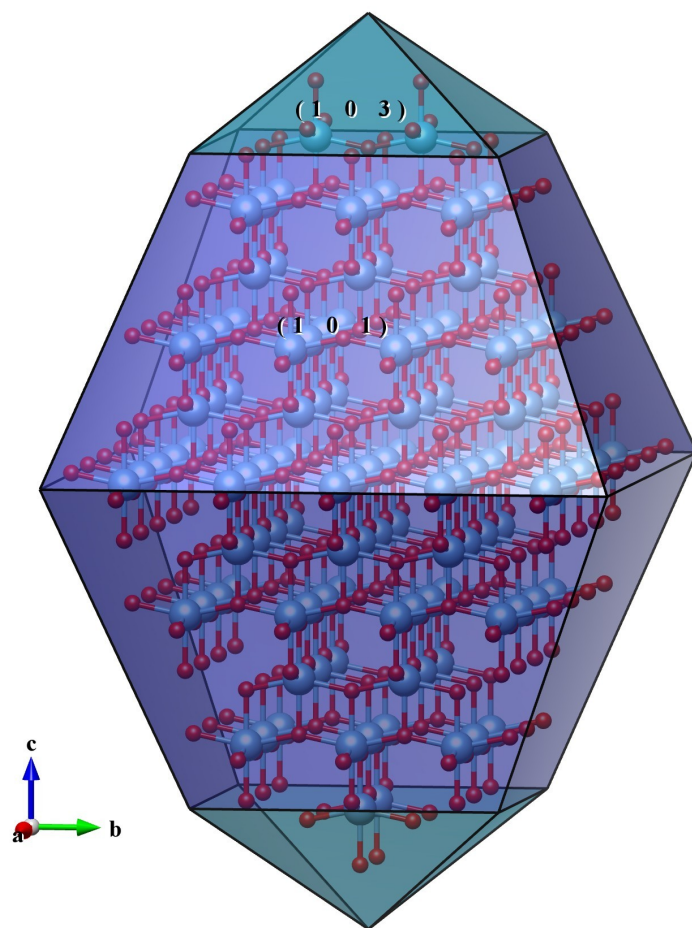


Figure 2.12: A crystal morphology of anatase-type TiO<sub>2</sub> superimposed on its structural model, where blue and red balls represent Ti and O atoms, respectively.

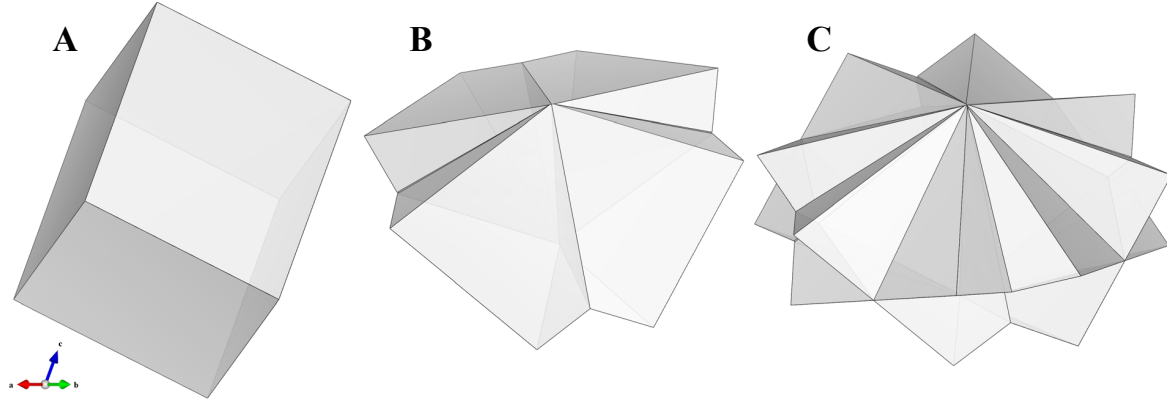


Figure 2.13: Crystal morphologies of adularia, a variant of orthoclase ( $\text{KAlSi}_3\text{O}_8$ ). (A) A single crystal. (B) A hypothetical morphology composed of four individual crystals twinned after the Babeno law. (C) An idealized morphology of repeated twins, which were found from Kobushi mine, Japan, composed of eight individual crystals twinned after the Babeno and Manebach laws.

## 2.5 Cooperation with External Programs

VESTA collaborates closely with external programs such as ORFFE [45], STRUCTURE TIDY [46], RIETAN-FP [12], and MADEL (see section 14.5). On selection of a bond (2 atoms) or a bond angle (3 atoms) in a dialog box relevant to geometrical parameters output by ORFFE, the corresponding object in a ball-and-stick model is highlighted in a graphic window, and *vice versa*. STRUCTURE TIDY allows us to standardize crystal-structure data and transform the current unit cell to a Niggli-reduced cell. RIETAN-FP makes it possible to simulate powder diffraction patterns from lattice and structure parameters. With MADEL, electrostatic site potentials and a Madelung energy can be calculated from occupancies, fractional coordinates, and oxidation states of all the sites.

## 2.6 Input and Output Files

VESTA can read in files with 42 kinds of formats such as CIF, ICSD, and PDB and output files with 15 kinds of formats such as CIF and PDB (see chapter 17). Users of RIETAN-FP [12] must be pleased to learn that standard input files, \*.ins, can be both input and output by VESTA. In addition, program ELEN [47] was built into VESTA for conversion of 3D electron densities into electronic-energy densities and Laplacians [48].

The entire crystal data and various settings can be saved in a small text file, \*.vesta, without incorporating huge volumetric data. File \*.vesta with the VESTA format contains relative paths to external data files of volumetric-data and optionally of structure-data that are automatically read in when \*.vesta is reopened. VESTA also makes it possible to export graphic-data files with 14 image formats including 4 vector-graphic ones (see section 17.5).

## 2.7 Programming Concept

The source code of VESTA comprises GUI and core parts. In this section, only the fundamental concept of programming is briefly described. For further details in algorithmic techniques adopted in VESTA, please refer to Ref. [11].

### **2.7.1 Graphical user interface**

The GUI of VESTA is built on top of a cross-platform application framework (toolkit), wxWidgets, written in the C++ language. The wxWidgets libraries are one of the best toolkits for cross-platform GUI programming. It provides us with a consistent look-and-feel inherent in each operating system. The license agreement of wxWidgets,<sup>2</sup> an LGPL-like license with some exceptions allowing binary distribution without source code and copyright, is flexible enough to permit us to develop any types of applications incorporating wxWidgets.

### **2.7.2 Core libraries**

In contrast to the GUI framework, the core parts of VESTA are carefully separated from the GUI parts to make it easier to reuse the former code. The core libraries are basically independent of the wxWidgets libraries. However, few classes and functions provided by wxWidgets are exceptionally used in some core parts. In such a case, the function is wrapped by another function in a separate file to make the core parts quite independent of GUI toolkits and to make clear which functions depend on external libraries.

---

<sup>2</sup><http://www.wxwidgets.org/about/newlicen.htm>

# Chapter 3

## GETTING STARTED

### 3.1 Minimum requirements of hardware

CPU: MMX Pentium 233 MHz or faster.

RAM: 64 MB or more.

Video RAM: 16 MB or more is desirable.

Video card: A graphics card capable of hardware acceleration of the OpenGL instruction set is recommended.

Display: A minimum resolution of  $1024 \times 768$  pixels with *ca.* 65,000 or *ca.* 16.7 million colors.

Because VESTA utilizes OpenGL technology, the use of an OpenGL-capable graphics processing unit (GPU) is highly recommended but not always mandatory. All the versions of VESTA were built with Intel C++ Composer XE 2011 and linked with the MKL library.<sup>1</sup>

### 3.2 Windows

Both 32- and 64-bit versions of VESTA are available for Windows. They were tested on Windows 10, 8, 7, Vista, and XP. VESTA does not run on Windows ME or older.

The Windows versions of VESTA are archived in the zip format. To get the 32-bit version of VESTA for Windows, download

<http://jp-minerals.org/vesta/archives/VESTA.zip>

To get the 64-bit version of VESTA for Windows, download

<http://jp-minerals.org/vesta/archives/VESTA-win64.zip>

Note that the 32-bit version of VESTA can also be used on 64-bit Windows. Extract the whole contents of the archive file in the same directory. VESTA can be launched in the following four fashions:

1. Double click the icon of VESTA.exe.
2. Type a command in a command line:

`VESTA file1 file2 ...`

This command will start VESTA and open specified files, *file1*, *file2*, etc. Input files may be omitted. When the current directory is different from the directory of VESTA, you

---

<sup>1</sup><http://software.intel.com/en-us/articles/intel-sdp-products/>

must input the absolute path of the executable binary file of VESTA. To execute VESTA by simply typing **VESTA** regardless of the current directory, set environment variable **PATH** to include absolute path of the directory where VESTA is placed.

3. Drag & drop file icons of supported file types on the icon of VESTA.exe.
4. Double click files with extensions associated with VESTA.

To associate an extension with VESTA, right click a file with the extension and select “Properties.” Then change the “Program” section in the **Properties** dialog box.

Beware that VESTA cannot be executed unless the zip file is decompressed. By default, double-clicking a zip file on Windows XP or later will open it with Explore, *i.e.*, the standard file manager of Windows. However, the contents of the archive file seen in the Explore window are actually not extracted but just ‘previewed’. In such a case, copy the whole contents of the ‘previewed’ archive into an appropriate directory, typically in C:\Program Files. Then, VESTA.exe in the VESTA folder can be executed as described above.

### 3.3 macOS

The macOS version of VESTA runs on OS X 10.9 or later using Macs equipped with Intel CPUs that support 64 bit instruction sets. For those using older machines, VESTA v3.4.4 or earlier runs on OS X 10.6 or later and Intel 64 bit CPU. VESTA 2.1.6 or earlier runs on Macs (Mac OS X 10.4) equipped with PowerPC or Intel 32 bit CPUs.

The macOS version is contained in VESTA.dmg with a disc image format. Download <http://jp-minerals.org/vesta/archives/VESTA.dmg> and mount its disc image by double-clicking the icon of VESTA.dmg. Copy the whole contents of the disc image into an appropriate directory, typically /Applications/VESTA.

VESTA can be launched in the following four fashions:

1. Double click the icon of VESTA (or VESTA.app).
2. Type a command in a command line:

```
open -a VESTA file1 file2 ...
```

3. Drag and drop file icons of supported file types on the icon of VESTA.
4. Double click files with extensions associated with VESTA.

### 3.4 Linux

Both 32- and 64-bit versions are available for Linux platforms.

#### 3.4.1 32-bit version

1. Dependency
  - (a) Gkt+ > 2.10
  - (b) Cairo > 1.0
  - (c) libstdc++.so.6
  - (d) Mesa OpenGL library

2. Distributions where VESTA is known to work
  - (a) Fedora 10, 11, 12, 13, 14
  - (b) openSUSE 11.2, 11.3
  - (c) Red Hat Enterprise Linux 5, 6
  - (d) Ubuntu 9.10, 10.10

### 3.4.2 64-bit version

1. Dependency
  - (a) Gkt+ > 2.10
  - (b) Cairo > 1.0
  - (c) libstdc++-so.6
  - (d) Mesa OpenGL library
2. Distributions where VESTA is known to work
  - (a) Fedora 10, 11, 12, 13, 14
  - (b) openSUSE 11.2, 11.3
  - (c) Red Hat Enterprise Linux 5, 6, 7
  - (d) Ubuntu 9.10, 10.10, 12.04, 16.04

Linux versions of VESTA are archived in the tar.bz2 format. For 32-bit OSs running on PCs equipped with Intel x86 CPUs, download

<http://jp-minerals.org/vesta/archives/VESTA-i686.tar.bz2>

For 64-bit OSs running on PCs equipped with AMD 64 CPUs, download

[http://jp-minerals.org/vesta/archives/VESTA-x86\\_64.tar.bz2](http://jp-minerals.org/vesta/archives/VESTA-x86_64.tar.bz2)

Extract the whole contents of the archive file to a directory. Then, execute VESTA in that directory by double-clicking the “VESTA” file on a file manager or by typing the following command in a command line:

**VESTA file1 file2 ...**

This command will start VESTA to open the specified files, *file1*, *file2*, etc. Of course, the input files may be omitted. When the current directory is different from that of VESTA, you must input the absolute path of the executable binary file of VESTA. To launch VESTA by simply typing **VESTA** regardless of the current directory, create a symbolic link of VESTA in a directory where environment variable **path** is set. You can optionally add VESTA to a panel, dock, or the application menu.

VESTA always uses “.” (period) as decimal points regardless of locale settings of OSs, even though some languages use “,” (comma) as decimal points. Such behavior is achieved by internally changing locale settings on execution of the VESTA program. This is necessary because most of file formats, such as Crystallographic Information Framework (CIF), use period as decimal points.

VESTA crashes on Ubuntu 6.06 with some locale settings. In this case, try the following command:

**GTK\_IM\_MODULE=xim VESTA**

## **3.5 Trouble Shooting**

VESTA may not function properly with part of graphics cards; most of such troubles seem to arise from bugs of their drivers. Updating drivers to latest ones may solve the problems. If some troubles are encountered on the use of VESTA, please try to run it on another machine to check whether or not the trouble is caused by a bug in it.

If you fail in executing VESTA on a Linux platform, try to execute it in a command line. Then you will probably get some information about the cause of the problem. Most likely, the failure is caused by missing libraries. In such a case, the names of missing libraries are output to the terminal.

## **3.6 Loading Files**

Files can be loaded in four different fashions. Files to be opened can be specified on execution of VESTA in a command line. Files can be specified in a file selection dialog box, which is opened from the “Open” item in the “File” menu. In the file selection dialog box, only files with supported formats can be selected. You can also drag and drop a file icon onto the main window of VESTA from a file manager (Finder in macOS or Explorer in Windows). If VESTA has been associated with some file extensions, files having these extensions can be opened with a file manager by double-clicking their icons.

# Chapter 4

## MAIN WINDOW

### 4.1 Components of the Main Window

**Figure 4.1** shows the main window of VESTA running on Windows 7. The Main Window consists of the following seven parts:

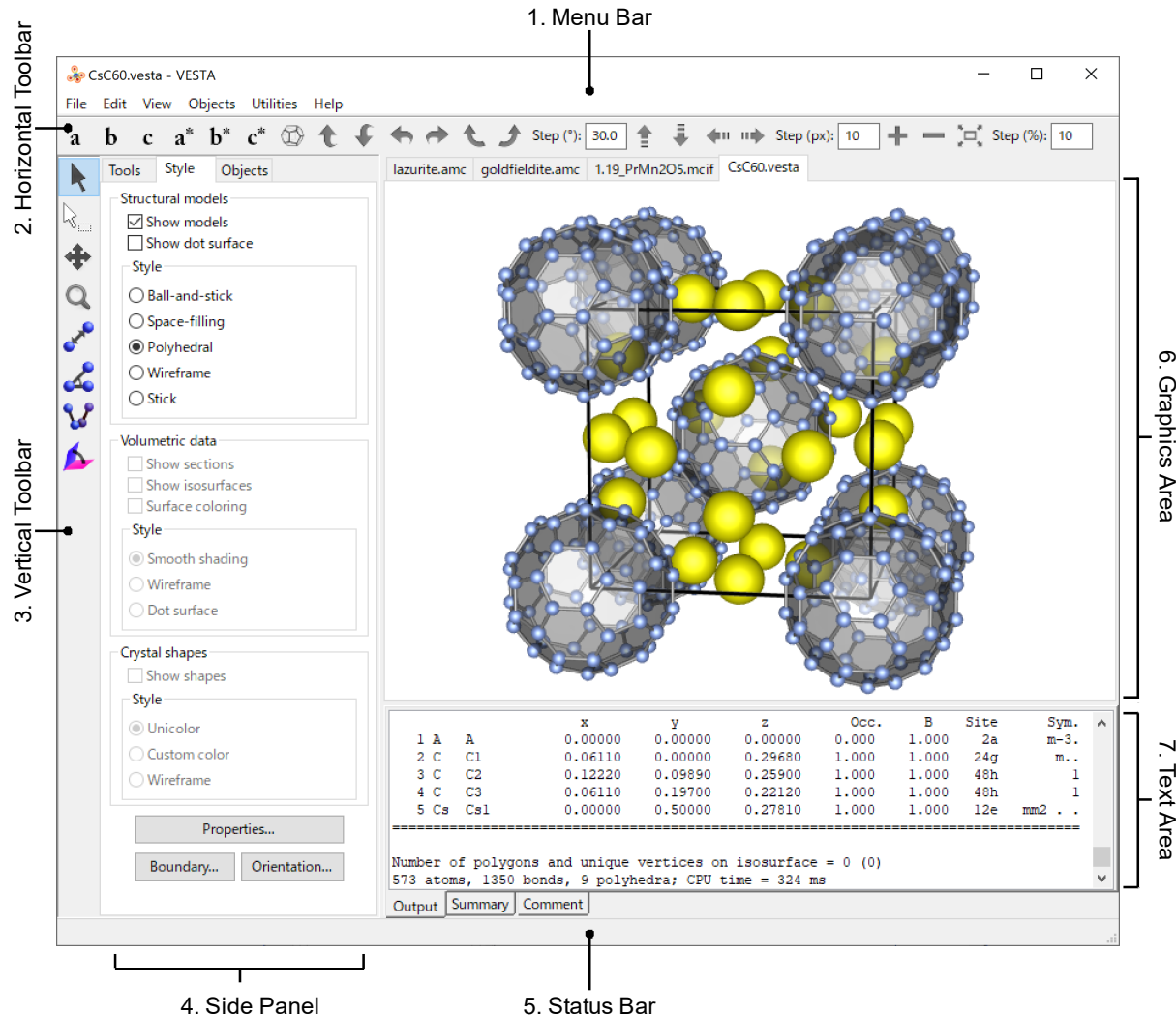


Figure 4.1: Main window of VESTA running on Windows 10.

1. **Menu bar:** “File”, “Edit”, “View”, “Objects”, “Utilities”, and “Help” menus are placed on the menu bar. The menu bar is placed at the top of the Main Window in Windows and Linux while the menus are displayed at the top of the screen in macOS.
2. **Horizontal Toolbar:** Tools used frequently (see section [4.3](#)).
3. **Vertical Toolbar:** Other tools used frequently (see section [4.4](#)).
4. **Side Panel:** Composed of three tab pages. The Tools tab contains options for GUI tools in the Vertical Toolbar (see chapter [11](#)). The Style tab contains GUI tools for display styles (see chapter [5](#)). The Objects tab shows a list of phases and objects in each phase (see chapter [12.2](#)).
5. **Status Bar:** An area to show brief information in a line of text.
6. **Graphics Area:** An area where various objects are displayed in three dimensions.
7. **Text Area:** Two types of texts are displayed here (see section [4.5](#)). A variety of information related to users’ operations is displayed in the Output tab. In the Comment tab, comments on data displayed currently can be input.

## 4.2 Menus

### 4.2.1 File menu

- **New Structure...:** Open a Edit Data dialog box to input crystal data of a new structure.
- **New Window...:** Open a new Main Window.
- **Open...:** Open files with a file selection dialog box.
- **Save...:** Save current data to a file, \*.vesta, with the VESTA format. If the current data has been input from \*.vesta or once saved as \*.vesta, \*.vesta is overwritten. Otherwise, a file selection dialog box will appear to prompt you to input a new file name.
- **Save As...:** Save current data to a new file, \*.vesta, with the VESTA format. A file selection dialog box will appear to prompt you to input a new file name.
- **Export Data...:** Export current data to a file with formats other than the VESTA format.
- **Export Raster Image...:** Export a graphic image to a file with a raster (pixel-based) format.
- **Export Vector Image...:** Export a graphic image to a file with a vector format.
- **Save Output Text...:** Save text data in the Text Area as a text file.
- **Close:** Close the current page. When no data are displayed, this menu is practically the same as the Exit menu.
- **Exit:** Exit VESTA.

#### 4.2.2 Edit menu

- **Undo:** Undo the last action.
- **Redo:** Redo an action that has just been undone.
- **Edit Data:**
  - **Phase...:** Open an Edit Data dialog box to select the Phase page.
  - **Unit Cell...:** Open an Edit Data dialog box to select the Unit Cell page.
  - **Structure Parameters...:** Open an Edit Data dialog box to select the Structure parameters page.
  - **Volumetric Data...:** Open an Edit Data dialog box to select the Volumetric data page.
  - **Crystal Shape...:** Open an Edit Data dialog box to select the Crystal shape page.
- **Bonds...:** Open a Bonds dialog box to create or edit data related to bonds.
- **Vectors...:** Open a Vectors dialog box.
- **Lattice Planes...:** Open a Lattice Planes dialog box.
- **Preferences...<sup>1</sup>:** Open a Preferences dialog box.

#### 4.2.3 View menu

- **Antialiasing:** Enable or disable antialiasing in the Graphics Area.
- **Parallel:** Switch to parallel representation.
- **Perspective:** Switch to perspective representation.
- **Zoom In:** Zoom in objects.
- **Zoom Out:** Zoom out objects.
- **Fit to Screen:** Scale and center justify objects to fit to the Graphics Area.
- **Overall Appearance...:** Open an Overall Appearance dialog box.
- **Clear Text Are:** Clear all the text in the Text Area.

#### 4.2.4 Objects menu

- **Structural Model:** items of this menu can be also selected in the Side Panel.
  - **Show Model:** Show or hide a structural model.
  - **Show Dot Surface:** Show or hide outer surfaces of atoms as dotted surfaces.
  - **Ball-and-Stick:** Show a ball-and-stick model.
  - **Space-filling:** Show a space-filling model.
  - **Polyhedral:** Show a polyhedral model.
  - **Wireframe:** Show a wireframe model.
  - **Stick:** Show a stick model.

---

<sup>1</sup>In the macOS version, the Preferences item is placed under the VESTA menu.

- **Volumetric Data:** items of this menu can be also selected in the Side Panel.
    - **Show Isosurfaces:** Show or hide isosurfaces.
    - **Show Sections:** Show or hide sections of isosurfaces.
    - **Surface Coloring:** Enable or disable the surface coloring of isosurfaces.
    - **Smooth Shading:** Show isosurfaces with a smooth-shading model.
    - **Wireframe:** Show isosurfaces with a wireframe model.
    - **Dot Surface:** Show isosurfaces as dotted surface.
  - **Properties**
    - **General...:** Open a Properties dialog box to select the General page.
    - **Atoms...:** Open a Properties dialog box to select the Atoms page.
    - **Bonds...:** Open a Properties dialog box to select the Bonds page.
    - **Polyhedra...:** Open a Properties dialog box to select the Polyhedra page.
    - **Isosurfaces...:** Open a Properties dialog box to select the Isosurfaces page.
    - **Sections...:** Open a Properties dialog box to select the Sections page.
  - **Boundary...:** Open a Boundary dialog box.
  - **Orientation...:** Open an Orientation dialog box.
- 4.2.5 Utilities menu**
- **Equivalent Positions...:** Open an Equivalent Positions dialog box to list general equivalent positions.
  - **Geometrical Parameters...:** Open a Geometrical Parameters dialog box.
  - **Standardization of Crystal Data...:** Standardize the space-group setting and fractional coordinates.
  - **Niggli-Reduced Cell:** Transform the current unit cell to a Niggli-reduced cell.
  - **Site Potentials and Madelung Energy...:** Calculate site potentials and the Madelung energy of the currently displayed crystal by an external program, MADEL.
  - **Powder Diffraction Pattern...:** Simulate a powder diffraction pattern with RIETAN-FP [12] and display the result with an external graph-plotting program.
  - **Structure Factors...:** Calculate structure factors.
  - **Fourier Synthesis...:** Calculate electron/nuclear densities from structure factors.
  - **Model Electron Densities:** Calculate electron densities from structure parameters.
  - **Model Nuclear Densities:** Calculate nuclear densities from structure parameters.
  - **Patterson Densities:**
    - **From Model Electron Densities...:** Calculate and display density distributions of Patterson function from model electron densities.
    - **From Model Nuclear Densities...:** Calculate and display density distributions of Patterson function from model nuclear densities.

- **From Volumetric Data...**: Calculate and display density distributions of Patterson function from the currently displayed volumetric data.
- **2D Data Display...**: Open a 2D Data Display window.
- **Line Profile...**: Calculate a line profile of volumetric data between two positions and output them in a text file.
- **Peak Search...**: Search peaks in volumetric data.
- **Conversion of Electron Densities...**: Convert 3D electron densities into electronic-energy densities and Laplacians.

#### 4.2.6 Help menu

- **Manual...**: Open the user's manual of VESTA in a PDF viewer.<sup>2</sup>
- **Check for Updates...**: Open the web page of VESTA<sup>3</sup> with a browser to check whether or not a new version of VESTA has been released.
- **About VESTA...**<sup>4</sup>: Show information about VESTA.

### 4.3 Tools in the Horizontal Toolbar

#### 4.3.1 Alignment

- a** View along the  $a$  axis
- b** View along the  $b$  axis
- c** View along the  $c$  axis
- $a^*$**  View along the  $a^*$  axis
- $b^*$**  View along the  $b^*$  axis
- $c^*$**  View along the  $c^*$  axis

The above six buttons are used to align objects parallel to the  $a$ ,  $b$ , or  $c$  axis, or parallel to the  $a^*$ ,  $b^*$ , or  $c^*$  axis, respectively.

---

<sup>2</sup>The present PDF file, VESTA\_Manual.pdf, need to share the same folder with a binary executable file of VESTA.

<sup>3</sup><http://jp-minerals.org/vesta/>

<sup>4</sup>In the macOS version, this item is placed under the VESTA menu.

#### 4.3.2 Rotation

-  Rotate around the x axis
-  Rotate around the x axis
-  Rotate around the y axis
-  Rotate around the y axis
-  Rotate around the z axis
-  Rotate around the z axis

These six buttons are used to rotate objects around the  $x$ ,  $y$ , or  $z$  axis. The step width of rotation (in degrees) is specified in the text box next to the sixth button:

Step (deg.):

#### 4.3.3 Translation

-  Translate upward
-  Translate downward
-  Translate leftward
-  Translate rightward

These four buttons are used to translate objects upward, downward, leftward, and rightward, respectively. The step width of translation (in pixels) is specified in the text box next to the fourth button:

Step (px.):

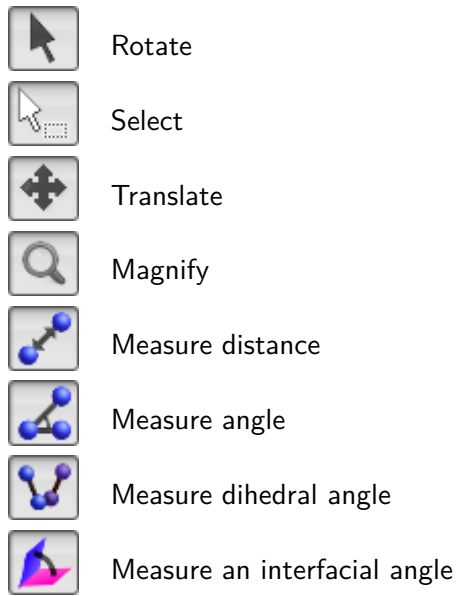
#### 4.3.4 Scaling

-  Zoom in
-  Zoom out
-  Fit to the screen

These three buttons are used to change object sizes. The step width of zooming (in %) is specified in a text box next to the third button:

Step (%):

## 4.4 Tools in the Vertical Toolbar



## 4.5 Text Area

### 4.5.1 Output tab

The **Output** area is a standard-output window corresponding to the Command Prompt window on Windows and a Terminal window on macOS or Linux. Just after launching VESTA, the **Output** area displays information about the PC you are using. **OpenGL version** denotes the version of OpenGL implementation supported by the system. **Video configuration** provides information about the GPU. For example, in a Windows PC equipped with Quadro FX 4600, a message

**Video configuration: Quadro FX 4600/PCI/SSE2**

is displayed in the **Text Area**. SSE2 means that Streaming SIMD Extensions 2 is supported in this graphics card. In the case of a Power Mac G5 (Dual 2.5 GHz) equipped with ATI Radeon 9600 XT, a message

**Video configuration: ATI Radeon 9600 XT OpenGL Engine**

is issued in the **Text Area**. If the GPU of your PC does not support any hardware acceleration of OpenGL, **Video configuration** would be **GDI Generic** on Windows, and **Software Rasterizer** or **Mesa GLX Indirect** on Linux.

When a new file is loaded, a summary of data appears in the **Output** area, including the absolute path of the file and the title of the data. For crystal-structure data, lattice parameters, a unit-cell volume, and structure parameters (element names, site names, fractional coordinates, occupancies, isotropic atomic displacement parameters, multiplicities plus Wyckoff letters, and site symmetries) are output. In the case of volumetric data, lattice parameters, number of grids along each axis, and number of polygons and unique vertices on slices and isosurfaces are displayed. For instance, a CIF of PbSO<sub>4</sub> affords the following output:

Title	04 Pb1 S1
Lattice type	P
Space group name	P n m a

Space group number 62  
Setting number 1

#### Lattice parameters

a	b	c	alpha	beta	gamma
8.51600	5.39900	6.98900	90.0000	90.0000	90.0000

Unit-cell volume = 321.339447

#### Structure parameters

		x	y	z	g	Occ	Site	Sym.
1	Pb	0.18820	0.25000	0.16700	1.000	1.200	4c	.m.
2	S	0.43700	0.75000	0.18600	1.000	0.700	4c	.m.
3	0	0.59500	0.75000	0.10000	1.000	1.600	4c	.m.
4	0	0.31900	0.75000	0.04300	1.000	1.600	4c	.m.
5	0	0.41500	0.97400	0.30600	1.000	1.600	8d	1

Such a type of a list is also output when pressing [OK] button in the Edit Data dialog box.

#### 4.5.2 Summary tab

The Summary tab gives a brief summary of data including data name, space group, unit cell parameters, unit cell volume, and number of grids of volumetric data. An example output is as follows.

NaV6011  
Space Group: P 63/m m c (#194-1)  
a = 5.70918 Å      α = 90.0000°      grid(x) = 120  
b = 5.70918 Å      β = 90.0000°      grid(y) = 120  
c = 13.08744 Å      γ = 120.0000°      grid(z) = 240  
V = 369.4305 Å<sup>3</sup>

#### 4.5.3 Comment tab

You can input any comments relevant to data displayed currently. VESTA also reads in some information on the data from files (\*.amc) of the American Mineralogist Crystal Structure Database format. For example, the following information is read in from \*.amc for anatase-type TiO<sub>2</sub> and displayed in the Comment area.

Horn M, Schwerdtfeger C F, Meagher E P  
Zeitschrift fur Kristallographie 136 (1972) 273–281  
Refinement of the structure of anatase at several temperatures  
Sample: T = 25 C  
Locality: Legenbach quarry, Binnatal, Switzerland  
\_database\_code\_amcsd 0010735

# Chapter 5

## DISPLAY STYLES

Display styles of structural models, volumetric data, and crystal shapes are controlled either from the Style tab of the Side Panel or from the “Objects” menu. Both of the methods allow us to use the same options.

### 5.1 Structural Models

The Structural model frame box in the Style tab of the Side Panel (**Fig. 5.1**) contains frequently used tools to control representation of structural models. The same options can also be used by selecting the Model item under the “Objects” menu. This frame box is disabled for data containing no structural model.

#### 5.1.1 Objects to be displayed

##### Show model

This option controls the visibility of a structural model. When this option is checked (default), a structural model is visible; otherwise, no structural model is shown. Uncheck this option when you want to see only isosurfaces and sections for data containing both structural and volumetric ones.

##### Show dot surface

In ball-and-stick, wireframe, and stick models, dot-surface spheres are added with radii corresponding to 100 % of user specified ones in the same manner as with a space-filling model if Show dot surface is checked (**Fig. 5.2**). This mode is designed to accentuate outer surfaces of atoms. Each sphere is represented as though it were a hollow shell with numerous dots placed on the surface. The combination of dot surface with a stick model is useful for understanding how atoms are combined with each other in a molecule. The density of dots is controlled by two parameters, {Stacks} and {Slices} in the Atoms page of the Properties dialog box as with the same manner as solid spheres.

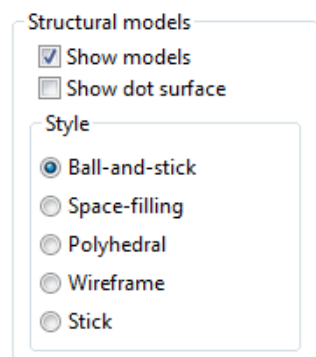


Figure 5.1: The Structural model frame box in the Style tab of the Side Panel.

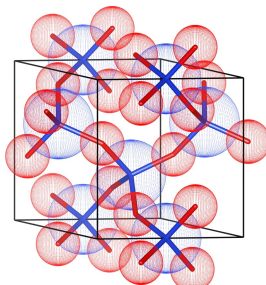


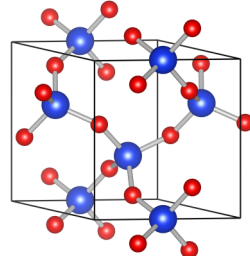
Figure 5.2: Crystal structure of quartz [49] represented by a stick model with dot surfaces. Si: blue, O: red.

### 5.1.2 Styles

As described in [2.2](#), VESTA represents crystal structures by the five different styles: ball-and-stick, space-filling, polyhedral, wireframe, and stick models. When atoms are drawn as spheres, they are rendered with radii corresponding to 40 % of actual atomic radii in all but the space-filling model, where atoms are rendered with the actual atomic radii. Default radii of atoms are selected from three types: atomic, ionic, and van der Waals radii. The radius of each element and a type of radii are specified at the [Atoms](#) page in the Properties dialog box (see section [12.1.2](#)). Features in each structural model are described below with screenshots of the structure for quartz [\[49\]](#) on the right side.

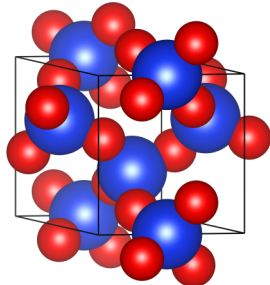
#### “Ball-and-stick”

In the “Ball-and-stick” model, all the atoms are expressed as solid spheres or displacement ellipsoids. Bonds are expressed as either cylinders or lines.



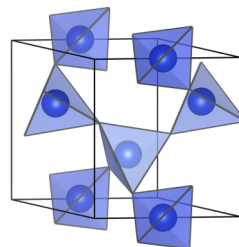
#### “Space-filling”

In the “Space-filling” model, atoms are drawn as interpenetrating solid spheres, with radii specified at the [Atoms](#) tab in the Properties dialog box (see section [12.1.2](#)). This model is useful for understanding how atoms are packed together in the structure.



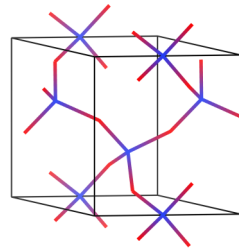
#### “Polyhedral”

In the polyhedral model, crystal structures are represented by coordination polyhedra where central atoms, bonds, and apex atoms may also be included. Bonds between central and apex atoms have to be searched with the [Bonds](#) dialog box to display coordination polyhedra comprising them. Atoms are expressed as solid spheres or displacement ellipsoids. Bonds are expressed as either cylinders or lines. Needless to say, the transparency of the coordination polyhedra must be high enough to make it possible to see the central atoms and bonds. One of six different styles for representing polyhedra is specified at the [Polyhedra](#) tab in the Properties dialog box (see section [12.1.4](#)).



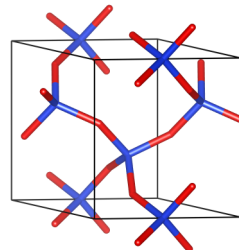
### “Wireframe”

In the “Wireframe” model, atoms having no bonds are drawn as wireframe spheres whereas those bonded to other atoms are never drawn. All the bonds are presented as lines with gradient colors. This model is useful for seeing and manipulating complex and/or large structures because this is usually the fastest model for rendering structures on the screen.



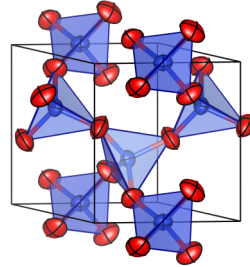
### “Stick”

In the “Stick” model, atoms with no bonds are drawn as solid spheres while atoms bonded to other atoms are never drawn. All the bonds are expressed as cylinders, whose properties can be changed at the **Bonds** tab in the Properties dialog box (see section 12.1.3). This model serves to see frameworks or molecular geometry.



### Displacement ellipsoids

In the ball-and-stick and polyhedral models, atoms can be rendered as displacement ellipsoids. The probability for atoms to be included in the ellipsoids is also specified in the Properties dialog box (see section 12.1.2).



## 5.2 Volumetric Data

The Volumetric data frame box in the **Style** tab of the Side Panel (Fig. 5.3) contains frequently used tools to control representation of volumetric data. The same options can also be used by selecting the “Volumetric Data” item under the “Objects” menu. This frame box is disabled for data containing no volumetric ones.

- Show sections

This option controls whether or not sections of isosurfaces are visible. When this option is checked (default), sections are visible, otherwise they are not shown.

- Show isosurfaces

This option controls whether or not isosurfaces of volumetric data are visible. When this option is checked (default), isosurfaces are visible, otherwise they are not shown. To see only a structural model for data containing both

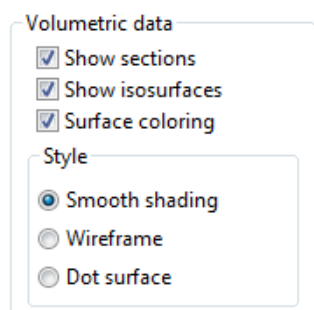


Figure 5.3: The Volumetric data frame box in the **Style** tab of the Side Panel.

structural and volumetric ones, uncheck this option in addition to the “Show sections” option.

- **Surface coloring**

“Surface coloring” means that colors of isosurfaces drawn from one data set are determined by a secondary data set. A typical example is coloring of electron-density isosurfaces on the basis of electrostatic potentials (see Fig. 12.9). This option is enabled only when the secondary volumetric data for surface coloring has been loaded with the **Volumetric data** tab in the **Edit Data** dialog box (see 6.4.2).

Styles of isosurfaces are chosen from the following three representations:

- Smooth shading
- Wireframe
- Dot surface

Isosurfaces are drawn as solid surfaces with variable opacity in the **Smooth shading** mode whereas isosurfaces are represented by lines and points, respectively, in the **Wireframe** and **Dot surface** modes.

## 5.3 Crystal Shapes

The **Crystal Shapes** frame box in the **Style** tab of the **Side Panel** (Fig. 5.4) provides us with tools to control representation of crystal morphologies. The same options can also be used by selecting the “**Crystal Shapes**” item under the “**Objects**” menu. This frame box is disabled for data containing no morphology data (faces).

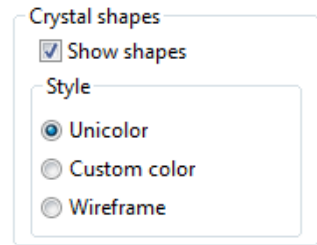


Figure 5.4: The **Crystal shapes** frame box in the **Style** tab of the **Side Panel**.

- **Show shapes**

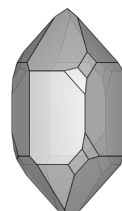
This option controls whether or not the external morphology of crystals are visible. When this option is checked (default), morphologies are visible, otherwise they are not shown.

### 5.3.1 Styles

VESTA represents crystal morphologies by the following three styles:

#### “Unicolor”

All the faces of a crystal are filled with a single color, as the right figure (quartz) illustrates.



### **“Custom color”**

Each face is filled with a color assigned to symmetrically equivalent  $\{hkl\}$  faces specified in the Edit Data dialog box (see section [6.5](#)) or in the Side Panel.



### **“Wireframe”**

Only edges of a crystal shape are drawn with lines.



# Chapter 6

## GIVING PHASE DATA

To create a new structure, choose the “File” menu  $\Rightarrow$  “New Structure...”. To edit current data, choose “Edit” menu  $\Rightarrow$  “Edit Data”  $\Rightarrow$  “Phase...”. In both of the cases, the same dialog box named New Data or Edit Data appears (Fig. 6.1). This dialog box consists of the following five tab pages:

- Phase
- Unit cell
- Structure parameters
- Volumetric data
- Crystal shape

At the top of the dialog box, a serial number and a title are displayed for the selected phase.

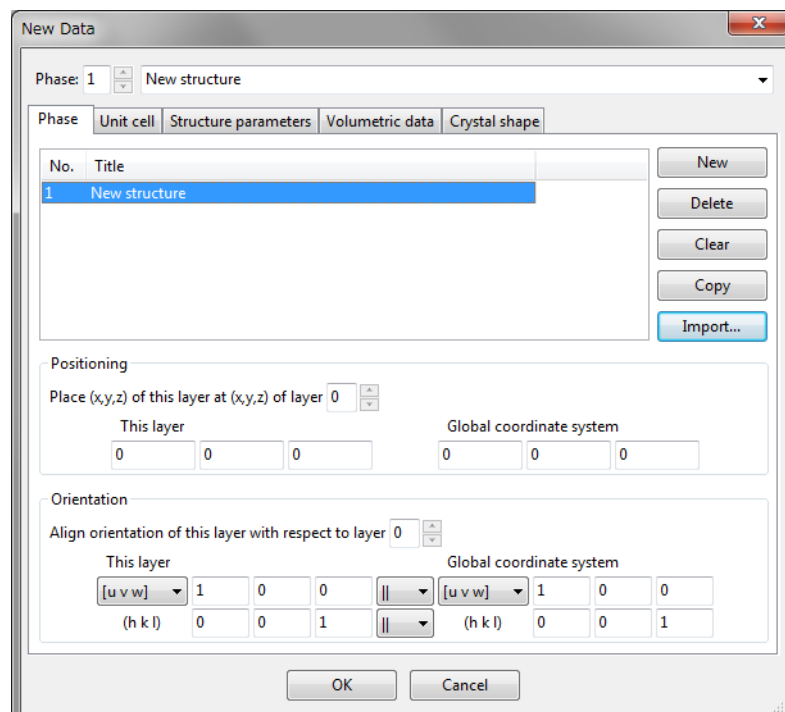


Figure 6.1: New Data dialog box.

## 6.1 Defining Phases

In the Phase tab (Fig. 6.1) of the Edit Data dialog box, you can add, delete, copy, or import phase data that are overlaid on the same **Graphics Area**. To edit the title of a phase, select a row in the list and click on the Title column. When dealing with a single phase, you have nothing to do with this tab except for editing the title. The **Positioning** and **Orientation** frame boxes are used when superimposing two or more phases. See chapter 7 for how to visualize multiple phase data in the same **Graphics Area**.

## 6.2 Symmetry and Unit Cell

The Unit cell tab in the Edit Data dialog box is used to give lattice parameters and the symmetry of a structure (Fig. 6.2).

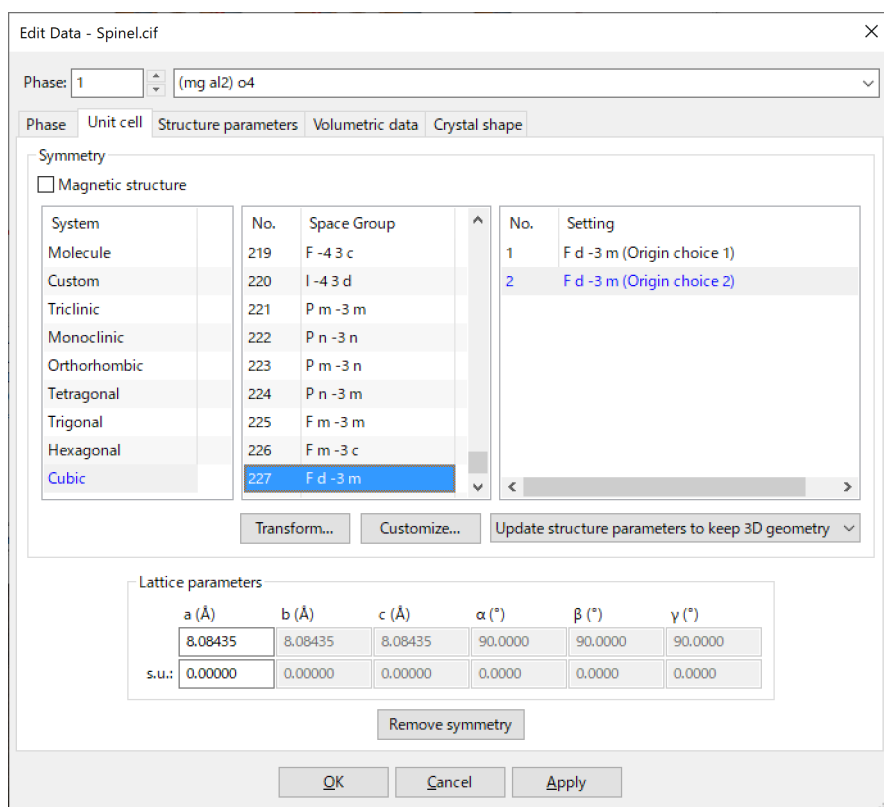


Figure 6.2: Unit cell page in the Edit Data dialog box.

### 6.2.1 Crystal systems and space groups

#### Selection of crystal systems

The **System** list box is used to filter a list of space-group symbols in the **Space group** list box. When an item in this list box is selected, only space groups belonging to the selected crystal system will be highlighted in the **Space group** list box. The following ten items are listed in the **System** list box.

- Molecule
- Custom

- Triclinic
- Monoclinic
- Orthorhombic
- Tetragonal
- Trigonal
- Hexagonal
- Cubic
- Rhombohedral

On selection of **Molecule**, a Cartesian-coordinate system is used instead of fractional-coordinate system, which leads to the absence of “unit cell”. Therefore, text boxes and list boxes for settings of a space group and lattice parameters are disabled. When **Custom** is selected, space-group settings cannot be specified, but symmetry operations can be manually customized (see page 36).

### Selection of a space group

Space group numbers and standard symbols are listed in the **Space Group** list box. Only space groups of a selected crystal system is highlighted in the list but you can select any space group. On selection of a space group, the list boxes of **System** and **Setting** will be updated.

### Settings for a space group

The number of available settings for the selected space group is listed in list box **Setting**. Settings available in the list box are basically those compiled in *International Tables for Crystallography*, volume A [30].

In some space groups, additional settings are contained in list box {**Setting**}. In the triclinic system, complex lattices, *A*, *B*, *C*, *I*, *F*, and *R*, may be selected with setting numbers of 2, 3, 4, 5, 6, and 7, respectively (Table 6.1). In the monoclinic system, settings with unique axes *a*, *b*, and *c* are all available as built-in settings (Table 6.2).

In the orthorhombic system, any of six settings, *i.e.*, **abc**, **ba $\bar{c}$** , **cab**,  **$\bar{c}ba$** , **bca**, and **a $\bar{c}b$**  listed in Table 4.3.2.1 in Ref. [30] may be selected with setting numbers of 1, 2, 3, 4, 5, and 6, respectively. In orthorhombic space groups having two origin choices, odd and even setting numbers adopts origin choices 1 and 2, respectively. Then, settings 1 and 2 are of axis choice **abc**, settings 3 and 4 are of **ba $\bar{c}$** , and so on (Table 6.3).

On changes in crystal axes, *e.g.*, rhombohedral or hexagonal axes in a trigonal crystal, lattice parameters are automatically converted.

When changing a setting number, consider whether you need to keep structure parameters or 3D geometries (see the following subsection).

Table 6.1: Non-standard settings in two triclinic space groups.

Setting number	Space group ( $P1$ )	Space group ( $P\bar{1}$ )
1	$P1$	$P\bar{1}$
2	$A1$	$A\bar{1}$
3	$B1$	$B\bar{1}$
4	$C1$	$C\bar{1}$
5	$I1$	$I\bar{1}$
6	$F1$	$F\bar{1}$
7	$R1$	$R\bar{1}$

Table 6.2: Setting numbers of monoclinic space groups.

Axis choice	$\underline{\mathbf{a}\mathbf{b}\mathbf{c}}$			$\mathbf{c}\bar{\mathbf{b}}\mathbf{a}$			$\underline{\mathbf{a}\mathbf{b}\mathbf{c}}$			$\mathbf{b}\mathbf{a}\bar{\mathbf{c}}$			$\underline{\mathbf{a}\mathbf{b}\mathbf{c}}$			$\bar{\mathbf{a}}\mathbf{c}\mathbf{b}$		
Cell choice	1	2	3	1	2	3	1	2	3	1	2	3	1	2	3	1	2	3
	Unique axis $b$						Unique axis $c$						Unique axis $a$					
$P2$	1						2						3					
$P2_1$	1						2						3					
$C2$	1	2	3				4	5	6				7	8	9			
$Pm$	1						2						3					
$Pc$	1	2	3				4	5	6				7	8	9			
$Cm$	1	2	3				4	5	6				7	8	9			
$Cc$	1	2	3	10	11	12	4	5	6	13	14	15	7	8	9	16	17	18
$P2/m$	1						2						3					
$P2_1/m$	1						2						3					
$C2/m$	1	2	3				4	5	6				7	8	9			
$P2/c$	1	2	3				4	5	6				7	8	9			
$P2_1/c$	1	2	3				4	5	6				7	8	9			
$C2/c$	1	2	3	10	11	12	4	5	6	13	14	15	7	8	9	16	17	18

Table 6.3: Axis choices in the orthorhombic space groups.

Axis choice	Space groups		
	No. 48, 50, 59, 68, and 70		Others
	Origin choice 1	Origin choice 2	
$\mathbf{a}\mathbf{b}\mathbf{c}$	1	2	1
$\mathbf{b}\mathbf{a}\bar{\mathbf{c}}$	3	4	2
$\mathbf{c}\mathbf{a}\mathbf{b}$	5	6	3
$\bar{\mathbf{c}}\mathbf{b}\mathbf{a}$	7	8	4
$\mathbf{b}\mathbf{c}\mathbf{a}$	9	10	5
$\mathbf{a}\bar{\mathbf{c}}\mathbf{b}$	11	12	6

### 6.2.2 Behavior when changing a space-group setting

The list box below the Setting controls the behavior when changing a space-group setting. There are two options:

- Update structure parameters to keep 3D geometry
- Keep structure parameters unchanged

On the use of the first option (default), lattice parameters and fractional coordinates are converted to keep the structural geometry of a crystal when the setting number of a space group is changed or a transformation matrix is specified. When the second option is used, lattice parameters and fractional coordinates remain unchanged instead of the geometry.

If a correct structure is displayed in the Graphic Area but another space-group setting is preferred to the current one, choose Update structure parameters to keep 3D geometry and change the space-group setting. The second option is typically used to change a setting number when the correct setting number is not recognized by VESTA after reading in a file such as CIF. In such a case, lattice parameters and fractional coordinates are correct whereas symmetry operations are incorrect. Then, choose Keep structure parameters unchanged and select the correct setting number. When a setting number cannot be uniquely determined from data recorded in a structural-data file, VESTA assumes setting number 2 (a setting with the inversion center at the origin) in centrosymmetric space groups with two origin choices, and setting number 1 in all the other space groups.

Note that even if structure parameters remain unchanged, some lattice parameters may be changed in conformity with constraints imposed on them in the current space-group setting.

### 6.2.3 Lattice parameters

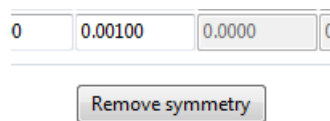
In the Lattice parameters frame box, lattice parameters are input in the unit of Å ( $a$ ,  $b$ , and  $c$ ) and degrees ( $\alpha$ ,  $\beta$ , and  $\gamma$ ). Lattice parameters input by the user are automatically constrained on the basis of a crystal system. Standard uncertainties (s.u.'s) of lattice parameters are used to calculate s.u.'s of geometrical parameters. For structural data based on the Cartesian coordinates (when Molecule is selected as the Crystal system), text boxes in this frame box are disabled.

### 6.2.4 Customization of symmetry operations

To customize symmetry operations, click the [Customize...] button. Then, the Equivalent Positions dialog box appears with an editing mode (**Fig. 6.3**), and a list of general equivalent positions is displayed in this dialog box. When one of the equivalent positions in the list is selected, the corresponding symmetry operation is displayed in a matrix form at the upper left of the dialog box. If you input a value in one of the text boxes, representation of the corresponding equivalent position in the list is updated. To add a new symmetry operation, click the [New] button. To remove a symmetry operation, select an item in the list and click the [Delete] button. Clicking the [Clear] button removes all the symmetry operations other than the identity operation.

### 6.2.5 Reducing symmetry

Clicking the [Remove symmetry] button generates all the atoms in the unit cell as virtual independent sites by reducing the symmetry of the crystal to  $P1$ . When the space group is changed to that with higher symmetry, or when the unit cell is transformed to a smaller one (see 6.2.6), the same atomic position may result from two or more sites. In such a case, the redundant sites can



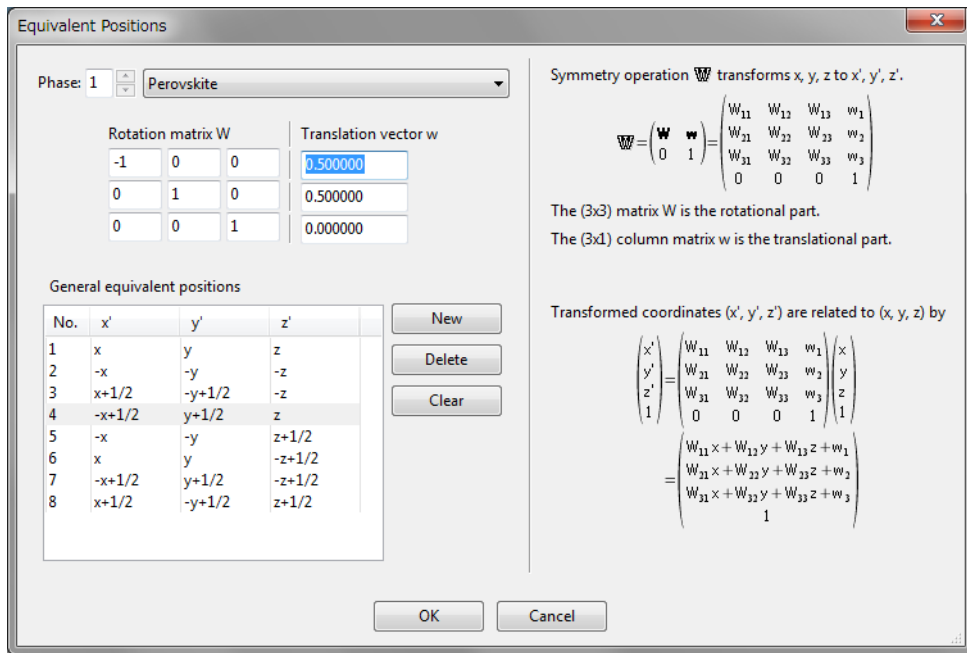


Figure 6.3: Equivalent Positions dialog box with an editing mode.

be removed by clicking the [Remove duplicate atoms] button in the Structure parameters tab (see page 48).

### 6.2.6 Transformation of the unit cell

Clicking the [Transform...] button opens the Unit Cell Transformation dialog box (Fig. 6.4). This dialog box allows you to transform crystal axes by specifying  $3 \times 3$  rotation matrix  $P$  and  $3 \times 1$  translation vector  $p$ . The [View general positions] button in the dialog box is used to open the Equivalent Positions dialog box to check the general equivalent positions and symmetry operations of the transformed unit cell (see 14.1). Clicking the [Initialize current matrix] button resets the transformation matrix to the identity matrix. Currently, this operation cannot be canceled. When option “Normalize the fractional coordinates” is checked, new atomic coordinates of the transformed unit cell will be normalized within a range of 0 to 1.

In what follows, a more detailed explanation and use cases of the Unit Cell Transformation dialog box will be given.

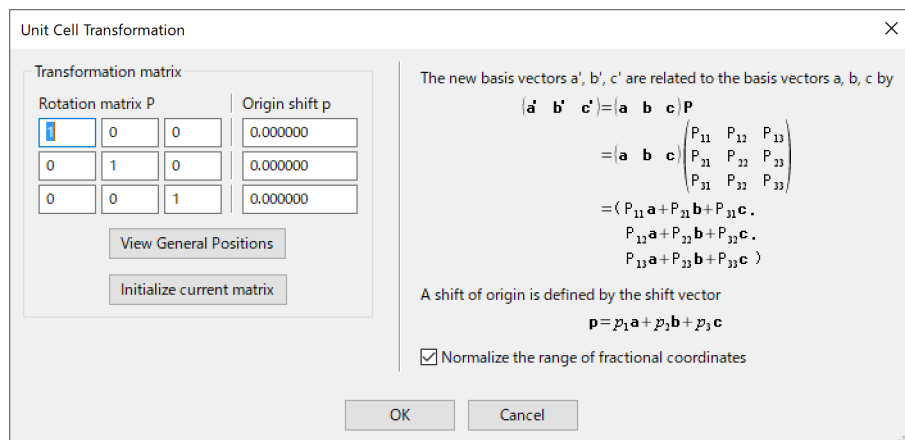


Figure 6.4: Unit Cell Transformation dialog box.

## Non-conventional space-group settings

To convert a structure from a conventional setting to a non-conventional one, you have to select a mode **Update structure parameters to keep 3D geometry** in the Unit cell tab of the **Edit Data** dialog box before opening the **Unit Cell Transformation** dialog box. With this mode, both lattice parameters and fractional coordinates are automatically transformed into new ones to keep the current geometry of the crystal structure. When the mode **Keep structure parameters unchanged** is selected, only symmetry operations are transformed to those of the new setting, whereas lattice parameters and fractional coordinates remain unchanged.

The new origin of the transformed unit cell is specified as the origin shift  $\mathbf{p}$ . For instance, if you specify  $(0.25, 0.25, 0.25)$  as an origin shift, a coordinate of  $(0.25, 0.25, 0.25)$  of a conventional setting becomes  $(0, 0, 0)$  of the transformed non-conventional unit-cell.

Orientations of the transformed crystal axes  $\mathbf{a}'$ ,  $\mathbf{b}'$ , and  $\mathbf{c}'$  are specified as column vectors in the  $3 \times 3$  rotation matrix  $\mathbf{P}$ , i.e., the first, second, and third columns of  $\mathbf{P}$  represent  $\mathbf{a}'$ ,  $\mathbf{b}'$ , and  $\mathbf{c}'$  respectively. For example, the following transformation matrix is used to swap the  $a$  and  $b$  axes.

$$\mathbf{P} = \begin{pmatrix} 0 & 1 & 0 \\ 1 & 0 & 0 \\ 0 & 0 & -1 \end{pmatrix}. \quad (6.1)$$

Note that the orientation of the  $c$  axis is inverted in this case, or otherwise the transformed structure becomes enantiomorphic with respect to the original structure in non-centrosymmetric space groups. In general, when the determinant of  $\mathbf{P}$ ,  $\det(\mathbf{P})$ , is negative, the crystal-coordinate system is transformed from right-handed to left-handed, and *vice versa*. When such a matrix is specified as  $\mathbf{P}$ , a warning dialog box will appear to confirm whether or not you proceed to the next step.

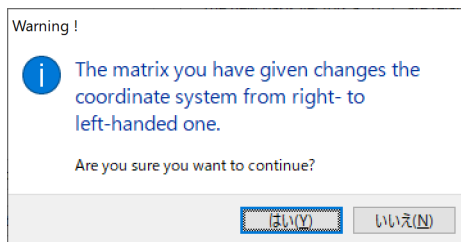


Figure 6.5: A warning dialog box for conversion of structure handedness.

The unit-cell volume,  $V$ , is transformed to  $V'$  by

$$V' = \det(\mathbf{P})V. \quad (6.2)$$

Therefore, the unit-cell volume changes on the transformation unless  $\det(\mathbf{P})$  is 1.

The entire transformation including both a rotation and an origin shift can be expressed by single  $4 \times 4$  transformation matrix  $\mathbb{P}$ , which consists of the  $3 \times 3$  rotation matrix  $\mathbf{P}$ , the  $3 \times 1$  translation vector  $\mathbf{p}$ , and the row vector  $\mathbf{o} = (0, 0, 0)$  [50]:

$$\mathbb{P} = \begin{pmatrix} \mathbf{P} & \mathbf{p} \\ \mathbf{o} & 1 \end{pmatrix} = \begin{pmatrix} P_{11} & P_{12} & P_{13} & p_1 \\ P_{21} & P_{22} & P_{23} & p_2 \\ P_{31} & P_{32} & P_{33} & p_3 \\ 0 & 0 & 0 & 1 \end{pmatrix}. \quad (6.3)$$

Then each of the following crystallographic variables, *i.e.*, primitive translation vectors  $\mathbf{a}$ ,  $\mathbf{b}$ ,  $\mathbf{c}$ , reciprocal lattice vectors  $\mathbf{a}^*$ ,  $\mathbf{b}^*$ ,  $\mathbf{c}^*$ , metric tensor  $\mathbf{G}$ , metric tensor of reciprocal lattice  $\mathbf{G}^*$ , atomic coordinate  $\mathbf{X}$ , symmetry operation  $\mathbb{W}$ , and anisotropic atomic displacement parameters  $\beta$ , are transformed as described below.

Primitive translation vectors  $\mathbf{a}$ ,  $\mathbf{b}$  and  $\mathbf{c}$  are transformed by  $\mathbf{P}$  as

$$\begin{aligned} (\mathbf{a}', \mathbf{b}', \mathbf{c}') &= (\mathbf{a}, \mathbf{b}, \mathbf{c})\mathbf{P} \\ &= (\mathbf{a}, \mathbf{b}, \mathbf{c}) \begin{pmatrix} P_{11} & P_{12} & P_{13} \\ P_{21} & P_{22} & P_{23} \\ P_{31} & P_{32} & P_{33} \end{pmatrix} \\ &= (P_{11}\mathbf{a} + P_{21}\mathbf{b} + P_{31}\mathbf{c}, P_{12}\mathbf{a} + P_{22}\mathbf{b} + P_{32}\mathbf{c}, P_{13}\mathbf{a} + P_{23}\mathbf{b} + P_{33}\mathbf{c}). \end{aligned} \quad (6.4)$$

The shift of the origin, *i.e.*,  $(0, 0, 0)$ , is defined with a shift vector  $\mathbf{t}$  as

$$\begin{aligned} \mathbf{t} &= (\mathbf{a}, \mathbf{b}, \mathbf{c})\mathbf{p} \\ &= (\mathbf{a}, \mathbf{b}, \mathbf{c}) \begin{pmatrix} p_1 \\ p_2 \\ p_3 \end{pmatrix} \\ &= p_1\mathbf{a} + p_2\mathbf{b} + p_3\mathbf{c}. \end{aligned} \quad (6.5)$$

Let  $\mathbf{A}$  be the representation matrix of primitive translation vectors,  $\mathbf{a}$ ,  $\mathbf{b}$ , and  $\mathbf{c}$ , on the basis of a set of orthonormal vectors,  $\mathbf{x}$ ,  $\mathbf{y}$ , and  $\mathbf{z}$ :

$$\mathbf{A} = (\mathbf{a}, \mathbf{b}, \mathbf{c}) = \begin{pmatrix} a_x & b_x & c_x \\ a_y & b_y & c_y \\ a_z & b_z & c_z \end{pmatrix}. \quad (6.6)$$

Then the transformation by Eq. (6.4) can be rewritten as

$$\mathbf{A}' = \mathbf{AP}. \quad (6.7)$$

Alternatively, the use of the metric tensor,  $\mathbf{G}$ , is often preferable to the direct use of  $\mathbf{A}$  owing to the unique definition of  $\mathbf{G}$ . On the other hand, the number of representations for  $\mathbf{A}$  is infinite because the orthonormal bases,  $\mathbf{x}$ ,  $\mathbf{y}$ , and  $\mathbf{z}$ , may be arbitrarily chosen. The metric tensor (matrix) of the direct lattice is defined as

$$\mathbf{G} = \mathbf{A}^t \mathbf{A} = \begin{pmatrix} \mathbf{a} \cdot \mathbf{a} & \mathbf{a} \cdot \mathbf{b} & \mathbf{a} \cdot \mathbf{c} \\ \mathbf{b} \cdot \mathbf{a} & \mathbf{b} \cdot \mathbf{b} & \mathbf{b} \cdot \mathbf{c} \\ \mathbf{c} \cdot \mathbf{a} & \mathbf{c} \cdot \mathbf{b} & \mathbf{c} \cdot \mathbf{c} \end{pmatrix} = \begin{pmatrix} a^2 & ab \cos \gamma & ac \cos \beta \\ ba \cos \gamma & b^2 & bc \cos \alpha \\ ca \cos \beta & cb \cos \alpha & c^2 \end{pmatrix}, \quad (6.8)$$

where  $t$  denotes transposition. Then,  $\mathbf{G}$  is transformed into  $\mathbf{G}'$  by

$$\mathbf{G}' = (\mathbf{A}')^t \mathbf{A}' = (\mathbf{AP})^t (\mathbf{AP}) = \mathbf{P}^t (\mathbf{A}^t \mathbf{A}) \mathbf{P} = \mathbf{P}^t \mathbf{GP}. \quad (6.9)$$

Similarly, the representation matrix of the reciprocal basis vectors  $\mathbf{a}^*$ ,  $\mathbf{b}^*$ , and  $\mathbf{c}^*$  is defined as

$$\mathbf{A}^* = (\mathbf{a}^*, \mathbf{b}^*, \mathbf{c}^*) = \begin{pmatrix} a_x^* & b_x^* & c_x^* \\ a_y^* & b_y^* & c_y^* \\ a_z^* & b_z^* & c_z^* \end{pmatrix}. \quad (6.10)$$

The direct and reciprocal basis vectors are related by

$$\mathbf{A}^* = (\mathbf{A}^{-1})^t = (\mathbf{A}^t)^{-1} \quad (6.11)$$

and

$$(\mathbf{A}^*)^t \mathbf{A} = \mathbf{A}(\mathbf{A}^*)^t = \mathbf{A}^* \mathbf{A}^t = \mathbf{A}^t \mathbf{A}^* = \mathbf{E}, \quad (6.12)$$

where  $\mathbf{E}$  is the identity matrix:

$$\mathbf{E} = \begin{pmatrix} 1 & 0 & 0 \\ 0 & 1 & 0 \\ 0 & 0 & 1 \end{pmatrix}. \quad (6.13)$$

The metric tensor of the reciprocal lattice is defined as

$$\mathbf{G}^* = (\mathbf{A}^*)^t \mathbf{A}^* = \begin{pmatrix} \mathbf{a}^* \cdot \mathbf{a}^* & \mathbf{a}^* \cdot \mathbf{b}^* & \mathbf{a}^* \cdot \mathbf{c}^* \\ \mathbf{b}^* \cdot \mathbf{a}^* & \mathbf{b}^* \cdot \mathbf{b}^* & \mathbf{b}^* \cdot \mathbf{c}^* \\ \mathbf{c}^* \cdot \mathbf{a}^* & \mathbf{c}^* \cdot \mathbf{b}^* & \mathbf{c}^* \cdot \mathbf{c}^* \end{pmatrix} = \begin{pmatrix} a^{*2} & a^* b^* \cos \gamma^* & a^* c^* \cos \beta^* \\ b^* a^* \cos \gamma^* & b^{*2} & b^* c^* \cos \alpha^* \\ c^* a^* \cos \beta^* & c^* b^* \cos \alpha^* & c^{*2} \end{pmatrix}. \quad (6.14)$$

The transformation of  $\mathbf{G}^*$  into  $\mathbf{G}^{*\prime}$  is represented by

$$\mathbf{G}^{*\prime} = (\mathbf{A}^{*\prime})^t \mathbf{A}^{*\prime} = (\mathbf{AP})^{-1} ((\mathbf{AP})^t)^{-1} = \mathbf{P}^{-1} ((\mathbf{A}^*)^t \mathbf{A}^*) (\mathbf{P}^{-1})^t = \mathbf{Q} \mathbf{G}^* \mathbf{Q}^t, \quad (6.15)$$

where  $\mathbf{Q} = \mathbf{P}^{-1}$ .

The coordinates  $x$ ,  $y$ , and  $z$  in the direct space are transformed by the  $4 \times 4$  transformation matrix  $\mathbb{Q}$  as

$$\begin{pmatrix} x' \\ y' \\ z' \\ 1 \end{pmatrix} = \mathbb{Q} \begin{pmatrix} x \\ y \\ z \\ 1 \end{pmatrix}, \quad (6.16)$$

where

$$\begin{aligned} \mathbb{Q} &= \begin{pmatrix} \mathbf{P}^{-1} & -\mathbf{P}^{-1} \mathbf{p} \\ \mathbf{o} & 1 \end{pmatrix} \\ &= \begin{pmatrix} \mathbf{Q} & \mathbf{q} \\ \mathbf{o} & 1 \end{pmatrix} \\ &= \begin{pmatrix} Q_{11} & Q_{12} & Q_{13} & q_1 \\ Q_{21} & Q_{22} & Q_{23} & q_2 \\ Q_{31} & Q_{32} & Q_{33} & q_3 \\ 0 & 0 & 0 & 1 \end{pmatrix} \\ &= \mathbb{P}^{-1}. \end{aligned} \quad (6.17)$$

In short, Eq. (6.16) can be expressed as:

$$\mathbf{X}' = \mathbb{Q} \mathbf{X}. \quad (6.18)$$

The  $4 \times 4$  symmetry operation matrix  $\mathbb{W}$  transforms the coordinates  $x$ ,  $y$ , and  $z$ , of point  $\mathbf{X}$  to

a symmetrically equivalent point  $\tilde{\mathbf{X}}$  with the coordinates,  $\tilde{x}$ ,  $\tilde{y}$ , and  $\tilde{z}$ , by

$$\begin{aligned} \begin{pmatrix} \tilde{x} \\ \tilde{y} \\ \tilde{z} \\ 1 \end{pmatrix} &= \begin{pmatrix} W_{11} & W_{12} & W_{13} & w_1 \\ W_{21} & W_{22} & W_{23} & w_2 \\ W_{31} & W_{32} & W_{33} & w_3 \\ 0 & 0 & 0 & 1 \end{pmatrix} \begin{pmatrix} x \\ y \\ z \\ 1 \end{pmatrix} \\ &= \begin{pmatrix} W_{11}x + W_{12}y + W_{13}z + w_1 \\ W_{21}x + W_{22}y + W_{23}z + w_2 \\ W_{31}x + W_{32}y + W_{33}z + w_3 \\ 1 \end{pmatrix}, \end{aligned} \quad (6.19)$$

or in short notation,

$$\tilde{\mathbf{X}} = \mathbb{W}\mathbf{X}. \quad (6.20)$$

The matrix  $\mathbb{Q}$  transforms both  $\mathbf{X}$  and  $\tilde{\mathbf{X}}$  to  $\mathbf{X}'$  and  $\tilde{\mathbf{X}}'$ , respectively:

$$\tilde{\mathbf{X}}' = \mathbb{W}'\mathbf{X}', \quad (6.21)$$

$$\mathbb{Q}\mathbb{W}\mathbf{X} = \mathbb{W}'\mathbb{Q}\mathbf{X}. \quad (6.22)$$

Then, the symmetry operation  $\mathbb{W}$  is transformed with the relation

$$\mathbb{W}' = \mathbb{Q}\mathbb{W}\mathbb{P}. \quad (6.23)$$

Let  $\mathbf{Q}^t$  be the transposed matrix of  $\mathbf{Q}$  defined in Eq. (6.17). Then, anisotropic atomic displacement parameters,  $\beta$ , are transformed by

$$\begin{aligned} \beta' &= \begin{pmatrix} \beta'_{11} & \beta'_{12} & \beta'_{13} \\ \beta'_{12} & \beta'_{22} & \beta'_{23} \\ \beta'_{13} & \beta'_{23} & \beta'_{33} \end{pmatrix} \\ &= \begin{pmatrix} Q_{11} & Q_{12} & Q_{13} \\ Q_{21} & Q_{22} & Q_{23} \\ Q_{31} & Q_{32} & Q_{33} \end{pmatrix} \begin{pmatrix} \beta_{11} & \beta_{12} & \beta_{13} \\ \beta_{12} & \beta_{22} & \beta_{23} \\ \beta_{13} & \beta_{23} & \beta_{33} \end{pmatrix} \begin{pmatrix} Q_{11} & Q_{21} & Q_{31} \\ Q_{12} & Q_{22} & Q_{32} \\ Q_{13} & Q_{23} & Q_{33} \end{pmatrix} \\ &= \mathbf{Q}\beta\mathbf{Q}^t. \end{aligned} \quad (6.24)$$

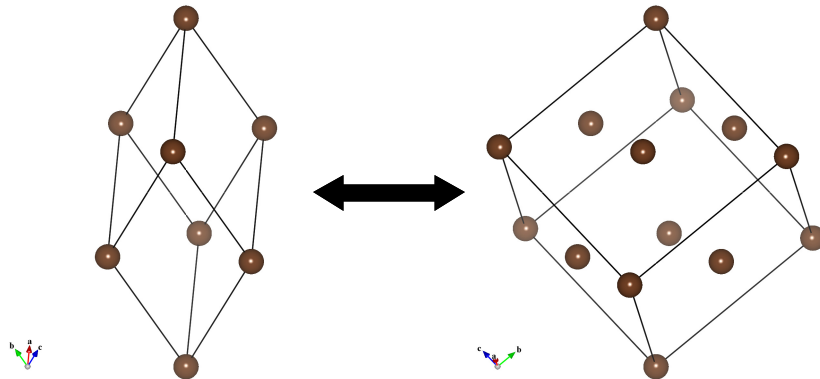


Figure 6.6: An example of lattice transformation between primitive and face-centered-cubic lattices.

## Creation of superstructures and substructures

The transformation matrix is also used to convert (primitive lattice) $\rightleftharpoons$ (complex lattice) (**Fig. 6.6**), and to create superstructures and averaged substructures. To convert a structure, you have to select mode **Update structure parameters to keep 3D geometry** in the Unit cell tab of the **Edit Data** dialog box before opening the **Unit Cell Transformation** dialog box.

When the determinant of  $\mathbf{P}$ ,  $\det(\mathbf{P})$  is larger than 1, the transformed unit-cell becomes larger than the original one, and when  $\det(\mathbf{P})$  is smaller than 1, the transformed unit-cell becomes smaller than the original one. In such cases, a dialog box appears to confirm whether you intend to change the unit cell volume (**Fig. 6.7**).

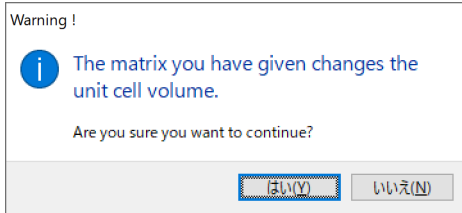


Figure 6.7: A dialog box for confirmation of unit cell transformation.

When a rotation matrix with  $\det(\mathbf{P}) > 1$  is specified, or the transformed unit cell contains additional lattice points even when  $\det(\mathbf{P}) = 1$ , a dialog box appears to ask you how to convert the structure (**Fig. 6.8**). There are the following three options:

- “Add new equivalent positions to a list of symmetry operations”
- “Search atoms in the new unit cell and add them as new sites”
- “Do nothing”

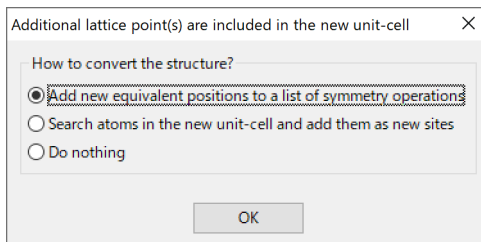


Figure 6.8: A dialog box showing options for how to create a larger unit cell.

In the first and second options, the structural geometry of the original data will remain unchanged. On the other hand, on selection of the third option, some atoms in the new unit cell will be missing. On selection of the first option, a superstructure will be created by examining the following equation to find additional symmetry operations  $\mathbb{W}'$  having a translational component in between  $(0, 0, 0)$  and  $(1, 1, 1)$ :

$$\mathbb{W}' = \begin{pmatrix} W'_{11} & W'_{12} & W'_{13} & w'_1 \\ W'_{21} & W'_{22} & W'_{23} & w'_2 \\ W'_{31} & W'_{32} & W'_{33} & w'_3 \\ 0 & 0 & 0 & 1 \end{pmatrix} = \mathbb{Q} \begin{pmatrix} W_{11} & W_{12} & W_{13} & w_1 + n_x \\ W_{21} & W_{22} & W_{23} & w_2 + n_y \\ W_{31} & W_{32} & W_{33} & w_3 + n_z \\ 0 & 0 & 0 & 1 \end{pmatrix} \mathbb{P}, \quad (6.25)$$

$(n_x, n_y, n_z = 0, \pm 1, \pm 2, \dots).$

On selection of the second option, a superstructure will be created by examining the following equation to find additional sites lying in between  $(0, 0, 0)$  and  $(1, 1, 1)$ :

$$\begin{pmatrix} x' \\ y' \\ z' \\ 1 \end{pmatrix} = \mathbb{Q} \begin{pmatrix} x + n_x \\ y + n_y \\ z + n_z \\ 1 \end{pmatrix}. \quad (n_x, n_y, n_z = 0, \pm 1, \pm 2, \dots) \quad (6.26)$$

Note that the transformed new unit-cell should be symmetrically consistent with the space group currently in use. Otherwise, reduce symmetry to  $P1$  by clicking [Remove symmetry] before creating a superstructure, and input a new space group after the superstructure has been created. If  $\det(\mathbf{P}) < 1$ , the same position may result from two or more sites. In such a case, the redundant sites can be removed by clicking [Remove duplicate atoms] button in the Structure parameters tab (see page 48).

### 6.2.7 Magnetic Structures

VESTA fully supports 1651 magnetic space groups. Check the “Magnetic structure” check box to use magnetic space groups. Then, the title of the Setting list box changes to BNS Setting, which shows a list of magnetic space groups for a selected space group. There are two types of notations of magnetic space groups: the Belov–Neronova–Smirnova (BNS) notation [51] and the Opechowski–Guccione (OG) notation [52]. VESTA uses the BNS notation because symmetry operations of the BNS notation are described with respect to the magnetic unit-cell with translational parts never exceeding 1. Atomic coordinates, displacement parameters, and occupancies of a magnetic structure are specified exactly the same way as conventional structure (see Section 6.3). Magnetic moments of atoms are specified in the Vectors dialog box (see Section 9.1).

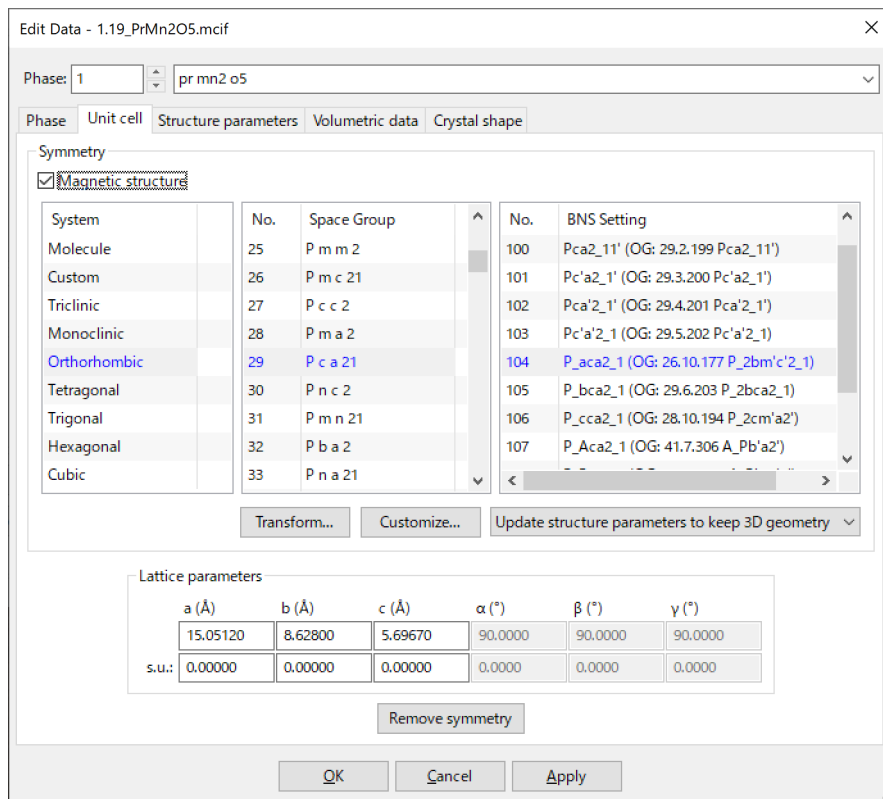


Figure 6.9: The Unit cell page in the Edit Data dialog box, with the “Magnetic structure” option checked.

### 6.3 Structure Parameters

The Structure parameters tab in the Edit Data dialog box (**Fig. 6.10**) is used to input and edit parameters related to atomistic structures. The following structural information is input or edited by using text boxes at the upper half of the page:

- {Symbol...}: Symbol of an element (up to two characters).
- {Label}: Site name (up to six characters).
- {Charge}: Formal charge (oxidation number; optional)
- {x}, {y}, and {z}: Fractional coordinates,  $x$ ,  $y$ , and  $z$  (dimensionless).
- {s.u.(x)}, {s.u.(y)}, and {s.u.(z)}: Standard uncertainties of the fractional coordinates (default values: zero).
- {Occ}: Occupancy (dimensionless; optional).
- {B} or {U}: Isotropic atomic displacement parameter,  $B$  or  $U$  (in  $\text{\AA}^2$ ; optional).
- {U11}, {U22}, {U33}, {U12}, {U13}, and {U23}: Anisotropic atomic displacement parameters,  $U_{ij}$  (in  $\text{\AA}^2$ , optional).
- {beta11}, {beta22}, {beta33}, {beta12}, {beta13}, and {beta23}: Anisotropic atomic displacement parameters,  $\beta_{ij}$  (dimensionless; optional).

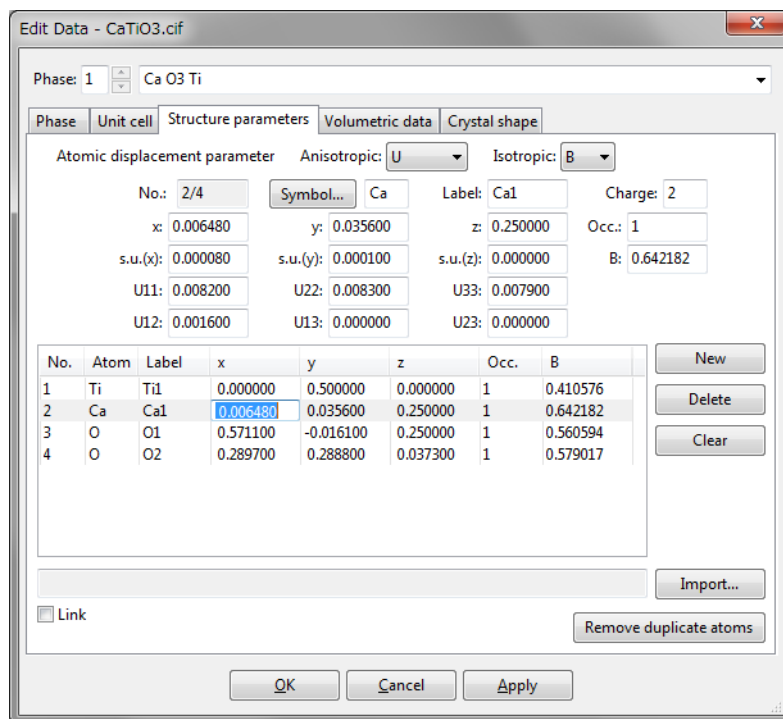


Figure 6.10: Structure parameter page in the Edit Data dialog box.

A list of sites in the asymmetric unit is shown at the lower half of the page. Text boxes are disabled when no site is selected in the list. When an item in the list is selected, the text boxes are updated to show data relevant to the selected site. In-place editing of a list item is also supported, as **Fig. 6.10** shows.

To add a new site, click the [New] button at first, and edit texts in the text boxes. A modification in a text box is applied to the selected site immediately after the focus (caret) has moved to another text box or another GUI control. In the case of text boxes for numerical values, modifications will be discarded if an input text is not a valid numerical value, or if the text box is empty. Therefore, if you have accidentally changed a value in a text box, the original value can be restored by erasing the entire text in the text box before moving the focus to another GUI control.

To delete a site, select an item in the list, and click the [Delete] button or press the <Delete> key. Clicking the [Clear] button will delete all the sites in the list.

### 6.3.1 Symbols and Labels

Up to two characters are input as an element symbol while up to nine characters are input as a label of a site. Click the [Symbol...] button to select an element symbol from the Periodic Table dialog box (**Fig. 6.11**).



Figure 6.11: Periodic Table dialog box.

### 6.3.2 Formal charge

Strictly speaking, formal charges are not structure parameters. They are, however, used to estimate a bond length from a bond valence parameter [38, 39, 40] (see 11.4.3), evaluate charge distribution from bond lengths [35, 36, 37] (see 11.4.3), and calculate electrostatic site potentials and a Madelung energy by the Fourier method (see 14.5).

### 6.3.3 Fractional coordinates

For special positions, input fractional numbers, *e.g.*, 1/4, 1/2, and 1/3, or a sufficient number of digits should be given, *e.g.*, 0.333333 and 0.666667.

When displacement ellipsoids are drawn from anisotropic atomic displacement parameters refined with RIETAN-FP [12], fractional coordinates corresponding to the first equivalent position described in *International Tables for Crystallography*, volume A [30] for each Wyckoff position have to be entered. For example, input not (1/2, 0, *z*) but (0, 1/2, *z*) for a 4*i* site in space group *P*4/*mmm* (No. 123).

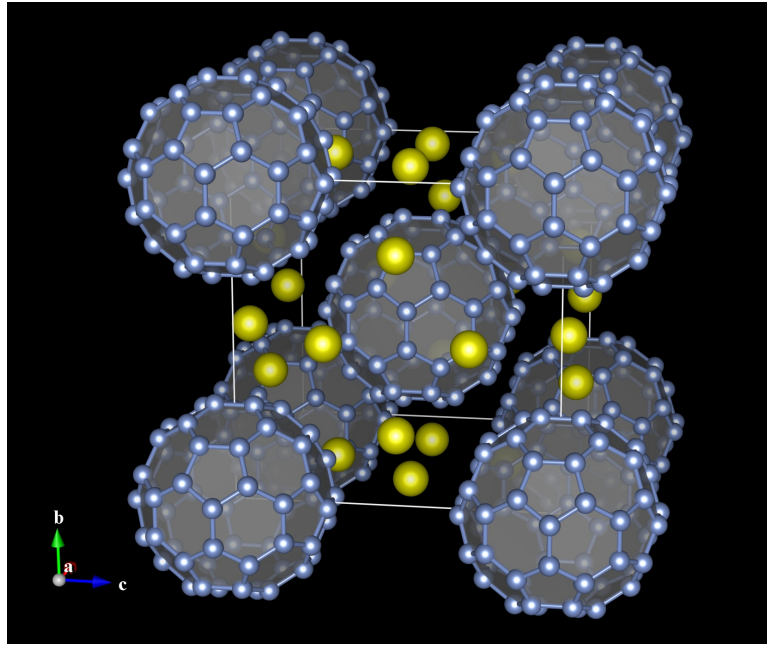


Figure 6.12: Crystal structure of  $\text{Cs}_6\text{C}_{60}$  [53], with  $\text{C}_{60}$  represented by translucent polyhedra. A virtual site X with an occupancy of  $g = 0$  was added at the center of  $\text{C}_{60}$ . Polyhedra of  $\text{C}_{60}$  were created by specifying X–C bonds in the **Bonds** dialog box. C–C bonds are also searched by a “Search molecules” mode to represent polyhedral edges by solid cylinders. See chapter 8 for details in creating bonds and polyhedra.

### 6.3.4 Occupancy

The occupancy is unity for full occupation and zero for virtual sites. If the occupancy of a site is less than unity, atoms occupying there are displayed as circle graphs for occupancies. If unicolor balls are preferred to bicolor ones, change the occupancy to unity for convenience.

If the occupancy of a site is zero, the site is treated as a virtual site that is not occupied by any atoms in the real structure. Neither the virtual sites nor bonds connecting them are displayed on the screen. Virtual sites are used to visualize, for example, cage structures of porous crystals as solid polyhedra without creating a large number of unnecessary bonds (Fig. 6.12).

### 6.3.5 Atomic displacement parameters

The Debye–Waller factor,  $T_j(\mathbf{h})$ , which is often referred to as the temperature factor, is included in formulae for structure factors,  $F(\mathbf{h})$ , to represent the effect of static and dynamic displacement of atom  $j$  (see Eqs. 14.8 and 14.11). The displacement of atom is formulated in two different ways: anisotropic and isotropic atomic displacement.

#### Anisotropic models

The anisotropic Debye–Waller factor,  $T(\mathbf{h})$ , is defined as

$$\begin{aligned} T(\mathbf{h}) &= \exp \left[ -2\pi^2 (h^2 a^{*2} U_{11} + k^2 b^{*2} U_{22} + l^2 c^{*2} U_{33} + 2hka^*b^*U_{12} + 2hla^*c^*U_{13} + 2klb^*c^*U_{23}) \right] \\ &= \exp \left[ - (h^2 \beta_{11} + k^2 \beta_{22} + l^2 \beta_{33} + 2hk\beta_{12} + 2hl\beta_{13} + 2kl\beta_{23}) \right], \end{aligned} \quad (6.27)$$

where  $a^*, b^*, c^*, \alpha^*, \beta^*$ , and  $\gamma^*$  are reciprocal lattice parameters.

The type of anisotropic atomic displacement parameters must be specified in list box {Anisotropic}: ‘None’ to omit anisotropic atomic displacement parameters, ‘U’ to input  $U_{ij}$  ( $U_{11}, U_{22}, U_{33}, U_{12}, U_{13}$ , and  $U_{23}$ ), and ‘beta’ to input  $\beta_{ij}$  ( $\beta_{11}, \beta_{22}, \beta_{33}, \beta_{12}, \beta_{13}$ , and  $\beta_{23}$ ). Using this list box, we can convert  $U_{ij}$  into  $\beta_{ij}$  and *vice versa*.

Anisotropic atomic displacement parameters defined in different ways must be converted into  $U_{ij}$  or  $\beta_{ij}$  defined above.

On refinement of  $\beta_{ij}$ ’s by the Rietveld method with RIETAN-FP [12],  $\beta_{ij}$ ’s for each site have to satisfy linear constraints imposed on them [54, 55].

### Isotropic models

The isotropic Debye–Waller factor,  $T(\mathbf{h})$ , is given by

$$\begin{aligned} T(\mathbf{h}) &= \exp \left[ -B \left( \frac{\sin \theta}{\lambda} \right)^2 \right] \\ &= \exp \left( -\frac{B}{4d^2} \right) \\ &= \exp \left( -\frac{2\pi^2 U}{d^2} \right), \end{aligned} \tag{6.28}$$

where  $B$  and  $U$  are the isotropic atomic displacement parameters ( $U = B/8\pi^2$ ),  $\theta$  is the Bragg angle,  $\lambda$  is the X-ray or neutron wavelength, and  $d$  is the lattice-plane spacing.  $B$  and  $U$  are related to the mean square displacement,  $\langle u^2 \rangle$ , along the direction perpendicular to the reflection plane with

$$B = 8\pi^2 U = 8\pi^2 \langle u^2 \rangle. \tag{6.29}$$

For example, a  $B$  value of  $3 \text{ \AA}^2$  corresponds to a displacement of about  $0.2 \text{ \AA}$ .

The type of isotropic atomic displacement parameters must be specified in list box {Isotropic}. Using this list box, we can convert  $U$  into  $B$  and *vice versa*.

Isotropic atomic displacement parameters defined in different ways must be converted into  $B$  or  $U$  defined above.

In crystallographic sites for which anisotropic atomic displacement parameters,  $U_{ij}$  or  $\beta_{ij}$ , have been input, equivalent isotropic atomic displacement parameters,  $B_{\text{eq}}$  or  $U_{\text{eq}}$ , are calculated from  $U_{ij}$ ,  $a^*$ ,  $b^*$ ,  $c^*$ , and the metric tensor  $\mathbf{G}$  [56, 57]:

$$B_{\text{eq}} = 8\pi^2 U_{\text{eq}} \tag{6.30}$$

with

$$\begin{aligned} U_{\text{eq}} &= \frac{1}{3} \sum_i \sum_j U_{ij} a_i^* a_j^* \mathbf{a}_i \cdot \mathbf{a}_j \\ &= \frac{1}{3} [U_{11} (aa^*)^2 + U_{22} (bb^*)^2 + U_{33} (cc^*)^2 \\ &\quad + 2U_{12} a^* b^* ab \cos \gamma + 2U_{13} a^* c^* ac \cos \beta + 2U_{23} b^* c^* bc \cos \alpha]. \end{aligned} \tag{6.31}$$

$B_{\text{eq}}$  and  $U_{\text{eq}}$  are regarded as  $B$  and  $U$  in the Structure parameters tab of the Edit Data dialog box after reopening it.

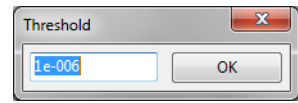
#### 6.3.6 Importing structure parameters

Structure parameters can be imported from a file storing structure parameters by clicking the [Import...] button at the bottom right of the Structure parameters page. Then, select a file with a format supported by VESTA in the file selection dialog box.

Option “Link” specifies the manner of outputting current structure data in a file, \*.vesta, with the VESTA format. Structure data are usually recorded in \*.vesta. On the other hand, for volumetric data, relative paths (including a file name) of data files are recorded in \*.vesta instead of recording the volumetric data directly in it. When option “Link” is checked, structural data are also recorded as the relative path of the data file. Then, even if the structural-data file is changed after saving \*.vesta, the changes are reflected in VESTA when \*.vesta is reopened. This option is useful in preparing a file, \*.vesta, with the VESTA format as a template file for setting objects and overall appearances. This option disables text boxes and list boxes in the **Structure parameters** tab to prohibit users from editing structure data because any modifications to structure data will not be saved to a file when this option is enabled.

### 6.3.7 Removing duplicate atoms

When the space group is changed to that with higher symmetry, or when the unit cell is transformed to a smaller one (see 6.2.6), the same atomic position may result from two or more sites. In such a case, the redundant sites can be removed by clicking the [Remove duplicate atoms] button. Then, a dialog box (right figure) opens, prompting you to input a threshold of distances between two atoms to be regarded as a single site. The threshold value is input in the unit of Å. Increasing the threshold value enables us, for example, to extract an average structure from a large cell calculated by computational simulations.



## 6.4 Volumetric Data

To input volumetric data for drawing isosurfaces with or without surface coloring, click the **Volumetric data** tab in the Edit Data dialog box (Fig. 6.13):

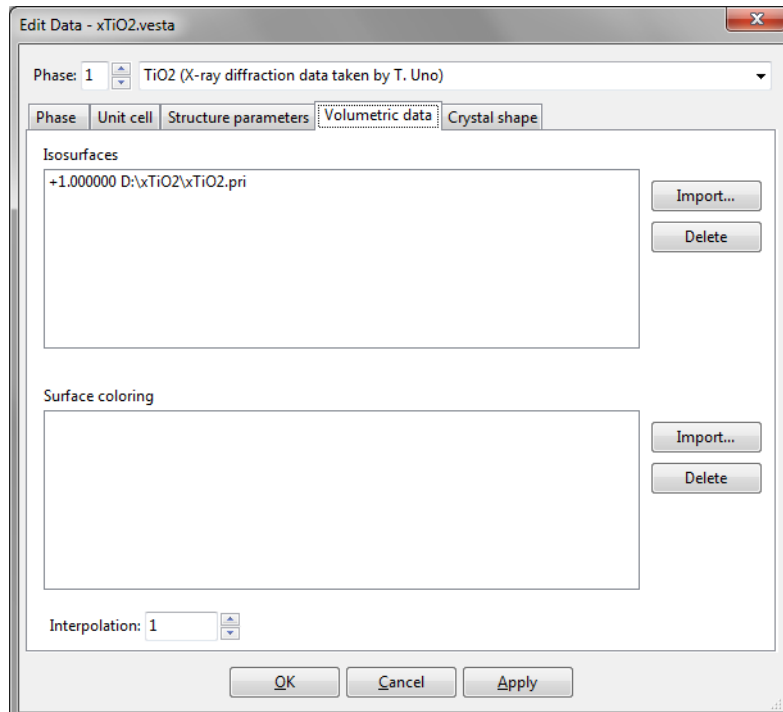


Figure 6.13: Volumetric data page in the Edit Data dialog box.

#### 6.4.1 Volumetric data to draw isosurfaces

VESTA enables us to deal with more than two volumetric data sets. Click [Import...] to select a file in the file selection dialog box. Only files with extensions of supported formats are visible in the file selection dialog box. After selecting a volumetric data file, a Choose operations dialog box appears (**Fig. 6.14**).

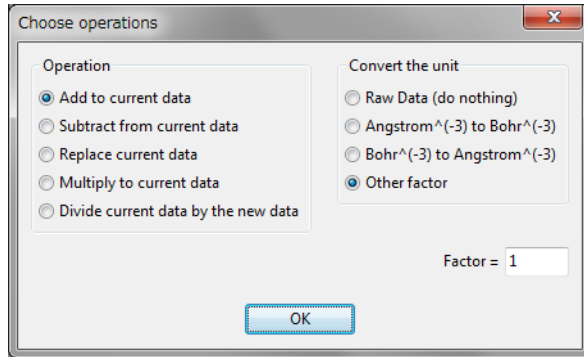


Figure 6.14: A dialog box to choose operations for volumetric data.

#### Operation

In the Operation radio box, one of the following five data operations can be selected in addition to conversion of data units.

- “Add to current data”
- “Subtract from current data”
- “Replace current data”
- “Multiply to current data”
- “Divide current data by new data”

“Multiply to current data” is convenient when squaring wave functions to obtain electron densities (existing probabilities for electrons). The last two options are not displayed when no volumetric data are contained in the current data. In such a case, the first and third options have also the same effect.

#### Convert the unit

In the Convert the unit radio box, the unit of data can be converted from Å<sup>-3</sup> to bohr<sup>-3</sup>, and *vice versa*. Select option “Other factor” to multiply the data by an arbitrary factor. Then, click [OK] to import data. Repeating the above procedures allows you to import multiple data, as exemplified in **Fig. 6.15**.

#### 6.4.2 Volumetric data for surface coloring

Volumetric data for surface coloring can be imported in the same manner as with data for isosurfaces. A typical application of surface coloring is to color isosurfaces of electron densities according to electrostatic potentials.

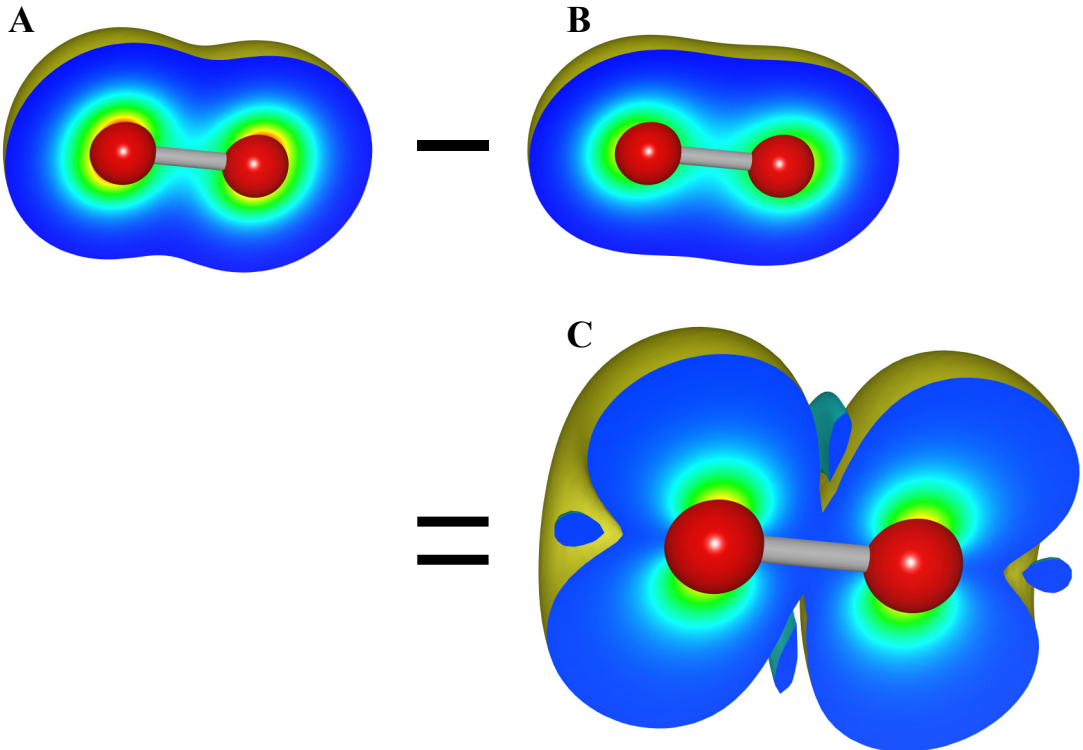


Figure 6.15: Distributions of electron densities and effective spin densities in an  $\text{O}_2$  molecule. (A) up-spin electron densities,  $\rho_\uparrow$ , (B) down-spin electron densities,  $\rho_\downarrow$ , and (C) effective spin densities,  $\Delta\rho = \rho_\uparrow - \rho_\downarrow$ , calculated with VESTA. Both  $\rho_\uparrow$  and  $\rho_\downarrow$  were calculated with DVSCAT [58]. Isosurface levels were set at  $0.01a_0^{-3}$  in (A) and (B), and at  $0.001a_0^{-3}$  in (C). where  $a_0$  is the Bohr radius.

### Interpolation

The spacial resolution of volumetric data can be increased using the algorithm of cubic spline interpolation. The interpolation level is specified in the {Interpolation} text box.

## 6.5 Crystal Shape

The Crystal Shape tab in the Edit Data dialog box (Fig. 6.16) is used to input and edit the external morphology of crystals. To add a new crystal face, click the [New] button at first, input Miller indices  $hkl$ , and the distance from the origin,  $(0, 0, 0)$ . The distance may be specified in the unit of either its lattice-plane spacing,  $d$ , or Å. The color and opacity of the face are specified either as four integers ranging from 0 to 255, or using a color selection dialog box and a slider, which are opened after clicking the square buttons on the right side of the text boxes. When option “Apply symmetry operations” is checked, all the symmetrically equivalent faces are automatically generated.

To delete a face, select an item in the list, and click the [Delete] button or press the <Delete> key. Clicking the [Clear] button will delete all the faces in the list.

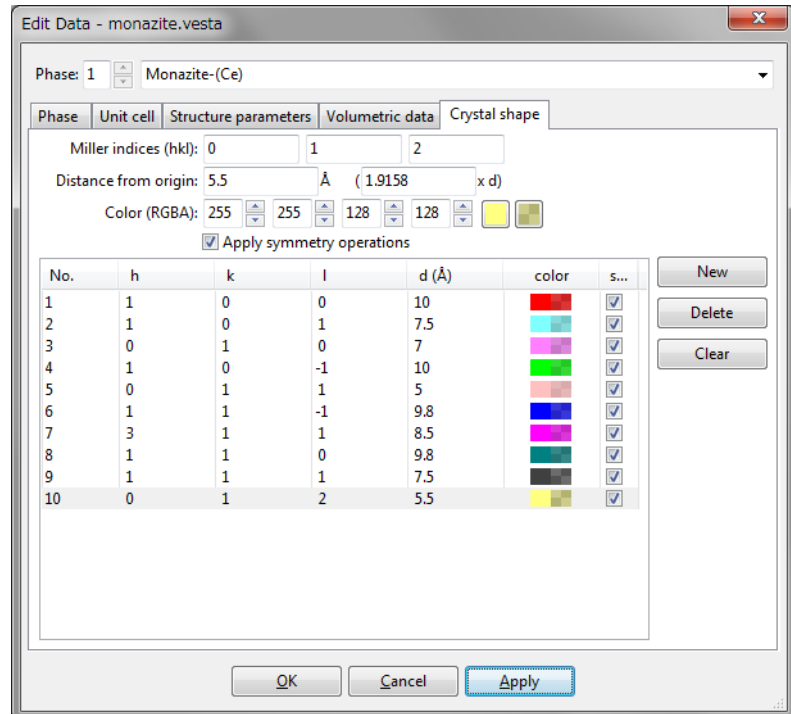


Figure 6.16: Crystal shape page in the Edit Data dialog box.

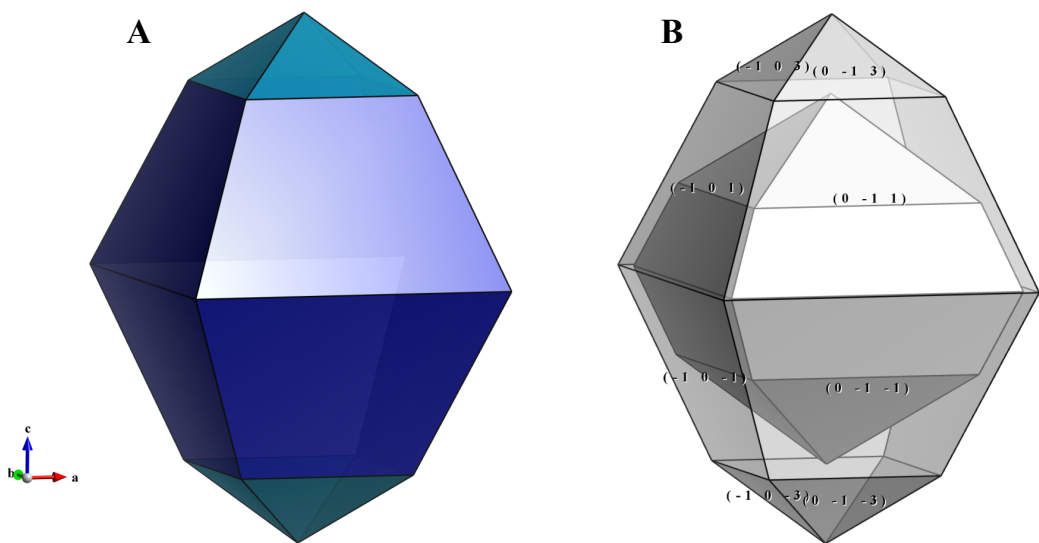


Figure 6.17: Crystal morphologies of anatase-type  $\text{TiO}_2$  crystals. In the inner crystal in (B), distances from the origin are set at 3.5 Å for both {101} and {103}. In the outer crystal, distances from the origin are set at 3.8 Å for {101} and 5 Å for {103}.

### 6.5.1 Examples

**Figure 6.17** shows morphologies of anatase-type  $\text{TiO}_2$  crystals composed of  $\{101\}$  and  $\{103\}$  faces. To visualize crystal morphologies, make sure that specified faces compose a closed polyhedron. For example, if only  $\{100\}$  is specified for a tetragonal crystal, it has to form a prismatic shape having an infinite length along the  $c$  axis. In this case, no objects are visible in the Graphics Area.

To adjust relative sizes of faces, edit the distance from the origin to the face. In general, the relative area of the face decreases with increasing distance as **Fig. 6.17B** illustrates. When the distance of  $\{103\}$  faces is set at a larger value of 5 Å, these faces become smaller with respect to  $\{101\}$  faces. The origin of the crystal shape is just the same as that of a structural model, *i.e.*, a position with the fractional coordinate of  $(0, 0, 0)$  is placed at the center of the crystal shape.

When option “Apply symmetry operations” is unchecked, faces that do not follow space-group symmetry may be inserted (**Fig. 6.19A**). If multiple faces with the same indices are specified, the face with the smallest distance from the origin is visible (**Fig. 6.19B, C**). These features make it possible to represent crystal habits of real crystals.

To display indices of faces as demonstrated in **Fig. 6.17B**, select the Objects tab in the Side Panel (**Fig. 6.18, a**), choose “Shape” in the list of phases at the upper half of the page (**Fig. 6.18, b**), and then click check boxes labeled as “L” (**Fig. 6.18, c**). See also section 12.2 for the function of the Objects tab.

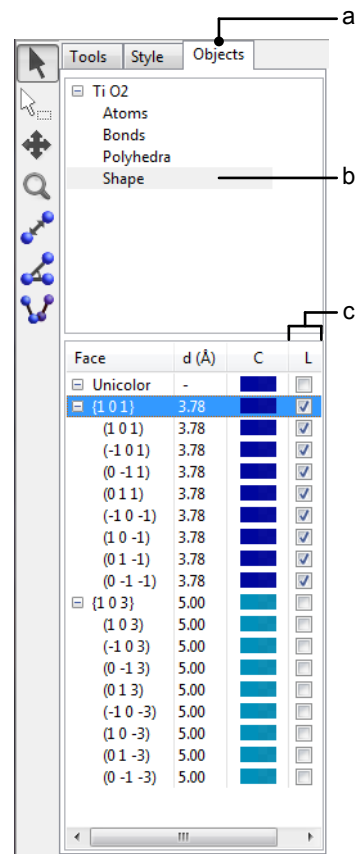


Figure 6.18: The Objects tab of the Side Panel showing a list of crystallographic faces.

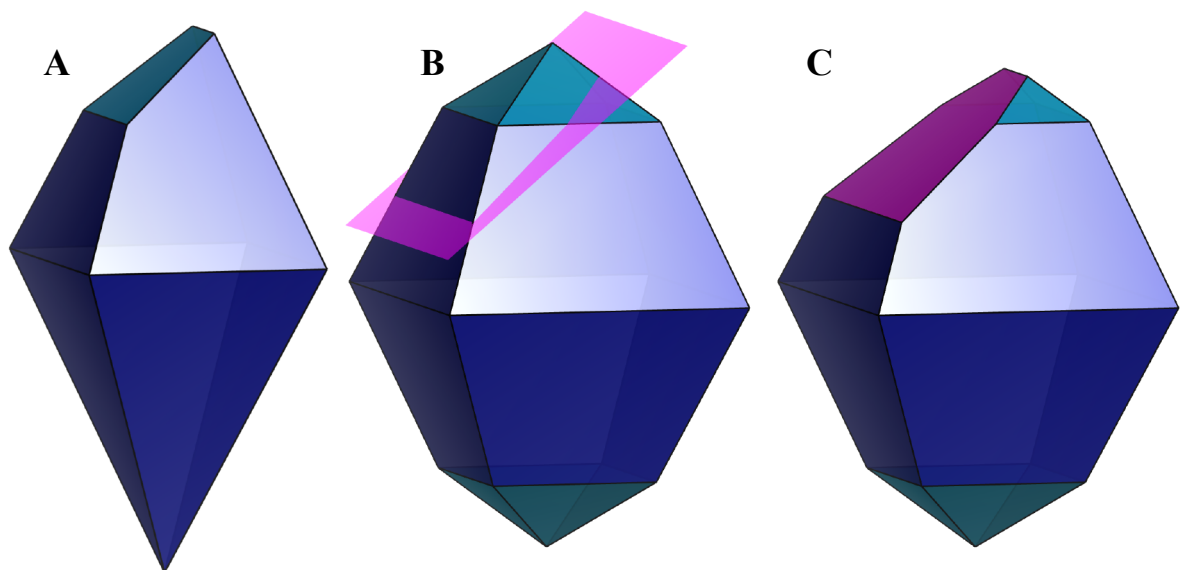


Figure 6.19: Crystal morphologies of anatase having faces that do not follow symmetry operations. (A) Option “Apply symmetry operations” is unchecked for a  $(\bar{1}03)$  face. (B) The distance from the origin was set at 3.8 Å for  $\{101\}$  and 5 Å for  $\{103\}$ , and a  $(\bar{1}03)$  lattice plane was inserted by setting a distance from the origin at 3.8 Å. (C) A  $(\bar{1}03)$  face, which overlaps with the  $(\bar{1}03)$  lattice plane in (B), was further added.

# Chapter 7

## OVERLAYING MULTIPLE DATA

To display multiple-phase data in a single Graphics Area, set positioning and orientation of each phase after clicking the Phase tab in the Edit Data dialog box (Fig. 7.1). The positioning and orientation of a phase are specified relative to another phase or the Cartesian coordinate system that is commonly used as internal representation of all phases. By default, the origin,  $(0, 0, 0)$ , of a phase is placed at that of the internal coordinate system. The orientation of a phase is set such that the  $[1\ 0\ 0]$  axis of a phase is parallel to the  $x$  axis of the internal coordinate system with the  $[0\ 1\ 0]$  axis parallel to the  $x-y$  plane.

To avoid the circular reference of phases, positioning and orientation must be set in descending order of the phase list.

### 7.1 Positioning of Phases

At first, select a phase to edit in the phase list (Fig. 7.1, a). In the Positioning frame box, select another phase (layer) which is used as a reference of positioning (Fig. 7.1, b). Layer 0 denotes

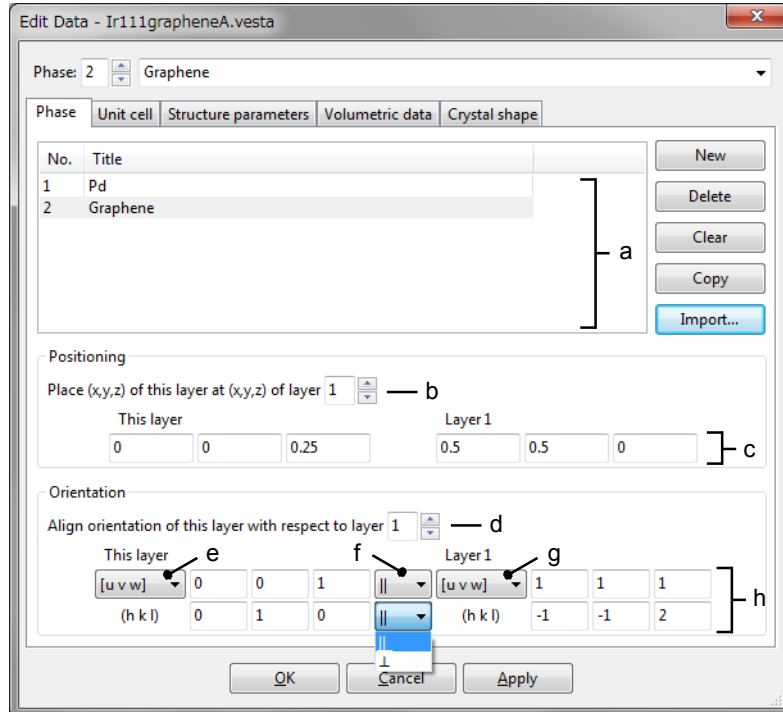


Figure 7.1: Phase page in the Edit Data dialog box.

the internal Cartesian coordinate system. Then, input  $(x, y, z)$  coordinates of the selected and reference layers; they are exactly overlapped with each other (**Fig. 7.1, c**).

## 7.2 Relative Orientation of Phases

Select a phase to edit in the phase list, and select ID's of another phase (layer) in the Orientation frame box (**Fig. 7.1, d**). As described above, layer 0 represents the internal Cartesian coordinate system. A set of a lattice vector and a reciprocal-lattice vector is specified for both of the current and reference layers. When the first vector is specified by a vector,  $[u \ v \ w]$ , in the direct space, the other one is specified by a reciprocal-lattice vector,  $[h \ k \ l]^*$ , and *vise versa*. The direct- and reciprocal-lattice vectors must be perpendicular to each other; in other words, the lattice vector,  $[u \ v \ w]$ , must be parallel to the lattice plane,  $(h \ k \ l)$ . Thus, the following condition must be satisfied:

$$hu + kv + lw = 0. \quad (7.1)$$

The type of the first vector is set by a pull down menu (**Fig. 7.1, d, g**). If a vector of the current layer is parallel to that of the reference layer, select  $\parallel$  in the pull down menu (**Fig. 7.1, f**). If the two vectors are perpendicular to each other, select  $\perp$  in the pull down menu. Then input indices in text boxes (**Fig. 7.1, h**).

## 7.3 Examples

**Figure 7.2** shows two kinds of organic molecules approaching a surface of calcite-type  $\text{CaCO}_3$ . **Figure 7.3** illustrates graphene on a (111) surface of Ir [59]. An example of overlaying isostuctural crystals is displayed in **Fig. 7.4**.

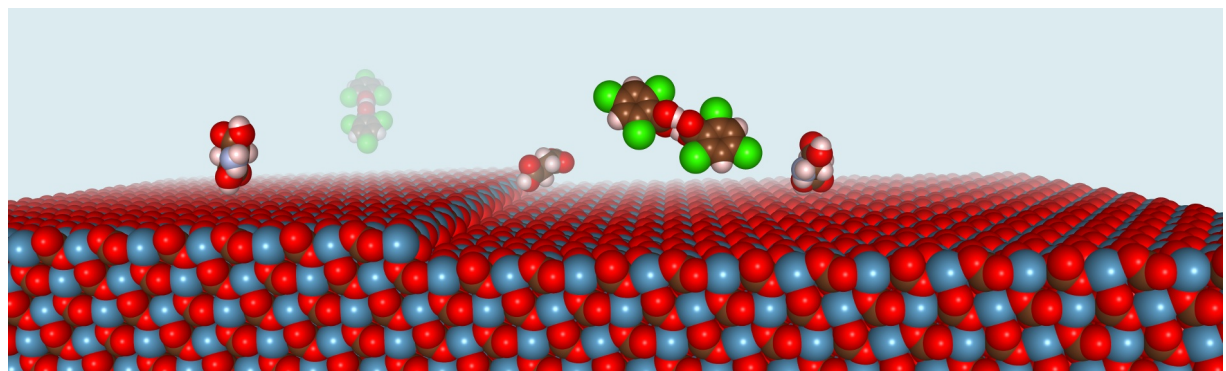


Figure 7.2: Molecules of L-aspartic acid and 2,4,6-trichlorobenzoic acid near a  $(10\bar{1}4)$  surface of calcite ( $\text{CaCO}_3$ ) having a  $[44\bar{1}]$  step.

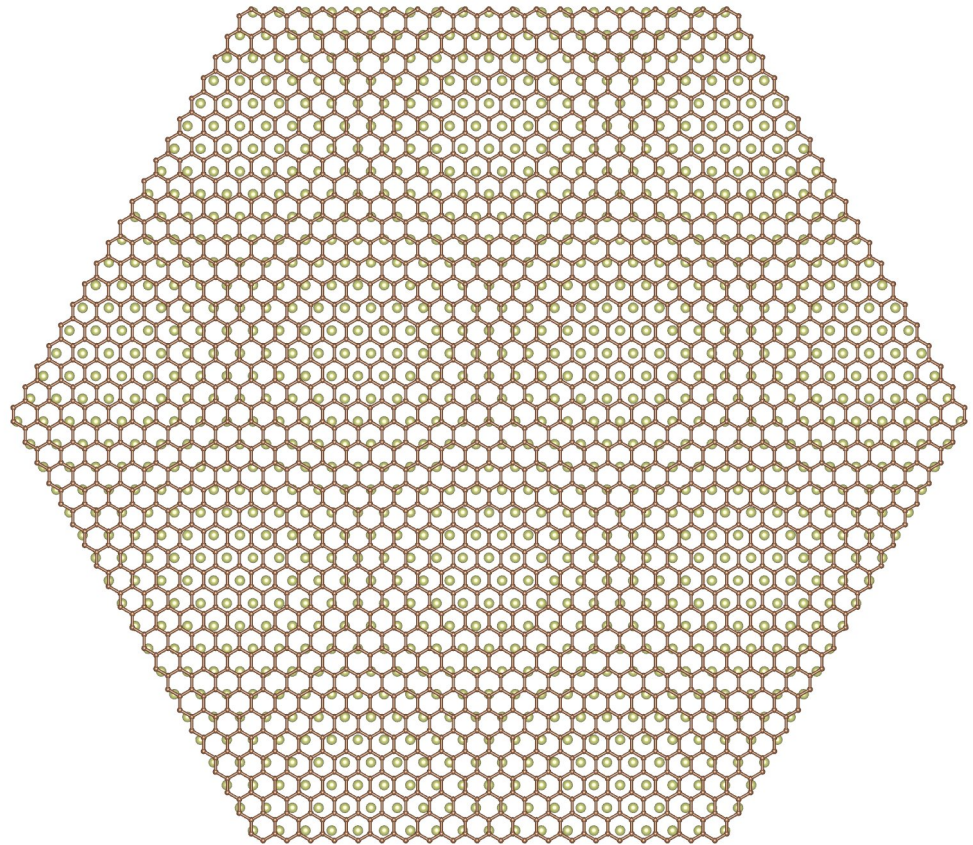


Figure 7.3: A moire pattern of graphene on the (111) surface of Ir.

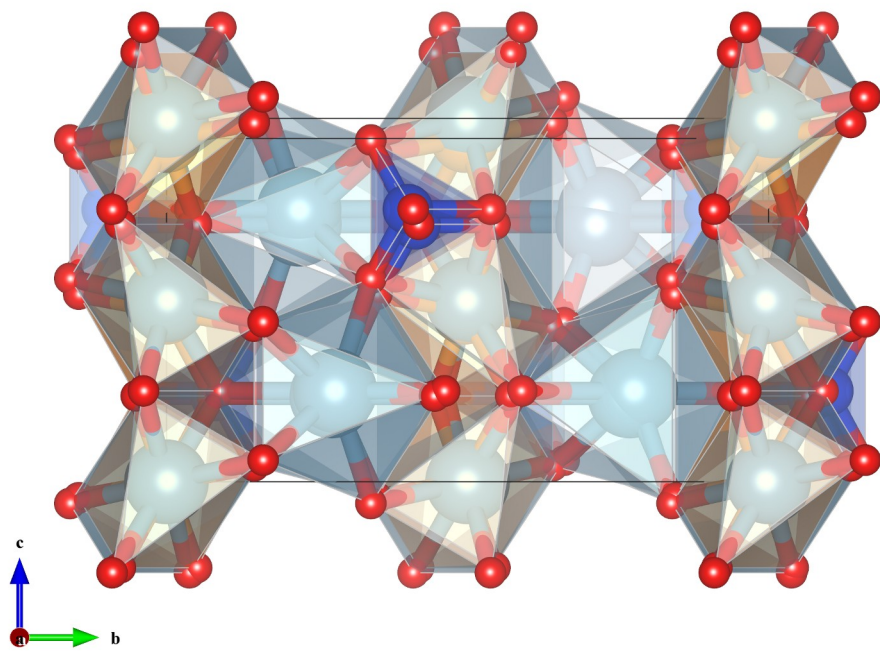


Figure 7.4: Crystal structures of Ca-olivine ( $\text{Ca}_2\text{SiO}_4$ ) and isostructural monticellite ( $\text{CaMgSiO}_4$ ) overlapped with each other.

# Chapter 8

## CREATING BONDS AND POLYHEDRA

To search for bonds and atoms connected by them, and to create coordination polyhedra, choose the “Edit” menu  $\Rightarrow$  “Bonds...”. At the top of the Bonds dialog box (Fig. 8.1), select a phase to edit. A list of bond specifications is shown at the lower half of the dialog box. GUI controls in the Search bonds and atoms frame box are used to edit a bond specification. They are disabled when no bond specification is selected in the list.

To add a new bond specification, click the [New] button at first, select atoms relevant to the bond, and edit minimum and maximum lengths. Modifications in the GUI control are applied to the list either immediately or after the focus (caret) has moved from a text box to another GUI control. To delete a bond specification, select it in the list, and then click the [Delete] button or press the <Delete> key. Clicking the [Clear] button deletes all the bond specifications in the list. Press the [OK] or [Apply] button to reflect editing results in the Graphics Area.

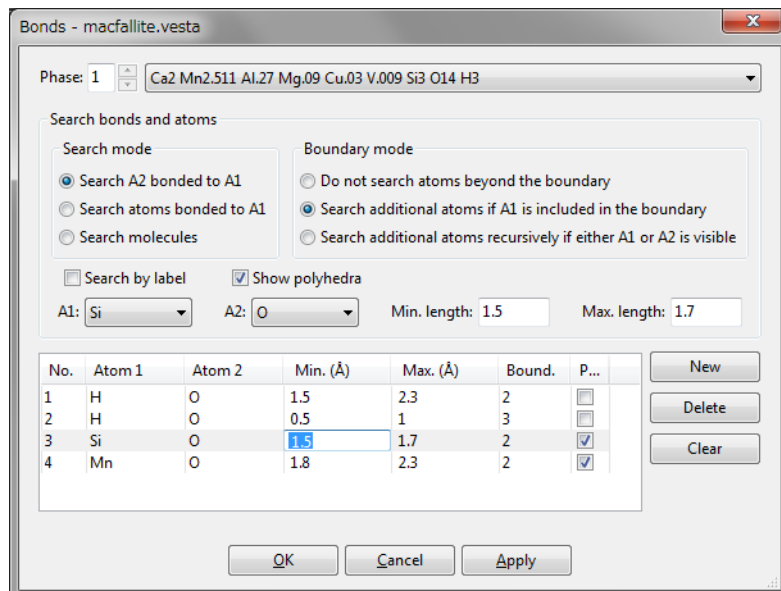


Figure 8.1: Bonds dialog.

## 8.1 Specifications of Searching for Bonds

### 8.1.1 Search mode

Bonds and, in turn, atoms connected by them are searched in one of the following three search modes:

- “Search A2 bonded to A1”

*A*2 atoms bonded to *A*1 atoms are searched on the basis of user-specified minimum and maximum interatomic distances: {Min. length} and {Max. length}.

- “Search atoms bonded to A1”

All the atoms bonded to *A*1 atoms are searched on the basis of user-specified {Min. length} and {Max. length} regardless of the species of the *A*2 atoms.

- “Search molecules”

All the pairs of atoms are searched on the basis of user-specified {Min. length} and {Max. length}. Neither *A*1 nor *A*2 is specified in this option. This mode best meets searching for atoms and bonds in molecular crystals.

### 8.1.2 Boundary mode

The Boundary mode specifies the extent of searching for atoms. Basically, atoms and bonds are searched within a drawing boundary defined by ranges along *x*, *y*, and *z* axes, and by optional cutoff planes (see chapter 10.1). However, on selection of a proper Boundary mode, atoms and bonds outside the drawing boundary are also searched so that all the atoms in coordination polyhedra or molecules are included.

- “Do not search atoms beyond the boundary”

Only atoms within the drawing boundary are searched.

- “Search additional atoms if A1 is included in the boundary”

All the *A*2 atoms bonded to *A*1 atoms are searched even if *A*2 atoms are placed outside the drawing boundary. If the *A*2 and *A*1 atoms are, respectively, located inside and outside the boundary, the *A*1 atom is not searched. This mode is the default for the “Search A2 bonded to A1” and “Search atoms bonded to A1” modes.

- “Search additional atoms recursively if either A1 or A2 is visible”

All the pairs of *A*1 and *A*2 atoms are searched if either *A*1 or *A*2 has already been found. When using this mode in inorganic crystals, beware lest bonds are infinitely connected. This mode is the default for the “Search molecules” mode.

### 8.1.3 Options

- “Search by label”

On selection of this option, a pair of atoms is specified by labels of sites. When this option is unchecked, a pair of atoms is specified by elemental symbols.

- “Show polyhedra”

This option specifies that *A*1 atoms are central atoms of coordination polyhedra. This option has no effect on bond specifications in the “Search molecules” mode because no coordination polyhedra are searched in that mode.

#### 8.1.4 A pair of atoms

Atoms  $A_1$  and  $A_2$  may be specified by entering either elemental symbols or site names. The  $\{A_1\}$  and  $\{A_2\}$  list boxes list elemental symbols of atoms if option “Search by label” is unchecked (default). On the other hand,  $\{A_1\}$  and  $\{A_2\}$  list site labels if option “Search by label” is checked.

The minimum and maximum bond lengths,  $\{\text{Min. length}\}$  and  $\{\text{Max. length}\}$ , are input in the unit of Å. Though  $\{\text{Min. length}\}$  is usually set at zero, it may be positive when dealing with a disordered structure whose split-atom model gives seemingly very short bonds.

## 8.2 Operating Instructions

### 8.2.1 Creating coordination polyhedra

To build up coordination polyhedra, either the “Search  $A_2$  bonded to  $A_1$ ” or “Search atoms bonded to  $A_1$ ” mode should be selected. The central atoms of the coordination polyhedra must be specified as  $A_1$ . In the “Search molecules” mode, no coordination polyhedra are created because VESTA does not have any information about central atoms. In the first two bond search modes, the Boundary mode 2 (“Search additional atoms if  $A_1$  is included in the boundary”) enables us to search for all the  $A_2$  atoms bonded to  $A_1$  atoms so that no coordination polyhedra are truncated even if  $A_2$  atoms lie outside the boundary.  $A_1$  atoms lying outside the boundary are never searched.

To search for additional atoms bonded to  $A_2$  atoms, use the Boundary mode 3 (“Search additional atoms recursively if either  $A_1$  or  $A_2$  is visible”). For example, if hydrogen atoms are coordinated to some  $A_2$  atoms, those hydrogen atoms can be searched even if  $A_2$  atoms lie outside the boundary ([Fig. 8.2](#)).

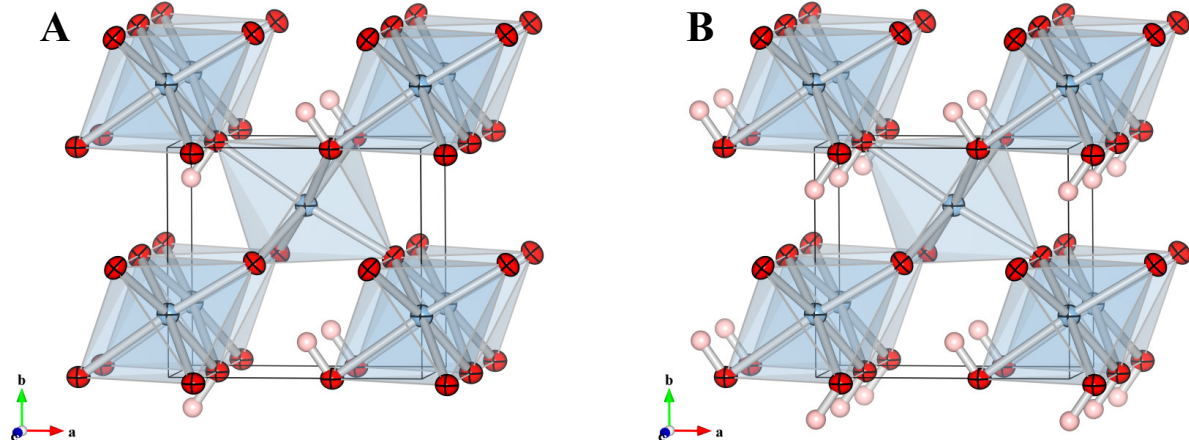


Figure 8.2: Crystal structure of  $\delta$ -AlOOH, a high-pressure modification of aluminum oxide hydroxide, with displacement ellipsoids at a 99 % probability level [60]. The structures were drawn in a coordinate range from (0, 0, 0) to (1, 1.5, 1). O-H bonds were searched (A) in the “Search additional atoms if  $A_1$  is included in the boundary” mode and (B) in the “Search additional atoms recursively if either  $A_1$  or  $A_2$  is visible” mode. In (A), some H atoms were omitted when O atoms lay outside of the boundary specified in the Boundary dialog box. On the hand, all the H atoms bonded to O atoms displayed in the screen were searched in (B).

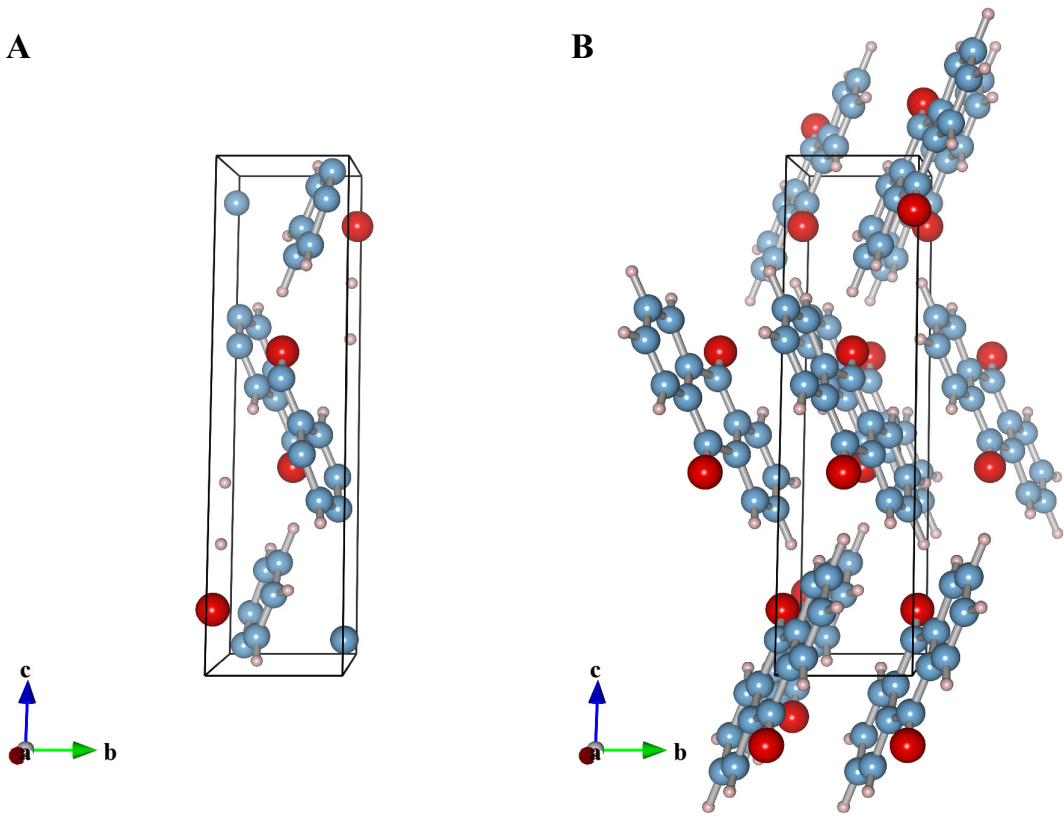


Figure 8.3: Crystal structure of anthraquinone [61]. Bonds are searched in the “Search molecules” mode with the boundary modes (A) “Do not search atoms beyond the boundary” and (B) “Search additional atoms recursively if either A1 or A2 is visible”. In both cases, the bounding box has a range of coordinates from (0, 0, 0) to (1, 1, 1).

### 8.2.2 Searching for molecules and clusters

The “Search molecules” mode is similar to 406 instruction in ORTEP-III<sup>1</sup> [62], *i.e.*, “reiterative convoluting sphere of enclosure add.” This mode is generally used in combination with the Boundary mode 3 to avoid some atoms in molecules being “truncated” (omitted) even if they lie outside the boundary (Fig. 8.3). In this mode, neither A1 nor A2 is specified; only {Min. length} and {Max. length} are input.

A maximum distance of 1.6 Å is appropriate in typical organic compounds containing H, C, N, O, and F atoms having covalent radii of 0.32, 0.77, 0.74, 0.66, and 0.72 Å, respectively. Inputting a larger value may generate unreal bonds. To search for atoms and bonds in molecules and clusters containing larger atoms such as P, S, Cl, and Br having covalent radii of 1.10, 1.04, 0.99, and 1.14 Å, respectively, add bond specifications in the “Search A2 bonded to A1” mode in combination with the Boundary mode 3 (Fig. 8.4).

### 8.2.3 Applications of the “Search molecules” mode to inorganic crystals

In general, combination of the “Search molecules” mode and the Boundary mode 3 is unsuitable for inorganic compounds or metals because a network of bonds may continue infinitely in their structures. In practice, an infinite number of atoms must be searched in such a case. Nevertheless, VESTA actually searches and shows a huge number of atoms and bonds in a finite range

<sup>1</sup><http://www.ornl.gov/sci/ortep/doc/i400.html>

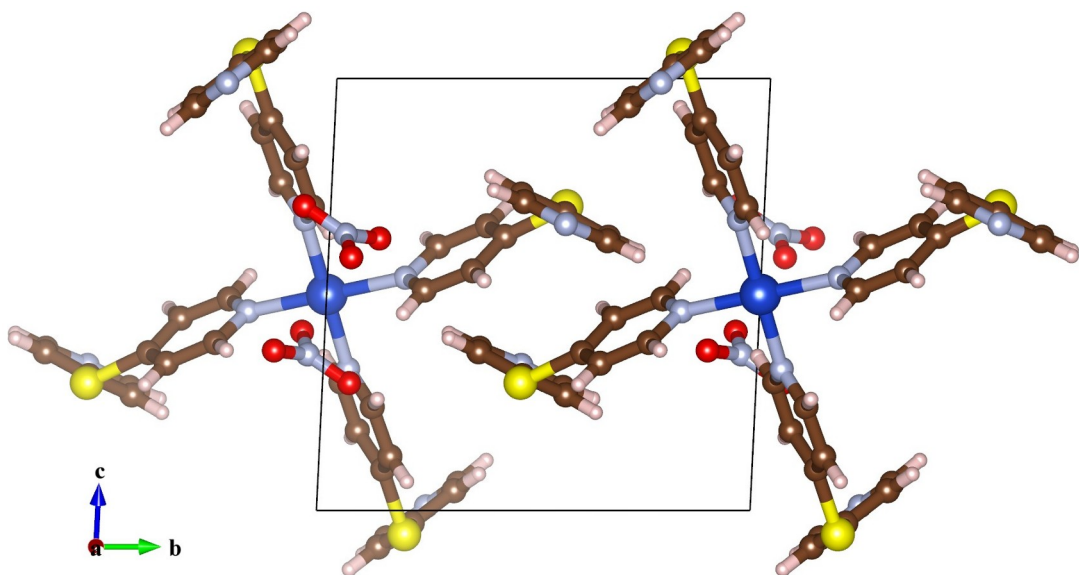


Figure 8.4: Crystal structure of tetrakis(di-4-pyridylsulfane)dinitratocopper(II) [63]. Bonds are searched in the “Search molecules” mode with a maximum distance of 1.6 Å in combination with the “Search A2 bonded to A1” mode for Cu–N and S–C bonds. The Boundary mode 3 was used.

because searching within a certain area ensures that all the atoms contained in molecules in the boundary are searched in cases of periodic structures.

There are exceptions where the combination of such modes is well-suited to search for bonds in inorganic crystals, *e.g.*, searching for O–H bonds. Usually, no bonds are shorter than O–H ones; thus, the use of this mode is safe with a small value of {Max. length}. The maximum bond length of *ca.* 1.1 Å leads to a search for all the H atoms bonded to O atoms in the Graphics Area.

#### 8.2.4 Searching for hydrogen bonds

To display X–H $\cdots$  Y hydrogen bonds, select the “Search A2 bonded to A1” mode in the Search mode frame box, set A1 at H and A2 at Y, and input the minimum and maximum distances of H $\cdots$  Y bonds in {Min. length} and {Max. length}. Styles of the H $\cdots$  Y bonds can be set at Objects tab in the Side Panel.

#### 8.2.5 Visualizing cage-like structures

To represent cage-like voids in porous crystals by a polyhedral model, put a virtual site at the center of a cage (see page 46) and add a bond specification between the virtual site and atoms at corners of the cage. Then, to visualize framework structures with solid bonds, add a bond specification between the corner atoms. If Y atoms are bonded to X atoms at the corners, add X–Y bonds. All of these bond specifications should be given with the Boundary mode 2 so that neither atoms nor bonds in cages displayed are omitted (Fig. 8.5).

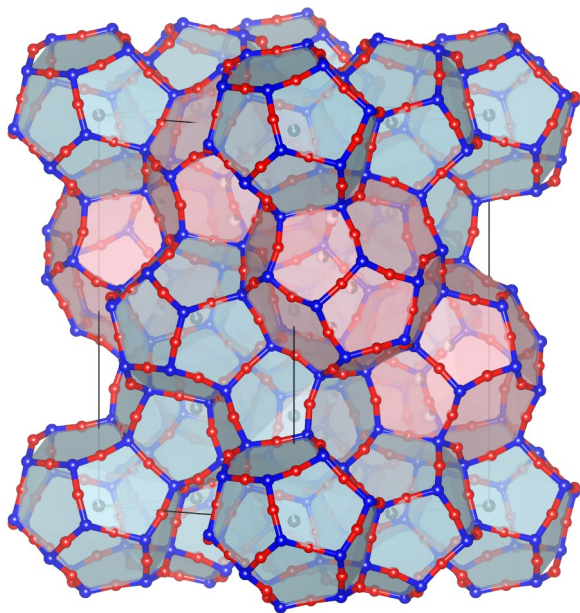


Figure 8.5: Crystal structure of the tetragonal variant of chibaite represented by a polyhedral model [64].

# Chapter 9

## ADDITIONAL OBJECTS

### 9.1 Vectors on Atoms

To attach vectors (arrows) to part of atoms, choose “Edit” menu  $\Rightarrow$  “Vectors...”. These arrows serve to represent magnetic moments or directions of static and dynamic displacements of atoms. At the top of the **Vectors** dialog box (Fig. 9.1), select a phase to edit. When option “Preview” is checked (default), changes in the dialog box are reflected in the **Graphics Area** in real time.

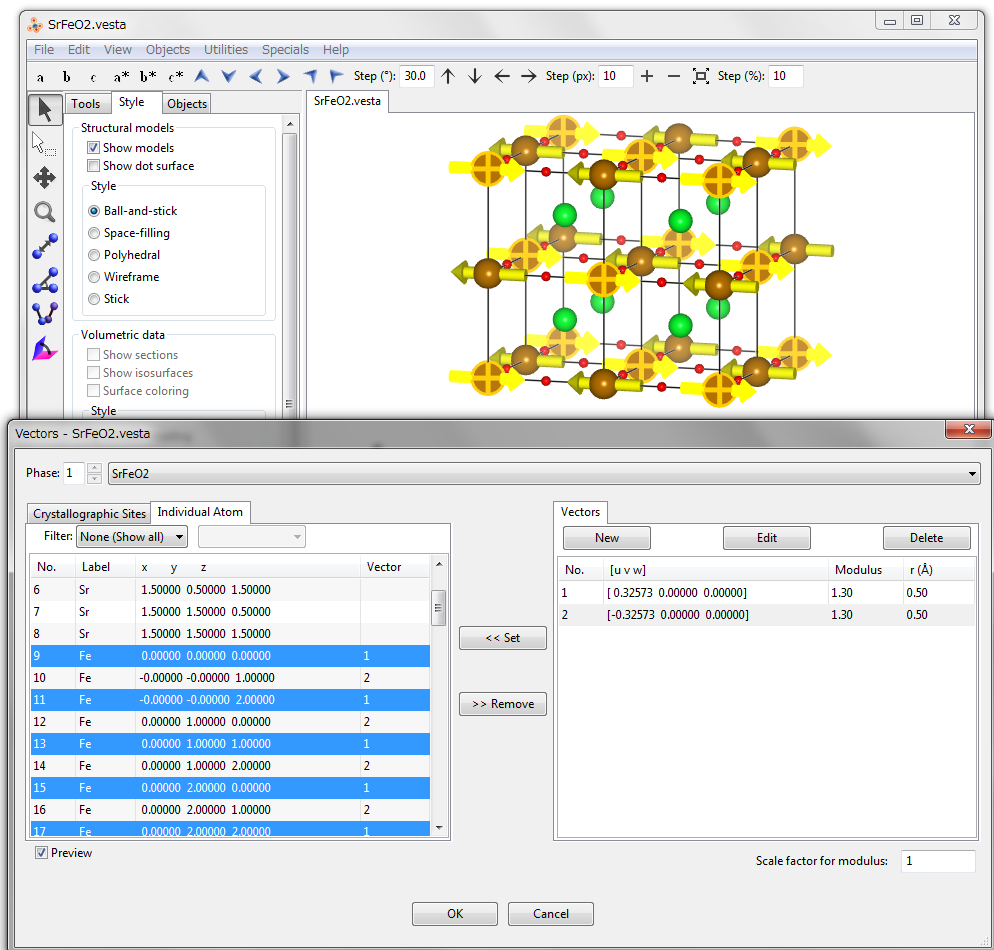


Figure 9.1: Vectors dialog box showing a list of atoms in SrFeO<sub>2</sub> [65], with the atom list filtered by elements. Atoms selected in the dialog box are highlighted in the underlying Graphics Area displaying the magnetic structure of SrFeO<sub>2</sub>.

Vectors can be assigned to either crystallographic sites or individual atoms in the Graphic Area. When a vector is attached to a crystallographic site, all of its symmetrically equivalent atoms will bear the same vector, which is properly rotated in accordance with symmetry operations applied to the atoms. When a vector is assigned to each atom, only that atom will have the vector whereas no other symmetrically equivalent atoms will bear the vector. Multiple numbers of vectors can be attached to atoms and sites, and a vector can be attached to more than two atoms and sites. The length of arrows, which are vectors rendered in the Graphics Area, is scaled by moduli of the vectors multiplied by the input value of the {Scale factor for modulus}. For more details about the scaling of vectors, see [9.1.1](#) and [Fig. 9.4](#).

### 9.1.1 Creation and editing of a vector

At the right pane of the Vectors dialog box, all the vectors are listed with the following three buttons placed above the list ([Fig. 9.1](#)):

[New]: Add a new vector.

[Edit]: Edit the selected vector.

[Delete]: Delete the selected vector.

The [Edit] and [Delete] buttons cannot be clicked unless a vector in the list has been selected.

Click the [New] button to create a new vector. Select a vector in the list of vectors, and click the [Edit] button to edit it. Then, a dialog box appears to edit properties of the selected vector ([Fig. 9.2](#)).

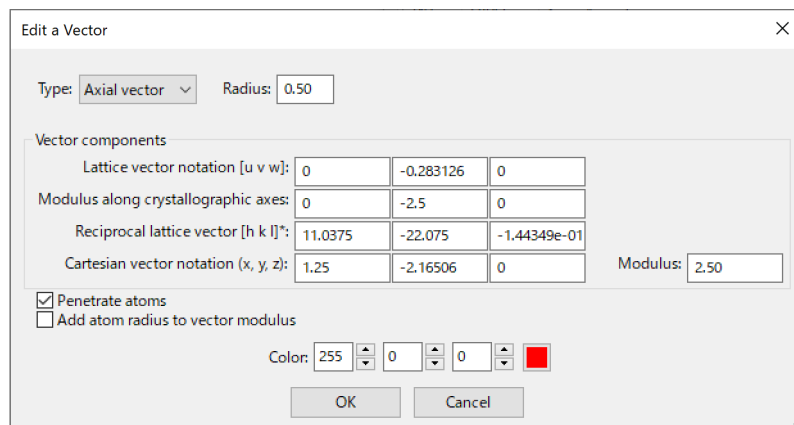


Figure 9.2: A dialog box to create or edit a vector.

Two types of vectors can be specified: {Axial vector} and {Polar vector}. Because these two differ from each other in the mode of applying symmetry operations, the vector type affects only vectors attached to crystallographic sites. When a vector is attached to individual atoms, no symmetry operation is applied to the vector, with no differences between the two types of the vectors.

Typical examples of axial and polar vectors are magnetic moment,  $\mu$ , and electrostatic polarization vector,  $p$ , respectively. The magnetic moment is induced by tiny electrical currents resulting from electrons moving around the nucleus of an atom. The direction of the moment vector is determined by that of the current. For example, counter-clockwise and clockwise currents generate upward and downward moment vectors, respectively. A mirror plane perpendicular to the moment vector does not change the current direction, while a mirror plane parallel to the moment vector inverses the current direction. As a result, magnetic moments are transformed by a mirror plane as [Fig. 9.3A](#) illustrates. In the case of the electrostatic polarization vector,

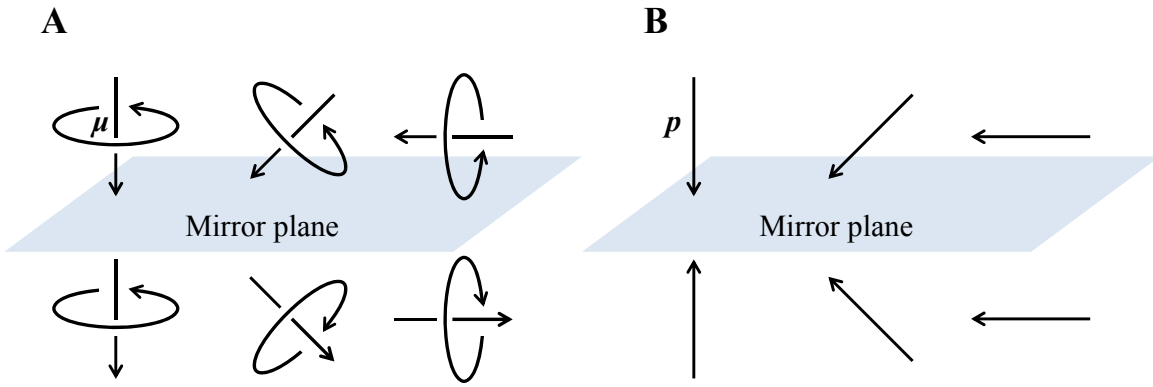


Figure 9.3: Results of applying a mirror operation to (A) magnetic moments  $\mu$  and (B) polarization vectors  $p$

on the other hand, a mirror plane perpendicular to the moment vector inverses the polarization vector, while a mirror plane parallel to the polarization vector does not change the polarization vector (**Fig. 9.3B**). To be more specific,  $p$  is transformed to  $p'$  by a  $3 \times 3$  operator matrix,  $M$ , as

$$p' = M p \quad (9.1)$$

while  $\mu$  is transformed to  $\mu'$  as

$$\mu' = P M \mu, \quad (9.2)$$

where  $P$  is the determinant of  $M$  and referred to as the “parity” of the operator  $M$ . Note that the term  $P M$  is a scalar-matrix multiplication.

Aside from conventional symmetry operations  $M$ , there is another important symmetry element for vectors, *i.e.* time reversal. In view of time reversal, the current direction around an atom is changed, with a result that the direction of  $\mu$  is reversed. Let the time reversal be  $T$  ( $= 1$  or  $-1$ ), then the transformation of  $\mu$  is represented by

$$\mu' = T P M \mu. \quad (9.3)$$

For the polarization vector, time reversal has no effect at all.

In the Edit a Vector dialog box, three different representations of vector components are shown: {Lattice vector notation ( $u, v, w$ )}, {Modulus along crystallographic axes}, and {Cartesian vector notation ( $x, y, z$ )}. Editing one representation of the vector components updates the rest of the representations as well as the {Modulus} of the vector. After the {Modulus} has been edited, vector components are linearly scaled.

When the “Penetrate atoms” check box is on (default), the length of an arrow (vector drawn in the Graphic Area) is doubled with its center placed at the center of an atom (**Figs. 9.4A** and **9.4B**). When this option is off, one end of an arrow is placed at the center of an atom so that it appears only one side above the atom sphere (**Figs. 9.4C** and **9.4D**).

When option “Add atom radius to the vector modulus” is checked, the length of an arrow appearing above an atom sphere is linearly scaled by the vector modulus, regardless of the radius of the atom sphere (**Figs. 9.4B** and **9.4D**). Even if a vector with a very small modulus is attached to an atom having a very large sphere, the arrow will not be hidden by the atom sphere. If this option is disabled (default behavior), the arrow length including the part hidden by an atom sphere is linearly correlated to the vector modulus (**Figs. 9.4A** and **9.4C**); consequently, a very short arrow may be completely hidden by the atom sphere.

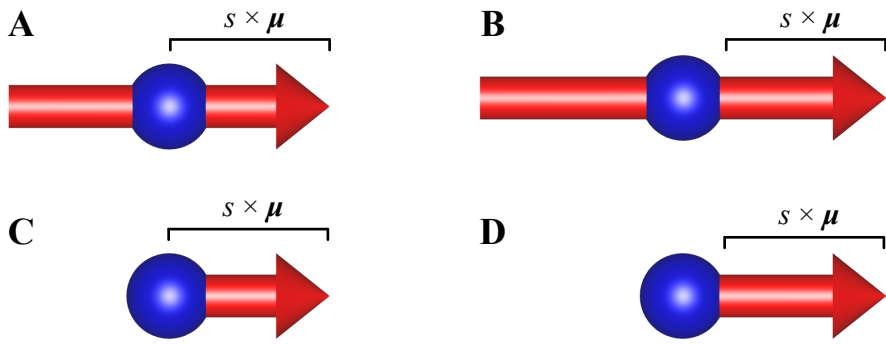


Figure 9.4: Effects of two options for vector styles. Option “Penetrate atoms”: on (A, B) and off (C, D), and option “Add atom radius to the vector modulus”: off (A, C) and on (B, D). When the latter option is on, the length of an arrow appearing above an atom sphere is linearly scaled by  $\mu$  multiplied by the {Scale factor for modulus},  $s$ .

### 9.1.2 Attachment of vectors to crystallographic sites

To attach a vector to crystallographic sites, select the Crystallographic sites tab at the left pane of the **Vectors** dialog box. Then, select sites in the left pane, select a vector in the right pane, and click the [ $<<$  Set] button. In a similar manner, select crystallographic sites in the left pane, and click the [ $>>$  Remove] button to detach a vector from the sites.

### 9.1.3 Attachment of vectors to individual atoms

To attach a vector to individual atoms in the **Graphics Area**, select the Individual atoms tab at the left pane of the **Vectors** dialog box. Select atoms from a list in the left pane or by clicking atoms in the **Graphics Area**. Then, select a vector in the right pane of the **Vectors** dialog box, and click the [ $<<$  Set] button. In a similar manner, select atoms in the left pane, and click the [ $>>$  Remove] button to detach a vector from the atoms. When atoms in the list in the left pane are selected, the corresponding ones are highlighted in the **Graphics Area**, and *vice versa*.

## 9.2 Lattice Planes

To insert lattice planes in structural models, or to add 2D slices of volumetric data in 3D images, choose “Edit” menu  $\Rightarrow$  “Lattice Planes...”. At the top of the **Lattice Planes** dialog box (Fig. 9.5), select a phase to edit. A list of lattice planes is shown at the lower half of the dialog box. Some of buttons and text boxes are disabled when no lattice plane is selected in the list. On selection of an item in the list, the text boxes are updated to show data relevant to the selected lattice plane. When option “Preview” is checked (default), changes in the dialog box are reflected in the **Graphics Area** in real time.

To add a new lattice plane, click the [New] button at first, input Miller indices  $hkl$ , and the distance from the origin,  $(0, 0, 0)$ . The distance may be specified in the unit of either its lattice-plane spacing,  $d$ , or Å. The color and opacity of the lattice plane is specified either as four integers ranging from 0 to 255 or from a color selection dialog box, which is opened after clicking the square button on the right side of the text boxes.

To delete a lattice plane, select an item in the list, and then click the [Delete] button or press the  $<\text{Delete}>$  key. Clicking the [Clear] button deletes all the lattice planes in the list.

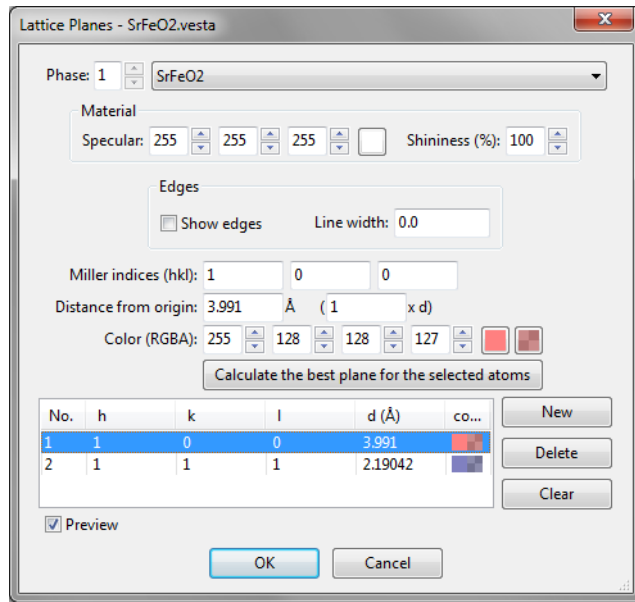


Figure 9.5: Lattice Plane dialog box.

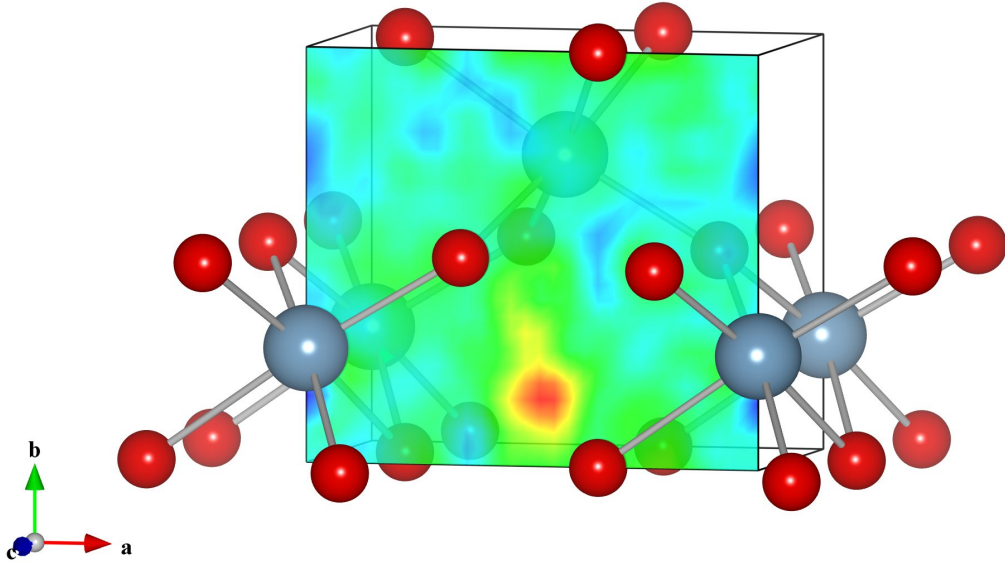


Figure 9.6: A section of a difference Fourier map inserted in a ball-and-stick model of  $\delta$ -AlOOH [60]. The maximum in the section corresponds to a position of an H atom, which is not included in the structural model.

### 9.2.1 Appearance of lattice planes

When volumetric data are included in the current data, lattice planes are colored according to volumetric data on the lattice planes. Saturation levels of colors are specified at [Sections](#) page in the Properties dialog box (Fig. 9.6; see 12.1.6). When only structural information is included in the current data, lattice planes are drawn with colors specified in this dialog box. To draw lattice planes with specified colors for data having both structural and volumetric information, volumetric data should be deleted at the Edit Data dialog box (see 6.4).

Material settings of lattice planes, *i.e.* specular color and shininess are input in the Material

frame box. Drawing of edges for lattice planes can be controlled in the Edge frame box. These settings are common to all the lattice planes.

### 9.2.2 Calculate the best plane for selected atoms

To calculate the best plane for a group of atoms (Fig. 9.7), add a new lattice plane at first, select three or more atoms in the Graphics Area, and press [Calculate the best plane for the selected atoms] button.

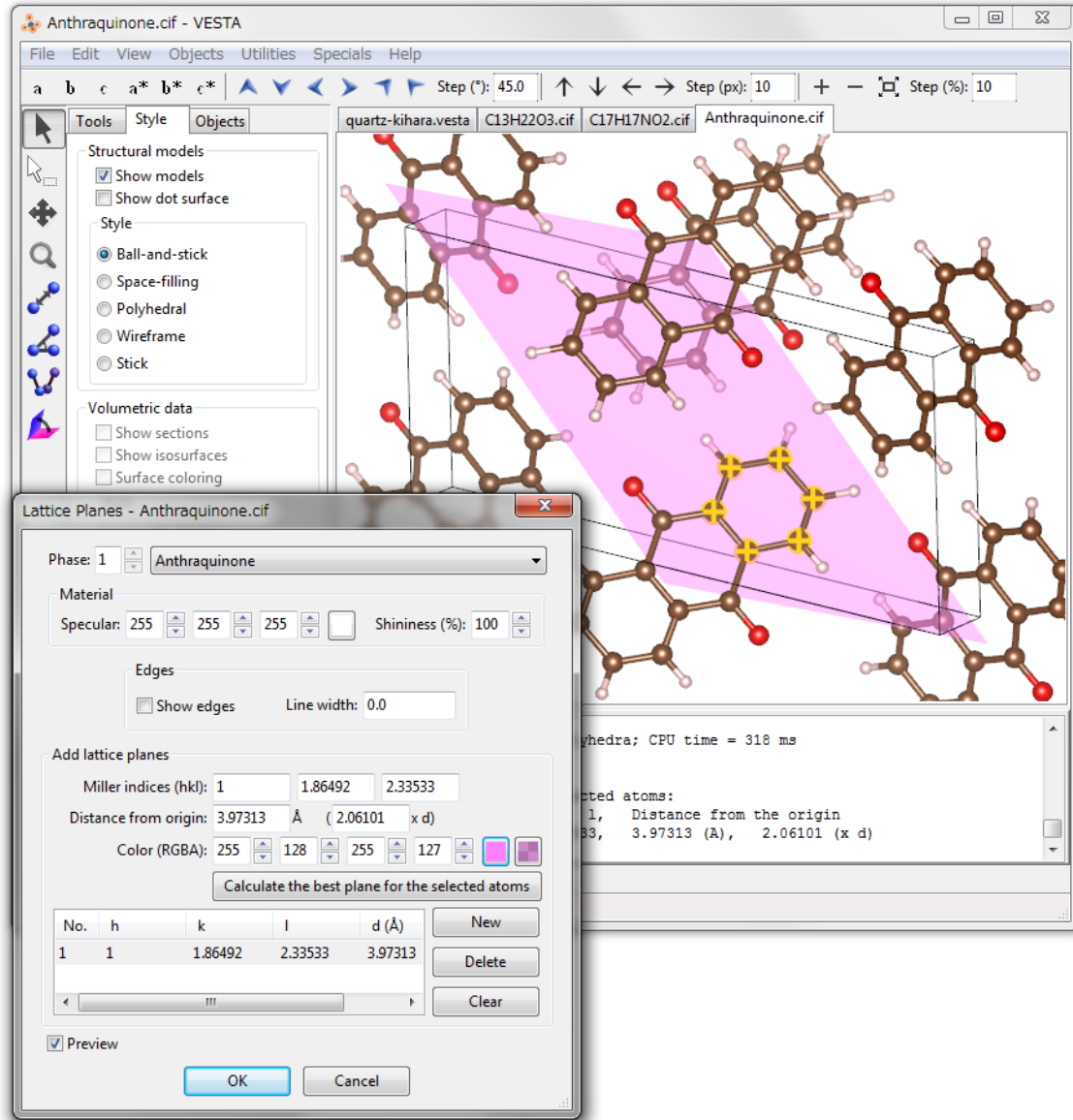


Figure 9.7: The best plane calculated for an aromatic ring in anthraquinone [61].

# Chapter 10

## DEFINING DRAWING BOUNDARIES AND VIEW DIRECTIONS

### 10.1 Drawing Boundaries

To change the size of a drawing boundary (box), select the [Boundary] button in the Side Panel, or choose “Objects” menu  $\Rightarrow$  “Boundary...”. Then, the Boundary dialog box appears as **Fig. 10.1** illustrates. This dialog box can also be opened with a keyboard shortcut of  $<\text{Ctrl}> + <\text{Shift}> + <\text{B}>$ . At the top of the dialog box, select a phase to edit. Press the [OK] or [Apply] button to reflect editing results in the Graphics Area.

Changing the boundary regenerates all the atoms in the Graphics Area and reset all the properties of objects to default values. Selected or hidden states of atoms, bonds, and polyhedra are reset to the default states.

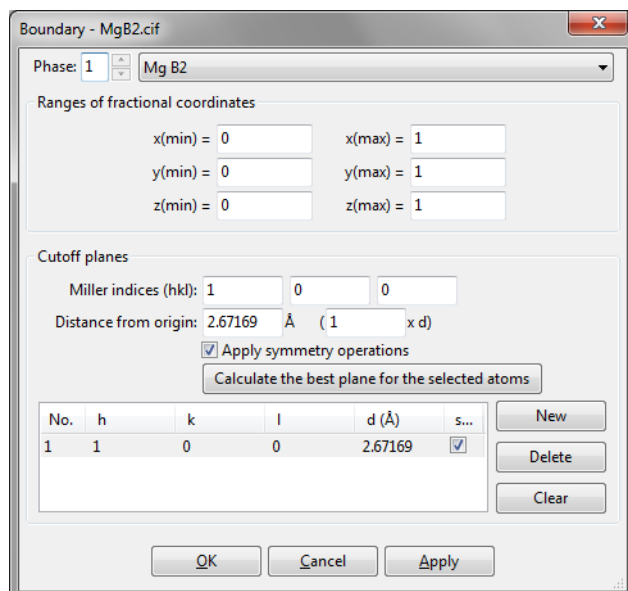


Figure 10.1: Boundary dialog box.

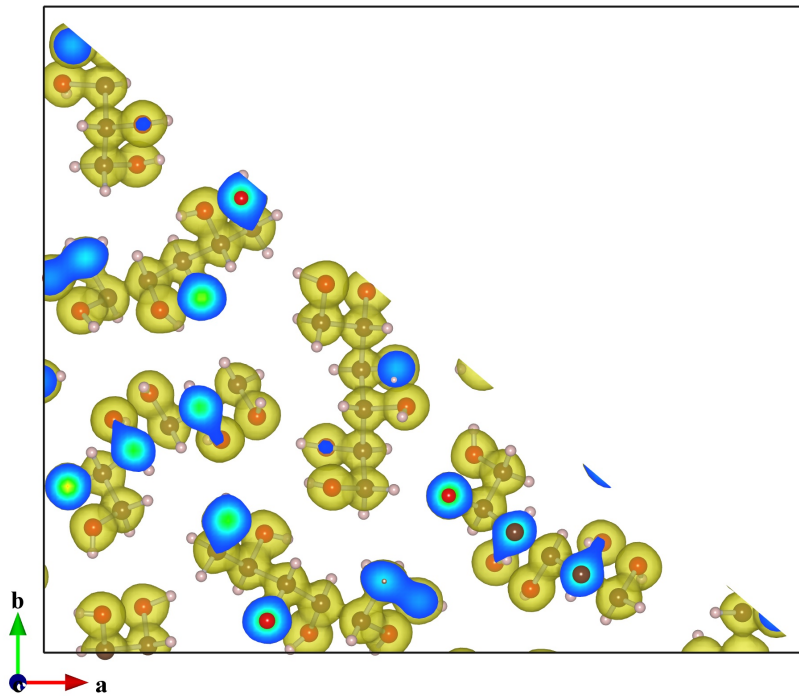


Figure 10.2: Electron density distribution determined for D-sorbitol [66] by the maximum-entropy method from synchrotron X-ray powder diffraction data. Drawn in ranges from  $(0, 0, 0)$  to  $(1, 1, 1)$  with a cutoff plane  $(1\bar{1}0)$ .

### 10.1.1 Ranges of fractional coordinates

Drawing boundaries are fundamentally specified by inputting ranges of fractional coordinates along  $x$ ,  $y$ , and  $z$  axes.

### 10.1.2 Cutoff planes

In addition to ranges of fractional coordinates, we can further specify “cutoff planes,” as exemplified in **Fig. 10.2**. After atoms, bonds, and isosurfaces within the  $x$ ,  $y$ , and  $z$  ranges have been generated, those lying outside of the cutoff planes are excluded. Even though atoms, bonds, and polyhedra can be hidden by another procedure described in 11.4, this is the only way to remove part of isosurfaces and sections. This feature is, therefore, particularly useful for visualizing 2D distribution of volumetric data on lattice planes in addition to isosurfaces. Each cutoff plane is specified as Miller indices  $hkl$  and a distance from the origin,  $(0, 0, 0)$ . The distance of a cutoff plane from the origin may be specified in the unit of either its lattice-plane spacing,  $d$ , or Å.

When option “Apply symmetry operations” is checked, all the symmetrically equivalent Miller planes are used as cutoff planes (**Fig. 10.3**). To define a cutoff plane with selected atoms, select three or more atoms in the Graphics Area and press the [Calculate the best plane for the selected atoms] button.

The Cutoff planes frame box lists cutoff planes. Some of buttons and text boxes are disabled when no cutoff plane is selected in the list. On selection of an item in the list, the text boxes are updated to show data relevant to the selected cutoff plane. To add a new cutoff plane, click the [New] button at first, and input Miller indices,  $hkl$ , and the distance from the origin. To delete a cutoff plane, select an item in the list, and then click the [Delete] button or press the <Delete> key. Clicking the [Clear] button deletes all the cutoff planes in the list.

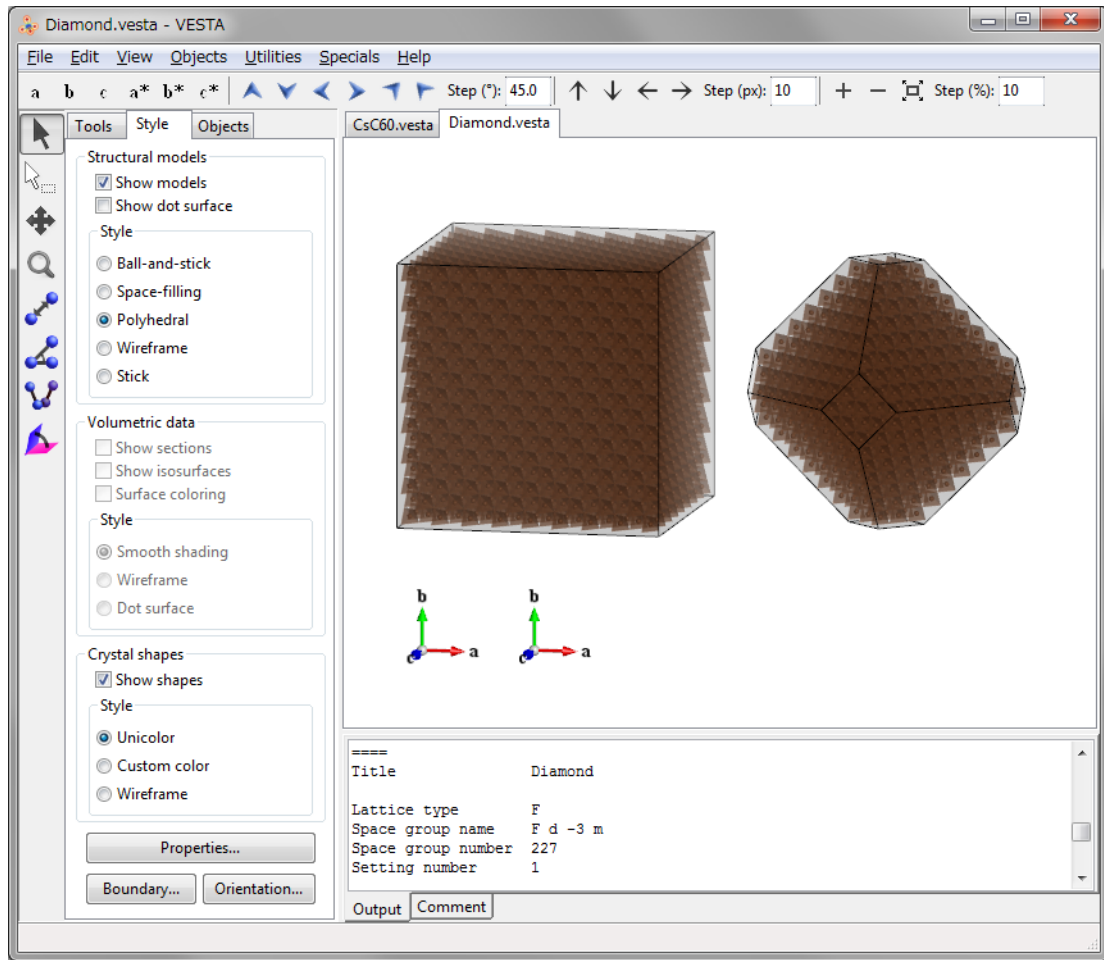


Figure 10.3: Crystal structure of diamond drawn in ranges from  $(-8, -8, -8)$  to  $(8, 8, 8)$  with and without a cutoff plane  $\{111\}$ . The drawing boundaries are displayed as transparent faces.

## 10.2 View Direction

To specify a direction of viewing objects, select the [Orientation] button in Side Panel, or choose “Objects” menu  $\Rightarrow$  “Orientation...”. Then, the Orientation dialog box appears as Fig. 10.4 shows. This dialog box can also be opened with a keyboard shortcut of  $<\text{Ctrl}> + <\text{Shift}> + <\text{O}>$ . At the top of the dialog box, specify a phase to which the viewing direction is applied. To change relative orientation of each phase, use the Phase tab in the Edit Data dialog box (see chapter 7).

### 10.2.1 Manner of specifying directions

Either a lattice vector,  $[uvw]$ , or a reciprocal-lattice vector,  $[hkl]^*$ , perpendicular to a lattice plane  $(hkl)$  is specified as the direction of projection.

- Project along  $[uvw]$   
The direction of projection is a lattice vector  $ua + vb + wc$ .
- Project along the normal to  $(hkl)$   
The direction of projection is a reciprocal-lattice vector  $ha^* + kb^* + lc^*$ .

### 10.2.2 Orientation matrix

A  $3 \times 3$  rotation matrix of the current orientation is displayed.

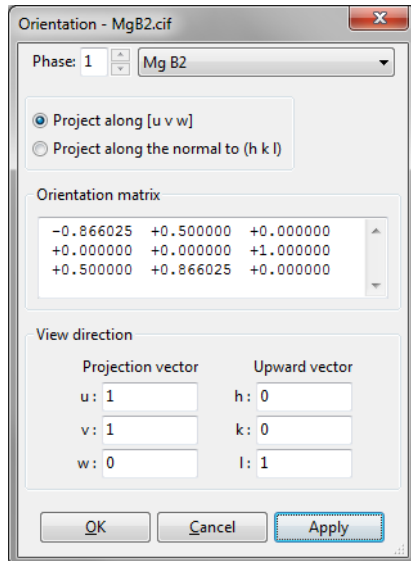


Figure 10.4: Orientation dialog box.

### 10.2.3 View direction

Two directions, *i.e.*, the direction of projection (direction from the viewpoint to the screen) and the upward direction on the screen are specified by a set of a lattice vector and a reciprocal-lattice vector. The two vectors are perpendicular to each other. When the lattice vector,  $ua + vb + wc$ , lies on the  $(hkl)$  plane,  $u, v, w, h, k$ , and  $l$  must satisfy the condition:

$$hu + kv + lw = 0. \quad (10.1)$$

This condition must, therefore, be satisfied in order to specify the upward direction on the screen, otherwise the upward direction on the screen is automatically determined by VESTA.

- **Projection vector:** Direction of projection.  
In the “Project along [uvw]” mode, this vector is  $u, v$ , and  $w$  in  $ua + vb + wc$ .  
In the “Project along the normal to (hkl) plane” mode, this vector is  $h, k$ , and  $l$  in  $ha^* + kb^* + lc^*$ .
- **Upward vector:** Upward direction on the screen.  
In the “Project along [uvw]” mode, this vector is  $h, k$ , and  $l$  in  $ha^* + kb^* + lc^*$ .  
In the “Project along the normal to (hkl) plane” mode, this vector is  $u, v$ , and  $w$  in  $ua + vb + wc$ .

### 10.2.4 Viewing along crystallographic axes

**a   b   c   a\*   b\*   c\***

To view the contents of Graphics Area along basis vectors of a unit cell or a reciprocal cell, simply press one of the above buttons in the Horizontal Toolbar. When two or more phases are visualized in the same Graphics Area, the above buttons set the viewing direction relative to the first phase. To set a viewing direction relative to a phase other than the first one, use the Orientation dialog box.

# Chapter 11

## INTERACTIVE MANIPULATIONS

### 11.1 Rotate

In the Rotation mode, mouse behavior can be changed after clicking the Tools tab in the Side Panel ([Fig. 11.1](#)).

#### 11.1.1 Drag mode

In the “Drag” mode, drag the mouse while pressing the left mouse button to rotate objects in the Graphics Area. The objects are rotated while dragging with the mouse. They are never rotated after releasing the mouse button. In the [Free rotation] mode, the rotation axis becomes normal to the direction along which the mouse is moved. To restrict the rotation axis, select [Around X axis], [Around Y axis], or [Around Z axis] in the pull-down menu of the Rotation modes frame box.

#### 11.1.2 Animation mode

Three types of animation modes can be used in VESTA: “Click”, “Push”, and “Random” modes. The step width of rotation (in degrees/frame) and intervals between frames (in ms) are specified in the Preferences dialog box (see chapter [16](#)).

##### “Click” mode

In the “Click” mode, click the left mouse button to rotate the objects. In the “Click” plus [Free] rotation modes, the rotation axis is perpendicular to a line connecting the clicked position and the central point. To restrict the rotation axis, select [Around X axis], [Around Y axis], or [Around Z axis] in the pull down menu of the Rotation modes frame box. To stop rotating the objects, select either the “Drag” or “Push” mode. The animation speed (intervals between frames in ms) is specified in the Preferences dialog box.

##### “Push” mode

In the “Push” mode, press the left mouse button at point 1 and drag the mouse to point 2. In the [Free rotation] mode, objects are rotated around an axis perpendicular to a line connecting points 1 and 2. The rotation speed is proportional to the speed of moving the mouse. The objects stop rotating immediately after releasing the left mouse button. To restrict the rotation

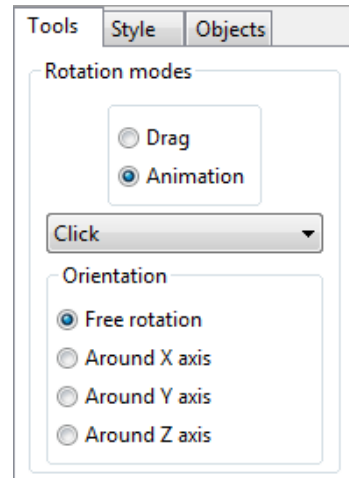


Figure 11.1: The Tools tab of the Side Panel.

axis, select [Around X axis], [Around Y axis], or [Around Z axis] in the pull down menu of the **Rotation modes** frame box.

### “Random” mode

In the “Random” mode, the rotation axis is automatically set and it changes dynamically. To stop the rotation of the objects, select either the “Drag” or “Push” mode.

## 11.2 Magnify

Objects are magnified in proportion to the distance of dragging the mouse upward. On the other hand, they are shrunk in inverse proportion to the distance of dragging the mouse downward.

## 11.3 Translate

Drag the mouse in the **Graphics Area** to translate objects. When a lattice plane with a color specified in the **Lattice Planes** dialog box is selected and dragged in this mode, it is interactively moved. Otherwise the entire objects are translated with the mouse along the same direction.

## 11.4 Select

Several ways of selecting objects can be used. On the use of the select mode in the **Vertical Toolbar**, left click on an object to select it. To select all the objects in a certain area, press the left mouse button and drag the mouse to specify an area. On selection of new objects, objects that have previously been selected are reset to the normal state. To select additional objects while keeping the present objects alive, press **<Shift>** while clicking or dragging the **Graphics Area**. Regardless of the current manipulation mode, two or more objects can be selected by clicking or dragging on them while pressing the **<Shift>** key. A single object is selectable by double-clicking on it. Objects other than atoms, bonds, and polyhedra cannot be selected. For example, atoms behind isosurfaces can be selected.

After a single object has been selected, a variety of information about it is output in the **Text Area**. The estimated standard uncertainty is also displayed for interatomic distance, bond angle, and dihedral angle if those of lattice parameters and fractional coordinates have been supplied. However, note that VESTA gives only rough estimates of standard uncertainties by neglecting off-diagonal elements of the variance-covariance matrix because no off-diagonal elements are included in crystal-data files.

Objects can also be selected by using the **Objects** tab in the **Side Panel** (see section 12.2), the **Vectors** dialog box (see section 11.4), and the **Geometrical Parameters** dialog box (see section 14.2).

Press the **<Delete>** key to hide selected objects. The hidden objects are not actually deleted but just made invisible. To restore all the hidden objects, press the **<Esc>** key. By hiding part of coordination polyhedra, you can easily mix polyhedra with a ball-and-stick model.

### 11.4.1 Atom

On selection of an atom, site number, site name, symbol of the element, fractional coordinates ( $x, y, z$ ), translation vector, symmetry operations (coordinate triplet), occupancy, isotropic atomic displacement parameter, site multiplicity plus Wyckoff symbol, and site symmetry are displayed for the atom. For example, selection of Al and O atoms connected with each other in a ball-and-stick model of  $\alpha\text{-Al}_2\text{O}_3$  gives the following lines:

```

Atom: 1 Al Al 0.00000 1.00000 -0.15000 ( 0, 1,-1)+ -y, -x, z+1/2
      Occ. = 1.000 Ueq = 0.17370 12c 3.
Atom: 2 O O 0.33333 0.97667 -0.08333 ( 0, 0,-1)+ -y+1/3, x-y+2/3, z+2/3
      Occ. = 1.000 Ueq = 0.19915 18e .2

```

When atoms are rendered as displacement ellipsoids, information about principal axes and mean square displacements are also output:

```

Atom: 2 O O 0.97667 0.64333 0.08333 ( 0, 0, 0)+ x-y+2/3, x+1/3, -z+1/3
      Occ. = 1.000 Ueq = 0.19915 18e .2

```

#### Principal axes of the anisotropic atomic displacement parameters

	MSD (Å^2)	x	y	z	u	v	w
1	0.003223	-0.043986	0.027435	-0.023150	-0.005924	0.006668	-0.001785
2	0.002471	0.027516	0.041255	-0.003390	0.010805	0.010027	-0.000261
3	0.001873	-0.013219	0.012054	0.039403	-0.001318	0.002930	0.003038

### 11.4.2 Bond

When a bond is selected, its length is displayed with its estimated standard uncertainty, if any, in the **Text Area** as well as the **Status Bar**. Site number, site name, symbol of the element, fractional coordinates ( $x, y, z$ ), translation vector, and symmetry operations are also displayed for two atoms connected with the bond. For example, on selection of an Al–O bond in the ball-and-stick model of  $\alpha$ -Al<sub>2</sub>O<sub>3</sub>, the following three lines are output:

```

Bond: l(Al-0) = 1.96249(0) Angstrom
      1 Al Al 1.00000 0.00000 0.15000 ( 1, 0, 0)+ y, x, -z+1/2
      2 O O 1.00000 0.31000 0.25000 ( 1, 0, 0)+ -y, x-y, z

```

### 11.4.3 Coordination polyhedron

When a coordination polyhedron with a coordination number of  $n$  is selected, information on the central atom and coordinating atoms (ligands), distances between the central atom and coordinating atoms are listed in the **Text Area**. Further, geometric information described below is displayed in the **Text Area**; the polyhedral volume,  $D$ ,  $\langle\lambda\rangle$ , and  $\sigma^2$  are useful when investigating structural changes under high/low temperature and high pressure [67].

#### Polyhedral volume

The volume of the selected coordination polyhedron is calculated as a fundamentally important physical quantity [31]. For example, distortion in perovskite-type compounds,  $ABO_3$  can be quantified with polyhedral volume ratios,  $V_A/V_B$ , rather than with tilting angles [68].

#### Distortion index

A distortion index,  $D$ , based on bond lengths was defined by Baur [32] as

$$D = \frac{1}{n} \sum_{i=1}^n \frac{|l_i - l_{av}|}{l_{av}}, \quad (11.1)$$

where  $l_i$  is the distance from the central atom to the  $i$ th coordinating atom, and  $l_{av}$  is the average bond length.

## Quadratic elongation

The quadratic elongation,  $\langle \lambda \rangle$  [33], is defined only for tetrahedra, octahedra, cubes, dodecahedra, and icosahedra:

$$\langle \lambda \rangle = \frac{1}{n} \sum_{i=1}^n \left( \frac{l_i}{l_0} \right)^2, \quad (11.2)$$

where  $l_0$  is the center-to-vertex distance of a regular polyhedron of the same volume.  $\langle \lambda \rangle$  is dimensionless, giving a quantitative measure of polyhedral distortion which is independent of the effective size of the polyhedron.

## Bond angle variance

The bond angle variance,  $\sigma^2$  [33], is calculated only for tetrahedra, octahedra, cubes, dodecahedra, and icosahedra:

$$\sigma^2 = \frac{1}{m-1} \sum_{i=1}^m (\phi_i - \phi_0)^2, \quad (11.3)$$

where  $m$  is (number of faces in the polyhedron)  $\times 3/2$  (*i.e.*, number of bond angles),  $\phi_i$  is the  $i$ th bond angle, and  $\phi_0$  is the ideal bond angle for a regular polyhedron (for example,  $90^\circ$  for an octahedron or  $109^\circ 28'$  for a tetrahedron).

## Effective coordination number

The coordination number denotes the number of atoms coordinated to a central atom in a coordination polyhedron. However, stating the coordination of the central atom as a single number is somewhat difficult in relatively distorted coordination polyhedra. Several proposals are made for calculation of a mean or ‘effective’ coordination number (ECoN) by adding all surrounding atoms with a weighting scheme, where the atoms are not counted as full atoms but as fractional atoms with numbers between 0 and 1. This number gets closer to zero with an increase in distance from the central atom to a surrounding atom.

VESTA adopts ECoN [33, 34, 35, 36] defined as

$$\text{ECoN} = \sum_i w_i, \quad (11.4)$$

where the quantity

$$w_i = \exp \left[ 1 - \left( \frac{l_i}{l_{\text{av}}} \right)^6 \right] \quad (11.5)$$

is called the “bond weight” of the  $i$ th bond. In Eq. (11.5),  $l_{\text{av}}$  represents a weighted average bond length defined as

$$l_{\text{av}} = \frac{\sum_i l_i \exp \left[ 1 - (l_i/l_{\text{min}})^6 \right]}{\sum_i \exp \left[ 1 - (l_i/l_{\text{min}})^6 \right]}, \quad (11.6)$$

where  $l_{\text{min}}$  is the smallest bond length in the coordination polyhedron.

## Charge distribution

Let  $q_X$  be the formal charge (oxidation number) of the central atom, X. Then, the fraction of the charge received by an ion at a corner of a coordination polyhedron is calculated as

$$\Delta q_i = \frac{w_i q_X}{\text{ECoN}_X}. \quad (11.7)$$

The total charge,  $Q_A$ , received by an ion  $A$  is obtained by summing the relevant charge fractions,  $-\Delta q_i$ 's, over its  $n$  bonds. Similarly, the charge,  $Q_X$ , received by the ion at the center of a coordination polyhedron is calculated by

$$Q_X = \left[ \sum_i \frac{w_i(q_A/Q_A)_i}{\text{ECoN}_X} \right] q_X. \quad (11.8)$$

Calculation of the charge distribution [35, 36, 37] in the crystal structure depends on the current bond specifications. In other words, the fraction of the charge is not given to or received by ions that are not bonded to each other. Formal charges of ions are read in from data files when ICSD files or CIFs (see 17.4.1) including oxidation states (oxidation numbers) are opened. For other file formats, formal charges of ions have to be input in the Structure parameters tab of the **Edit Data** dialog box to calculate the charge distribution. Note that charge distribution in nonstoichiometric compounds can be calculated because occupancies are used in the calculation.

### Bond valence sum

In addition to the above physical quantities, the bond valence sum,  $V$ , defined as

$$V = \sum_{i=1}^n \exp\left(\frac{l_0 - l_i}{b}\right) \quad (11.9)$$

is also obtainable from the bond valence parameter,  $l_0$ , of the central atom [38, 39, 40]. In VESTA, the empirical constant,  $b$ , in Eq. (11.9) is fixed at a typical value of 0.37 Å.

The bond valence model, which is a development of Pauling's rules, has been theoretically described in terms of classical electrostatic theory without resorting to quantum mechanics. Nevertheless,  $V$  serves, in practice, to estimate the oxidation state of the central atom only from bond lengths determined by X-ray or neutron diffraction.

A CIF, bparm2011.cif, storing bond valence parameters of most chemical species is available for download from

<http://www.iucr.org/resources/data/datasets/bond-valence-parameters>

This CIF is also included in the folder where the executable binary file of VESTA is located so as to refer to it when  $l_0$  values are required. In bparm2009.cif, an  $l_0$  value for a pair of a cation and an anion is obtained, *e.g.*,  $l_0 = 1.620$  Å for Al<sup>3+</sup> and O<sup>2-</sup> and  $l_0 = 2.172$  Å for La<sup>3+</sup> and O<sup>2-</sup> ( $b = 0.37$  Å). Never select an  $l_0$  value for which  $b \neq 0.37$  Å.

If a coordination polyhedron is clicked in the **Graphic Area** while pressing the <Ctrl> key in the manipulation mode of **Select**, you are asked to input a bond valence parameter,  $l_0$ , for the central metal of the selected coordination polyhedron. After entering  $l_0$ , the bond valence sum [38, 39, 40] for the central atom is calculated and displayed in the **Text Area** from all the bond lengths,  $l_i$ , for the current polyhedron and  $l_0$ .

### Expected bond length

Unless oxidation states of sites have been input in the Structure parameters tab of the **Edit Data** dialog box or from some kinds of structural files, VESTA prompts you to enter an oxidation number corresponding to  $V$  in Eq. (11.9); pressing the <Enter> key skips the subsequent calculation. After entering the value, an bond length expected with Eq. (11.9) is calculated and given in the **Text Area**.

## An example of getting information on a coordination polyhedron

Suppose that a  $\text{TiO}_6$  octahedron is selected in a structural model of perovskite ( $\text{CaTiO}_3$ ) [69] while pressing the <Ctrl> key. You are asked to enter the bond valence parameter of  $\text{Ti}^{4+}$  ( $l_0 = 1.815 \text{ \AA}$ ) and the oxidation state of Ti (= +4) unless it has already been input in the Structure parameters tab of the **Edit Data** dialog box. Then, the following data including the physical quantities described above are output to the **Text Area**:

### POLYHEDRON:

1	Ti1	Ti	1.00000	0.50000	0.00000	( 1, 0, 0)+ x, y, z
---	-----	----	---------	---------	---------	---------------------

4	02	0	0.71030	0.71120	-0.03730	( 1, 1, 0)+ -x, -y, -z
4	02	0	0.78970	0.21120	-0.03730	( 0, 0, 0)+ x+1/2, -y+1/2, -z
3	01	0	0.92890	0.48390	0.25000	( 1, 0, 0)+ -x+1/2, y+1/2, z
3	01	0	1.07110	0.51610	-0.25000	( 0, 0, 0)+ x+1/2, -y+1/2, -z
4	02	0	1.28970	0.28880	0.03730	( 1, 0, 0)+ x, y, z
4	02	0	1.21030	0.78880	0.03730	( 1, 0, 0)+ -x+1/2, y+1/2, z

$l(\text{Ti1-02}) = 1.9571(11) \text{ \AA}$

$l(\text{Ti1-02}) = 1.9569(11) \text{ \AA}$

$l(\text{Ti1-01}) = 1.9497(4) \text{ \AA}$

$l(\text{Ti1-01}) = 1.9497(4) \text{ \AA}$

$l(\text{Ti1-02}) = 1.9571(11) \text{ \AA}$

$l(\text{Ti1-02}) = 1.9569(11) \text{ \AA}$

Average bond length = 1.9546  $\text{\AA}$

Polyhedral volume = 9.9546  $\text{\AA}^3$

Distortion index (bond length) = 0.00168

Quadratic elongation = 1.0001

Bond angle variance = 0.3773 deg.^2

Effective coordination number = 5.9994

### Charge distribution

delta\_q: Fraction of the charge received by the ion

Q: Total charge received by the ion

q: Formal charge (oxidation number)

	x	y	z	delta_q	Q	q
4	02	0	0.71030	0.71120	-0.03730	0.661 -1.994 -2.000
4	02	0	0.78970	0.21120	-0.03730	0.662 -1.994 -2.000
3	01	0	0.92890	0.48390	0.25000	0.677 -2.013 -2.000
3	01	0	1.07110	0.51610	-0.25000	0.677 -2.013 -2.000
4	02	0	1.28970	0.28880	0.03730	0.661 -1.994 -2.000
4	02	0	1.21030	0.78880	0.03730	0.662 -1.994 -2.000

1	Ti1	Ti	1.00000	0.50000	0.00000	4.000 4.000
---	-----	----	---------	---------	---------	-------------

Input a bond valence parameter: 1.815000

Bond valence sum = 4.115

Oxidation state of the cation: +4

Expected bond length = 1.965 Angstrom

All the fractional coordinates, translations, equivalent positions, bond lengths with their estimated standard uncertainties for the  $\text{TiO}_6$  octahedron are output before the polyhedral volume.

## 11.5 Distance

To calculate an interatomic distance, select the fifth button in the Vertical Toolbar. In this mode, only atoms can be selected. Select a pair of atoms,  $A$  and  $B$ , to obtain the interatomic distance between  $A$  and  $B$ . Then, the two atoms are highlighted, and a dashed line connecting them is plotted on the screen. The  $A-B$  distance is displayed on the Status Bar with its estimated standard uncertainty [70], if any, enclosed by a pair of parentheses. The estimated standard uncertainty is calculated only when those of lattice parameters and fractional coordinates have been input.

To obtain a bond length in a ball-and-stick model, selecting the relevant bond (see 11.4.2) is faster than clicking two atoms. More information on the interatomic distance is displayed in the Text Area, where site number, site name, symbol of the element, fractional coordinates ( $x, y, z$ ), symmetry operations, and translation vector are displayed for each of atoms  $A$  and  $B$ .

For example, an interatomic distance for  $A = \text{C}7$  and  $B = \text{O}2$  in 2'-Hydroxyl-4''-dimethylaminothalcone [71] is output as follows:

```
l(C7-02) = 1.254(4) Angstrom
15      C7  C  0.75640  0.11620  0.34510 ( 1,-1, 0)+ -x, y+1/2, -z+1/2
        4      02  O  0.80530  0.04440  0.43470 ( 1,-1, 0)+ -x, y+1/2, -z+1/2
```

## 11.6 Bond angle

To calculate a bond angle, select the sixth button in the Vertical Toolbar. Then select three atoms  $A$ ,  $B$ , and  $C$  to calculate the bond angle (in degrees) with atom  $B$  at the apex. The angle is displayed on the Status Bar with its estimated standard deviation, if any, in a pair of parentheses. The estimated standard uncertainty [70] is calculated only when those of lattice parameters and fractional coordinates have been input.

More information on the bond angle is displayed in the Text Area, where site number, site name, symbol of the element, fractional coordinates ( $x, y, z$ ), translation vector, and symmetry operations are displayed for each of atoms  $A$ ,  $B$ , and  $C$ .

For example, a bond angle for  $A = \text{O}1$ ,  $B = \text{Al}1$ , and  $C = \text{O}1$  in  $\text{Al}_2\text{O}_3$  [72] is output as follows:

```
phi(01-Al1-01) = 86.37(3) deg.
1      01  O  1.33333 -0.02698  0.41667 ( 1, 0, 0)+ y+1/3, -x+y+2/3, -z+2/3
2      Al1 Al  1.00000  0.00000  0.35217 ( 1, 0, 0)+ x, y, z
1      01  O  1.00000 -0.30635  0.25000 ( 1,-1, 0)+ -y, x-y, z
```

## 11.7 Dihedral angle

To calculate a dihedral angle defined by four atoms, select the seventh button in the Vertical Toolbar. For a sequence of four atoms  $A$ ,  $B$ ,  $C$ , and  $D$ , the dihedral angle,  $\omega$ , is defined as the positive angle between  $ABC$  and  $BCD$  planes. Let  $\alpha = \angle(B-C-D)$ ,  $\beta = \angle(B-A-D')$ , and  $\gamma = \angle(A-B-C)$ , where  $D'$  denotes the  $D$  atom when  $C-D$  is translated in such a way that the  $C$  atom overlaps with the  $A$  atom. Then,  $\cos \omega$  is formulated as [73]

$$\cos \omega = \frac{\cos \alpha \cos \gamma - \cos \beta}{\sin \alpha \sin \gamma}. \quad (11.10)$$

Select four atoms,  $A$ ,  $B$ ,  $C$ , and  $D$ . The dihedral angle (in degrees) for atom  $D$  and a plane on which atoms  $A$ ,  $B$ , and  $C$  lie is displayed on the Status Bar with its estimated standard uncertainty, if any, in a pair of parentheses. The estimated standard uncertainty [70] is calculated only when those of lattice parameters and fractional coordinates have been input.

More information about the dihedral angle is output in the Text Area, where site number, site name, symbol of the element, fractional coordinates ( $x, y, z$ ), symmetry operations, and translation vector are displayed for each of atoms  $A$ ,  $B$ ,  $C$ , and  $D$ . For example, in the case of C1 (=  $A$ ), C2 (=  $B$ ), C3 (=  $C$ ), and C4 (=  $D$ ) atoms contained in an aromatic ring of 3-[4-(dimethylamino)phenyl]-1-(2-hydroxyphenyl)prop-2-en-1-one [71] (Fig. 11.2), the following five lines are output in the text area:

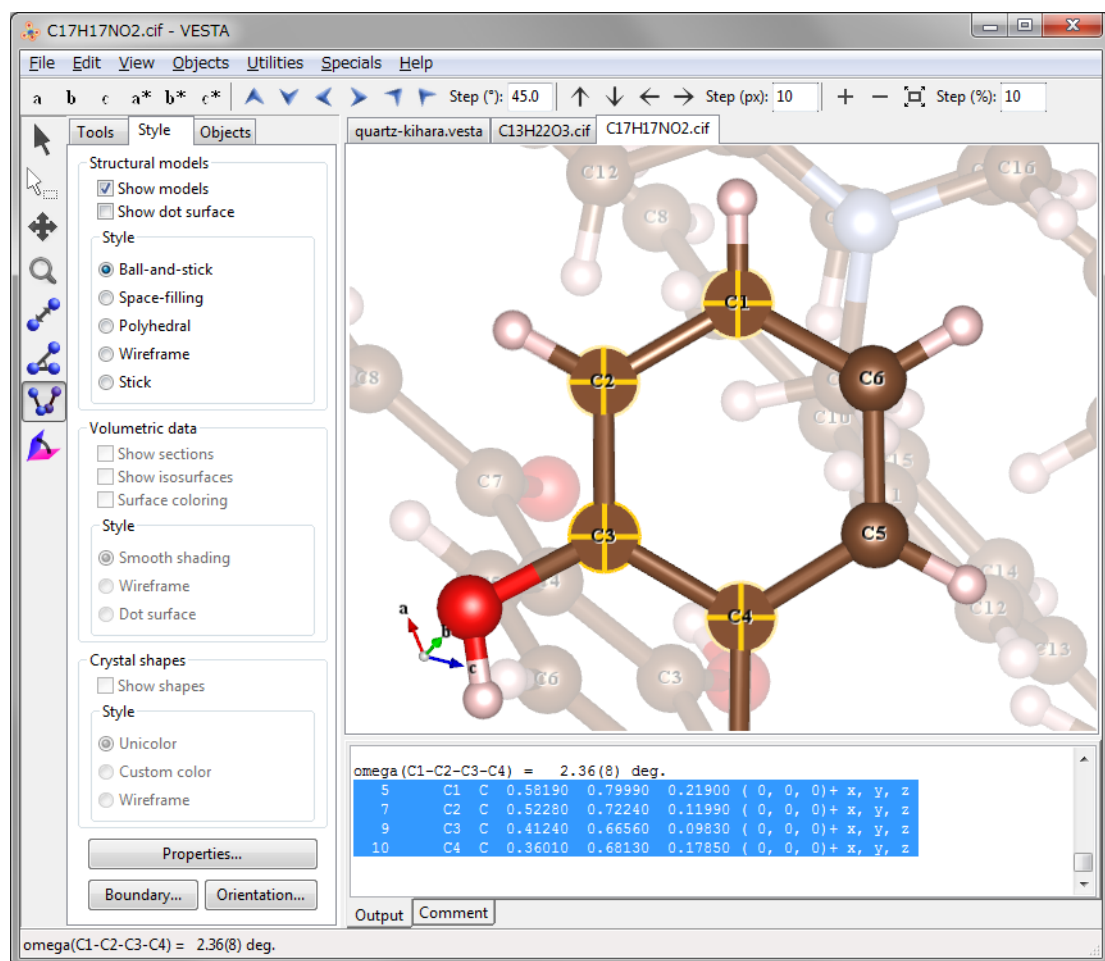


Figure 11.2: Calculation of a dihedral angle for four carbon atoms in an aromatic ring in 3-[4-(dimethylamino)phenyl]-1-(2-hydroxyphenyl)-prop-2-en-1-one

```

omega(C1-C2-C3-C4) = 2.36(8) deg.
5      C1  C  0.58190  0.79990  0.21900 ( 0, 0, 0)+ x, y, z
7      C2  C  0.52280  0.72240  0.11990 ( 0, 0, 0)+ x, y, z
9      C3  C  0.41240  0.66560  0.09830 ( 0, 0, 0)+ x, y, z
10     C4  C  0.36010  0.68130  0.17850 ( 0, 0, 0)+ x, y, z

```

Data in lines No. 2–5 (selected lines in the Text Area in Fig. 11.2) can be used when imposing nonlinear restraints on the dihedral angle in Rietveld refinement with RIETAN-FP [12].

## 11.8 Interfacial angle

To calculate an interfacial angle, *i.e.*, an angle between two crystal faces, select the eighth button in the Vertical Toolbar. In this mode, only crystal faces can be selected. Selection of a pair of faces A and B gives an angle between their normal vectors (Fig. 11.3).

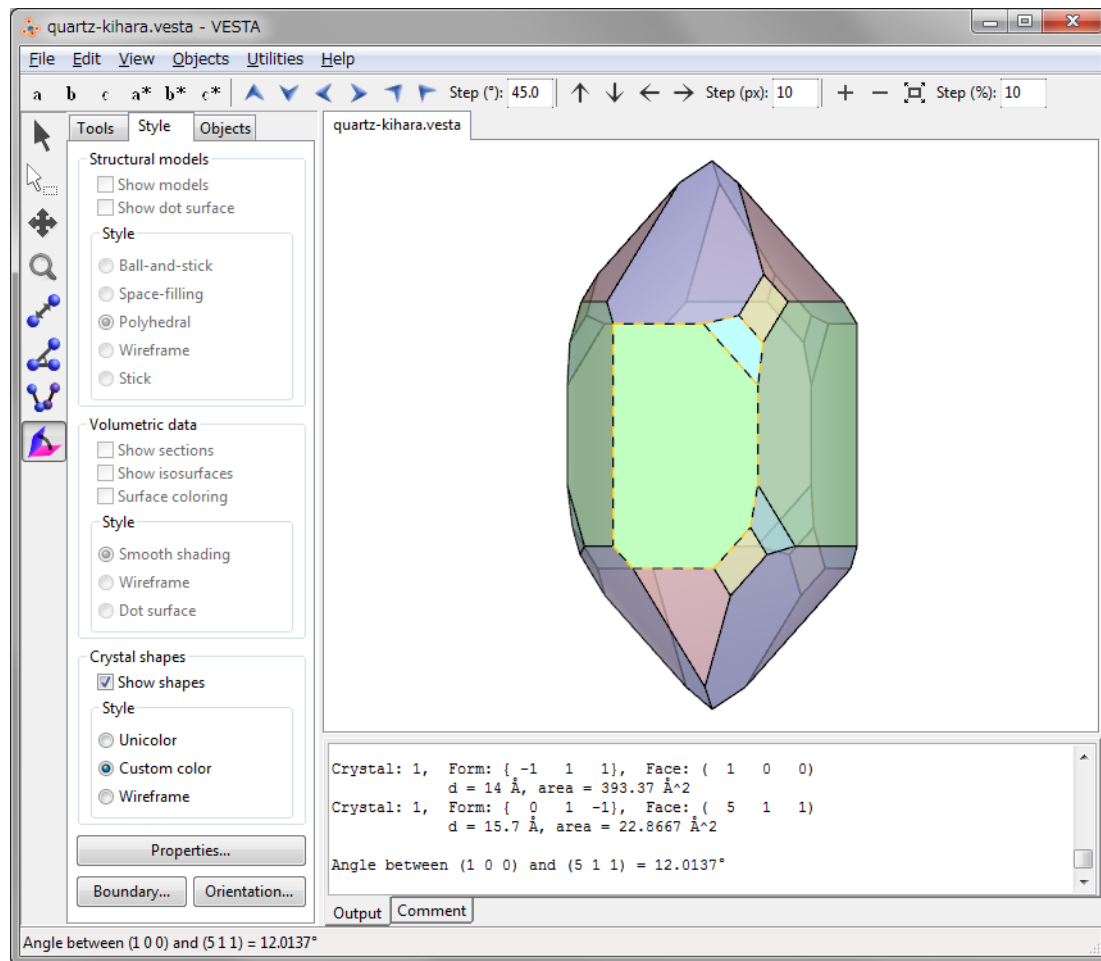


Figure 11.3: Calculation of an interfacial angle between (100) and (511) faces in quartz.

# Chapter 12

## PROPERTIES OF OBJECTS

Properties of various objects are edited in the **Properties** dialog box and the Objects tab of the Side Panel.

### 12.1 Properties Dialog Box

To open the **Properties** dialog box, press the **[Properties]** button in the Style tab of the Side Panel. The same dialog box can be open by choosing one of submenus in the “Objects” menu ⇒ “Properties”. When “Preview” is checked, changes in the **Properties** dialog box are reflected on the **Graphics Area** in real time. Click **[OK]** to apply all the changes or **[cancel]** to discard the changes. Current properties are saved as default values in VESTA by clicking the **[Save as default]** button.

#### 12.1.1 General

The first page in the **Properties** dialog box is General (Fig. 12.1).

##### Unit cell

The display of Unit cell edges in the **Graphics Area** is controlled with the following three radio buttons:

- “Do not show”: Do not show unit cell edges.
- “Single unit cell”: Show edges of a single unit cell.
- “All unit cells”: Show all the edges of unit cells within the drawing boundary.

Line styles of the unit cell edges are selected from three styles: “Solid lines”, “Dotted lines”, and “Dashed lines”. The width of lines is input in text box {Line width}. The color of lines is specified either (A) by entering R, G, and B values ranging from 0 to 255 or (B) by picking a color from a color selection dialog box opened after clicking the **[Select]** button.

##### Axes

“Show Compass” is used to turn on or off a display of three arrows indicating *a*, *b*, and *c* axes (or *x*, *y*, and *z* axes in the case of Cartesian coordinates). “Show Axis Labels” is used to turn on or off a display of axis labels, ‘*a*’, ‘*b*’, and ‘*c*’ (or ‘*x*’, ‘*y*’, and ‘*z*’ in the case of Cartesian coordinates).

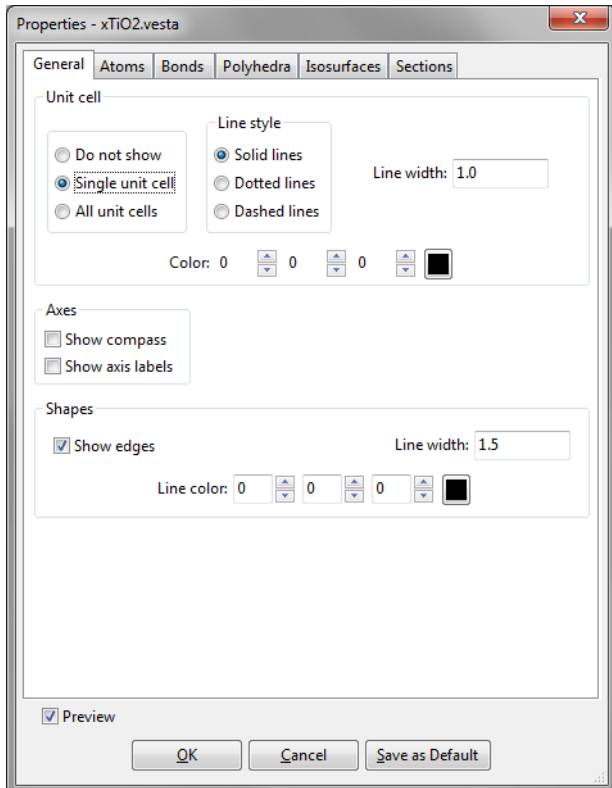


Figure 12.1: General page in the Properties dialog box.

## Shapes

The visibility, line width, and color of edges of crystal morphologies are input in the **Shapes** frame box.

### 12.1.2 Atoms

The second page in the Properties dialog box is Atoms (Fig. 12.2).

## Material

- {Specular} is a color of reflected light that bounces sharply in a particular direction in the manner of a mirror. A highly specular light tends to cause a bright spot on the surface it shines upon, which is called the specular highlight.
- {Shininess} is a property, which specifies how small and focused the specular highlight. A value of 0 specifies an unfocused specular highlight.

## Resolution

{Stacks} and {Slices} are parameters common to all the atoms, allowing you to change the resolution (quality) of atoms displayed on the screen. {Stacks} denotes the numbers of subdivisions along the Z axis (similar to lines of latitude) while {Slices} denotes the number of subdivisions around the Z axis (similar to lines of longitude). {Stacks} and {Slices} should be equal to each other in ball-and-stick and space-filling models where atoms are represented by perfect spheres. In general, decreasing {Stacks} and {Slices} accelerates the rendering of objects in the Graphics Area.

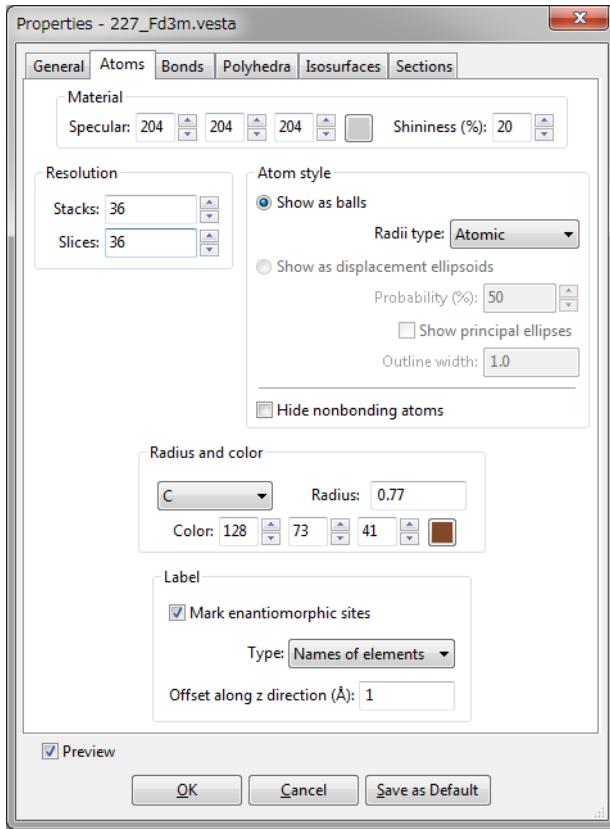


Figure 12.2: Atoms page in the Properties dialog box.

## Atom style

Select either of the following two radio buttons for the mode of displaying atoms on the Graphics Area: (1) “Show as balls” or (2) “Show as displacement ellipsoids”.

- “Show as balls”: Atoms are rendered as spheres. List box {Radii type} is used to select a type of default atomic radii from the following three:
  - **Atomic**: Metallic or covalent radii, whose values were mostly taken from Refs. [74, 75, 76].
  - **Ionic**: Effective ionic radii compiled by Shannon [77] for representative oxidation states and coordination numbers.
  - **van der Waals**: van der Waals radii [78].

The user may modify default values of atomic, ionic, and van der Waals radii by editing a text file, elements.ini, in the program folder of VESTA.

- “Show as displacement ellipsoids”: Atoms are rendered as ellipsoids to represent anisotropic displacement of atoms whose shapes are calculated from anisotropic atomic displacement parameters,  $\beta_{ij}$  or  $U_{ij}$  (see 6.3.5). The probability (in percentage) for atomic nuclei to be included in the ellipsoids is input in text box {Probability}. It is common to all the atoms when drawing displacement ellipsoids. If option “Show principal ellipses” is checked, three principal ellipses corresponding to three principal planes are plotted on the surface of each ellipsoid (**Fig. 12.3**). The line width of the principal ellipses is input in text box {Line width}.



Figure 12.3: Displacement ellipsoids of an atom (A) with principal ellipses and (B) without them.

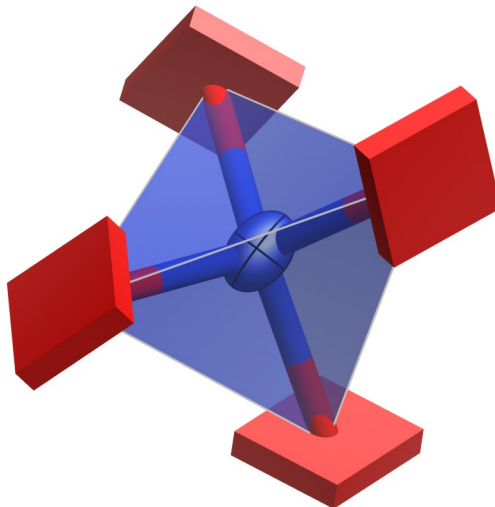


Figure 12.4: A displacement ellipsoid model of a structure with four atoms having negative mean square displacements.

If one or more of principal axes have negative mean square displacements, atoms are represented by cuboids so that the unusual atomic displacement parameters can easily be recognized (**Fig. 12.4**). Each cuboid is oriented in accordance with principal axes with the dimension of the cuboid scaled according to the absolute value of the mean-square displacement.

- “Hide non-bonding atoms”: This option hides atoms that are connected by no bonds but the crystallographic site for those atoms have a coordination number larger than 0. In other words, atoms are made invisible if all the coordinated atoms are lying outside of the drawing boundary.

### Radius and color

Select a symbol of an element from list box {Symbol} and then specify its {Radius}. The color of an atom (element) is specified either (a) by entering R, G, and B values ranging from 0 to 255 or (b) by picking a color from a color selection dialog box opened when clicking the [Select] button.

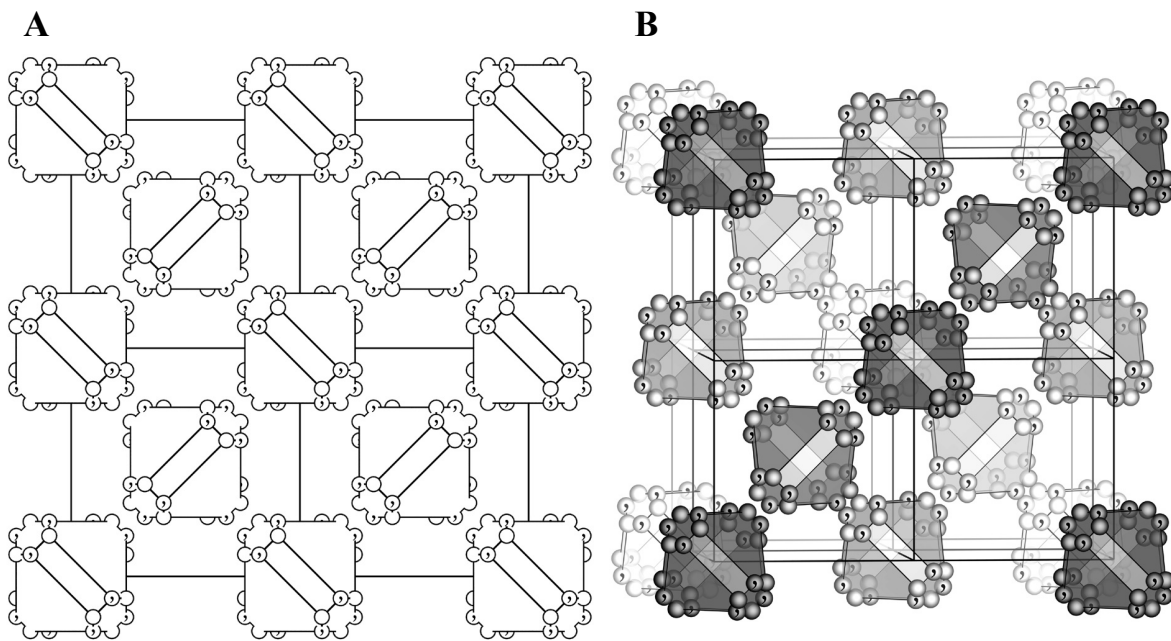


Figure 12.5: General-position diagrams of space group  $Fd\bar{3}m$  with (A) light disabled and (B) light enabled.

## Labels

Select either of the following two types for atom labels: (1) “Names of elements” or (2) “Names of sites”. Labels are displayed near atoms with an offset along the  $z$  axis, which is specified in the unit of Å. When option “Mark enantiomeric sites” is checked, atoms generated by symmetry operations of inversion, rotoinversion, or mirror are marked with a ‘,’ symbol. These positions are enantiomorphs with respect to non-marked positions. This option can be used to draw general position diagrams (Fig. 12.5) similar to those illustrated in “International Tables for Crystallography,” Vol. A [30]. When an atom position coincides with an enantiomeric symmetry element, the original and enantiomeric positions coincide. Such an atom is represented by a ‘,’ mark on the left half of the atom separated with ‘|’ at its center.

### 12.1.3 Bonds

The third page in the Properties dialog box is **Bonds** (Fig. 12.6).

#### Material

It is the same as that in Atoms (see 12.1.2).

#### Resolution

It is the same as that in Atoms (see 12.1.2).

#### Bond style

One of the following six types of bonds are specified in this frame box:

- “Unicolor cylinder”: Each bond is drawn as a cylinder, whose color can be changed in the Color panel.

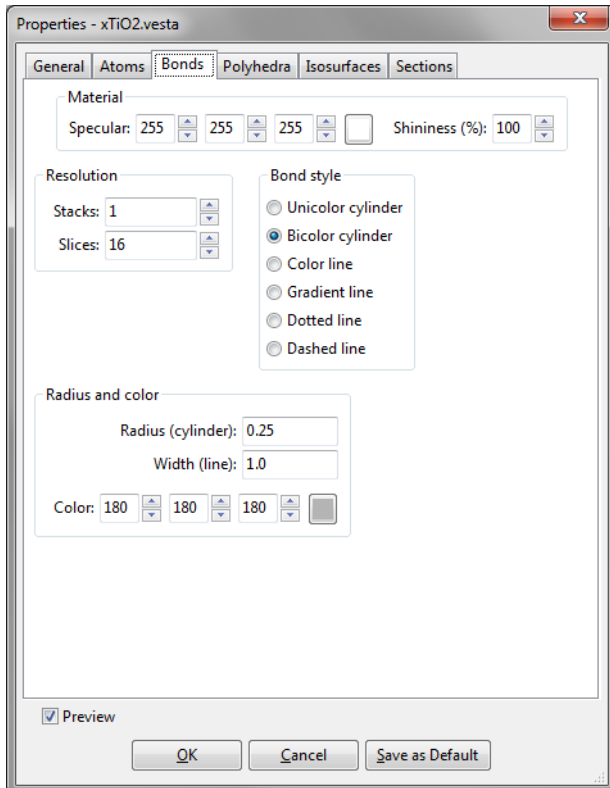


Figure 12.6: Bonds page in the Properties dialog box.

- “Bicolor cylinder”: Each bond is drawn as a cylinder with colors of two atoms connected with each other. The two colors of the bond are just the same as those of atoms connected by bonds.
- “Color line”: Each bond is drawn as a straight line, whose color is changed in the Color panel.
- “Gradient line”: Each bond is drawn as a line connecting two atoms with gradient distribution of colors. Colors of each bond at the ends of the line are the same as those of the atoms.
- “Dotted line”
- “Dashed line”

### Radius and color

The radius of each cylindrical bond in the stick model is changed in text box {Radius (cylinder)}. The actual radius of cylinders is 40 % of the input value. The line width of line-style bonds is changed in text box, {Width (line)}. The color of bonds in the single color style is changed in the Color tool below these two text boxes.

#### 12.1.4 Polyhedra

The fourth page in the Properties dialog box is Polyhedra (Fig. 12.7).

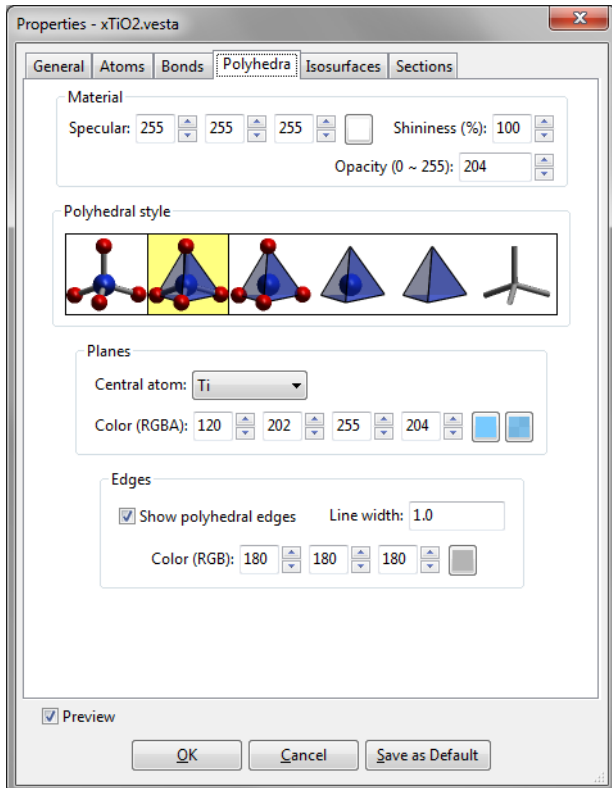


Figure 12.7: Polyhedra page in the Properties dialog box.

## Material

{Specular} and {Shininess} are just the same as those in Atoms page (see 12.1.2). The {Opacity} of coordination polyhedra is input with 255 corresponding to opaque planes (the inside of each coordination polyhedron is invisible) and 0 corresponding to fully transparent planes (coordination polyhedra are invisible).

## Polyhedral style

Styles of coordination polyhedra are selected from the following six types of expressions that are schematically illustrated in the Polyhedral style frame box:

- Show atoms and bonds without any coordination polyhedra.
- Show atoms, bonds, and coordination polyhedra (default).
- Show atoms and coordination polyhedra.
- Show central atoms and coordination polyhedra.
- Show only coordination polyhedra.
- Show only bonds.

## Planes

The surface color of each coordination polyhedron is specified here. Select an element from list box {Central atom} to specify its color. Default colors of coordination polyhedra are the same as those of the central atoms.

## Edges

The visibility, line width, and color of edges of coordination polyhedra are input in the Edges frame box.

### 12.1.5 Isosurfaces

The fifth page in the Properties dialog box is Isosurface (Fig. 12.8).

## Material

It is the same as that in Atoms (see 12.1.2).

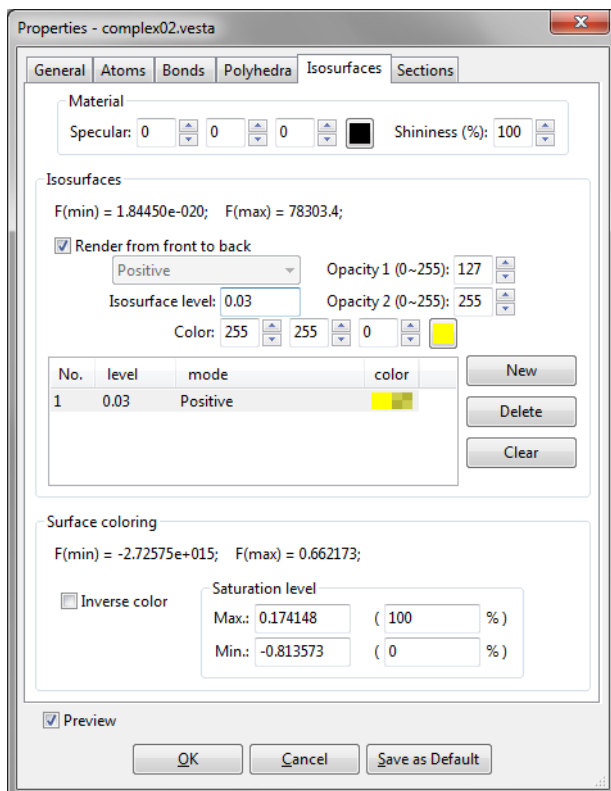


Figure 12.8: Isosurfaces page in the Properties dialog box.

## Isosurfaces

At the top of the Isosurfaces frame box, the minimum and maximum data values are displayed in the unit of the raw data. Data values such as electron and nuclear densities, and wave functions on isosurfaces are equal to {Isosurface level},  $d(\text{iso})$ . All the points with densities larger than  $d(\text{iso})$  lie inside the isosurfaces whereas those with densities smaller than  $d(\text{iso})$  are situated outside the isosurfaces.

At the lower half of the frame box, a list of isosurface levels is shown. To add a new isosurface level, add the [New] button, and edit the isosurface level and color. To delete an isosurface level, select an item in the list, and press the [Delete] button. Pressing the [Clear] button deletes all the isosurfaces.

**Order of rendering polygons** The sequence of drawing polygons can be changed with option "Render from front to back." By default, polygons are rendered from behind so that isosurfaces

behind the nearest surface are visible through translucent isosurfaces. In some cases with complex isosurfaces, it may become difficult to understand the shape of isosurfaces because they heavily overlap each other. When option “Render from front to back” is checked, only the nearest surfaces are rendered. The use of this option may sometimes improve the visibility of complex isosurfaces because neither back surfaces nor internal ones are drawn.

**Figure 12.9** illustrates a difference between the two rendering modes in 3D visualization of results of an electronic-state calculation for the  $[Cd\{S_4Mo_3(Hnta)_3\}_2]^{4-}$  ion ( $H_{3nta}$ : nitrilotriacetic acid) [79] by a discrete variational  $X\alpha$  method with DVSCAT [58].

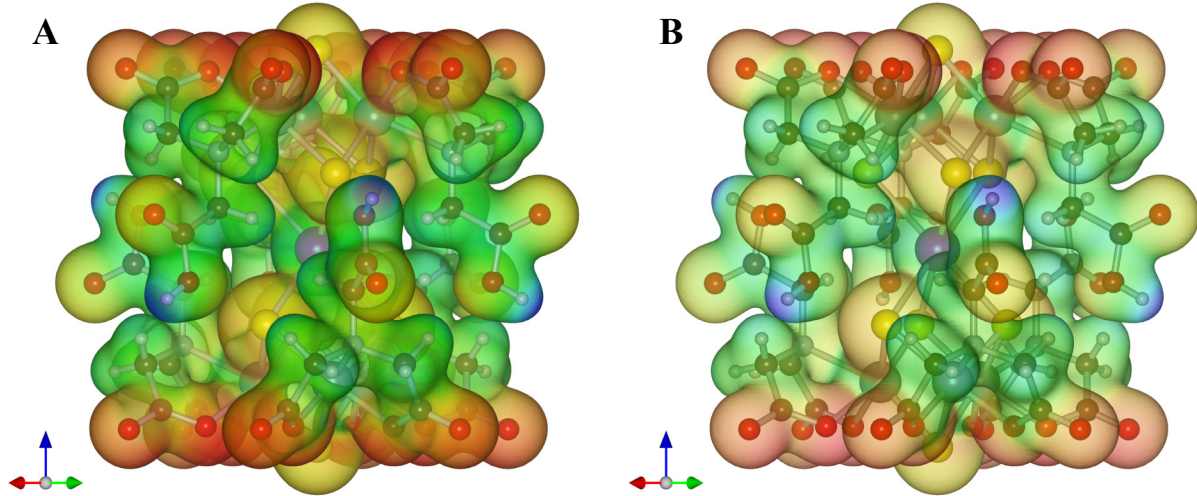


Figure 12.9: Comparison between the two modes of rendering isosurfaces for a molybdenum-cadmium cluster  $[Cd\{S_4Mo_3(Hnta)_3\}_2]^{4-}$ . (A) “Render from behind (default)” and (B) “Render from front to back.” Composite images of electron-density isosurfaces colored according to electrostatic potentials and a ball-and-stick model are shown with an isosurface level of  $0.03a_0^{-3}$  and electrostatic potentials on the isosurface ranging from  $-0.814$  Ry (blue) to  $0.174$  Ry (red).

**Kinds of isosurfaces** For volumetric data having both positive and negative values, you can select which surfaces are visible:

- {Positive and negative},
- {Positive},
- {Negative}.

**Figure 12.10** exemplifies isosurfaces of wave functions calculated with DVSCAT [58] for a complex ion with a ball-and-stick model superimposed on the isosurfaces. Yellow and blue surfaces show positive and negative values, respectively.

**Opacity of isosurfaces** The opacity of isosurfaces is specified by two parameters, {Opacity 1} ( $O_1$ ) and {Opacity 2} ( $O_2$ ), as exemplified in **Fig. 12.11**.  $O_1$  is the opacity for polygons parallel to the screen, and  $O_2$  is that for polygons perpendicular to the screen (**Fig. 12.12**). The opacity,  $O(p)$ , for polygon  $p$  with a normal vector of  $(x, y, z)$  is calculated with a linear combination of  $O_1$  and  $O_2$ :

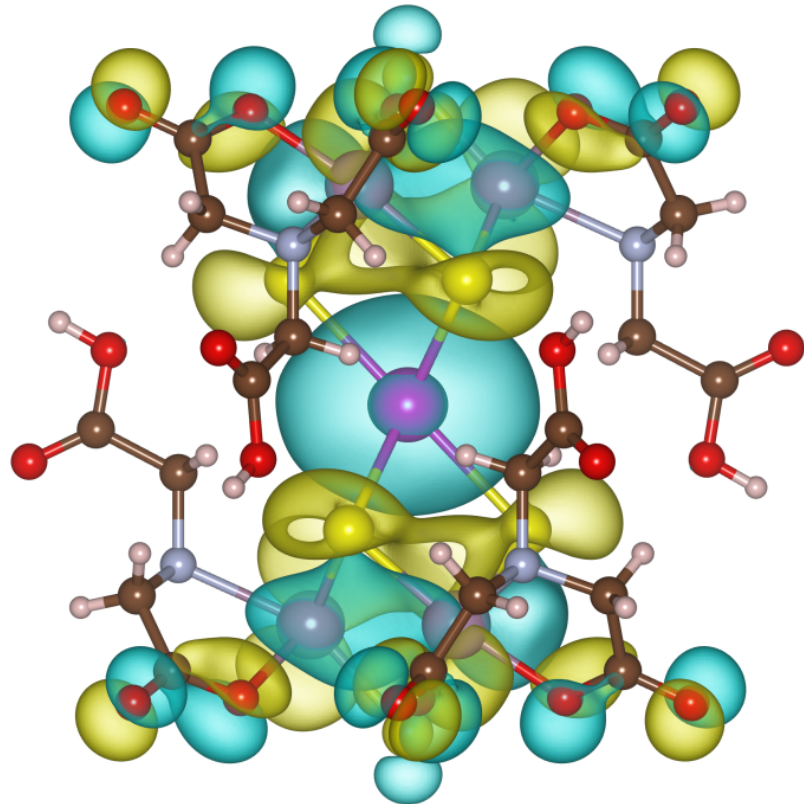


Figure 12.10: The  $64a_{1g}$  orbital for the  $\{Cd[S_4Mo_3(Hnta)_3]_2\}^{4-}$  ion [79] with a ball-and-stick model. The isosurface levels of the wave function were set at  $0.01a_0^{-3/2}$  (yellow) and  $-0.01a_0^{-3/2}$  (blue), where  $a_0$  is the Bohr radius.

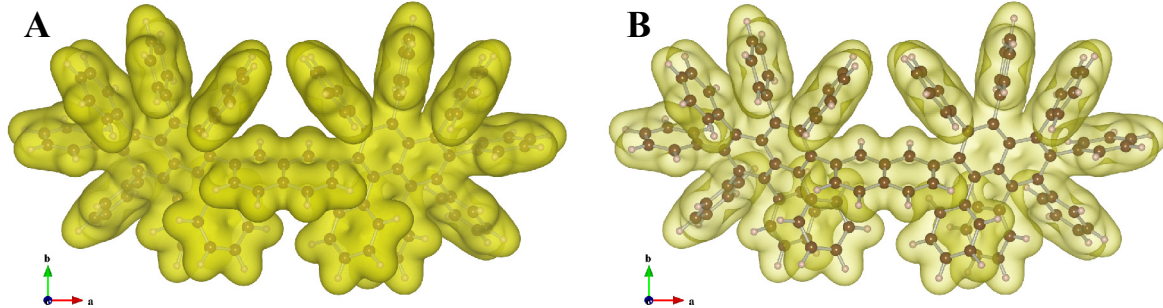


Figure 12.11: Composite images of electron-density isosurfaces and a ball-and-stick model drawn for albatrossene ( $C_{114}H_{76}$ ) [80] with two pairs of opacity parameters: (A)  $O_1 = 153$  and  $O_2 = 255$ ; (B)  $O_1 = 26$  and  $O_2 = 179$ . The electron densities were calculated with DVSCAT [58] and visualized with an equi-density level of  $0.01a_0^{-3}$ .

### Surface coloring

After volumetric data for surface coloring have been loaded, isosurfaces can be colored according to those data. The saturation level of colors is specified as (a) a value normalized between 0 and 100, and (b) a value corresponding to raw data. This is mostly equal to color settings for lattice planes and sections of isosurfaces (see 12.1.6), except that the normalized values of 0 and 100 corresponds to the minimum and maximum data values on the current isosurfaces, not the

data set itself.

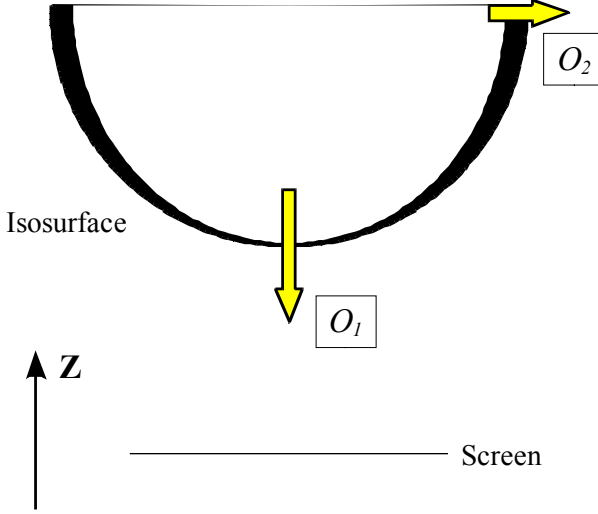


Figure 12.12: Schematic representation of relations between orientation of an isosurface and the two opacity parameters,  $O_1$  and  $O_2$ .

The color index,  $T$ , to determine the color of a data point with a value of  $d$  is calculated from the unit of the raw data: the minimum saturation level,  $S_{\min}$ , and the maximum one,  $S_{\max}$ , in the unit of the raw data:

$$T = \frac{d - S_{\min}}{S_{\max} - S_{\min}}. \quad (12.1)$$

Data points with values larger than  $S_{\max}$  and smaller than  $S_{\min}$  are given the same colors as those assigned to  $S_{\min}$  and  $S_{\max}$ , respectively.

$$O_p = O_1 z + O_2 (1 - z). \quad (12.2)$$

### 12.1.6 Sections

The seventh (final) page in the Properties dialog box is Sections (Fig. 12.13).

For volumetric data, both lattice planes and sections of isosurfaces are colored according to numerical values on them (Fig. 12.14). The saturation level of colors is specified as (a) a value normalized between 0 and 100 corresponding the minimum and maximum data values, respectively, and (b) a value corresponding to raw data. The color index,  $T$ , for a data point with a value of  $d$  is calculated from the minimum saturation level,  $S_{\min}$ , and the maximum one,  $S_{\max}$ , in the unit of the raw data:

$$T = \frac{d - S_{\min}}{S_{\max} - S_{\min}}. \quad (12.3)$$

Data points with numerical values larger than  $S_{\max}$  and smaller than  $S_{\min}$  are given the same colors as those assigned to  $S_{\min}$  and  $S_{\max}$ , respectively. The color of each point is determined from  $T$ , depending on color modes. One of six color modes, that is, B-G-R, R-G-B, C-M-Y, Y-M-C, gray scale (from black to white), and inverse gray scale, is selected from a list box. For example, blue is assigned to 0, green to 0.5, and red to 1 in the B-G-R mode, as shown in Fig. 12.15.

When option “Absolute values” is checked, colors are assigned on the basis of absolute values of data.

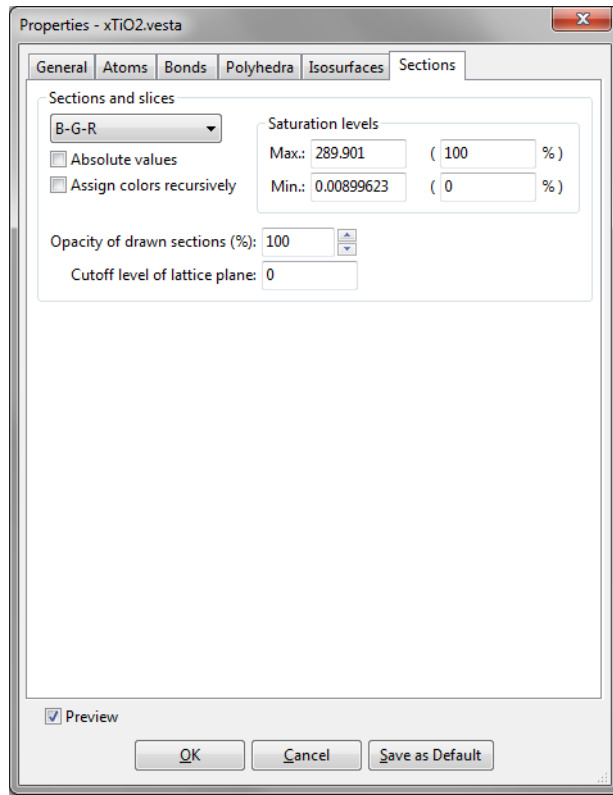


Figure 12.13: Sections page in the Properties dialog box.

Option “Assign colors recursively” assigns rainbow colors recursively to data points with values smaller or larger than the saturation levels, which affords an effect similar to contour lines with gradient colors in between them. The opacity of sections are specified in the {Opacity of drawn sections} box, and that of lattice planes in the Lattice Planes dialog box (see 9.2). When {Cutoff level of lattice plane} is larger than 0, some parts of lattice planes with data values smaller than the cutoff level are omitted.

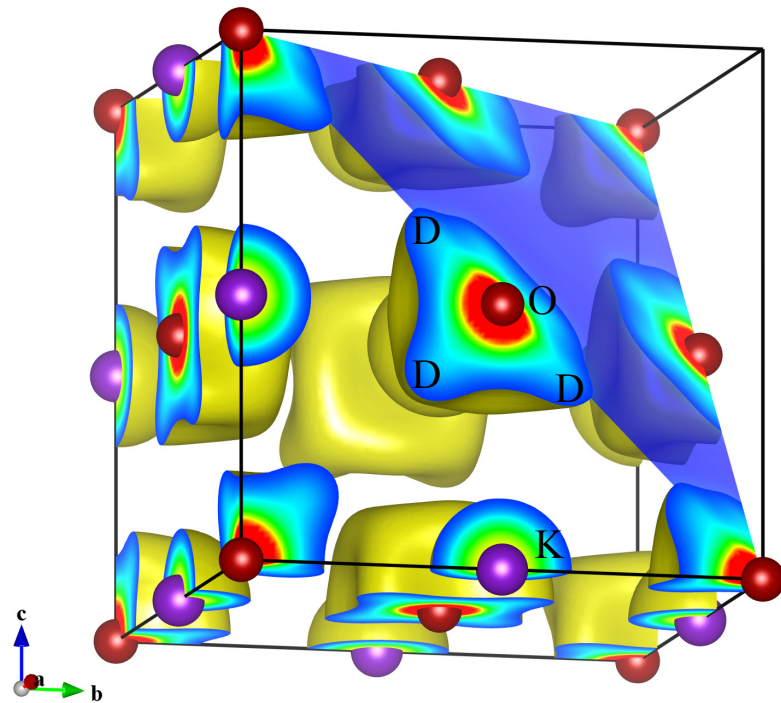


Figure 12.14: Distribution of nuclear densities obtained for KOD at 580 K by MEM from single-crystal neutron diffraction data [81]. Coordinate ranges from (0, 0, 0) to (1, 1, 1) were drawn with a cutoff plane of (111). D atoms are highly disordered around O atoms.

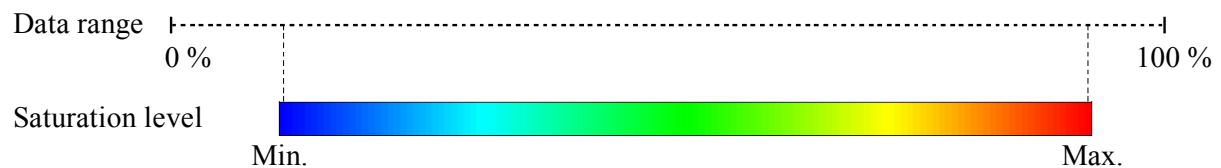


Figure 12.15: Relations among saturation levels, data values, and colors of sections.

## 12.2 Objects Tab in the Side Panel

### 12.2.1 List of phases and objects

At the upper half of the Objects page, an overview of objects contained in each phase is listed (Fig. 12.16). Atoms, bonds, polyhedra, slices, and shapes are shown for each phase if they are contained in the phase data. Select one of them to see more details in objects at the lower half of the page.

### 12.2.2 Atoms

The first column (Site) lists crystallographic sites grouped by elements. The second column ( $r(\text{\AA})$ ) gives radii for elements and crystallographic sites. To edit these data, select a row and click on the text. The third column (C) shows colors of atoms, which can be edited by double-clicking square areas. The fourth to sixth columns (L, S, and V) control visual properties of atoms, *i.e.*, labels, selection states, and visibility. If properties of an element are edited, the modifications are applied to all the sites of the element.

### 12.2.3 Bonds

When a list of bond specifications is displayed in the lower half of the Objects page (Fig. 12.17), the first column (Bond) gives pairs of atoms that are bonded to each other. The second column (S) shows styles of bonds, which can be changed by double-clicking the second column of a bond. The third column ( $r/w$ ) gives radii or line widths of bonds. When bonds are rendered as cylinders (styles 1 and 2), they are specified in the unit of  $\text{\AA}$ , which are then rescaled by a factor of 0.4 on rendering of bonds. When bonds are rendered as solid, dashed, or dotted lines (styles 3–6), they are specified in the unit of pixels. The fourth column (C) displays colors of bonds, which are edited by double-clicking the colored square. The fifth and sixth columns (S and V) control selection states and visibilities of bonds, respectively.

### 12.2.4 Polyhedra

When a list of polyhedra is displayed in the lower half of the Objects page (Fig. 12.18), the first column (polyhedra) gives crystallographic sites grouped by elements. The second column (C) shows colors and opacities of polyhedra. The third and fourth columns (S and V) control selection states and visibilities of polyhedra, respectively. If polyhedral properties of an element are edited, the modifications are applied to all the sites of the element.

Objects						
TiO2 (X-ray diffraction data)						
Atoms		Bonds	Polyhedra	Slices		
TiO2 shape						Shape
Site	$r(\text{\AA})$	C	L	S	V	
Ti	1.00		<input type="checkbox"/>	<input type="checkbox"/>	<input checked="" type="checkbox"/>	
Ti	1.00		<input type="checkbox"/>	<input type="checkbox"/>	<input checked="" type="checkbox"/>	
O	0.74		<input type="checkbox"/>	<input type="checkbox"/>	<input checked="" type="checkbox"/>	
O	0.74		<input type="checkbox"/>	<input type="checkbox"/>	<input checked="" type="checkbox"/>	

Figure 12.16: The Objects tab in the Side Panel showing a list of crystallographic sites for the first phase.

Bond	S	$r/w$	C	S	V
H - O	5	5.0 px		<input type="checkbox"/>	<input checked="" type="checkbox"/>
H - O	1	0.25 $\text{\AA}$		<input type="checkbox"/>	<input checked="" type="checkbox"/>
Si - O	1	0.25 $\text{\AA}$		<input type="checkbox"/>	<input checked="" type="checkbox"/>
Mn - O	1	0.25 $\text{\AA}$		<input type="checkbox"/>	<input checked="" type="checkbox"/>

Figure 12.17: A list of bond specifications in the Objects tab of the Side Panel.

Polyhedra	C	S	V
Mn		<input type="checkbox"/>	<input checked="" type="checkbox"/>
MnMn1		<input type="checkbox"/>	<input checked="" type="checkbox"/>
MnMn2		<input type="checkbox"/>	<input checked="" type="checkbox"/>
MnMn3		<input type="checkbox"/>	<input checked="" type="checkbox"/>
Si		<input type="checkbox"/>	<input checked="" type="checkbox"/>
Si1		<input checked="" type="checkbox"/>	<input checked="" type="checkbox"/>
Si2		<input type="checkbox"/>	<input checked="" type="checkbox"/>
Si3		<input type="checkbox"/>	<input checked="" type="checkbox"/>

Figure 12.18: A list of polyhedra in the Objects tab of the Side Panel.

### 12.2.5 Slices

When a list of slices is displayed in the lower half of the Objects page (**Fig. 12.19**), the first column (Slice) gives Miller indices of slices. The second column ( $d(\text{\AA})$ ) is distances from the origin to the slices, and the third column (C) shows colors and opacities of slices.

Slice	$d(\text{\AA})$	C
{0 1 1}	0.00	Red
{1 0 0}	2.30	Blue

Figure 12.19: A list of slices in the Objects tab of the Side Panel.

### 12.2.6 Shapes

When a list of forms and faces of crystal morphologies is displayed in the lower half of the Objects page (**Fig. 12.20**), the first row is assigned to a special item to control a color of shape in the “Unicolor” style and the visibility of labels all at once. The first column (Face) gives Miller indices of faces grouped by crystallographically equivalent forms. The second column ( $d(\text{\AA})$ ) is distances from the origin to faces, and the third one (C) shows colors and opacities of faces. The fourth column (L) controls the visibility of labels for faces. If properties of a form are edited, the modifications are applied to all the faces that are crystallographically equivalent.

Face	$d(\text{\AA})$	C	L
Unicolor	-	Blue	Visible
{1 0 0}	10.00	Red	Visible
(1 0 0)	10.00	Red	Visible
(-1 0 0)	10.00	Red	Visible
{1 0 1}	7.50	Cyan	Visible
(1 0 1)	7.50	Cyan	Visible
(-1 0 -1)	7.50	Cyan	Visible
{0 1 0}	7.00	Magenta	Visible
(0 1 0)	7.00	Magenta	Visible
(0 -1 0)	7.00	Magenta	Visible
{1 0 -1}	10.00	Green	Visible
(1 0 -1)	10.00	Green	Visible

Figure 12.20: A list of forms and faces of crystal morphologies in the Objects tab of the Side Panel.

# Chapter 13

## OVERALL APPEARANCE

The Overall Appearance dialog box (**Fig. 13.1**) appears on selection of the “Overall appearance...” item under the “View” menu.

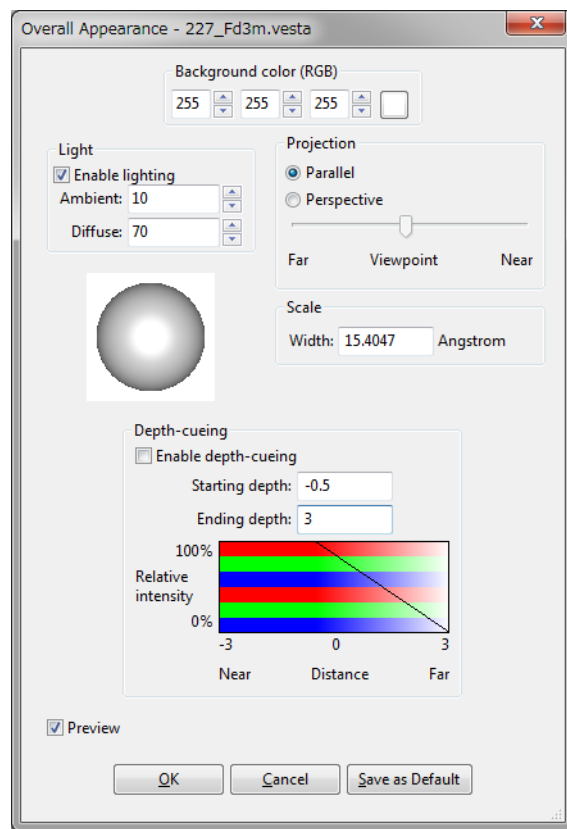


Figure 13.1: Overall Appearance dialog box.

### 13.1 Background

The background color is specified with three values in between 0 to 255, or selected from a color selection dialog box after clicking the button at the right of the text boxes.

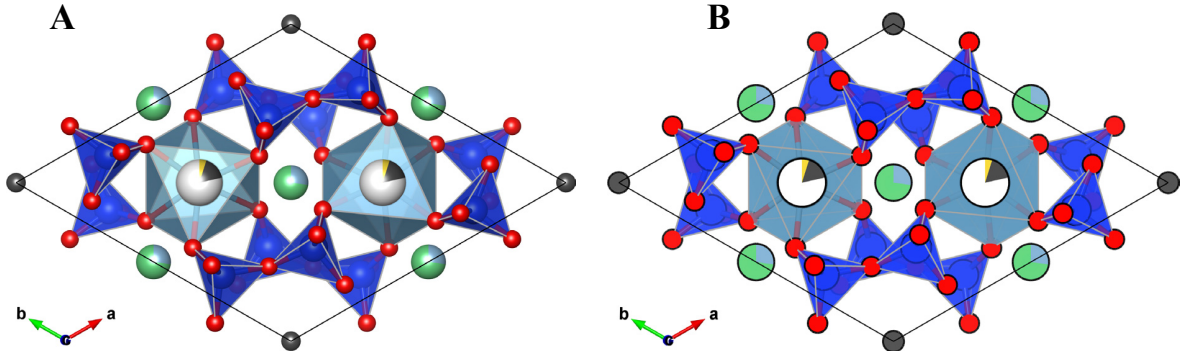


Figure 13.2: Crystal structure of milarite drawn with light effects (A) enabled and (B) disabled.

## 13.2 Lighting

When option “Enable lighting” is checked, the following light properties are set. When lighting is disabled, the resulting figure looks like a traditional 2D plot with no gradients ([Fig. 13.2](#)).

- **Ambient:** A light that comes from all directions equally and is scattered in all directions equally by objects. Specified by a value in between 0 to 100.
- **Diffuse:** A light that comes from a particular direction and hits objects with an intensity that depends on the orientation of their surfaces. However, once the light hits a surface, it reflects evenly off a surface and radiates in all directions. Specified by a value in between 0 to 100.
- **Lighting direction:** This can be changed by dragging the “track ball” placed below the “Lighting” frame box.

Even though the ambient and diffuse lights are evenly reflected, some part of lights are reflected more in the manner of a mirror where most of the light bounces off in a particular direction. A light having such a reflection component is called “specular” light. In VESTA, the intensity of the specular light is fixed at 100 %, and a color of a reflected specular light, *i.e.*, “specular color” is controlled by two properties of objects, {Specular} and {Shininess}. The final color of a surface is the sum of all three components of lights. A object surface appears to be brighter than the color of object if the specular light is reflected in the direction of viewpoint.

## 13.3 Projection Mode

- **Parallel:** Objects are rendered by parallel projection.
- **Perspective:** Objects are rendered by perspective projection. Accentuation of the perspective view is controlled by the slider placed below the radio button.

[Figure 13.3](#) shows the structure of post-perovskite,  $\text{MgSiO}_3$  [82], visualized in the parallel and perspective modes.

$$f = \frac{\text{end} - z}{\text{end} - \text{start}}. \quad (13.1)$$

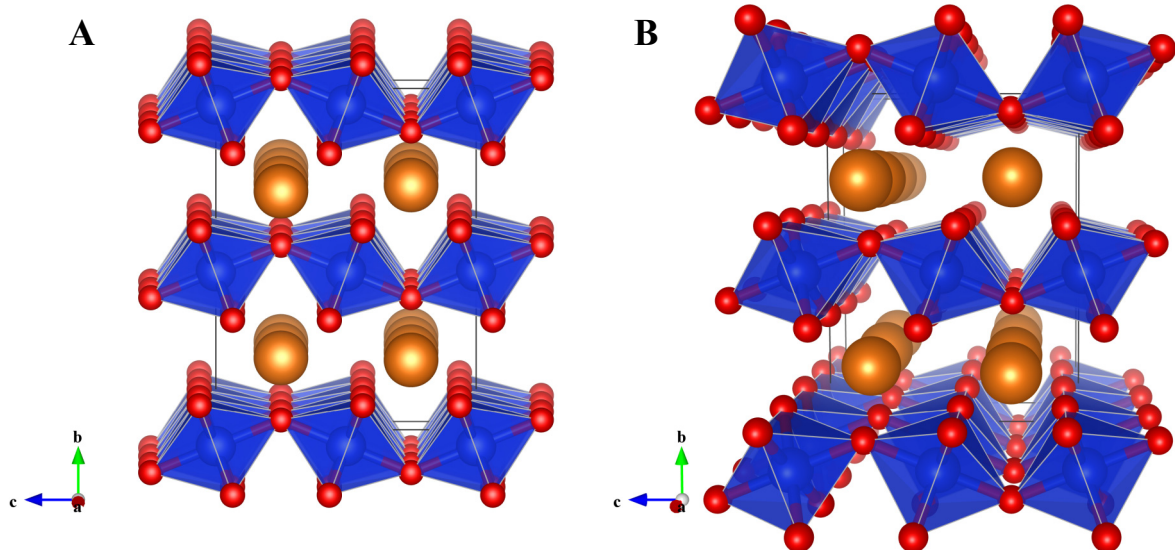


Figure 13.3: Crystal structure of post-perovskite, a high-pressure form of  $\text{MgSiO}_3$ , rendered by (A) parallel and (B) perspective projections.

### 13.4 Depth-Cueing

Depth-cueing blends a “fog” color with the original color of each object using the blending factor  $f$ . The factor  $f$  at depth  $z$  is computed by both of the starting depth,  $start$ , and the ending depth,  $end$ , are input by the user. VESTA automatically assigns the background color of the **Graphics Area** to the fog color  $C_f$ . Then, the color of a rendering object,  $C_r$ , is replaced by

$$C'_r = f * C_r + (1 - f) * C_f. \quad (13.2)$$

When VESTA renders objects in the **Graphics Area**, internal coordinates of the OpenGL scene are normalized in such a way that a radius of the bounding sphere for the scene becomes 0.9 and that the center of the scene is placed at 0. Objects at  $z < start$  are clearly rendered without any fog whereas objects at  $z > end$  are completely invisible.

Depth-cueing can be enabled or disabled in check box **Enable depth-cueing**. The effect of depth-cueing is schematically displayed below the two text boxes **Starting depth** and **Ending depth**.

**Figure 13.4** illustrates the effect of depth-cueing on images of mordenite [83] viewed along the  $c$  axis in the perspective-projection mode.

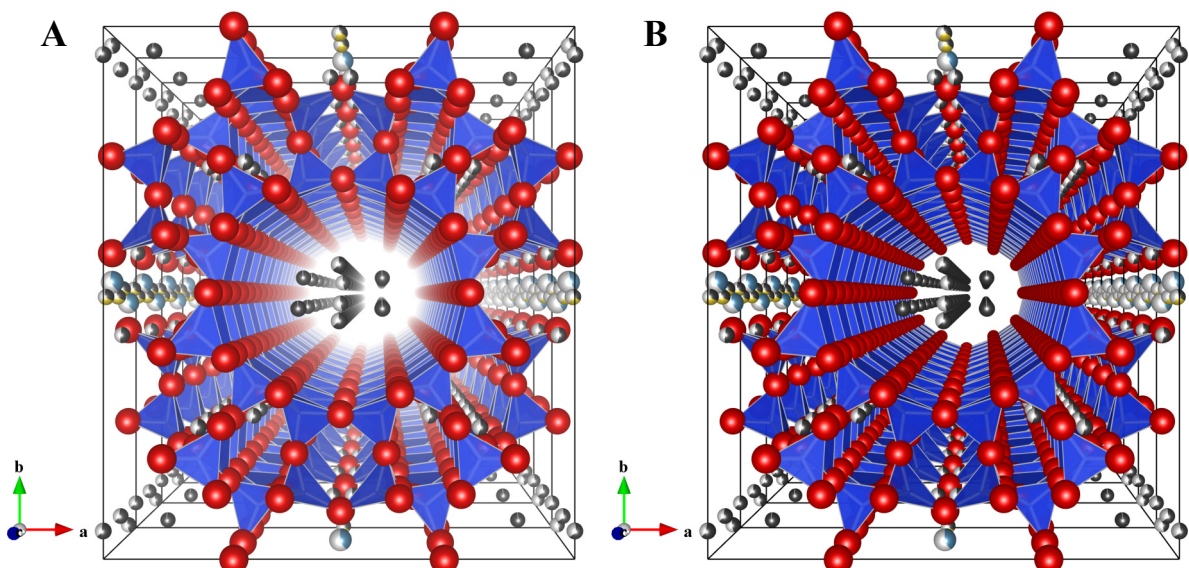


Figure 13.4: Crystal structure of mordenite rendered with and without depth-cueing. (A) Depth-cueing enabled by setting *start* and *end* parameters at -1.2 and 1.0, respectively. (B) Depth-cueing disabled.

# Chapter 14

## UTILITIES

### 14.1 Equivalent Positions

The Equivalent Positions dialog box (Fig. 14.1) appears on selection of the “Equivalent Positions...” item under the “Utilities” menu.

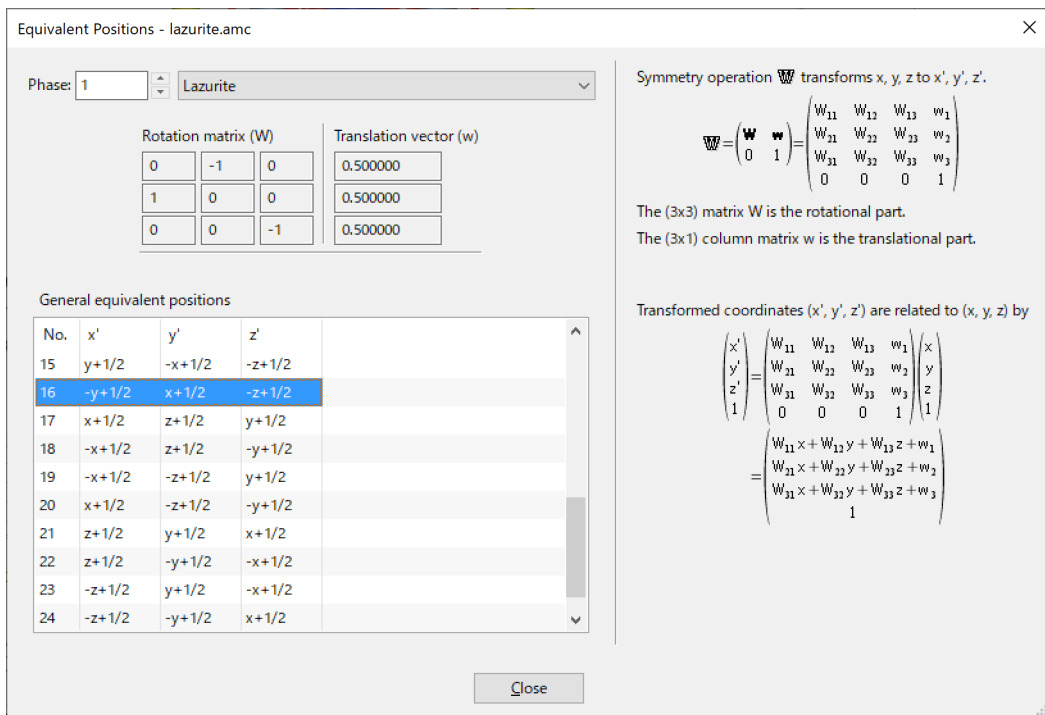


Figure 14.1: Equivalent Positions dialog box.

A list of general equivalent positions is displayed in this dialog box. When one of the equivalent positions in the list is selected, the corresponding symmetry operation is displayed in a matrix form at the upper left of the dialog box. In the right side of this dialog box, symmetry operation  $\bar{W}$  and transformation of fractional coordinates  $(x, y, z)$  with it are explicitly described (see 6.2.6).

In the case of magnetic space groups, the time reversal term  $t$  and the resultant magnetic moments  $mx$ ,  $my$ , and  $mz$  are also displayed in the list as well as the  $x$ ,  $y$ ,  $z$  notation of general positions.

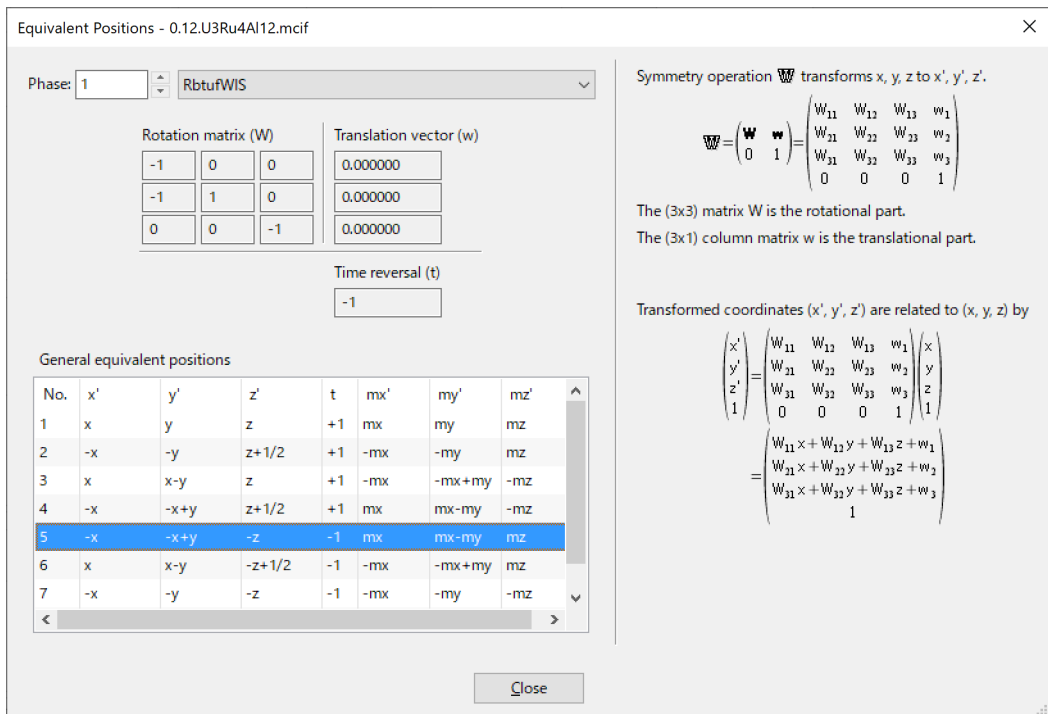


Figure 14.2: The Equivalent Positions dialog box showing magnetic data.

## 14.2 Geometrical Parameters

This dialog box lists interatomic distances and bond angles recorded in a file \*.ffe output by ORFFE [45]. ORFFE calculates geometrical parameters from crystal data in file \*.xyz created by RIETAN-FP [12], outputting them in file \*.ffe. When reading in input and/or output files of RIETAN-FP (\*.ins, \*.lst), VESTA also inputs \*.ffe automatically provided that \*.ffe shares the same folder with \*.lst and/or \*.ins. Otherwise, \*.ffe can be input by clicking the [Read \*.ffe] button in the Geometrical Parameters dialog box.

VESTA allows us to locate the bonds and bond angles displayed in the Geometrical Parameters dialog box in the Graphic Area. On selection of a bond (2 atoms) or a bond angle (3 atoms) in this dialog box, the corresponding objects in a ball-and-stick model is selected (highlighted), and *vice versa*. Thus, atom pairs and triplets associated with geometrical parameters on which restraints are imposed in Rietveld analysis with RIETAN-FP are easily recognized in the ball-and-stick model.

**Figure 14.3** exemplifies visualization of a bond in a ball-and-stick model of fluorapatite; a P–O<sub>3</sub> bond (grey line) selected in the dialog box is highlighted in the structural model in the graphic window. The upper part of the dialog box displays detailed information on the P–O<sub>3</sub> bond.

Because ORFFE calculates standard uncertainties of geometrical parameters from both diagonal and off-diagonal terms in the variance-covariance matrix output by RIETAN-FP, the resulting standard uncertainties are more accurate than those evaluated by VESTA from only the diagonal terms. Accordingly, the standard uncertainties output by ORFFE should be described in papers rather than those calculated by VESTA.

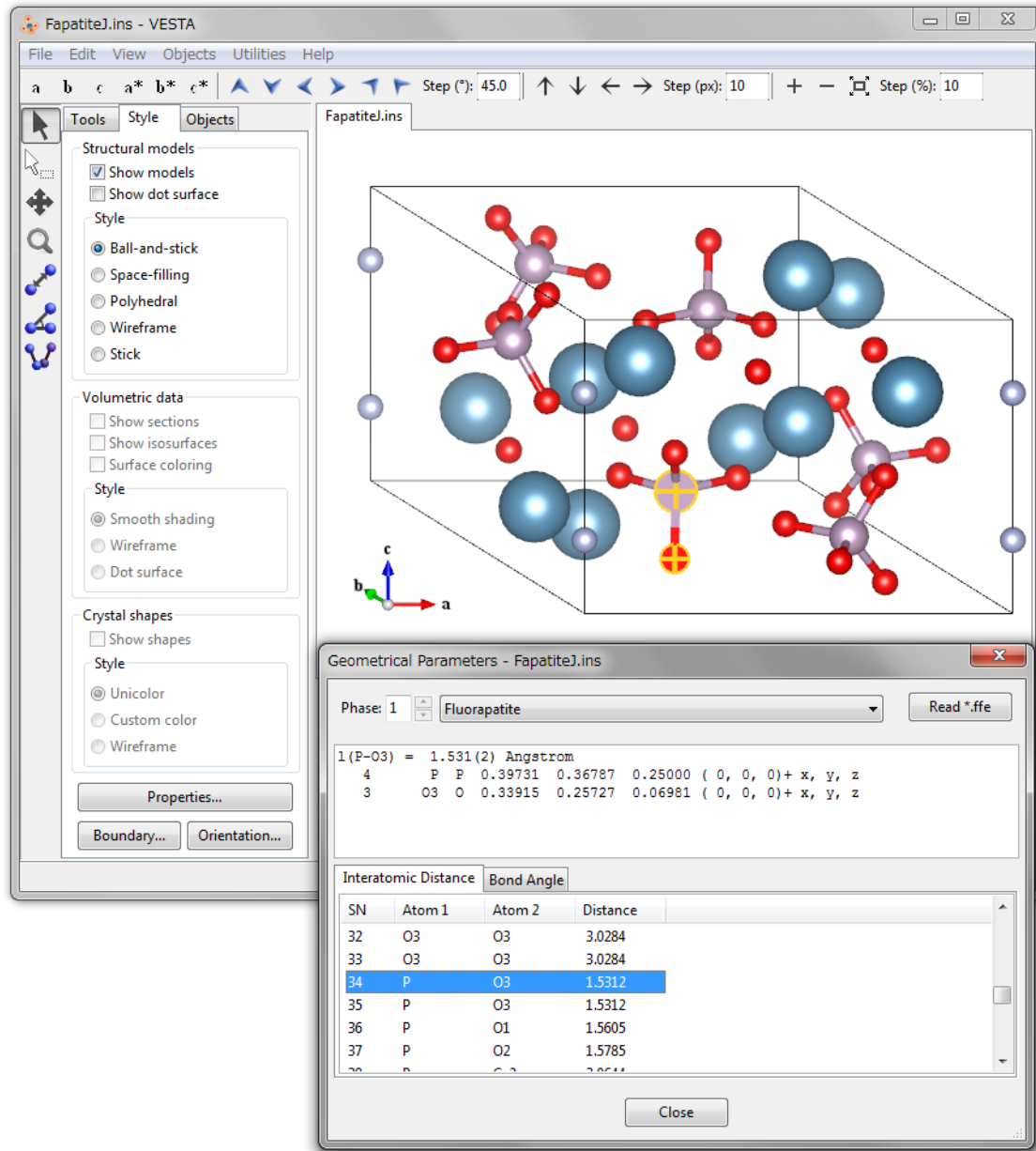


Figure 14.3: The Geometrical Parameters dialog box showing a list of bonds recorded for fluorapatite [84] in FapatiteJ.ffe.

### 14.3 Standardization of Crystal Data

On the use of RIETAN-FP [12], it is highly desirable for an axis setting and fractional coordinates to be standardized in compliance with definite rules [85]. In RIETAN-FP, the following lattice settings are inhibited:

1. monoclinic system:  $c$ -axis unique setting ( $\gamma \neq 90^\circ$ ),
2. trigonal system: rhombohedral lattice ( $a = b = c$  and  $\alpha = \beta = \gamma \neq 90^\circ$ ),
3. cubic and tetragonal systems: an inversion center not at the origin.

Unless standard settings are adopted, standardization of crystal axes and fractional coordinates is indispensable for Rietveld analysis using RIETAN-FP; otherwise LAZY PULVERIX [86] built in RIETAN-FP fails in generating diffraction indices  $hkl$  and their multiplicities.

Standardized crystal data are generally suitable for structure refinement because atoms in the asymmetric unit are confined in a relatively narrow region. VESTA is capable of launching STRUCTURE TIDY [46] for this purpose.

This feature of standardization of crystal-structure data is particularly useful when searching for compounds with similar structures using the Inorganic Crystal Structure Database (ICSD) [87].

In both STRUCTURE TIDY and LAZY PULVERIX, the following three standard settings are preferred to other settings:

1. monoclinic system:  $b$ -axis unique setting ( $\beta \neq 90^\circ$ ),
2. trigonal system: hexagonal lattice ( $a = b \neq c$  and  $\gamma = 120^\circ$ ),
3. centrosymmetric space groups: an inversion center at the origin.

Let  $n$  be the number of atoms in the asymmetric unit, and  $(x_j, y_j, z_j; j = 1, 2, \dots, n)$  their fractional coordinates. Then, the standardization parameter,  $\Gamma$ , is defined as

$$\Gamma = \sum_{j=1}^n \left( x_j^2 + y_j^2 + z_j^2 \right)^{\frac{1}{2}}. \quad (14.1)$$

Note that this equation does not contain occupancies,  $g_j$ . STRUCTURE TIDY selects a set of  $x_j$ ,  $y_j$  and  $z_j$  ( $j = 1, 2, \dots, n$ ) minimizing the  $\Gamma$  value. For better distinction between different structure-type branches, STRUCTURE TIDY further outputs another standardization parameter, CG, depending also on lattice parameters:

$$\begin{aligned} \text{CG} = & \frac{1}{nV} \left[ \left( a \sum_{j=1}^n x_j \right)^2 + \left( b \sum_{j=1}^n y_j \right)^2 + \left( c \sum_{j=1}^n z_j \right)^2 \right. \\ & \left. + 2ab \cos \gamma \left( \sum_{j=1}^n x_j y_j \right) + 2ac \cos \beta \left( \sum_{j=1}^n x_j z_j \right) + 2bc \cos \alpha \left( \sum_{j=1}^n y_j z_j \right) \right]^{\frac{1}{2}}, \end{aligned} \quad (14.2)$$

where  $V$  denotes the unit-cell volume.

VESTA automatically normalize the fractional coordinates between 0 to 1 before standardization of crystal-structure data because the absolute value of each fractional coordinate to be converted by STRUCTURE TIDY should be less than unity; otherwise, the corresponding part of the output text becomes disordered. If lattice parameters and fractional coordinates of atoms in the asymmetric unit are changed on the transformation of the crystal lattice, current crystal data are replaced with the standardized ones. The resulting data are output in the Text Area while standard input and output files of STRUCTURE TIDY are, respectively, saved as `data.stin` and `data.sto` in directory `tmp` under a directory for user settings (see 17.2); `data.sto` provides us with more detailed information on the standardization of the crystal data.

For example, suppose that a structure data file for Si (space group:  $Fd\bar{3}m$ ) is created on the basis of the first setting where Si in the asymmetric unit occupies the  $8a$  site at  $(0, 0, 0)$ . Subsequent standardization using STRUCTURE TIDY moves Si from  $(0, 0, 0)$  to  $(1/8, 1/8, 1/8)$  in such a way that a center of symmetry is present at the origin (second setting). When lattice parameters ( $a$  and  $\alpha$ ) and fractional coordinates based on a rhombohedral lattice are input in a trigonal compound, STRUCTURE TIDY converts them into lattice parameters ( $a$  and  $c$ ) and fractional coordinates based on a hexagonal lattice.

An example of standardization of crystal data is given below. The structure of a high- $T_c$  superconductor  $\text{YBa}_2\text{Cu}_4\text{O}_8$  is usually represented with the  $c$  axis perpendicular to the  $\text{CuO}_2$

conduction sheet and space group *Ammm* (No. 65) [88]. However, the standard setting described in *International Tables for Crystallography*, volume A [30] is *Cmmm*; Rietveld analysis with RIETAN-FP has to be carried out on the basis of *Cmmm*.

Running STRUCTURE TIDY by selecting the “Standardization of Crystal Data” item under the “Utilities” menus in VESTA, we obtain optimum crystal data based on space group *Ammm*; they are listed at the tail of `data.sto`:

Axes changed to : b,c,a

```
Setting x,y,z          origin  0.00000 0.00000 0.00000   gamma =  2.9785
( 65) C m m m      - j2 i5 c          oS30
-----
DATA  YBa2Cu4O8          2.9785  0.7284
CELL    3.8708 27.2309  3.8402          *
ATOM   01     4(j)   0    0.05253  1/2      02
ATOM   Ba     4(j)   0    0.36498  1/2      Ba
ATOM   Cu1    4(i)   0    0.06138  0        Cu2
ATOM   02     4(i)   0    0.14562  0        01
ATOM   Cu2    4(i)   0    0.21296  0        Cu1
ATOM   03     4(i)   0    0.28178  0        04
ATOM   04     4(i)   0    0.44786  0        03
ATOM   Y      2(c)  1/2    0    1/2        Y
TRANS b,c,a
REMARK Transformed from setting A m m m.
```

STRUCTURE TIDY converted *a*, *b*, and *c* axes in *Ammm* into *b*, *c*, and *a* axes in *Cmmm*, respectively. The value of **2.9785** is the standardization parameter ‘gamma’, the last data, **0.7284**, in the ‘DATA’ line is CG, and the last data of each site is the site name input by the user.

## 14.4 Niggli-Reduced Cell

Low-symmetry unit cells can be selected in a variety of ways regardless of the method of determining the unit cell suitable for indexing the whole diffraction pattern. To compare and analyze different indexing solutions, the lattice has to be reduced to a certain unique, preferably standard form, which is usually achieved in the following way [89]:

- In the orthorhombic system, the lattice parameters should be  $a \leq b \leq c$ .
- In the monoclinic system, the lattice parameters should be  $a \leq c$  with the *b*-axis unique setting.
- In the triclinic system, the reduction becomes more complicated owing to possible multiple choices of basis vectors in the lattice.

Niggli’s approach to unit-cell reduction [89, 90] defines the reduced cell in terms of the shortest vectors:

$$\nu_1 + \nu_2 + \nu_3 = \text{minimum}. \quad (14.3)$$

STRUCTURE TIDY [46] transforms the given unit cell to a Niggli-reduced cell to describe the structure in space group *P1* or *P̄1* when ‘\*’ precedes a space-group symbol in an input file. If the Niggli-reduction is successful, the solution is output in the Text Area.

From the reduced form, we can obtain the metric symmetry of the lattice, which is the highest symmetry possible for the lattice on the basis of only geometric considerations. A

second application of the Niggli-reduced cell is that different deformation variants of a basis type (arstotype), probably conventionally described with different space groups and probably non-comparable unit cells, can be compared if they have been standardized in their corresponding Niggli-reduced cells.

The output in the Text Area on transformation to a Niggli-reduced cell for a spinel-type oxide  $\text{CoAl}_2\text{O}_4$  is given below:

Lattice type F  
 Space group name F d -3 m  
 Space group number 227  
 Setting number 1

## Lattice parameters

a	b	c	alpha	beta	gamma
8.09500	8.09500	8.09500	90.0000	90.0000	90.0000

Unit-cell volume = 530.457520

## Structure parameters

```

      x           y           z           g           B       Site   Sym.
 1 Co  Co1    0.00000  0.00000  0.00000  1.000  1.000    8a -43m
-----
```

18 atoms, 16 bonds, 0 polyhedra; CPU time = 0 ms

## Transformation to a Niggli-reduced cell

Setting x,y,z origin 0.00000 0.00000 0.00000 gamma = 0.2165  
ratio volume Niqqli-reduced cell/original cell : 0.25

$$(-2) \cdot P - 1 = i \cdot aP_2$$

```

DATA                               0.2165  0.3437
CELL      5.7240  5.7240  5.7240   60.000   60.000   60.000   *
ATOM    Co        2(i)   0.12500  0.12500  0.12500                         Co1
TRANS   0.5a+0.5b,0.5b+0.5c,0.5a+0.5c
REMARK Niggli-reduced cell

```

## 14.5 Site Potentials and Madelung Energy

VESTA utilizes an external program, MADEL [91], to calculate electrostatic site potentials,  $\phi_i$ , and the Madelung energy,  $E_M$ , of a crystal. Three methods are used to calculate Madelung energies: Ewald, Evjen, and Fourier methods; the Fourier method is adopted in MADEL. MADEL was originally written by Katsuo Kato (old National Institute for Research in Inorganic Materials) and slightly modified later by one of the authors (F.I.). An advantage of using MADEL in VESTA is that troublesome inputting of formatted data, particularly symmetry operations, is avoidable.

The electrostatic potential,  $\phi_i$ , for site  $i$  is computed by

$$\phi_i = \sum_j \frac{Z_j}{4\pi\epsilon_0 l_{ij}}, \quad (14.4)$$

where  $Z_j$  is the valence (oxidation state) of the  $j$ th ion in the unit of the elementary charge,  $e$  ( $= 1.602177 \times 10^{-19}$  C),  $\epsilon_0$  is the vacuum permittivity ( $= 8.854188 \times 10^{-12}$  F m $^{-1}$ ), and  $l_{ij}$  is the

distance between ions  $i$  and  $j$ ; the summation is carried out over all the ions  $j$  ( $i \neq j$ ) in the crystal. In case site  $j$  is partially occupied,  $Z_j$  should be multiplied by its occupancy,  $g_j$ .  $E_M$  per asymmetric unit is calculated by using the formula

$$E_M = \frac{1}{2} \sum_i \phi_i Z_i W_i, \quad (14.5)$$

with

$$W_i = \frac{(\text{occupancy}) \times (\text{number of equivalent positions})}{(\text{number of general equivalent positions})}. \quad (14.6)$$

The summation in Eq. (14.5) is carried out over all the sites in the asymmetric unit. To obtain the Madelung energy for the unit cell,  $E_M$  must be multiplied by the number of general equivalent positions.

Prior to the execution of MADEL, the oxidation numbers of atoms in the asymmetric unit must be input in the Structure parameters tab of the Edit Data dialog box. Just after launching MADEL, you are prompted to input two parameters, RADIUS and REGION:

RADIUS: Radius of an ionic sphere,  $s$ , in Å. The charge-density distribution,  $r$ , is given by

$$\rho(r) = \rho_0 [1 - 6(r/s)^2 + 8(r/s)^3 - 3(r/s)^4], \quad (14.7)$$

where  $r$  is the distance from the center of the ionic sphere ( $r < s$  and  $\rho(r) = 0$  for  $r \geq s$ ). When lines for interstitial sites are not given in the input file, set RADIUS at a value that is large enough but less than the smallest interatomic distance (not half of it!).

REGION: Reciprocal-space range (in Å<sup>-1</sup>) within which Fourier coefficients are summed up. MADEL sums up the Fourier coefficients with respect to all  $hkl$ 's within a sphere having a radius equal to RADIUS. Choose an appropriate value ranging from 2 Å<sup>-1</sup> to 4 Å<sup>-1</sup> according to the desired precision of calculation. Also, check whether or not a curve for Madelung energy versus REGION is nearly flat around the selected value of REGION.

The standard output of MADEL is displayed in the Text Area. The unit of  $\phi_i$  is  $e/\text{\AA}$  ( $1 e/\text{\AA} = 14.39965 \text{ V}$ ). The accuracy of  $\phi_i$  and  $E_M$  obtained using MADEL is limited to 3 or 4 digits.

The following lines give part of an output file when this feature is applied to investigating distribution of hole carriers in a high- $T_c$  superconductor,  $\text{YBa}_2\text{Cu}_4\text{O}_8$  [88, 92]:

#### Potentials of sites in the asymmetric unit

	Charge	W	X	Y	Z	phi
Ba	2.000000	0.250000	0.500000	0.135000	0.500000	-1.330304E+00
Y	3.000000	0.125000	0.500000	0.000000	0.500000	-1.639974E+00
Cu1	2.000000	0.250000	0.000000	0.213000	0.000000	-2.164424E+00
Cu2	2.500000	0.250000	0.000000	0.061400	0.000000	-1.798502E+00
01	-2.000000	0.250000	0.000000	0.145600	0.000000	1.310975E+00
02	-2.000000	0.250000	0.000000	0.052500	0.500000	1.931017E+00
03	-2.000000	0.250000	0.500000	0.052100	0.000000	1.925720E+00
04	-2.000000	0.250000	0.500000	0.218200	0.000000	1.133873E+00

#### Electrostatic energy per asymmetric unit

-3.318605 e\*\*2/\AA = -47.78676 eV = -4.610721 MJ/mol

The electrostatic energy per mole is calculated by multiplying a factor of the Avogadro constant ( $6.02214 \times 10^{23} \text{ mol}^{-1}$ ) and  $E_M$  together. In the above calculation, all the holes are assumed

to be doped into the Cu<sub>2</sub> atoms on the CuO<sub>2</sub> conduction sheet with the Cu<sub>1</sub> atoms having an oxidation state of +2.

Standard input files, \*.pme, (see p. 141) for MADEL can be output by selecting the Export Data... item under the File menu. This file is helpful in appending fractional coordinates of interstitial sites to obtain their site potentials using the RIETAN-FP–VENUS integrated assistance environment.

## 14.6 Powder Diffraction Pattern

VESTA utilizes RIETAN-FP [12] to simulate X-ray and neutron powder diffraction patterns from lattice and structure parameters. As described in 16.1, a binary executable file of RIETAN-FP, a graph plotting program, and a template input file, \*.ins, for RIETAN-FP are specified in the Preferences dialog box. Setting a variable **NMODE** at 1 (simulation of a powder diffraction pattern) in the template file is recommended. In addition, change the following data in the template file if necessary:

- Radiation (neutron, characteristic X-ray, or synchrotron X-ray diffraction).
- Wavelength (neutron and synchrotron X-ray diffraction) or target (diffraction using characteristic X rays).
- Geometry (Bragg–Brentano, transmission, or Debye–Scherrer geometry).
- Profile functions and profile parameters.
- Range of diffraction angles:  $2\theta_{\min}$  and  $2\theta_{\max}$ .
- Profile cutoff.

Profile parameters refined from typical diffraction data measured on a powder diffractometer, which is often used on a routine basis, are preferable to those in one of template files included in the distribution files of the RIETAN-FP–VENUS system. Further, a variable, **NPAT**, must be given in the template file to specify a graph plotting program:

1. **NPAT = 1**: a pair of files, \*.plt including commands to plot a graph and \*.gpd storing data to be graphed, for gnuplot<sup>1</sup> (default),
2. **NPAT = 2**: an Igor text file, \*.itx, for Igor Pro<sup>2</sup> or WinPLOTR,<sup>3</sup>
3. **NPAT = 3**: a text file, \*.itx, for RietPlot.<sup>4</sup>

The use of gnuplot is highly recommended because it is free software supporting many features; commands may be modified and added in \*.plt to change the appearance of a graph. For details in the content of \*.plt, refer to RIETAN-FP\_manual.pdf. If **NPAT = 1**, no graph plotting program need to be specified in the Preferences dialog box.

Stable versions of gnuplot are included in the distribution files of the RIETAN-FP–VENUS system<sup>5</sup> for Windows and macOS.

Gnuplot can output a PDF file, \*.pdf, whose margins are automatically cut, which is very convenient when exporting the resulting PDF file to an application such as T<sub>E</sub>X, Microsoft PowerPoint and Word, and Adobe Illustrator. (Windows) or ps2pdf (macOS).

<sup>1</sup><http://www.gnuplot.info/>

<sup>2</sup><http://www.wavemetrics.com/>

<sup>3</sup><http://www.llb.cea.fr/winplotr/winplotr.htm>

<sup>4</sup>[http://www.nims.go.jp/denzai/publ\\_rietplot.html](http://www.nims.go.jp/denzai/publ_rietplot.html)

<sup>5</sup>[http://fujioizumi.verse.jp/download/download\\_Eng.html](http://fujioizumi.verse.jp/download/download_Eng.html)

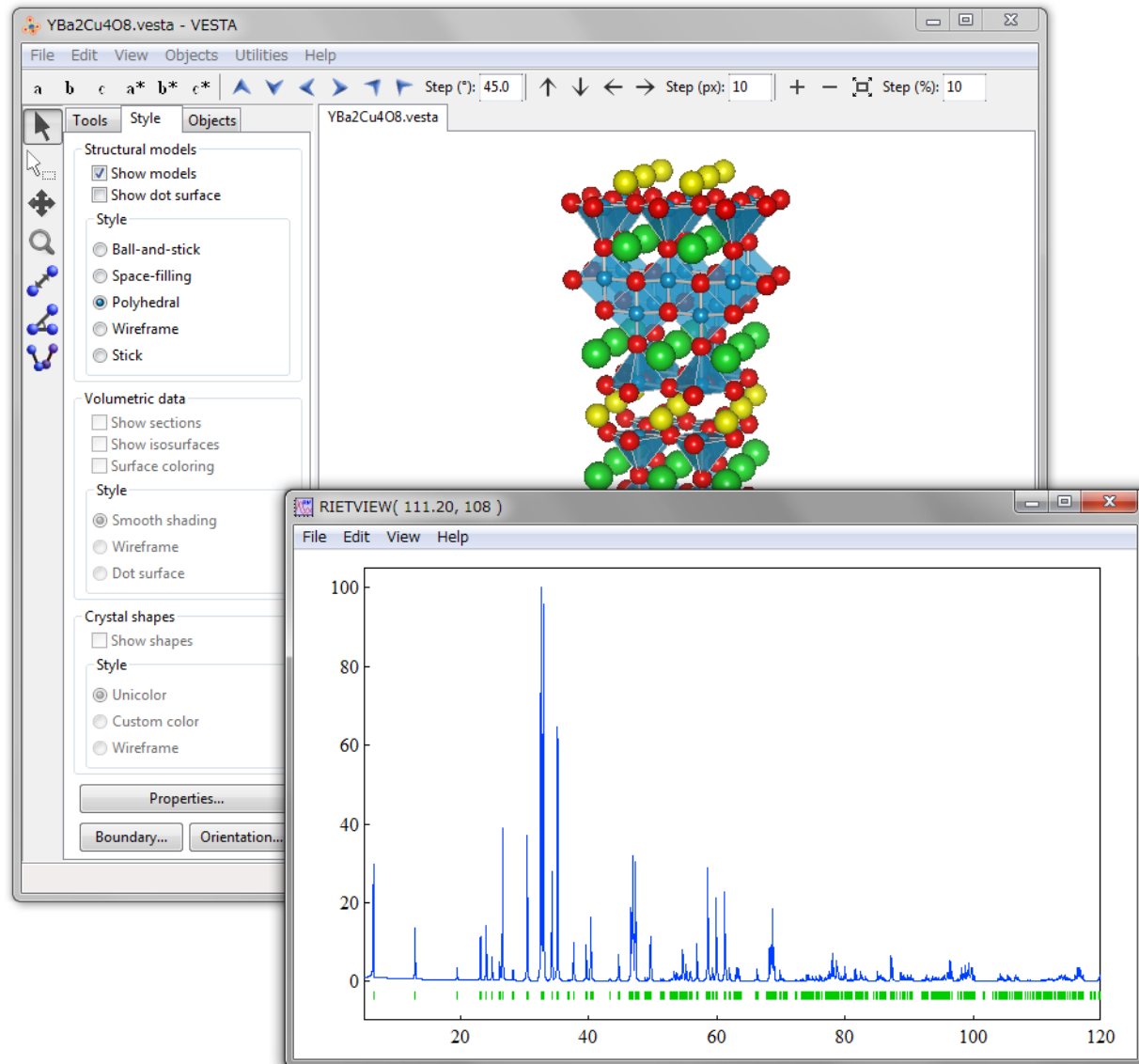


Figure 14.4: Simulation of an X-ray powder diffraction pattern of a high- $T_c$  superconductor, YBa<sub>2</sub>Cu<sub>4</sub>O<sub>8</sub> [88], which was plotted with Igor Pro.

On selection of the “Powder Diffraction Pattern...” item under the “Utilities” menu, a series of procedures, *i.e.*, (a) generation of an input file, \*.ins, for RIETAN-FP, (b) execution of RIETAN-FP in the simulation mode (**NMODE** = 1), and (c) representation of the resulting text file(s) by a graphing program are executed by VESTA as if the two programs were implemented in VESTA (Fig. 14.4). Text files, \*.ins, \*.lst (standard output), and a pair of files (\*.plt and \*.gpd for gnuplot) or \*.itx, output by RIETAN-FP are saved in folder tmp under the settings directory (see 17.2).

For those who have not any program to plot data in \*.itx with the Igor text format, a small Java program named PowderPlot,<sup>6</sup> which was developed by one of the authors (K.M.), is included in the archive file of VESTA.

VESTA automatically standardizes lattice settings when outputting \*.ins to satisfy conditions required by LAZY PULVERIX [86], which is embedded in RIETAN-FP to generate

<sup>6</sup><http://jp-minerals.org/powderplot/>

diffraction indices,  $hkl$ , and their multiplicities,  $m$ . Standard lattice settings adopted in LAZY PULVERIX are just the same as those in STRUCTURE TIDY (see 14.3) [85, 46]: second settings in centrosymmetric space groups with more than one origin choice and first settings in the other space groups. Then, beware that diffraction indices displayed in PowderPlot are incompatible with the coordinate system adopted in VESTA if the lattice setting in VESTA is other than a standard one.

A list of reflections output at the tail of \*.lst if **NPRINT > 0** provides us with a variety of information about  $hkl$  reflections included in a  $2\theta$  range specified by the user. For instance, simulation of an X-ray diffraction pattern for fluorapatite gives the following output where line heads were deleted for convenience:

<b>h</b>	<b>k</b>	<b>l</b>	<b>Code</b>	<b>2-theta</b>	<b>d</b>	<b>Ical</b>	<b> F(crys) </b>	<b> F(magn) </b>	<b>POF</b>	<b>FWHM</b>	<b>m</b>	<b>Dd/d</b>
1	0	0	+1	10.895	8.11382	12287	16.7800	-	1.001	0.07451	6	0.013637
1	0	0	+2	10.923	8.11382	6113	16.7800	-	1.001	0.07451	6	0.013602
1	0	1	+1	16.877	5.24919	4465	11.1545	-	0.999	0.07443	12	0.008757
1	0	1	+2	16.919	5.24919	2221	11.1545	-	0.999	0.07443	12	0.008734
1	1	0	+1	18.929	4.68452	2079	12.0931	-	1.001	0.07445	6	0.007795
1	1	0	+2	18.976	4.68452	1034	12.0931	-	1.001	0.07445	6	0.007775
2	0	0	+1	21.891	4.05691	9679	30.2953	-	1.001	0.07453	6	0.006726
2	0	0	+2	21.946	4.05691	4814	30.2953	-	1.001	0.07453	6	0.006709
1	1	1	+1	22.945	3.87283	8580	21.1855	-	1.000	0.07457	12	0.006413
1	1	1	+2	23.003	3.87283	4268	21.1855	-	1.000	0.07458	12	0.006397
.....												

where **Code +1** and **Code +2** are, respectively,  $K\alpha_1$  and  $K\alpha_2$  reflections ('+' means not  $\bar{h}\bar{k}\bar{l}$  but  $hkl$  reflection in Friedel pairs), **2-theta** is the diffraction angle  $2\theta$ , **d** is the lattice-plane spacing, **Ical** is the calculated integrated intensity adjusted in such a way that the strongest reflection has an intensity of  $10^5$ , **F(nucl)** and **F(magn)** are, respectively, the crystal-structure and magnetic-structure factors, **POF** is the preferred-orientation function, **FWHM** is the full-width at the half-maximum intensity, **m** is the multiplicity, and **Dd/d** is the resolution,  $\Delta d/d$ .

## 14.7 Structure Factors

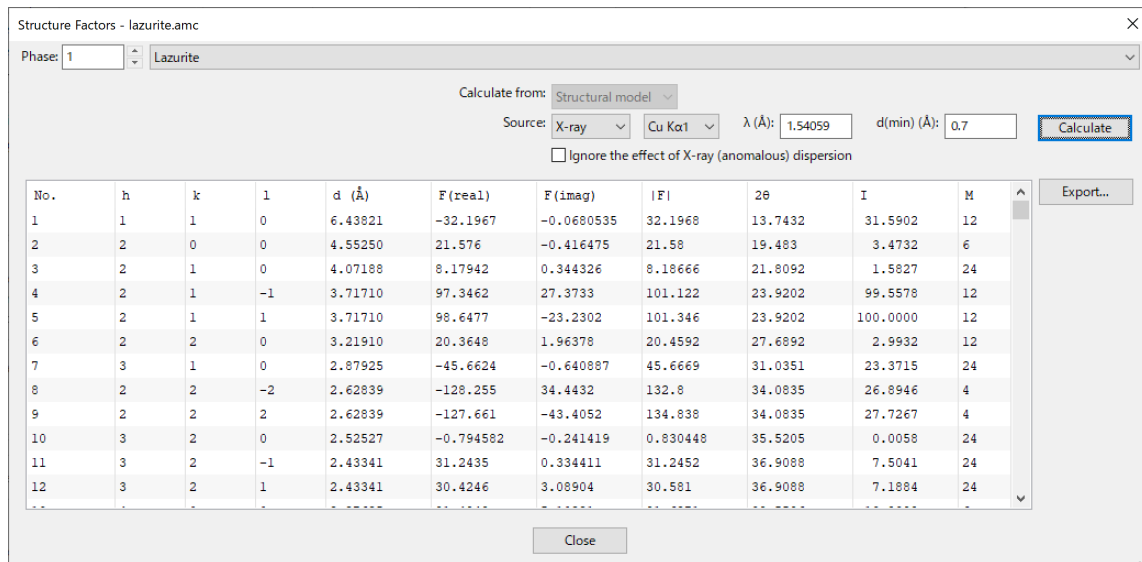


Figure 14.5: Structure Factors dialog box.

Selection of “Utilities” menu ⇒ “Structure Factors...” pops up the Equivalent Positions dialog box (Fig. 14.5), whose use makes it possible to calculate structure factors from structural models (structure parameters) or volumetric data (electron or coherent-scattering length densities,  $\rho$ ).

If multiple phase data are included in the data set, select a phase, for which structure factors are calculated, at the top of the dialog box. If the phase data contain both structural and volumetric data, select {Structural model} or {Volumetric data} in the list box to specify the type of data from which structure factors are calculated. In the Source list box, {X-ray} and {Neutron} beam sources can be switched, and some typical characteristic X-rays can be selected at a list box next to the Source list box. For the neutron source and the X-ray source with its target specified as {Custom}, the wavelength can be edited in the text box. The minimum lattice-plane spacing,  $d$ , of reflections whose structure factors are calculated is also specified in the text box.

In X-ray diffraction, structure factor  $F$  of reflection  $\mathbf{h}$  with diffraction indices  $hkl$  is formulated as

$$F(\mathbf{h}) = \sum_{j=1}^n g_j f_j(\mathbf{h}) T_j(\mathbf{h}) \exp[2\pi i(hx_j + ky_j + lz_j)], \quad (14.8)$$

where  $j$  is the atom number,  $n$  is the total number of atoms in the unit cell,  $g_j$  is the occupancy,  $f_j(\mathbf{h})$  is the (X-ray) atomic form factor,  $T_j(\mathbf{h})$  is the Debye–Waller factor, and  $x_j$ ,  $y_j$ , and  $z_j$  are the fractional coordinates. The atomic form factor  $f(\mathbf{h})$  is a complex number that can be divided into four separate components as

$$f(\mathbf{h}) = f_0(\mathbf{h}) + f' + i f'' + f_{NT}, \quad (14.9)$$

where  $f_0(\mathbf{h})$  is the coherent scattering factor,  $f'$  and  $f''$  are the real and imaginary components of the dispersion correction, and  $f_{NT}$  is the nuclear Thomson scattering [93]. The coherent atomic scattering factor  $f_0$ , which is a function of  $\sin \theta / \lambda$ , is usually analytically approximated by a sum of exponentials plus a constant:

$$f_0(\sin \theta / \lambda) = \sum_{i=1}^N a_i \exp\left(-b_i \frac{\sin^2 \theta}{\lambda^2}\right) + c. \quad (14.10)$$

VESTA utilizes a set of parameters ( $a_i$ ,  $b_i$ , and  $c$ ) with  $N = 5$  tabulated in [94]. These parameters can be used in the range of  $0 < \sin \theta / \lambda < 6$ . The real and imaginary parts,  $f'$  and  $f''$ , of the dispersion correction are calculated by linear interpolation of theoretically calculated form factors in energy ranges of  $E = 1\text{--}10$  eV and  $E = 0.4\text{--}1.0$  MeV [95, 96]. The nuclear Thompson scattering term  $f_{NT}$  is small and negative in the phase relative to the electronic form factor, with small (negligible) dependences on  $\lambda$  and  $\sin \theta / \lambda$ .

In the case of neutron diffraction,  $f_j(\mathbf{h})$  has to be replaced by the coherent-scattering length [10],  $b_c$ :

$$F(\mathbf{h}) = \sum_{j=1}^n g_j b_{cj} T_j(\mathbf{h}) \exp[2\pi i(hx_j + ky_j + lz_j)]. \quad (14.11)$$

The value of  $b_c$  is constant regardless of  $\mathbf{h}$  because scattering of neutrons by negligibly small atomic nuclei does not depend on  $\sin \theta / \lambda$  (in the absence of magnetic atoms).

On calculation of structure factors from structural models,  $a_i$ ,  $b_i$ ,  $c_i$ ,  $b_c$ ,  $f'$ ,  $f''$ ,  $f_{NT}$ , and the mass attenuation coefficient,  $\mu/\rho$  ( $\mu$ : linear attenuation coefficient,  $\rho$ : density), of each element are output in the Text Area as follows:

	a1	a2	a3	a4	a5	c
	b1	b2	b3	b4	b5	bc
Cu:	14.014192	4.784577	5.056806	1.457971	6.932996	-3.254477
	3.738280	0.003744	13.034982	72.554793	0.265666	7.718000
Se:	17.354071	4.653248	4.259489	4.136455	6.749163	-3.160982
	2.349787	0.002550	15.579460	45.181201	0.177432	7.970000
O:	2.960427	2.508818	0.637853	0.722838	1.142756	0.027014

14.182259 5.936858 0.112726 34.958481 0.390240 5.803000

X-ray dispersion coefficients for $\lambda = 0.154059$ nm			
f'	f''	f_NT	$\mu/\rho$ (cm <sup>2</sup> /g)
Cu: -2.02777E+00,	5.83511E-01,	-7.26020E-03,	5.01091E+01
Se: -7.87865E-01,	1.13462E+00,	-8.03140E-03,	7.75653E+01
O: 4.77543E-02,	3.20501E-02,	-2.19440E-03,	1.09804E+01

If all the parameters of some elements are 0, the element names are not recognized by the program; consequently, such elements do not contribute to calculated structure factors at all. The element names can be edited in the Structure parameters page of the **Edit Data** dialog box. When an option of “Ignore the effect of X-ray (anomalous) dispersion” is enabled,  $f'$ ,  $f''$ , and  $f_{NT}$  are set at 0, and none of these values are output in the **Text Area**.

Structure factors,  $F(\mathbf{h})$ , can be calculated by the Fourier transform of  $\rho(x, y, z)$ :

$$F(\mathbf{h}) = \iiint \rho(x, y, z) \exp[2\pi i(hx + ky + lz)] dx dy dz. \quad (14.12)$$

In the {Volumetric data} mode, Eq. (14.12) is approximated by numerical integration of discrete densities:

$$F(\mathbf{h}) = \sum_{x=0}^1 \sum_{y=0}^1 \sum_{z=0}^1 \rho(x, y, z) dV \exp[2\pi i(hx + ky + lz)]. \quad (14.13)$$

In this mode, only the minimum  $d$  value can be specified, and no other options affect calculation results.

## 14.8 Fourier Synthesis

On selection of “Utilities” menu  $\Rightarrow$  “Fourier Synthesis...”, structure factors can be imported from an external file to carry out Fourier synthesis from them to visualize one of observed, calculated, or difference densities. Prior to the use of this menu, lattice parameters and space-group symmetry have to be given. The **Fourier Synthesis** dialog box is used to import and edit structure factors (**Fig. 14.6**). To import structure factors, click the [Import...] button. One of observed, calculated, or difference structure factors ( $F_o$ ,  $F_c$ , or  $F_o - F_c$ ) can be imported from \*.fcf files output by SHELX-97 [97] with a “LIST 3” command.  $F_o$  can also be imported from input files, \*.mem and \*.fos, for MEM analysis [7, 8, 9]. To import structure factors from files with formats other than the above ones, create a text file where each line contains the following data in free format:

$h \ k \ l \ |F_o| \ |F_c| \ Fc(\text{real}) \ Fc(\text{imag}) \ sigma(F)$

Only unique reflections should be given in the file because all the equivalent reflections are automatically generated according to the current space group. If parts of reflections in the list do not satisfy conditions limiting possible reflections in the space group, a warning message will appear, and their structure factors will be reset to 0.  $F(000)$  is separately input in the text box placed above the list of structure factors. In addition, the spacial resolution in real space must be specified in the unit of Å. After all the data have been input, press the [Calculate] button to carry out Fourier synthesis from them.

## 14.9 Model Electron Densities

On selection of the “Utilities” menu  $\Rightarrow$  “Model Electron Densities”, electron densities are calculated by the Fourier transform of structure factors,  $F(\mathbf{h})$ , that are calculated from structure parameters and atomic scattering factors of free atoms [94] with Eq. (14.8). The spacial resolution of

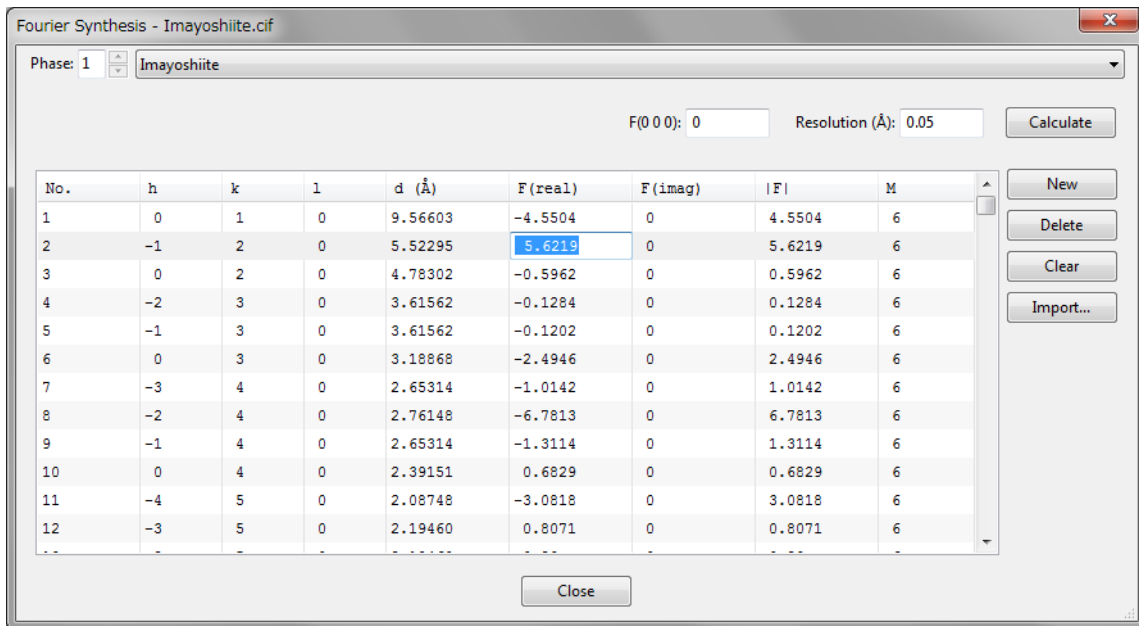


Figure 14.6: Fourier Synthesis dialog box.

electron densities is specified in the unit of Å. The number of grids along each crystallographic axis,  $N_x$ , is automatically set such that  $N_x$  gives a resolution close to the specified value and that  $N_x$  satisfies symmetrical constraints. Then, the electron density,  $\rho(x, y, z)$ , at the coordinates of  $(x, y, z)$  is calculated by

$$\rho(x, y, z) = \frac{1}{V} \sum_{h=-\frac{N_x}{2}}^{\frac{N_x}{2}} \sum_{k=-\frac{N_y}{2}}^{\frac{N_y}{2}} \sum_{l=-\frac{N_z}{2}}^{\frac{N_z}{2}} F(\mathbf{h}) \exp[-2\pi i(hx + ky + lz)]. \quad (14.14)$$

If the resolution is not sufficiently high, spurious noises appear in the resulting densities because of the so-called termination effect in Fourier synthesis. On the other hand, atomic scattering factors compiled in Ref. [94] are reliable only in a range of  $\sin \theta / \lambda < 6 \text{ \AA}^{-1}$ , which corresponds to a spacial resolution of approximately 0.042 Å. VESTA simply extrapolates the atomic scattering factors given in Ref. [94] even when the specified resolution is smaller than 0.042 Å.

## 14.10 Model Nuclear Densities

On selection of the “Utilities” menu ⇒ “Model Nuclear Densities”, densities of coherent-scattering lengths [10],  $b_c$ , are calculated by the Fourier transform of structure factors,  $F(\mathbf{h})$ , that are calculated from structure parameters and  $b_c$ 's of atoms with Eq. 14.11. The spacial resolution is set in the same manner as with the calculation of model electron densities (see section 14.9).

## 14.11 Patterson Densities

On selection of the “Utilities” menu ⇒ “Patterson Densities”, Patterson functions in the unit cell are calculated in three different modes:

1. “From Model Electron Densities” submenu: from structure parameters and atomic scattering factors of free atoms [94].

2. "From Model Nuclear Densities" submenu: from structure parameters and coherent-scattering lengths of atoms.
3. "From Volumetric Data" submenu: by convolution of volumetric data that are currently displayed.

On selection of the first two submenu, structure factors are calculated with Eqs. 14.8 and 14.11, respectively, with the spacial resolution of electron or coherent-scattering-length densities specified in the unit of Å. Then, the Patterson density,  $P(x, y, z)$ , at the coordinates of  $(x, y, z)$  is calculated by

$$P(x, y, z) = \frac{1}{V} \sum_{h=-\frac{N_x}{2}}^{\frac{N_x}{2}} \sum_{k=-\frac{N_y}{2}}^{\frac{N_y}{2}} \sum_{l=-\frac{N_z}{2}}^{\frac{N_z}{2}} |F(\mathbf{h})|^2 \exp[-2\pi i(hx + ky + lz)], \quad (14.15)$$

where  $N_x$ ,  $N_y$ , and  $N_z$  are the numbers of grids along the  $x$ ,  $y$ , and  $z$  axes, respectively (see section 14.9).

When Patterson functions are calculated from the current volumetric data, structure factors are calculated by

$$F(h, k, l) = \sum_x \sum_y \sum_z \rho(x, y, z) \exp[2\pi i(hx + ky + lz)], \quad (14.16)$$

and then  $P(x, y, z)$  is computed by Eq. (14.15). Therefore, the spacial resolution of the Patterson function is the same as that of the volumetric data.

## 14.12 2D Data Display

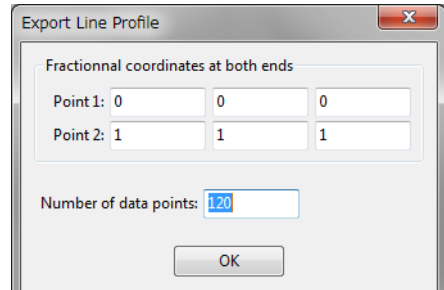
We sometimes wish to visualize 2D distribution of a physical quantity on a plane. In such a case, open the 2D Data Display window to display 2D images of volumetric data. Details in the feature of 2D Data Display are described in chapter 15.

## 14.13 Line Profile

Numerical values on a line segment with an equal step are calculated from volumetric data by linear interpolation of volumetric data and output in a text file to plot a line profile by a graphing program such as Igor Pro, gnuplot, and WinPLOTR. After this item has been selected, a dialog box (right figure) is opened to input fractional coordinates,  $(x, y, z)$ , of both ends and the total number of data points to be calculated. After clicking the [OK] button, a file selection dialog box appears and prompts you to input the name of an output file.

The top part of an output file when dealing with electron densities in rutile-type TiO<sub>2</sub> is listed below:

```
TiO2 (rutile)
Point 1: 0.00000 0.00000 0.00000
Point 2: 0.30530 0.30530 0.00000
50
0.000000E+000 2.899010E+002
4.047903E-002 2.582953E+002
```



```

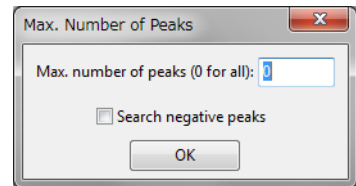
8.095806E-002 2.272991E+002
1.214371E-001 1.836505E+002
1.619161E-001 1.328268E+002
.....

```

The first line gives a title, followed by two lines for the fractional coordinates of both ends, those of Ti and O atoms in this case. The fourth line is the total number of data points (= 50), followed by 50 lines. In each of the 50 lines, the first and second columns give a distance from “Point 1” in the unit of Å and an interpolated value, respectively.

## 14.14 Peak Search

To search for peak positions in volumetric data, choose “Peak Search” under the “Utilities” menu. When this item is selected, a dialog box (right figure) is opened to restrict the maximum number of peaks listed in the Text Area. Enter 0 to list all the peaks detected in the volumetric data. The following data are listed in the Text Area: integrated value of volumetric data, number of peaks, peak positions, peak values, integrated value of volumetric data for each peak, and Voronoi volume [21] calculated for each peak.



Results of peak search for electron densities in the unit cell of rutile-type  $\text{TiO}_2$  are exemplified below:

Integrated value of volumetric data over the unit cell: 75.999979, 0.000000

Number of peaks in the volumetric data = 10  
Number of voxels at Voronoi boundaries = 60870/262144

	x	y	z	Peak value	Integrated	Volume
1	0.00000	0.00000	0.00000	2.89901E+02	1.99855E+01	7.64201E+00
2	0.50000	0.50000	0.50000	2.89901E+02	1.99855E+01	7.64201E+00
3	0.29688	0.29688	0.00000	5.66020E+01	9.00724E+00	1.17901E+01
4	0.70312	0.70312	0.00000	5.66020E+01	9.00724E+00	1.17901E+01
5	0.79688	0.20312	0.50000	5.66020E+01	9.00724E+00	1.17901E+01
6	0.20312	0.79688	0.50000	5.66020E+01	9.00724E+00	1.17901E+01

The integrated values represent numbers of electrons per each site, which is calculated by summation of numbers of electrons over the Voronoi volume of the site.

## 14.15 Conversion of Electron Densities

We can extract some important physical quantities from electron densities obtained experimentally from X-ray diffraction experiments. Let  $\rho(\mathbf{r})$  be the electron density at the position vector  $\mathbf{r}$ , and  $\nabla\rho(\mathbf{r})$  the gradient vector field of  $\rho(\mathbf{r})$ . With VESTA, we can calculate Laplacians of electron densities  $\nabla^2\rho(\mathbf{r})$ , electronic kinetic-energy densities  $g(\mathbf{r})$ , electronic potential-energy densities  $\nu(\mathbf{r})$ , and electronic energy densities  $h_e(\mathbf{r})$  from electron densities displayed in the current page according to Tsirelson’s procedures [48]. Consideration of these functions, particularly  $\nabla^2\rho(\mathbf{r})$  and  $h_e(\mathbf{r})$ , is not restricted by the bond critical point,  $\mathbf{r}_b$ , where  $\nabla\rho(\mathbf{r}) = 0$ , providing us with a comprehensive characterization of chemical bonding in molecules and crystals.

The electronic kinetic-energy density is expressed as

$$g(\mathbf{r}) = \frac{\hbar^2}{m} \left\{ \frac{3}{10} (3\pi^2)^{2/3} [\rho(\mathbf{r})]^{5/3} + \frac{\lambda [\nabla\rho(\mathbf{r})]^2}{\rho(\mathbf{r})} + \frac{k\nabla^2\rho(\mathbf{r})}{2} \right\}, \quad (14.17)$$

where  $\hbar^2$  is Dirac's constant, and  $m$  is the electron mass; the gradient  $\hbar$ -expansion of the Green function around the classical Thomas-Fermi approximation [98] yields  $\lambda = 1/72$  and  $k = 1/6$ . The electronic-energy density equals the sum of  $g(\mathbf{r})$  and  $\nu(\mathbf{r})$ :

$$h_e(\mathbf{r}) = g(\mathbf{r}) + \nu(\mathbf{r}) \quad (14.18)$$

with

$$\nu(\mathbf{r}) = \frac{\hbar^2}{4m} \nabla^2 \rho(\mathbf{r}) - 2g(\mathbf{r}). \quad (14.19)$$

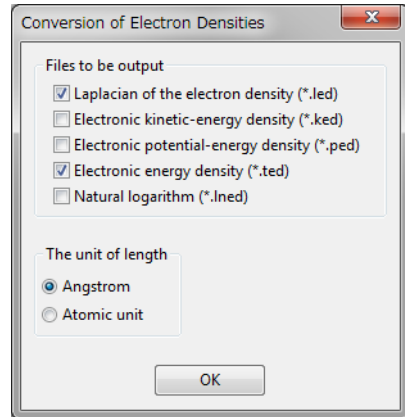
The electronic-energy density at  $\mathbf{r}_b$  gives a straightforward criterion for the recognition of the atomic interaction type. That is,  $h_e(\mathbf{r}) < 0$  is observed in shared-type atomic interactions whereas  $h_e(\mathbf{r}) > 0$  is observed in closed-shell interactions. In a similar manner, if the electrons are locally concentrated around  $\mathbf{r}_b$  [ $\nabla^2 \rho(\mathbf{r}_b) < 0$ ], the electrons are shared by both nuclei, which is typical for shared or covalent atomic interactions. Otherwise the electrons are concentrated in each of the atomic basins [ $\nabla^2 \rho(\mathbf{r}_b) > 0$ ], and the atomic interaction belongs to the closed-shell type.

On selection of the "Conversion of Electron Densities" item in the "Utilities" menu, a dialog box appears (right figure) to specify files to be output. The user-selected files are output in the general volumetric-data format (see p. 135) to either a directory where the electron densities are recorded or a directory specified by the user if VESTA fails in writing the files under that directory. By default, files storing volumetric data of  $\nabla^2 \rho(\mathbf{r})$  and  $h_e(\mathbf{r})$  are, respectively, output to files \*.led and \*.ted with their contents visualized in two pages.

The unit of input data should also be specified: either angstrom ( $\text{\AA}^{-3}$ ) or atomic unit ( $a_0^{-3}$ ).

**Table 14.1** lists units of output data.

Table 14.1: Units of converted volumetric data.



Input data	Output data			
	$\nabla^2 \rho(\mathbf{r})$	$g(\mathbf{r})$	$\nu(\mathbf{r})$	$h_e(\mathbf{r})$
$\text{\AA}^{-3}$	$\text{\AA}^{-5}$	$E_h a_0^{-3}$	$E_h a_0^{-3}$	$E_h a_0^{-3}$
$a_0^{-3}$	$a_0^{-5}$	$E_h a_0^{-3}$	$E_h a_0^{-3}$	$E_h a_0^{-3}$

$a_0 = 0.529177211 \text{ \AA}$  ( $a_0$ : Bohr radius), and  $E_h = 4.3597443 \times 10^{-18} \text{ J}$  ( $E_h$ : hartree).

# Chapter 15

## TWO-DIMENSIONAL DATA DISPLAY

### 15.1 Components of the 2D Data Display Window

Figure 15.1 shows the 2D Data Display window of VESTA running on Windows 7.

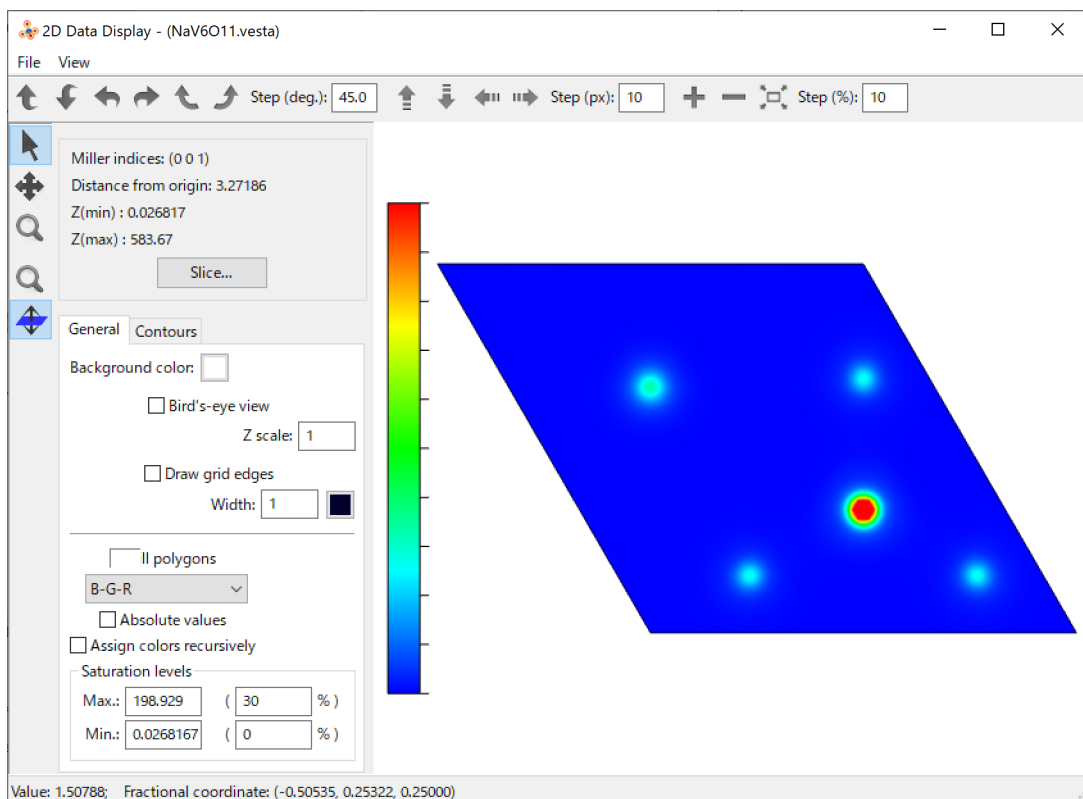


Figure 15.1: 2D Data Display window.

This window comprises the following four components:

- **Menu bar:** On Windows and Linux, the menu bar is placed at the top of the Main Window. On macOS, menus are displayed at the top of the screen. “File” and “View” menus are available in this window.
- **Toolbar:** Tools used frequently.

- **Side Panel:** Colors, contours, and other properties of a 2D image are controlled in the Side Panel. The minimum and maximum values in the 2D slice/projection data are displayed at the top of the panel.
- **Graphics Area:** Display an 2D image of volumetric data.

If a 2D image has been previously displayed, it is restored as soon as this window is opened. The default preferences of colors and width of contour lines, and the background color can be changed when no 2D image is displayed in this window. To change these default settings, edit values in the Side Panel and then close the window to save the settings.

## 15.2 Menus

- **File menu**
  - **Export 2D Data...**: Export 2D data as a text file.
  - **Export Raster Image...**: Export a graphic image as a file with a raster (pixel-based) format.
  - **Close**: Close the 2D Data Display window.
- **View menu**
  - **Zoom In**: Zoom in an image.
  - **Zoom Out**: Zoom out an image.

## 15.3 Tools in the Toolbar

### 15.3.1 Rotation

- |  |                          |
|--|--------------------------|
|  | Rotate around the x axis |
|  | Rotate around the x axis |
|  | Rotate around the y axis |
|  | Rotate around the y axis |
|  | Rotate around the z axis |
|  | Rotate around the z axis |

These six buttons are used to rotate objects around one of the  $x$ ,  $y$ , and  $z$  axes. The step width of rotation (in degrees) is specified in a text box next to the sixth button:

Step (deg.): 30.0

### 15.3.2 Translation

-  Translate upward
-  Translate downward
-  Translate leftward
-  Translate rightward

These four buttons are used to translate objects toward up, down, left, and right, respectively. The step width of translation (in pixels) is specified in a text box next to the fourth button:

Step (px):

### 15.3.3 Scaling

-  Zoom in
-  Zoom out
-  Fit to the screen

These three buttons is used to change object sizes. The step width of zooming (in %) is specified in a text box next to the third button:

Step (%):

## 15.4 Tools in the Vertical Toolbar

-  Rotate
-  Translate
-  Magnify
-  Magnify by mouse wheel
-  Shift slice by mouse wheel

## 15.5 Create and Edit a 2D Image

Click the [Slice...] button in the Side Panel to create a new image. Then, a dialog box named Create New Slice is opened (**Fig. 15.2**).

Three different methods of creating a slice or a projection image can be used:

1. (hkl) plane in the bounding box
2. (hkl) plane defined by two vectors
3. Project along [hkl] axis.

**Figure 15.3** schematically illustrates how a 2D image is created in each mode.

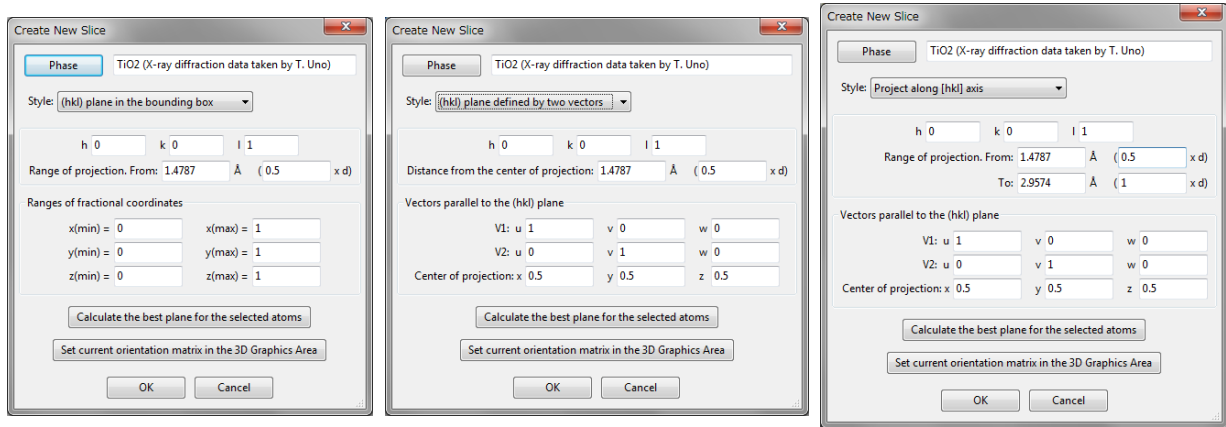


Figure 15.2: A dialog box for three different modes to draw a 2D image

### 15.5.1 (hkl) plane in the bounding box

In this mode, a slice that cuts a bounding box is created. The size of the bounding box is specified by ranges along  $x$ ,  $y$ , and  $z$  axes. The position of the slice is given as a distance from the origin of 3D data in the unit of either its lattice-plane spacing,  $d$ , or Å.

### 15.5.2 (hkl) plane defined by two vectors

In this mode, the size of the slice is defined by two lattice vectors:  $[u_1 v_1 w_1]$  and  $[u_2 v_2 w_2]$ .

**h, k, and l:** Three values in an equation to represent the lattice vector,  $\mathbf{R} = h\mathbf{a} + k\mathbf{b} + l\mathbf{c}$ , where  $\mathbf{a}$ ,  $\mathbf{b}$ , and  $\mathbf{c}$  denote fundamental lattice vectors.

**Distance from the center of projection:** The Center of projection lies on the projection vector that passes through the center of the slice (Fig. 15.4). The distance between the center of slice and the Center of projection is specified in the unit of either its lattice-plane spacing,  $d$ , or Å. For example, when this value is 0, the  $(x, y, z)$  position specified as the Center of projection corresponds to the center of the slice.

**Vectors parallel to the (hkl) plane:** A pair of vectors,  $\mathbf{V}_1$  and  $\mathbf{V}_2$ , is specified in the expression of the lattice vector,  $u\mathbf{a} + v\mathbf{b} + w\mathbf{c}$ , on the  $(hkl)$  plane. The two lattice vectors should be parallel to the  $(hkl)$  plane but should not be parallel to each other.

**Center of projection:** Projection of this point along the  $[hkl]$  direction intersects the slice at the center of the slice.

In this mode, two-dimensional data on the slice are recalculated by linear interpolation. When the numbers of data points along  $x$ ,  $y$ , and  $z$  directions in the volumetric data are  $N[0]$ ,  $N[1]$ , and  $N[2]$ , respectively, the number of data points,  $N_x$ , along the  $[u_1 v_1 w_1]$  direction is computed by

$$N_x = (\text{int})(N[0] * u_1 + N[1] * v_1 + N[2] * w_1). \quad (15.1)$$

The same procedure is applied to the number of data points along the  $[u_2 v_2 w_2]$  direction.

### 15.5.3 Project along [hkl] axis

This mode draws cumulative data of a series of  $(hkl)$  slices summed up along the  $[hkl]$  direction in a user-specified range. The number of data points is calculated in the same way as with the “(hkl) plane defined by two vectors” mode.

In the Slice Properties dialog box for this mode, four kinds of data have to be input:

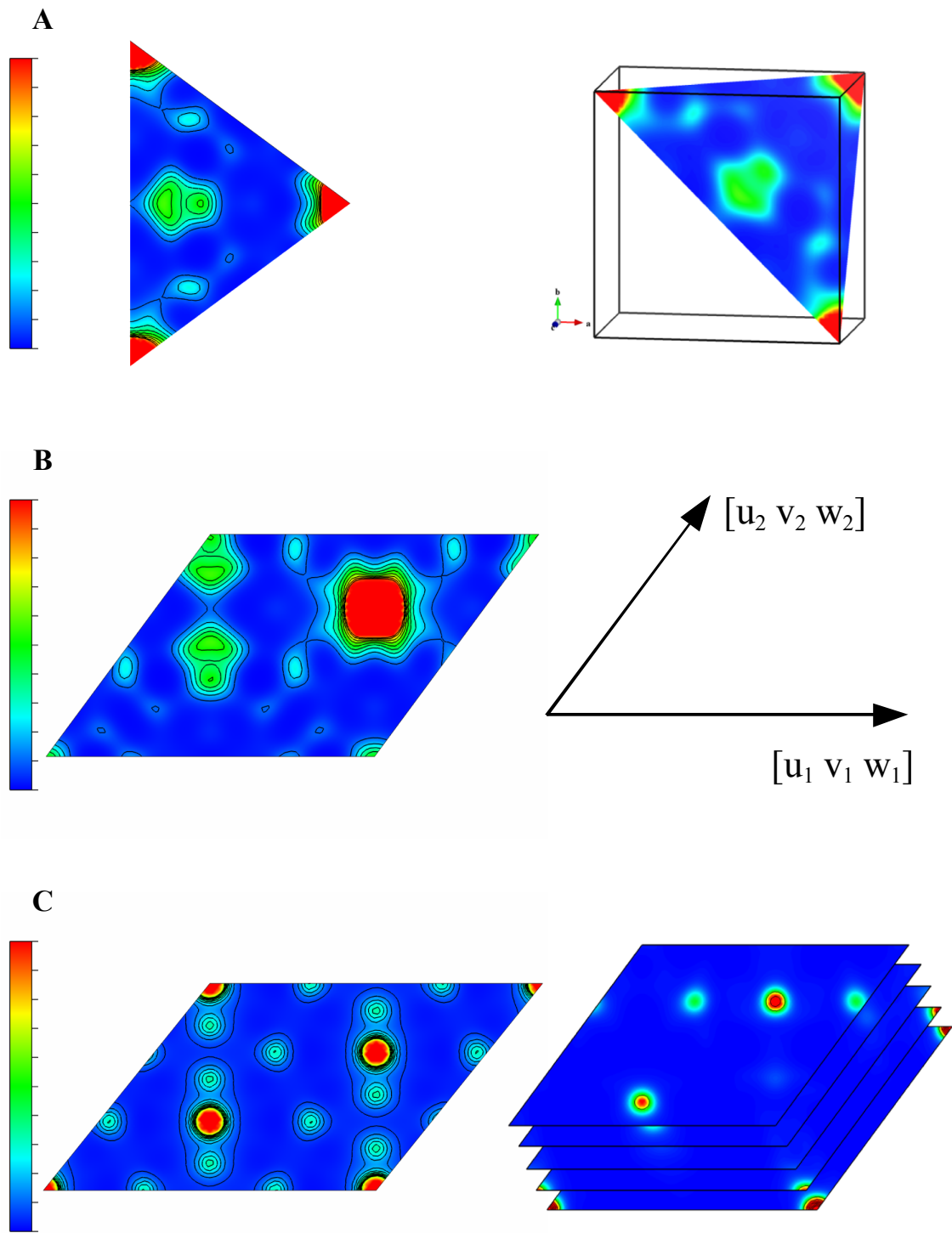


Figure 15.3: Electron-density distribution drawn with the three different modes for the (111) plane in rutile-type  $\text{TiO}_2$ . (A) “(hkl) plane in the bounding box” mode, (B) “(hkl) plane defined by two vectors” mode, and (C) “Project along [hkl] axis” mode. The electron densities were determined by MEM from X-ray powder diffraction data.

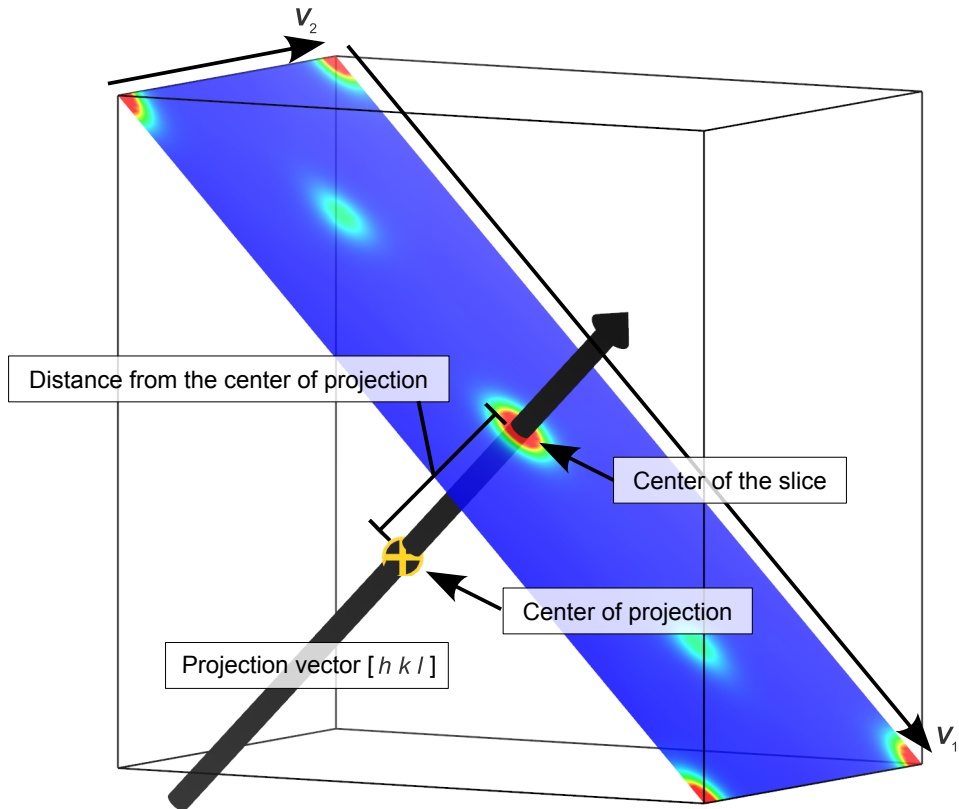


Figure 15.4: Schematic image of the relation between the center of the projection and the center of the slice.

**h, k, and l:** Three values in an equation to represent the lattice vector,  $\mathbf{R} = h\mathbf{a} + k\mathbf{b} + l\mathbf{c}$ , where  $\mathbf{a}$ ,  $\mathbf{b}$ , and  $\mathbf{c}$  denote fundamental lattice vectors. The  $[hkl]$  direction is defined with  $\mathbf{R}$ .

**Range of projection:** A pair of values specified by distances from the Center of projection. They are input in the unit of either its lattice-plane spacing,  $d$ , or Å.

**Vectors parallel to the (hkl) plane:** A pair of vectors,  $\mathbf{V}_1$  and  $\mathbf{V}_2$ , is specified in the expression of the lattice vector,  $u\mathbf{a} + v\mathbf{b} + w\mathbf{c}$ , on the  $(hkl)$  plane. The two lattice vectors should be parallel to the  $(hkl)$  plane but should not be parallel to each other.

**Center of projection:** Projection of this point along the  $[hkl]$  direction intersects the slice at the center of the slice.

## 15.6 Controlling Properties of a 2D Image

In the [General](#) page in the Side Panel, colors of the background and plane are mainly controlled (see Fig. 15.1).

Press a button at the right side of **Background color**: to change the background color. Check box “Bird’s eye view” enables or disables Bird’s eye view (Fig. 15.5). If “Draw grid edges” is checked, edges of grids are drawn with solid lines of a color and a width specified below the check box (Fig. 15.6).

When “Fill polygons” is checked, the surface of the plane is filled with colors corresponding to data values. Colors of the plane are controlled in the same manner as with sections of isosurfaces (see 12.1.6).

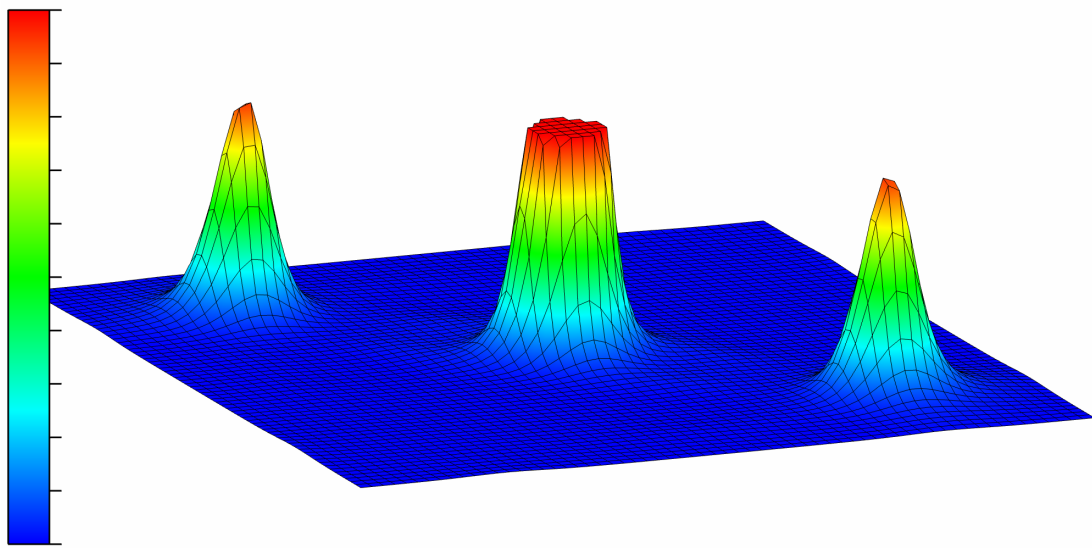


Figure 15.5: Bird's eye view of a (001) slice of rutile-type  $\text{TiO}_2$ .

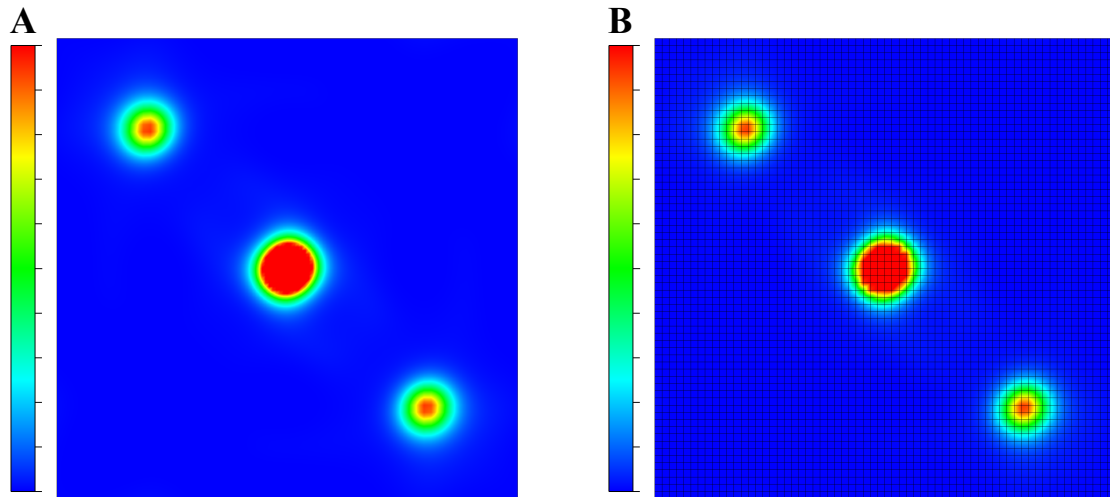


Figure 15.6: Electron-density distribution on the (001) plane in rutile-type  $\text{TiO}_2$ . (A) without grid edges and (B) with grid edges drawn with solid lines.

In the [Contours](#) page (**Fig. 15.7**), various properties of contour lines are specified. Check “Draw contour lines” to draw contour lines, which are plotted in two different modes: linear or logarithmic.

Contours are plotted in linear and logarithmic modes as solid lines (style L1) and dashed ones (style L2). The width and colors of these lines are specified in the text boxes and buttons in the Style frame box.

In the linear mode, lines are drawn at every Interval in data ranging from Min. to Max. The numerical value at the  $N$ th line,  $F(N)$ , is given by

$$F(N) = \text{Min.} + N \times \text{Interval.} \quad (15.2)$$

In this mode, line style L1 (solid line) is applied to lines of positive values, and line style L2 (dashed line) to lines of negative values.

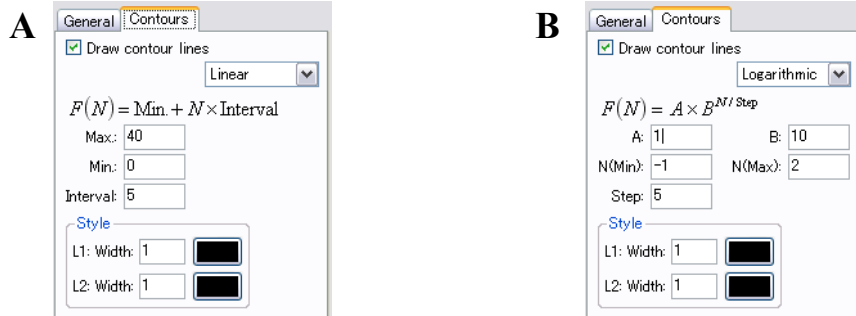


Figure 15.7: Contours page in the Side Panel. (A) Linear mode and (B) logarithmic mode.

In the logarithmic mode,  $F(N)$  is computed by

$$F(N) = A \times B^{N/\text{Step}}, \quad (15.3)$$

where  $A$  and  $B$  are constants specified by user. Line style L1 is applied to every “step” lines starting from the first one, and for other lines the L2 style is applied. For example, when  $N_{\min}$  is set to an integer value, the L1 style is used for lines with integer values of  $N/\text{Step}$ , and the L2 style is used for lines with non-integer values of  $N/\text{Step}$ .

## 15.7 Exporting 2D data

To export 2D data of the specified slice as a text file, choose “File” menu  $\Rightarrow$  “Export 2D Data...” in the 2D Data Display window. No 2D data files can be output on selection of style “(hkl) plane in the bounding box” in the Slice Properties dialog box.

# Chapter 16

## PREFERENCES

Default settings for the behavior of VESTA are changed in the Preferences dialog box (Fig. 16.1).

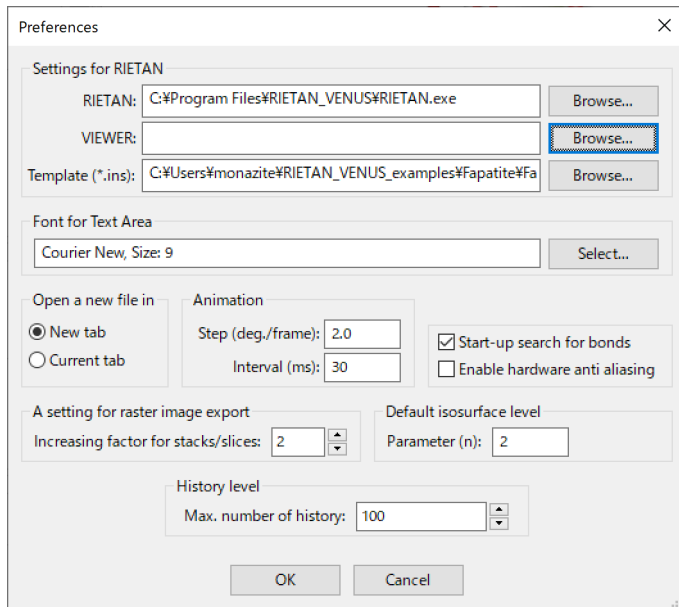


Figure 16.1: Preferences dialog box.

### 16.1 Settings for RIETAN

Settings for simulation of X-ray and neutron powder diffraction patterns are specified in frame box **Settings for RIETAN**.

Specify the absolute path of the executable binary file of RIETAN-FP [12], which is used for simulating powder diffraction patterns, after clicking the [Browse...] button at the right of text box {RIETAN}.

Click the [Browse...] button at the right of text box {Viewer} to specify an application to plot the powder diffraction pattern output to file \*.itx by RIETAN-FP. This text box may be left vacant on the use of Igor Pro because the extension, itx, is associated with Igor Pro by default if it has been installed.

VESTA uses a template file to export a standard input file of RIETAN-FP. The template file is specified in text box {Template (\*.ins)} by clicking the [Browse...] button at the right of the text box. In the exported file, data other than a space group, and lattice and structure

parameters are copied from the template file. Beware that the format of the template file must be compatible with the version of RIETAN-FP used by VESTA. The use of \*.ins for an older version of RIETAN-FP may cause an error on execution of its latest version. The default template file distributed with VESTA is that for the latest version of RIETAN-FP.

## 16.2 Font for Text Area

In frame box **Font for Text Area**, a text font for the **Text Area** is specified. Specify the text font after clicking the [Select...] button at the right of text box {**Font for Text Area**}.

## 16.3 Open a New File in

When VESTA reads in new data, a new page may be assigned to them, or an existing page may be reused. To input new data under a new page, select “New tab” in radio box **Open a new file in**. When “Current tab” is selected, data assigned to the current page are discarded, and new data are input in the current page. Unless changes in old data have been saved, VESTA asks you whether or not the changed data should be saved in a file.

## 16.4 Animation

Two settings for animation speed, *i.e.*, the rotation angle per frame and the interval between frames are specified in frame box **Animation**. The rotation angle per frame is specified in text box {**Step (deg./frame)**}. The interval between frames is specified in milliseconds in text box {**Interval (ms)**}. The number of frames per second is

$$1 / (t_{\text{draw}} + t_{\text{interval}}), \quad (16.1)$$

where  $t_{\text{draw}}$  is the time required to draw a single frame of an image on the **Graphics Area**, and  $t_{\text{interval}}$  is the interval between frames.

## 16.5 Start-up Search for Bonds

When this option is turned on, bonds will be automatically generated for atom pairs closer than certain distances when opening files. The list of element pairs to search for bonds, and bond distances, and styles for each pair are recorded in the “style.ini” file.

## 16.6 A Setting for Raster Image Export

Resolutions of atoms and cylindrical bonds are scaled when exporting pixel-based images. The numbers of stacks and slices for the graphics image,  $R_g$ , is scaled as

$$R_g = R_d \times s \times f, \quad (16.2)$$

where  $R_d$  is the number of stacks or slices for display on the screen,  $s$  is the scale of the image, and  $f$  is the factor to increase  $R_g$  specified in text box {**Increasing factor for stacks/slices**}.

## 16.7 Default isosurface level

The default isosurface level,  $d(\text{iso})$ , after opening a file storing volumetric data,  $\rho$ , is calculated as

$$d(\text{iso}) = \langle |\rho| \rangle + n \times \sigma(|\rho|), \quad (16.3)$$

where  $\langle |\rho| \rangle$  is the average of  $|\rho|$ 's,  $\sigma(|\rho|)$  is the standard deviation of  $|\rho|$ , and  $n$  is a parameter to adjust  $d(\text{iso})$ .

## 16.8 History level

VESTA supports for undoing and redoing user's operations. The default value of the maximum number of history level is 100.

# Chapter 17

## INPUT AND OUTPUT FILES

### 17.1 File Formats of Volumetric Data

Volumetric data are composed of regular grids in 3D space. A volume element, “voxel,” at each grid point represents a value on the grid point. Voxels are analogous to pixels, which represent 2D image data.

In general, two types of formats are used to record volumetric data in files: general and periodic grids. **Figure 17.1** schematically illustrates the general concepts of the two kinds of the formats.

The general grid is a uniform one spanned inside a bounding box for molecules and a unit cell for crystals. For crystal structures, part of data in the general grid are redundant owing to the periodicity of the data. For example, a numerical value at  $(1, 1, 1)$  are equal to that at the origin, *i.e.*,  $(0, 0, 0)$ . Grids where these redundant points have been omitted are called periodic ones.

VESTA distinguishes the grid types automatically from file extensions. For volumetric data with the periodic grid format, VESTA internally generates the general grid by adding redundant data points. On preparation of volumetric data using a self-made script or a program, the user must pay attention to the grid type of a file by himself.

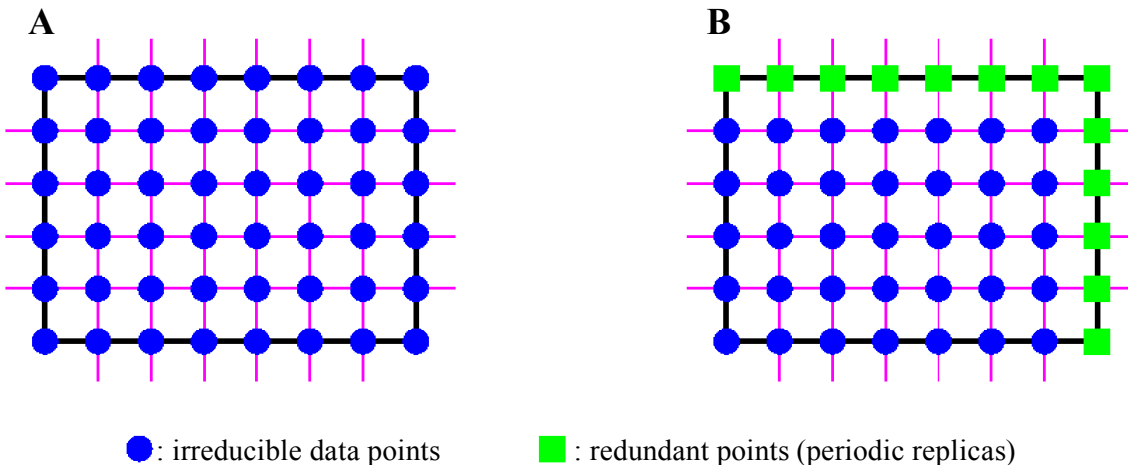


Figure 17.1: Two types of the grids for volumetric data on a plane. (A) general grid and (B) periodic grid.

## 17.2 Directories for User Settings

VESTA loads and saves two files, VESTA.ini and style/default.ini in a directory for user settings to store user settings for the program and for graphics, respectively. A directory, tmp, to store temporary files is also created in the same directory. The location of the settings directory depends on operating systems, and is determined in the following order of priority.

### 17.2.1 Windows

- When environmental variable `VESTA_PREF` is defined, the specified directory is used.
- When a directory named `VESTA` exists in `%HOMEPATH%\AppData\Roaming\`, it is used. (`%HOMEPATH%` represents the full path of the user's home directory, and `%HOMEPATH%\AppData\` is a hidden directory.)
- When the user has permission to write in the program directory of VESTA, that directory is used so as not to put the home directory in disorder.
- A directory `%HOMEPATH%\AppData\Roaming\VESTA\` is created on the first execution of VESTA to use it.

### 17.2.2 macOS

- When environmental variable `VESTA_PREF` is defined, the specified directory is used. To define environmental variables for GUI applications, they must be described in a text file named `environment.plist` under a hidden directory, `~/.MacOSX`. To make it easier to define `VESTA_PREF`, a utility called `set_VESTA_PREF.app` is included in the RIETAN-VENUS package<sup>1</sup>; refer to `Readme_mac.pdf` for details in `set_VESTA_PREF.app`.
- A directory `~/Library/Application Support/VESTA/` is created on the first execution of VESTA, and it is used. Note that `~/Library` is a hidden directory under the home directory (`~/`).

### 17.2.3 Linux

- When environmental variable `VESTA_PREF` is defined, the specified directory is used.
- A hidden directory `~/.VESTA/` is created on the first execution of VESTA to use it.

---

<sup>1</sup>[http://fujioizumi.verse.jp/download/download\\_Eng.html](http://fujioizumi.verse.jp/download/download_Eng.html)

## 17.3 Files Used by VESTA

Table 17.1: Files used by VESTA.

asfdc	A file storing parameters related to atomic form factors.
element.ini	A file storing default colors and radii of atoms.
spgra.dat	A file storing information on 230 space groups, <i>e.g.</i> , coordinates of equivalent positions compiled in <i>International Tables for Crystallography</i> , volume A [30].
spgro.dat	A file storing non-conventional symbols of orthorhombic space groups.
wyckoff.dat	A file storing information on wyckoff positions.
mspgr.dat	A file storing information on 1651 magnetic space groups.
style.ini	Default file for styles of the graphic scene.
template.ins	A template file for the standard input of RIETAN-FP [12]. It is used for exporting *.ins and simulating of powder diffraction patterns.
VESTA_def.ini	Default file for various settings of VESTA.
\$USER_DIR/VESTA.ini <sup>†</sup>	A file for user settings of VESTA. This file is copied from VESTA_def.ini when VESTA is executed for the first time by the user.
\$USER_DIR/style/default.ini <sup>†</sup>	User settings file for styles of the graphic scene. This file is copied from style.ini when VESTA is executed for the first time by the user.

<sup>†</sup> \$USER\_DIR is a directory for user settings (see 17.2).

## 17.4 Input Files

### 17.4.1 Structural data

#### 1. VESTA format (\*.vesta)

Text files containing the entire structure data and graphic settings. File \*.vesta saved by VESTA may contain relative paths to volumetric data files and a crystal-data file that are automatically read in when \*.vesta is reopened. If any one of keywords, **IMPORT\_STRUCTURE**, **IMPORT\_ORFFE**, **IMPORT\_DENSITY**, and **IMPORT\_TEXTURE**, is included in \*.vesta and followed by lines specifying relative paths to data files, these data files are also input by VESTA when \*.vesta are opened.

After Rietveld analysis with RIETAN-FP [12], lattice and structure parameters in \*.vesta are automatically updated provided that \*.vesta and \*.ins share the same folder.

#### 2. VICS format (\*.vcs)

<http://fujioizumi.verse.jp/visualization/VENUS.html>

VICS, which is the predecessor of the structure-drawing part of VESTA, is now obsolete. Nevertheless, this format is still supported in VESTA to maintain compatibility.

- American Mineralogist Crystal Structure Database [99] (\*.amc)  
<http://rruff.geo.arizona.edu/AMS/amcsd.php>

In part of AMCSD text files, extra characters are attached to space group names, and non-standard space-group symbols are used. Some of such non-standard space-group settings may not be read in correctly. In such a case, modify the space-group symbol appropriately and then change the setting number in the Unit cell tab of the **Edit Data** dialog box if necessary. Sometimes, you have to convert fractional coordinates by yourself if a non-standard setting that is not described in *International Tables for Crystallography*, volume A [30] is adopted.

- asse (\*.asse)  
<http://www.nims.go.jp/cmse/staff/arai/asse/>
- Chem3D (\*.cc1)  
[http://openbabel.org/docs/2.3.1/FileFormats/3D\\_viewer\\_Formats.html](http://openbabel.org/docs/2.3.1/FileFormats/3D_viewer_Formats.html)
- Crystallographic Information File (CIF; \*.cif) [100]  
<http://www.iucr.org/resources/cif/>

CIF has a variety of formats for crystal data. You can get detailed information about CIF from the above Web site. For example, CIF files may contain Cartesian coordinates, but VESTA cannot input them. Note that VESTA does not support all the formats allowed in the CIF format. For example, Cartesian coordinates included in CIFs cannot be input with VESTA; only fractional coordinates should be given in CIFs. For readable formats, refer to example files of \*.cif in **VENUS/examples/VICS/CIF**.

In the case of \*.cif containing multiphase data, all the data are input in the same tab and overlapped with each other. To visualize only one phase in such a case, select “Edit” menu ⇒ “Edit Data” ⇒ “Phase...”. Select an unnecessary phase in the list, and press [Delete] button.

The CIF specification presents multiple ways of inputting entries for space-group symmetry. VESTA searches the entries in the following order:

```
_symmetry_equiv_pos_as_xyz  
_symmetry_space_group_number  
_symmetry_space_group_name_H-M
```

If one of the above entries are given in \*.cif, VESTA recognizes space-group symmetry. For example, CIFs created by SHELX-97 [97] through WinGX [101] contain neither space-group number nor space-group symbol but have a list of symmetry operations.

If none of the above entries are correctly given, the space group is regarded as *P1*. In this case, set the space group in the Unit cell tab of the **Edit Data** dialog box after opening such a file, or modify a line relevant to the space group in the CIF in the following manner:

```
_symmetry_space_group_number 12  
or  
_symmetry_space_group_name_H-M 'P 21/n'
```

- CrystalMaker text file (\*.cmt, \*.cmtx)  
<http://www.crystalmaker.com>

CrystalMaker is a commercial program for building, displaying, and manipulating all kinds of crystal and molecular structures.

8. Crystal Structure Search and Retrieval (CSSR; \*.cssr)  
<http://www.maciejharanczyk.info/Zeopp/input.html>

In a file with the CSSR format, a setting numbers may be given after 'OPT ='. Unfortunately, we have no information about setting numbers in this format. Then, please change it in the Unit cell tab of the **Edit Data** dialog box if necessary.

9. Cambridge Structural Database [102] (CSD/FDAT; \*.csd, \*.fdt))  
<http://www.ccdc.cam.ac.uk/Solutions/CSDSystem/Pages/CSD.aspx>

10. DL\_POLY [103] format (CONFIG, REVCON, \*.config)  
[https://www.scd.stfc.ac.uk/Pages/DL\\_POLY.aspx](https://www.scd.stfc.ac.uk/Pages/DL_POLY.aspx)

11. FEFF input file (feff.inp)  
<http://www.feffproject.org/>

FEFF [104, 105] is an automated program for *ab initio* multiple-scattering calculations of X-ray Absorption Fine Structure (XAFS) and X-ray Absorption Near-Edge Structure (XANES) spectra for clusters of atoms. The names of input files for FEFF must be either **feff.inp** or **FEFF.INP**.

12. FHI-aims input file (\*.in)  
<https://aimsclub.fhi-berlin.mpg.de/>

FHI-aims is an accurate all-electron, full-potential electronic structure code package for computational materials science.

13. Output file of the Elk FP-LAPW Code (GEOMETRY.OUT)  
<http://elk.sourceforge.net/>

Elk is an all-electron full-potential linearised augmented-planewave (FP-LAPW) code for determining the properties of crystalline solids.

14. GSAS [18] format (\*.EXP)  
<http://www.ncnr.nist.gov/xtal/software/gsas.html>

15. Inorganic Crystal Structure Database [87] (ICSD; \*.ics)  
[http://www2.fiz-karlsruhe.de/icsd\\_home.html](http://www2.fiz-karlsruhe.de/icsd_home.html)

Two retrieval programs, RETRIEVE for MS-DOS and FindIt for Windows, of ICSD output text files with quite different formats. VESTA is capable of reading in both types of the crystal data files.

In these \*.ics files, extra characters are sometimes attached to space group names, *e.g.*, 'P 42/n m c S', which should be 'P 42/n m c' ( $P4_2/nmc$ ). In addition, full Hermann-Mauguin space-group symbols are sometimes given in ICSD text files. In such a case, an error message appears in both the Text Area and a message box. Read it carefully to proceed to a next operation. When you encounter this type of an error, it is strongly recommended to output a CIF instead of \*.ics.

16. ICSD-CRYSTIN: (\*.cry)

17. MDL Molfile (\*.mol)  
[http://en.wikipedia.org/wiki/Chemical\\_table\\_file](http://en.wikipedia.org/wiki/Chemical_table_file)

18. MINCRYST (Crystallographic Database for Minerals; \*.min)  
<http://database.iem.ac.ru/mincryst/>

In part of MINCRYST text files, extra characters are attached to space group names, and non-standard space-group symbols are used. In such a case, an error message appears in the **Text Area**. Such space group names need to be appropriately changed. Change the setting number in the Unit cell tab of the **Edit Data** dialog box if necessary.

19. MOLDA [106] (\*.mld)

<http://www3.u-toyama.ac.jp/kihara/cc/mld/readme.html>

The Web site of MOLDA has been closed because the author, Hiroshi Yoshida passed away in 2005. Then, the MODRAST/MOLDA format for \*.mld is briefly explained here. This format consists of the following lines:

- (a) Line No. 1: A comment about the compound, *e.g.*, its name
- (b) Line No. 2: Number of atoms,  $n_a$ , in the compound
- (c) Lines No. 3 –  $(3 + n_a)$ : Cartesian coordinates ( $x$ ,  $y$ , and  $z$ ) and an atomic number
- (d) Line No.  $(4 + n_a)$ : Number of bonds,  $n_b$ , in the compound
- (e) Lines No.  $(5 + n_a)$  –  $(5 + n_a + n_b)$ : A pair of atom numbers

For example, in the case of ethylene, where  $n_a = 6$  and  $n_b = 5$ , the following lines are required:

```
"Ethylene (CH2=CH2)"  
6  
.66958, 0, 0, 6  
1.23873, -.94397, 0, 1  
1.23873, .94397, 0, 1  
-.66958, 0, 0, 6  
-1.23873, -.94397, 0, 1  
-1.23873, .94397, 0, 1  
5  
1, 4  
1, 2  
1, 3  
4, 5  
4, 6
```

20. Protein Data Bank (PDB; \*.pdb) [107]

<http://www.wwpdb.org/>

PDB has a variety of formats for crystal data. You can get detailed information on PDB in a Web page <http://www.wwpdb.org/docs.html>. Note that VESTA does not support all the formats allowed in these two formats. For readable formats, refer to \*.pdb in **VENUS/examples/VICS/PDB**.

21. Input file of RIETAN-FP/2000 [12, 108] (\*.ins)

[http://fujioizumi.verse.jp/download/download\\_Eng.html](http://fujioizumi.verse.jp/download/download_Eng.html)

VESTA cannot input \*.ins for versions of RIETAN (*e.g.*, RIETAN-94) earlier than RIETAN-2000. In the case of \*.ins containing multiphase data, only the crystal data of the first phase are input.

In \*.ins, the volume name of *International Tables* should be not 'I' but 'A' in accordance with a specification in RIETAN-FP. For example, 'A-230-2' is input for the second setting

of space group  $Fd\bar{3}m$ . The input of 'I-230-2' causes an error. Lattice parameters must be given within one line in the following way:

```
CELLQ 9.36884 9.36884 6.88371 90.0 90.0 120.0 0.0 1010000
```

22. Output file of RIETAN-FP [12] (\*.lst)  
[http://fujioizumi.verse.jp/download/download\\_Eng.html](http://fujioizumi.verse.jp/download/download_Eng.html)  
Beware lest \*.lst output by RIETAN-2000 [108] is input.
23. Input file of SHELXL [97] (\*.ins)
24. Output file of STRUCTURE TIDY (\*.sto)
25. Structure data files output by USPEX (gatheredPOSCARS, BESTgatheredPOSCARS) [109, 110]  
<http://han.ess.sunysb.edu/~USPEX/>
26. WIEN2k [41] (\*.struct)  
<http://www.wien2k.at/>
27. XMol XYZ (\*.xyz)  
[http://en.wikipedia.org/wiki/XYZ\\_file\\_format](http://en.wikipedia.org/wiki/XYZ_file_format)  
[http://openbabel.org/docs/2.3.1/FileFormats/XYZ\\_cartesian\\_coordinates\\_format.html](http://openbabel.org/docs/2.3.1/FileFormats/XYZ_cartesian_coordinates_format.html)  
XMol developed at the Minnesota Supercomputer Center is a utility for creating and viewing graphic images of molecules.
28. F01 for SCAT [58, 111] and C04D for contrd  
<http://www.dvxa.org/>

VESTA need to read in c04d, which is an input file of contrd, in addition to f01 if a structural model is to be overlap with volumetric data. For this purpose, the dimensions of a boundary box (an area where volumetric data are output to text files) in c04d are required. For details in contrd, refer to **Readme\_contrd.txt** in the VENUS package [15, 16]. Of course, c04d and f01 should be placed in the same folder. If c04d has not been input by VESTA, atomic coordinates are treated in the Cartesian coordinate system, as is the case for \*.xyz files. In this case, volumetric data, \*.scat and \*.sca, cannot be overlapped with the structural model.

All the atoms recorded in f01 must be included within the above boundary box. Otherwise, atomic coordinates are normalized within the boundary box by assuming periodicity, which leads to the appearance of incorrect structures in the **Graphics Area**.

The assistance environment for the DV-X $\alpha$  method<sup>2</sup> using Hidemaru Editor is very convenient when carrying out a series of electronic-state calculations.

The Web site of Genta Sakane of Okayama University of Science:  
<http://www.chem.ous.ac.jp/~gsakane/>

is very useful for those who like to visualize physical quantities calculated with contrd. "Introduction to the assistance environment for the DV-X $\alpha$  method<sup>3</sup>" distributed there is a detailed Japanese document suitable for beginners in the DV-X $\alpha$  method as well as VESTA.

<sup>2</sup>[http://fujioizumi.verse.jp/visualization/VENUS.html#assistance\\_environment](http://fujioizumi.verse.jp/visualization/VENUS.html#assistance_environment)

<sup>3</sup>[http://www.chem.ous.ac.jp/~gsakane/dvxa\\_assistance\\_environment\\_1.html](http://www.chem.ous.ac.jp/~gsakane/dvxa_assistance_environment_1.html)

29. MXDORTO/MXDTRICL [112, 113] (FILE06.DAT, FILE07.DAT)  
<http://kats-labo.jimdo.com/mxdorto-mxdtric/>  
 MXDORTO and MXDTRICL are Fortran programs for molecular dynamics simulation.
30. XTL format (\*.xtl)  
 Text files used in Cerius2 (Accelrys, Inc.<sup>4</sup>). GULP [114] and GSAS [18] are capable of outputting crystal data with this format.

#### 17.4.2 Volumetric data

31. MEM densities in binary format (\*.pri, \*.prim)  
<http://fujioizumi.verse.jp/visualization/VENUS.html>  
<http://jp-minerals.org/dysnomia/en/>  
 Binary files of 3D electron and nuclear densities output by PRIMA [5] or Dysnomia [7, 8] and those of Patterson functions output by ALBA [17]. The unit of electron densities (strictly speaking, number densities of electrons) recorded in these files is Å<sup>-3</sup>, and that of nuclear densities is fm Å<sup>-3</sup>.
32. MEM densities in text format (\*.den)  
 Text files of 3D electron and nuclear densities output by PRIMA, Dysnomia, MEED [115], MEND [116], and ENIGMA [117]. The unit of electron densities recorded in these files is Å<sup>-3</sup> while that of nuclear densities is fm Å<sup>-3</sup>.
33. Energy Band (\*.eb)  
 Text files having practically the same format with \*.rho. Files \*.eb are used to visualize Fermi surfaces from results obtained with programs for band-structure calculations, *e.g.*, WIEN2k [41]. As a matter of convenience, a constant is added to all the energy eigenvalues in \*.eb so as to make them greater or equal to zero. Therefore, the isosurface level has to be set with this padding in mind.  
 Masao Arai of NIMS provides us with detailed information about \*.eb in his Web site:  
<http://www.nims.go.jp/cmse/staff/arai/>
34. General volumetric-data (text format) (\*.?ed)  
 A file with the general volumetric-data format stores one of the following physical quantities converted from electron densities according to procedures proposed by Tsirelson [48] (see 14.15):

- $\nabla^2\rho(\mathbf{r})$ : Laplacian of the electron density (\*.led).
- $g(\mathbf{r})$ : Electronic kinetic-energy density (\*.ked).
- $\nu(\mathbf{r})$ : Electronic potential-energy density (\*.ped).
- $h_e(\mathbf{r})$ : Electronic energy density (\*.ted).

with the format (common to all the files with the extension of ?ed):

- Title: Title up to 80 characters.
- $a, b, c, \alpha, \beta, \gamma$ : Lattice parameters with at least one space between two parameters (free format).
- N1+1, N2+1, N3+1: Numbers of voxels along the  $a, b$ , and  $c$  axes, respectively, with at least one space between two integers (free format).

---

<sup>4</sup><http://accelrys.com/>

followed by elements of a three-dimensional array, D

```
((D(I1, I2, I3), I3 = 1, N3+1), I2 = 1, N2+1), I1 = 1, N1+1)
```

with any number of data in each line and at least one space between two real data (free format). Note that voxels at N1+1, N2+1, and N3+1 lie on  $x = 1$ ,  $y = 1$ , and  $z = 1$ , respectively. A top part of an example of \*.ted is given below:

```
TiO2 (rutile)
 4.59393   4.59393   2.95886   90.00000   90.00000   90.00000
 65      65      65
-3.700291E+004 -3.355551E+004 -2.515189E+004 -1.581991E+004 -8.551052E+003 -4.096268E+003
-1.802126E+003 -7.564262E+002 -3.147750E+002 -1.347187E+002 -6.129182E+001 -3.045389E+001
-1.683229E+001 -1.043066E+001 -7.226008E+000 -5.529954E+000 -4.588889E+000 -4.036150E+000
-3.669965E+000 -3.365605E+000 -3.043458E+000 -2.664371E+000 -2.229370E+000 -1.771544E+000
-1.337361E+000 -9.658093E-001 -6.762105E-001 -4.680259E-001 -3.280885E-001 -2.393913E-001
....
```

VESTA allows you to save a file, \*.?ed, with the general volumetric-data format. Accordingly, VESTA serves as a converter from a binary file to a text one.

35. Periodic volumetric-data (text format) (\*.grd)

<http://www.ncnr.nist.gov/xtal/software/gsas.html>

Text files for 3D Fourier maps output by GSAS [18]. A program, 3DBVSMAPPER [118], for automatically generating bond-valence sum images is also capable of outputting files with this format. To create \*.grd files that can be input by VESTA, select option “C – Select section (X, Y, or Z) selection” in Fourier calculation setup and then enter “X” for prompt “Enter section desired (X,Y,Z - choose Z for DSN6 maps).”

The file format is essentially the same as the general volumetric-data format, except that the three-dimensional data array, D, are output in the following range:

```
((D(I1, I2, I3), I3 = 1, N3), I2 = 1, N2), I1 = 1, N1)
```

VESTA also allows you to export volumetric data in this format.

36. General volumetric-data format (binary) (\*.ggrid)

37. Periodic volumetric-data format (binary) (\*.pgrid)

38. Compressed volumetric-data format (\*.m3d)

39. SCAT volumetric-data files (\*.sca, \*.scat)

<http://www.dvxa.org/>

Electron densities, electrostatic potentials, and wave functions calculated with contrd from files F09 and F39 output by SCAT [58, 111]. Text files (CHG3D.SCA, POT3D.SCA, WXXX-3D.SCA, WXXXU-3D.SCA, and WXXXU-3D.SCA) created with a batch file named contrd.bat can directly be input by VESTA, where XXX denotes an integer assigned to a wave function. To learn details in \*.SCA, refer to **Readme\_contrd.txt** distributed

as a part of package [15, 16]. Three-dimensional numerical data recorded in \*.SCA or \*.SCAT are drawn without any conversion.

Units for electron densities, electrostatic potentials, and wave functions are, respectively, bohr<sup>-3</sup>, Ry (rydberg), and bohr<sup>-3/2</sup>, where bohr is the atomic unit for length, *i.e.*, 1 bohr =  $a_0 = 5.29177211 \times 10^{-11}$  m = 0.529177211 Å ( $a_0$ : Bohr radius), and 1 Ry =  $E_h/2 = 2.179\ 871\ 9 \times 10^{-18}$  J ( $E_h$ : hartree).

Refer to No. 23 in 17.4.1 for the assistance environment for the DV-X $\alpha$  method and its detailed document written in Japanese.

40. WIEN2k (\*.rho)

<http://www.wien2k.at/> (WIEN2k)

<http://www.nims.go.jp/cmsc/staff/arai/wien/venus.html> (wien2venus.py)

A script, wien2venus.py, coded in Python<sup>5</sup> by Masao Arai of NIMS makes it possible to export electron densities calculated with WIEN2k [41] to a text file, \*.rho, which is in turn visualized by VESTA. The unit of electron densities stored in this file is bohr<sup>-3</sup>.

41. WinGX 3D Fourier map (\*.fou)

<http://www.chem.gla.ac.uk/~louis/software/wingx/>

Text files of 3D Fourier Maps output by WinGX [101]. To create \*.fou that can be input with VESTA, open “FOURIER MAP Control Panel” of WinGX from Maps menu → FOURIER MAP → Slant plane. Select “3D Fouier (Beavers-Lipson)” and “Write MarchingCubes File” options and set “Projection” at Z axis. The minimum and maximum of “Summation limits” should be set at 0 and 1 for all of X, Y, and Z axes. A resolution for each axis should be carefully set in view of the following matter.

In this format, data points along each axis are not uniformly distributed but just placed at intervals of given resolutions. When length of an axis is  $L$  and resolution is set at  $d$ , the number of data points, NPIX, is set at the integer part of  $L/d + 1$ . The output files have a general grid format with nearly correct periodicity only if  $L/d$  is close to an integer. It is recommended that special positions lie exactly on data grid. For example, if mirror planes lie at  $x = 1/4$  and  $x = 3/4$ ,  $L/d$  should be multiples of 4.

42. X-PLOR/CNX (\*.xplor)

<http://en.wikipedia.org/wiki/X-PLOR> (CNX)

<http://superflip.fzu.cz/> (Superflip)

Superflip [119] is a computer program for *ab initio* structure solution of crystal structures by the charge-flipping method [120, 121, 122]. Superflip outputs electron densities in the unit cell in file \*.x-plor with the X-PLOR format [123], which can be directly visualized by VESTA.

### 17.4.3 Structural and volumetric data

43. CASTEP [124, 125] (\*.cell, \*.charg\_frm)

<http://www.castep.org/>

File \*.cell contains crystal-structure data while file \*.charg\_frm stores electron densities in the unit of Å<sup>-3</sup>. Only a structural model is visualized when \*.cell is opened by VESTA. On the other hand, both a structural model and electron-density distribution are displayed when opening \*.charg\_frm. Because no unit-cell dimensions are recorded in \*.charg\_frm, it must be accompanied by \*.cell.

---

<sup>5</sup><http://www.python.org/>

44. GAMESS [126] input and volumetric data files output by MacMolPlt [127]  
<http://www.msg.ameslab.gov/GAMESS/GAMESS.html> (GAMESS)  
<https://brettbode.github.io/wxmacmolplt/> (MacMolPlt)

A GAMESS input file, \*.inp, can readily be obtained from a GAMESS log file, \*.log, with MacMolPlt. At first, examine the unit of final Cartesian coordinates of atoms after convergence in this file using a text editor. Then, run MacMolPlt to open \*.log. In the Windows menu, select ‘Coordinates’ through the name of \*.log and check whether the unit of Cartesian coordinates is Å or bohr (au). The unit should be Å, as is usual with VESTA. If the unit is Bohr, select ‘Convert to Angstroms’ under the Molecule menu. Then, select ‘Input Builder’ through the name of \*.log in the Windows menu and click [Write File] to create \*.inp storing atomic symbols and Cartesian coordinates.

Next, a volumetric data file, \*.mmp, in which the origin of the 3D grid is recorded, has to be output. In the Windows menu, select ‘Surfaces’ through the name of \*.log. Specify an item from ‘3D Orbital’, ‘3D Total Electron Density’, and ‘3D Molecular Electrostatic Potential’. In the dialog box that appears subsequently, change the number of grid points and grid size appropriately, select an orbital (in the case of ‘3D Orbital’), and click [Update]. An isosurface plus a ball-and-stick model appear in the \*.log window. The number of grid points, origin, and grid increment are displayed by clicking [Parameters...]. Then, click [Export...]. Specify the name and location of \*.mmp with the same basename as \*.inp. Note that \*.inp and \*.mmp must share the same folder.

45. Gaussian Cube format (\*.cube, \*.cub)

<http://www.gaussian.com/>

Text files storing electron densities, spin densities, electrostatic potentials, wave functions, and so forth calculated with Gaussian [128, 129] with a keyword of ‘Cube’.<sup>6</sup>

Cube files can also be created by Firefly (previously known as PC GAMESS).<sup>7</sup>

46. VASP (\*.vasp, CHG, CHGCAR, PARCHG, LOCPOT, ELFCAR, POSCAR, CONTCAR)  
<http://www.vasp.at/>

<http://www.materialsdesign.com/medea> (commercial software MedeA including VASP as its component)

All the above files are text files storing crystal-structure and volumetric data output by VASP [130, 131].

CHG stores lattice vectors, atomic coordinates, and total charge densities multiplied by the unit-cell volume,  $V$ . PAW one-center occupancies are added to them in CHGCAR. Though both CHG and CHGCAR provide us with the same information on the valence charges, the file size of CHG is smaller than that of CHGCAR owing to the lower accuracy of the numerical data. PARCHG has the same format as CHG has, storing partial charge densities of a particular k-point and/or band. When these files are read in to visualize isosurfaces and sections, data values are divided by  $V$  in the unit of bohr<sup>3</sup>. The unit of charge densities input by VESTA is, therefore, bohr<sup>-3</sup>.

LOCPOT contains lattice vectors, atomic coordinates, and Coulomb potentials (unit: eV), *i.e.*, total potentials without exchange-correlation contributions (unless the line of LEXCHG=-1 is commented out in main.F). ELFCAR, which has the same format as CHG has, stores dimensionless electron localization functions (ELF). POSCAR and CONTCAR include lattice vectors, atomic coordinates, and optionally starting velocities and

<sup>6</sup>Units used in Gaussian 03 are described in [http://www.gaussian.com/g\\_tech/g\\_ur/k\\_constants.htm](http://www.gaussian.com/g_tech/g_ur/k_constants.htm)

<sup>7</sup><http://classic.chem.msu.su/gran/gamess/>

predictor-corrector coordinates for molecular-dynamics calculation. POSCAR and CONTCAR, respectively, correspond to the initial structure and the final one output by VASP at the end of a job; CONTCAR can be used to continue the job.

Owing to the absence of symbols of elements or atomic numbers in these files, they must accompany another file, OUTCAR, to display structural models. OUTCAR may be renamed \*.out having the same basename as \*.vasp has. Only lines following ‘POTCAR:’ at the top part of OUTCAR are required to obtain symbols of elements.

When files are read in for surface coloring, no data values are scaled unless the file name is CHGCAR or PARCHG.

#### 47. XCrySDen XSF format (\*.xsf)

<http://www.xcrysden.org/> (XCrySDen)

<http://www.abinit.org/> (ABINIT)

[http://www.abinit.org/documentation/helpfiles/for-v6.4/users/cut3d\\_help.html](http://www.abinit.org/documentation/helpfiles/for-v6.4/users/cut3d_help.html) (Cut3D)

<http://www.quantum-espresso.org/> (Quantum ESPRESSO)

The ABINIT package [132] for the *ab initio* computation of material properties has a feature to output binary files storing electron densities, electrostatic potentials, and wave functions. They can be converted into text files, \*.xsf, having the XSF format of XCrySDen [133, 134] using a converter named Cut3D. The unit of electron densities is bohr<sup>-3</sup>. Cut3D supports data Type 13 (XCrySDen/VENUS wavefunction real data), whereby wave functions can be directly output in \*.xsf.

Quantum ESPRESSO [135] for quantum simulations of materials has also a feature to output files with the XSF format.

Detailed information about the XSF format can be obtained from

<http://www.xcrysden.org/doc/XSF.html>

In general, \*.xsf consists of some sections that begins with keywords. VESTA reads in volumetric data from a **BEGIN\_BLOCK\_DATAGRID** section. To make it possible to overlap isosurfaces with a structural model, \*.xsf should also contain (1) **PRIMEVEC** and **PRIMCOORD** sections or (2) **CONVVEC** and **CONVCOORD** sections. Furthermore, lattice vectors in the **PRIMVEC** or **CONVVEC** section must agree with spanning vectors in the **BEGIN\_DATAGRID** section. The unit of primitive lattice vectors (**PRIMVEC**) and Cartesian coordinates is Å in the XSF format.

## 17.5 Output Files

### 17.5.1 Data files

#### Structure data

##### 1. Original format of VESTA (\*.vesta)

The entire information about data displayed currently are saved in a text file, \*.vesta, with the VESTA format. Files with the VESTA format contains all the structural data and graphic settings whereas volumetric data are not directly recorded in \*.vesta but imported from external files. Directories and names of files storing volumetric data are recorded in \*.vesta as relative paths to the volumetric-data files from the directory of \*.vesta, which makes it possible to save the entire information about the current data in a small file without duplicating huge volumetric data.

Structural data can be optionally imported from an external file in the same manner. To prevent the structural data from being recorded directly in \*.vesta, import structural data using the Import Data dialog box with option “Link” (see 6.3.6). A name of file \*.ffe output by ORFFE [45] is also recorded in \*.vesta so that geometrical parameters recorded in \*.ffe are automatically listed in the Geometrical Parameters dialog box after reopening \*.vesta (see 14.2). After Rietveld analysis with RIETAN-FP [12], lattice and structure parameters in \*.vesta are automatically updated provided that \*.vesta and a standard input file, \*.ins, share the same folder.

2. Chem3D (\*.cc1)

[http://openbabel.org/docs/2.3.1/FileFormats/3D\\_viewer\\_Formats.html](http://openbabel.org/docs/2.3.1/FileFormats/3D_viewer_Formats.html)

3. Crystallographic Information File (CIF; \*.cif)

<http://www.iucr.org/resources/cif/>

4. DL\_POLY input file (\*.config)

[https://www.scd.stfc.ac.uk/Pages/DL\\_POLY.aspx](https://www.scd.stfc.ac.uk/Pages/DL_POLY.aspx)

5. Protein Data Bank (PDB; \*.pdb)

<http://www.wwpdb.org/>

6. User input file of RIETAN-FP/2000 (\*.ins)

[http://fujioizumi.verse.jp/download/download\\_Eng.html](http://fujioizumi.verse.jp/download/download_Eng.html)

The feature of outputting \*.ins enables us to read in crystal data files of various formats with VESTA, simulate powder diffraction patterns, and carry out subsequent Rietveld refinements with RIETAN-FP [12]. Note that standard input files of RIETAN-2000 [108] and RIETAN-FP are incompatible with each other. VESTA uses a template file to export input files of RIETAN-FP/2000, and the default template file, template.ins, has the RIETAN-FP format. If a standard input file with the RIETAN-2000 format is desired, change the template file to a file with the RIETAN-2000 format in the Preferences dialog box (see 16).

In Rietveld refinement or simulations of powder diffraction patterns with RIETAN-FP, the following standard lattice settings of STRUCTURE TIDY [85, 46] embedded in RIETAN-FP should be selected:

- Monoclinic system:  $b$ -axis unique setting ( $\beta \neq 90^\circ$ ),
- Trigonal system: hexagonal lattice ( $a = b \neq c$  and  $\gamma = 120^\circ$ ),
- Centrosymmetric space groups: an inversion center at the origin (origin choice 2 in Ref. [30]).

Unless these three standard settings are adopted, LAZY PULVERIX [86], which is also incorporated in RIETAN-FP, fails in generating correct diffraction indices  $hkl$  and their multiplicities. Accordingly, VESTA automatically transforms the lattice setting of a crystal structure to the standard one when exporting \*.ins with the RIETAN-FP/2000 [108, 12] format.

It should be pointed out that fractional coordinates in part of crystal data recorded in databases have too small significant digits, *e.g.*, 0.3333 instead of 0.333333. In such a case, please increase the significant digit to 6 or 7 before outputting \*.ins.

7. VASP (POSCAR, \*.vasp)

<http://www.vasp.at/>

8. VRML (\*.wrl)  
<http://www.web3d.org/x3d/specifications/vrml/>
9. XMol XYZ (\*.xyz)  
[http://en.wikipedia.org/wiki/XYZ\\_file\\_format](http://en.wikipedia.org/wiki/XYZ_file_format)  
[http://openbabel.org/docs/2.3.1/FileFormats/XYZ\\_cartesian\\_coordinates\\_format.html](http://openbabel.org/docs/2.3.1/FileFormats/XYZ_cartesian_coordinates_format.html)
10. *P*1 structure (\*.p1)

Simple text files storing lattice parameters and atomic positions of all the atoms in the unit cell. Atomic positions are written in fractional coordinates, and the space group of the crystal is converted into *P*1 (triclinic, No. 1). This format is useful when preparing initial atomic configurations in computational simulations.

11. Fractional coordinates (\*.xtl)

Simple text files with the xtl file format storing atomic positions of all the atoms currently displayed in the **Graphics Area**. Atomic positions are written in fractional coordinates. The space group of the crystal is treated as *P*1 (triclinic, No. 1) for convenience.

12. MADEL input files (\*.pme)

Although MADEL can be executed from VESTA (see 14.5), input files of MADEL, \*.pme, should be manually edited to calculate electrostatic site potentials of interstitial (vacant) sites, whose fractional coordinates have to be input in **FORMAT(3F9.6)** at the tail of \*.pme. The use of the RIETAN-FP–VENUS integrated assistance environment included in the distribution file of the RIETAN-FP system is highly recommended to edit \*.pme and run MADEL to input it on Hidemaru Editor.<sup>8</sup> For details in the above assistance environment, read **Readme\_macros.txt** contained in the distribution file.

When exporting files with this format, you are prompted to input two parameters, RADIUS and REGION (see 14.5). Refer to the user's manual of MADEL for details in these parameters to be input in \*.pme.

13. Input files of STRUCTURE TIDY (\*.sto)

## Volumetric data

14. PRIMA binary format (\*.pri)
15. General volumetric-data format (\*.3ed)
16. Periodic volumetric-data format (\*.grd)
17. General volumetric-data format (binary) (\*.ggrid)  
The general volumetric-data format is the most recommended file format when exporting volumetric data. It is lossless, and yet files with this format have sizes much smaller than those for text formats or even some other binary formats. In the case of periodic volumetric data, \*.pgrid described below is preferred because of better compression efficiency.
18. Periodic volumetric data (binary format) (\*.pgrid)  
This file format is similar to \*.ggrid format but assumes the periodicity of grids to minimize data redundancies. When there are more than two symmetry operations, which are generated from space-group information set or directly edited by the user, only grid data in the asymmetric unit are recorded in \*.pgrid.

---

<sup>8</sup><http://hide.maruo.co.jp/software/hidemaru.html>

19. Compressed volumetric-data format (\*.m3d)

## Two-dimensional data

Suppose that the 2D Data Display window has been opened to choose option “(hkl) plane defined by two vectors” or “project along [hkl] axis” in the Create New Slice dialog box (see 15.5). Then, two-dimensional data shown in 2D Data Display window can be output by selecting the 2D Data Display item from the File menu. Note that this function is disabled on selection of the first option: “(hkl) plane in the bounding box.”

For example, electron densities on the (100) plane with a distance of  $0.5d$  from the origin in rutile-type TiO<sub>2</sub> are output as follows:

```
TiO2
(hkl) :      1      0      0
Vector 1:    0      1      0
Vector 2:    0      0      1
Distance from the origin: 2.29696 2.29696
       65      65
0.000000  0.000000  1.771768E-02
0.000000  0.046232  1.777942E-02
0.000000  0.092464  1.796342E-02
0.000000  0.138697  1.826639E-02
0.000000  0.184929  1.868208E-02
....
```

The two integers (65 and 65) in the sixth line are numbers of divisions along the  $x$  and  $y$  axes. Three data in each data line are  $X$ ,  $Y$ , and density, where  $X$  and  $Y$  are, respectively,  $x$  and  $y$  coordinates (unit: Å) from the origin in the two-dimensional plot.

### 17.5.2 Raster images

1. BMP
2. EPS
3. JPEG<sup>9</sup>
4. JPEG 2000<sup>10</sup>
5. PNG<sup>11</sup>
6. PPM
7. RAW
8. RGB (SGI)
9. TGA
10. TIFF

---

<sup>9</sup><http://www.jpeg.org/jpeg/index.html>

<sup>10</sup><http://www.jpeg.org/jpeg2000/index.html>

<sup>11</sup><http://www.libpng.org/pub/png/>

Images of structural and volumetric data displayed in the **Graphics Area** and the **2D Data Display** window can be recorded in files with a variety of graphics formats. When saving files storing bit-mapped images, select “**Export Raster Image...**” in the “**File**” menu. The image size of the exported graphics files is scaled up as a multiple of the size of the **Graphics Area**. The scale factor is input after the file name has been entered in a file selection dialog box. VESTA can export huge images that exceed the maximum width and height of the viewport, which are displayed in the **Text Area** just after launching VESTA, *e.g.*,

**Maximum supported width and height of the viewport: 4096 x 4096**

The resolution of objects, *i.e.*, the number of stacks and slices for atoms and bonds, are also scaled by two factors {**Scale**} and {**Increasing factor for stacks/slices**} specified in the Preferences dialog box (see [12.1.2](#), [12.1.3](#), and [16](#)).

### **17.5.3 Vector images**

1. Encapsulated PostScript (EPS)
2. Portable Document Format (PDF)
3. PostScript (PS)
4. Scalable Vector Graphics (SVG)

Images of structural and volumetric data displayed in the **Graphics Area** of the **Main Window** can be saved as vector images. When saving files storing vector images, select “**Export Vector Image...**” under the “**File**” menu. There are some limitations on exporting vector images. Colors of isosurfaces and sections colored according to volumetric data cannot be represented with vector image formats. Translucent polygons of polyhedra, lattice planes, and isosurfaces become opaque in all the formats except for PDF.

### **17.5.4 Output text**

The content of the **Text Area** can be saved as a text file by selecting “**Save Output Text...**” in the “**File**” menu.

# CLOSING REMARKS

## Feedback and Suggestions

The development of VESTA has been led by user feedback. Its phenomenal success results from the response from around the country. We assume that things are working fine provided that no feedback is received. If its users were so selfish as to behave like “black holes,” VESTA would not be improved very much. Please feel free to inform us of any bugs and your thoughts. Sending us files relevant to your troubles could facilitate the debug.

Encouraging responses would present us with driving forces for further development and refinement of VESTA.

## Acknowledgments

We wish to thank Ruben A. Dilanian of Melbourne University for his dedication to a great deal of programming for VICS and VEND, the two predecessors of VESTA. Akiji Yamamoto of NIMS coded a highly efficient compressed volumetric-data format (\*.m3d), and Takashi Ida of Nagoya Institute of Technology wrote Voronoi integration code for volumetric data. Masao Arai of NIMS and Masataka Mizuno of Osaka University kindly coded file converters, wien2venus.py for WIEN2k and contrd for SCAT, respectively. Hiroshi Ohki of Shinshu University helped us improve VICS, VEND and VICS-II significantly. Genta Sakane of Okayama University of Science, Takuji Ikeda of AIST, and Kazuki Komatsu of the University of Tokyo gave us many suggestions and helped us debug the program.

Finally, we thank for all who have helped us improve the program by reporting bugs and offering valuable ideas.

# Appendix A

## Keyboard Shortcuts

Table A.1: Keyboard shortcuts.

Global (Menu)	
Ctrl + N	File menu - New Structure...
Ctrl + O	File menu - Open...
Ctrl + S	File menu - Save...
Ctrl + Shift + S	File menu - Save as
Ctrl + W	File menu - Close
Ctrl + Q	File menu - Exit
Ctrl + E	Edit menu - Edit Data - Phase...
Ctrl + B	Edit menu - Bonds...
Ctrl + +	View menu - Zoom In
Ctrl + -	View menu - Zoom Out
Ctrl + Shift + A	View menu - Overall Appearance...
Ctrl + Shift + P	Objects menu - Properties...
Ctrl + Shift + B	Objects menu - Boundary...
Ctrl + Shift + O	Objects menu - Orientation...
When the Graphics Area has focus	
r	Change Manipulation to the Rotate mode
m	Change Manipulation to the Magnify mode
t	Change Manipulation to the Translate mode
s	Change Manipulation to the Select mode
d	Change Manipulation to the Distance mode
a	Change Manipulation to the Angle mode
Left	Rotate along $-y$
Right	Rotate along $+y$
Up	Rotate along $-x$
Down	Rotate along $+x$
Ctrl + Up	Rotate along $-z$
Ctrl + Down	Rotate along $+z$
Shift + Left	Rotate along $-y$ (1/10 step)
Shift + Right	Rotate along $+y$ (1/10 step)
Shift + Up	Rotate along $-x$ (1/10 step)

Table A.1: Continued from the previous page.

Shift + Down	Rotate along $+x$ (1/10 step)
Ctrl + Shift + Up	Rotate along $-z$ (1/10 step)
Ctrl + Shift + Down	Rotate along $+z$ (1/10 step)
Alt + Left	Translate along $-x$
Alt + Right	Translate along $+x$
Alt + Up	Translate along $+y$
Alt + Down	Translate along $-y$

# Bibliography

- [1] W. I. F. David, *J. Appl. Crystallogr.*, **20**, 316 (1987).
- [2] M. Sakata and M. Sato, *Acta Crystallogr., Sect. A: Found. Crystallogr.*, **46**, 263 (1990).
- [3] G. Bricogne and C. J. Gilmore, *Acta Crystallogr., Sect. A: Found. Crystallogr.*, **46**, 284 (1991).
- [4] R. J. Papoular, *Acta Crystallogr., Sect. A: Found. Crystallogr.*, **47**, 293 (1991).
- [5] F. Izumi and R. A. Dilanian, “Recent Research Developments in Physics,” Vol. 3, Part II, Transworld Research Network, Trivandrum (2002), pp. 699–726.
- [6] F. Izumi, *Solid State Ionics*, **172**, 1 (2004).
- [7] F. Izumi and K. Momma, *IOP Conf. Ser.: Mater. Sci. Eng.*, **18**, 022001 (2011).
- [8] K. Momma and F. Izumi, *Z. Kristallogr., Proc.*, **1**, 195 (2011).
- [9] K. Momma, T. Ikeda, A. A. Belik, and F. Izumi, *Powder Diffr.*, **28**, 184 (2013).
- [10] V. F. Sears, “International Tables for Crystallography,” Vol. C, 3rd ed., ed. by E. Prince, Kluwer, Dordrecht (2004), pp. 444–452.
- [11] K. Momma and F. Izumi, *Commission on Crystallographic Computing, IUCr Newsletter*, No. 7, 106 (2006).
- [12] F. Izumi and K. Momma, *Solid State Phenom.*, **130**, 15 (2007).
- [13] K. Momma and F. Izumi, *J. Appl. Crystallogr.*, **41**, 653 (2008).
- [14] K. Momma and F. Izumi, *J. Appl. Crystallogr.*, **44**, 1272 (2011).
- [15] F. Izumi, *Rigaku J.*, **36**, 18 (2005).
- [16] F. Izumi and R. A. Dilanian, *Commission on Powder Diffraction, IUCr Newsletter*, No. 32, 59 (2005).
- [17] F. Izumi, “Spectroscopy and Diffraction III,” Vol. 11: the 5th Series of Chemistry, Maruzen, Tokyo (2006), p. 220.
- [18] A. C. Larson and R. B. V. Dreele, “General Structure Analysis System (GSAS),” Report LAUR 86-748, Los Alamos National Laboratory, Los Alamos (2004).
- [19] J. Rodriguez-Carvajal, *Phys. B (Amsterdam, Neth.)*, **192**, 55 (1993).
- [20] J. Smart, K. Hock, and S. Csomor, “Cross-Platform GUI Programming with wxWidgets,” Prentice Hall (2005).

- [21] W. H. Press, B. P. Flannery, S. A. Teukolsky, and W. T. Vetterling, “Numerical Recipes: the Art of Scientific Computing,” 3rd ed., Vol. 11: the 5th Series of Chemistry, Maruzen, Tokyo (2007), pp. 1142–1146.
- [22] B. Quentrec and C. Brot, *J. Comput. Phys.*, **13**, 430 (1973).
- [23] M. P. Allen and D. J. Tildesley, “Computer Simulation of Liquids,” Clarendon Press, Oxford (1987), p. 149.
- [24] M. F. Brigatti, A. Mottana, D. Malferrari, and G. Cibin, *Am. Mineral.*, **92**, 1395 (2007).
- [25] T. Balasubramanian, S. R. Jebas, S. Thamotharan, G. Rheinwald, and A. G. Lang, *Acta Crystallogr., Sect. E: Struct. Rep. Online*, **62**, o290 (2006).
- [26] R. M. Hazen, A. Y. Au, and L. W. Finger, *Am. Mineral.*, **71**, 977 (1986).
- [27] I. Hassan, S. M. Antao, and J. B. Parise, *Am. Mineral.*, **89**, 359 (2004).
- [28] T. Nakagawa, K. Kihara, and K. Harada, *Am. Mineral.*, **86**, 1506 (2001).
- [29] M. R. Silva, V. M. Moreira, C. Cardoso, A. M. Beja, and J. A. R. Salvador, *Acta Crystallogr., Sect. C: Cryst. Struct. Commun.*, **64**, o217 (2008).
- [30] “International Tables for Crystallography,” Vol. A, 5th ed., ed. by Th. Hahn, Kluwer, Dordrecht (2005).
- [31] D. K. Swanson and R. C. Peterson, *Can. Mineral.*, **18**, 153 (1980).
- [32] W. H. Baur, *Acta Crystallogr., Sect. B: Struct. Sci.*, **30**, 1195 (1974).
- [33] K. Robinson, G. V. Gibbs, and P. H. Ribbe, *Science (Washington, DC, U. S.)*, **172**, 567 (1971).
- [34] R. Hoppe, *Z. Kristallogr.*, **150**, 23 (1979).
- [35] R. Hoppe, S. Voigt, H. Glaum, J. Kissel, H. P. Müller, and K. Bernet, *J. Less-Common Met.*, **156**, 105 (1989).
- [36] C. Ferraris, “Fundamentals of Crystallography,” 2nd ed., ed. by C. Giacovazzo, Oxford University Press, Oxford (2002), p. 526.
- [37] M. Nespolo, G. Ferraris, and H. Ohashi, *Acta Crystallogr., Sect. B: Struct. Sci.*, **55**, 902 (1999).
- [38] I. D. Brown and D. Altermatt, *Acta Crystallogr., Sect. B: Struct. Sci.*, **41**, 244 (1985).
- [39] N. E. Brese and M. O’Keeffe, *Acta Crystallogr., Sect. B: Struct. Sci.*, **47**, 192 (1991).
- [40] I. D. Brown, “The Chemical Bond in Inorganic Chemistry,” Oxford University Press, Oxford (2001).
- [41] P. Blaha, K. Schwarz, G. Madsen, D. Kvasnicka, and J. Luitz, “WIEN2k, an Augmented Plane Wave + Local Orbitals Program for Calculating Crystal Properties,” Technische Universität Wien, Wien (2001).
- [42] J. Nagamatsu, N. Nakagawa, T. Muranaka, Y. Zenitani, and J. Akimitsu, *Nature (London, U. K.)*, **410**, 63 (2001).

- [43] S. Kumazawa, S. Yamamura, E. Nishibori, M. Takata, M. Sakata, F. Izumi, and Y. Ishii, *J. Phys. Chem. Solids*, **60**, 1407 (1999).
- [44] P. Hartman, “Crystal Growth: An Introduction,” North-Holland Publishing Co., Amsterdam (1973), pp. 367–402.
- [45] W. R. Busing, K. O. Martin, and H. A. Levy, “A FORTRAN Crystallographic Function and Error Program,” Report ORNL-TM-306, Oak Ridge National Laboratory, Oak Ridge (1964).
- [46] L. M. Gelato and E. Parthé, *J. Appl. Crystallogr.*, **20**, 139 (1987).
- [47] F. Izumi, *J. Crystallogr. Soc. Jpn.*, **44**, 380 (2002).
- [48] V. G. Tsirelson, *Acta Crystallogr., Sect. B: Struct. Sci.*, **58**, 632 (2002).
- [49] K. Kihara, *Eur. J. Mineral.*, **2**, 63 (1990).
- [50] H. Arnold, “International Tables for Crystallography,” Vol. A, 5th ed., ed. by Th. Hahn, Kluwer, Dordrecht (2006), pp. 78–85.
- [51] N. V. Belov, N. N. Neronova, and T. S. Smirnova, *Sov. Phys. Crystallogr.*, **2**, 311 (1957).
- [52] W. Opechowski and R. Guccione, “Magnetism,” ed. by G. T. Rado and H. Shut, Vol. II, Part A, Academic Press, New York (1965), pp. 105–165.
- [53] O. Zhou and D. E. Cox, *J. Phys. Chem. Solids*, **53**, 1373 (1992).
- [54] W. J. A. M. Peterse and J. H. Palm, *Acta Crystallogr.*, **20**, 147 (1966).
- [55] E. Prince, L. W. Finger, and J. H. Konnert, “International Tables for Crystallography,” Vol. C, 3rd ed., ed. by E. Prince, Kluwer, Dordrecht (2004), p. 695.
- [56] Y. Ohashi, “X-Ray Crystal Structure Analysis,” Syôkabô, Tokyo (2005), p. 103.
- [57] F. Izumi, “Spectroscopy and Diffraction III,” Vol. 11: the 5th Series of Chemistry, Maruzen, Tokyo (2006), p. 161.
- [58] H. Adachi, M. Tsukada, and C. Satoko, *J. Phys. Soc. Jpn.*, **45**, 875 (1978).
- [59] A. T. N’Diaye, S. Bleikamp, P. J. Feibelman, and T. Michely, *Phys. Rev. Lett.*, **97**, 215501 (2006).
- [60] K. Komatsu, T. Kurabayashi, A. Sano, E. Ohtani, and Y. Kudoh, *Acta Crystallogr., Sect. E: Struct. Rep. Online*, **62**, i216 (2006).
- [61] A. Prakash, *Acta Crystallogr.*, **22**, 439 (1967).
- [62] M. N. Burnett and C. K. Johnson, “ORTEP-III: Oak Ridge Thermal Ellipsoid Plot Program for Crystal Structure Illustrations,” Report ORNL-6895, Oak Ridge National Laboratory, Oak Ridge (1996).
- [63] R. H. Gao, *Acta Crystallogr., Sect. E: Struct. Rep. Online*, **66**, m487 (2010).
- [64] K. Momma, T. Ikeda, K. Nishikubo, N. Takahashi, C. Honma, M. Takada, Y. Furukawa, T. Nagase, and Y. Kudoh, *Nat. Commun.*, **2**, 196 (2011).
- [65] Y. Tsujimoto, C. Tassel, N. Hayashi, T. Watanabe, H. Kageyama, K. Yoshimura, M. Takano, M. Ceretti, C. Ritter, and W. Paulus, *Nature (London, U. K.)*, **450**, 1062 (2007).

- [66] M. Rakiah, J. Refebvre, O. Hernandez, W. van Beek, and M. Serpelloni, *J. Appl. Crystallogr.*, **37**, 766 (2004).
- [67] R. M. Hazen, R. T. Downs, and C. T. Prewitt, “High-Temperature and High-Pressure Crystal Chemistry,” Vol. 41: Reviews in Mineralogy, Mineral. Soc. Am., Washington, D.C. (2000), Chap. 1.
- [68] M. Avdeev, E. N. Caspi, and S. Yakovlev, *Acta Crystallogr., Sect. B: Struct. Sci.*, **63**, 363 (2007).
- [69] A. Beran, E. Libowitzky, and T. Armbruster, *Can. Mineral.*, **34**, 803 (1996).
- [70] C. Giacovazzo, “Fundamentals of Crystallography,” 3rd ed., ed. by C. Giacovazzo, Oxford University Press, Oxford (2002), pp. 138–141.
- [71] Z.-Q. Liu, Q. Fang, W.-T. Yu, G. Xue, D.-X. Cao, and M.-H. Jiang, *Acta Crystallogr., Sect. C: Cryst. Struct. Commun.*, **58**, o445 (2002).
- [72] V. G. Tsirelson, M. Y. Antipin, R. G. Gerr, R. P. Ozerov, and Y. T. Struchkov, *Phys. Status Solidi A*, **87**, 425 (1985).
- [73] C. Giacovazzo, “Fundamentals of Crystallography,” 2nd ed., ed. by C. Giacovazzo, Oxford University Press, Oxford (2002), p. 80.
- [74] D. F. Shriver and P. W. Atkins, “Inorganic Chemistry,” 3rd ed., Oxford University Press, Oxford (1999), p. 24 and p. 71.
- [75] B. K. Vainshtein, V. M. Fridkin, and V. L. Indenbom, “Structure of Crystals,” 3rd ed., Springer, Berlin (2000), p. 69.
- [76] A. F. Wells, “Structural Inorganic Chemistry,” 5th ed., Clarendon Press, Oxford (1984), p. 1288.
- [77] R. D. Shannon, *Acta Crystallogr., Sect. A: Found. Crystallogr.*, **32**, 751 (1976).
- [78] A. Bondi, *J. Phys. Chem.*, **68**, 441 (1964).
- [79] G. Sakane, H. Kawasaki, T. Oomori, M. Yamasaki, H. Adachi, and T. Shibahara, *J. Cluster Sci.*, **13**, 75 (2002).
- [80] L. Tong, D. M. Ho, N. J. Vogelaar, C. E. Schutt, and J. R. A. Pascal, *J. Am. Chem. Soc.*, **119**, 7291 (1997).
- [81] K. D. Schotte, U. Schotte, H. J. Bleif, and R. Papoula, *Acta Crystallogr., Sect. A: Found. Crystallogr.*, **51**, 739 (1995).
- [82] M. Murakami, K. Hirose, K. Kawamura, N. Sata, and Y. Ohishi, *Science (Washington, DC, U. S.)*, **304**, 855 (2004).
- [83] E. Passaglia, G. Artioli, A. Gualtieri, and R. Carnevali, *Eur. J. Mineral.*, **7**, 429 (1995).
- [84] M. C. J. M. Hughes and K. D. Crowley, *Am. Mineral.*, **74**, 870 (1989).
- [85] E. Parthé and L. M. Gelato, *Acta Crystallogr., Sect. A: Found. Crystallogr.*, **40**, 169 (1984).
- [86] K. Yvon, W. Jeitschko, and E. Parthé, *J. Appl. Crystallogr.*, **10**, 73 (1977).

- [87] A. Belsky, M. Hellenbrandt, V. L. Karen, and P. Luksch, *Acta Crystallogr., Sect. B: Struct. Sci.*, **B58**, 364 (2002).
- [88] P. Lightfoot, S. Pei, J. D. Jorgensen, Y. Yamada, T. Matsumoto, F. Izumi, and Y. Kodama, *Acta Crystallogr., Sect. C: Cryst. Struct. Commun.*, **47**, 1143 (1991).
- [89] V. K. Pecharsky and P. Y. Zavalij, “Fundamentals of Powder Diffraction and Structural Characterization of Materials,” 2nd ed., Springer, New York (2009), pp. 447-450.
- [90] C. Giacovazzo, “Fundamentals of Crystallography,” 3rd ed., ed. by C. Giacovazzo, Oxford University Press, Oxford (2011), pp. 84–86.
- [91] K. Kato and F. Izumi, unpublished work (2008).
- [92] F. Izumi, *Phys. C (Amsterdam, Neth.)*, **190**, 35 (1991).
- [93] Z. Berant, R. Moreh, and S. Kahane, *Phys. Lett. B*, **69**, 281 (1977).
- [94] D. Waasmaier and A. Kirfel, *Acta Crystallogr., Sect. A: Found. Crystallogr.*, **51**, 416 (1995).
- [95] C. T. Chantler, *J. Phys. Chem. Ref. Data*, **24**, 71 (1995).
- [96] C. T. Chantler, *J. Phys. Chem. Ref. Data*, **29**, 597 (2000).
- [97] G. M. Sheldrick, *Acta Crystallogr., Sect. A: Found. Crystallogr.*, **64**, 112 (2008).
- [98] D. Kirzhnits, *Sov. Phys. JETP*, **5**, 64 (1957).
- [99] R. T. Downs and M. Hall-Wallace, *Am. Mineral.*, **88**, 247 (2003).
- [100] S. R. Hall, F. H. Allen, and I. D. Brown, *Acta Crystallogr., Sect. A: Found. Crystallogr.*, **47**, 655 (1991).
- [101] L. J. Farrugia, *J. Appl. Crystallogr.*, **45**, 849 (2012).
- [102] F. H. Allen, *Acta Crystallogr., Sect. B: Struct. Sci.*, **58**, 380 (2002).
- [103] W. Smith and T. Forester, *J. Mol. Graph.*, **14**, 136 (1996).
- [104] J. Rehr and R. Albers, *Phys. Rev. B: Condens. Matter Mater. Phys.*, **41**, 8139 (1990).
- [105] J. Rehr and R. Albers, *Rev. Mod. Phys.*, **72**, 621 (2000).
- [106] H. Yoshida, “Molecular Modeling on Computers – A Guidebook of Molda –,” Science House, Tokyo (2000).
- [107] H. Berman, K. Henrick, and H. Nakamura, *Nat. Struct. Biol.*, **10**, 980 (2003).
- [108] F. Izumi and T. Ikeda, *Mater. Sci. Forum*, **321**, 198 (2000).
- [109] A. Oganov and C. Glass, *J. Chem. Phys.*, **214**, 244704 (2006).
- [110] C. Glass, A. Oganov, and N. Hansen, *Comp. Phys. Comm.*, **175**, 713 (2006).
- [111] Y. Kowada, I. Tanaka, H. Nakamatsu, and M. Mizuno, “Hajimete no Denshi Jotai Keisan,” Sankyo Shuppan, Tokyo (1998).
- [112] K. Hirao and K. Kawamura, “Material Design Using Personal Computer,” Syôkabô, Tokyo (1994).

- [113] K. Kawamura, *Jpn. Chem. Prog. Exchange Newsletter*, **6**, No. 4, 91 (1995).
- [114] J. D. Gale, *J. Chem. Soc., Faraday Trans.*, **93**, 692 (1997).
- [115] S. Kumazawa, Y. Kubota, M. Takata, M. Sakata, and Y. Ishibashi, *J. Appl. Crystallogr.*, **26**, 453 (1993).
- [116] K. Burger and W. Prandl, *Acta Crystallogr., Sect. A: Found. Crystallogr.*, **55**, 719 (1999).
- [117] H. Tanaka, M. Takata, E. Nishibori, K. Kato, T. Iishi, and M. Sakata, *J. Appl. Crystallogr.*, **35**, 282 (2002).
- [118] M. Sale and M. Avdeev, *J. Appl. Crystallogr.*, **45**, 1054 (2012).
- [119] L. Palatinus and G. Chapuis, *J. Appl. Crystallogr.*, **40**, 786 (2007).
- [120] G. Oszlányi and A. Sütő, *Acta Crystallogr., Sect. A: Found. Crystallogr.*, **60**, 134 (2004).
- [121] G. Oszlányi and A. Sütő, *Acta Crystallogr., Sect. A: Found. Crystallogr.*, **61**, 147 (2005).
- [122] G. Oszlányi and A. Sütő, *Acta Crystallogr., Sect. A: Found. Crystallogr.*, **63**, 156 (2006).
- [123] A. T. Brünger, “X-Plor Version 3.1: A System for X-Ray Crystallography and NMR,” Yale University Press, New Haven (1993).
- [124] M. D. Segall, P. J. D. Lindan, M. J. Probert, C. J. Pickard, P. J. Hasnip, S. J. Clark, and M. C. Payne, *J. Phys.: Condens. Matter*, **14**, 2717 (2002).
- [125] S. J. Clark, M. D. Segall, C. J. Pickard, P. J. Hasnip, M. J. Probert, K. Refson, and M. C. Payne, *Z. Krystallogr.*, **220**, 567 (2002).
- [126] M. W. Schmidt, K. K. Baldridge, J. A. Boatz, S. T. Elbert, M. S. Gordon, J. J. Jensen, S. Koseki, N. Matsunaga, K. A. Nguyen, S. Su, T. L. Windus, M. Dupuis, and J. A. Montgomery, *J. Comput. Chem.*, **14**, 1347 (1993).
- [127] B. M. Bode and M. S. Gordon, *J. Mol. Graph. Mod.*, **16**, 133 (1998).
- [128] A.E. Frisch, M. J. Frisch, and G. W. Trucks, “Gaussian 03 User’s Reference,” Gaussian, Inc., Pittsburgh (2003).
- [129] M. J. Frisch, G. W. Trucks, H. B. Schlegel, G. E. Scuseria, M. A. Robb, J. R. Cheeseman, G. Scalmani, V. Barone, B. Mennucci, G. A. Petersson, H. Nakatsuji, M. Caricato, X. Li, H. P. Hratchian, A. F. Izmaylov, J. Bloino, G. Zheng, J. L. Sonnenberg, M. Hada, M. Ehara, K. Toyota, R. Fukuda, J. Hasegawa, M. Ishida, T. Nakajima, Y. Honda, O. Kitao, H. Nakai, T. Vreven, J. A. Montgomery, Jr., J. E. Peralta, F. Ogliaro, M. Bearpark, J. J. Heyd, E. Brothers, K. N. Kudin, V. N. Staroverov, R. Kobayashi, J. Normand, K. Raghavachari, A. Rendell, J. C. Burant, S. S. Iyengar, J. Tomasi, M. Cossi, N. Rega, J. M. Millam, M. Klene, J. E. Knox, J. B. Cross, V. Bakken, C. Adamo, J. Jaramillo, R. Gomperts, R. E. Stratmann, O. Yazyev, A. J. Austin, R. Cammi, C. Pomelli, J. W. Ochterski, R. L. Martin, K. Morokuma, V. G. Zakrzewski, G. A. Voth, P. Salvador, J. J. Dannenberg, S. Dapprich, A. D. Daniels, O. Farkas, J. B. Foresman, J. V. Ortiz, J. Cioslowski, and D. J. Fox, “Gaussian 09 Revision A.1,” Gaussian Inc., Wallingford CT (2009).
- [130] G. Kresse and J. Furthmüller, *Phys. Rev. B: Condens. Matter Mater. Phys.*, **54**, 11169 (1996).

- [131] G. Kresse and J. Furthmüller, *Comput. Mater. Sci.*, **6**, 15 (1996).
- [132] X. Gonze, J.-M. Beuken, R. Caracas, F. Detraux, M. Fuchs, G.-M. Rignanese, L. Sindic, M. Verstraete, G. Zerah, F. Jollet, M. Torrent, A. Roy, M. Mikami, P. Ghosez, J.-Y. Raty, and D. C. Allan, *Comput. Mater. Sci.*, **25**, 478 (2002).
- [133] A. Kokalj, *J. Mol. Graph. Mod.*, **17**, 176 (1999).
- [134] A. Kokalj, *Comput. Mater. Sci.*, **28**, 155 (2003).
- [135] P. Giannozzi, S. Baroni, N. Bonini, M. Calandra, R. Car, C. Cavazzoni, D. Ceresoli, G. L. Chiarotti, M. Cococcioni, I. Dabo, A. D. Corso, S. de Gironcoli, S. Fabris, G. Fratesi, R. Gebauer, U. Gerstmann, C. Goucoussis, A. Kokalj, M. Lazzeri, L. Martin-Samos, N. Marzari, F. Mauri, R. Mazzarello, S. Paolini, A. Pasquarello, L. Paulatto, C. Sbraccia, S. Scandolo, G. Sclauzero, A. P. Seitsonen, A. Smogunov, P. Umari, and R. M. Wentzcovitch, *J. Phys.: Condens. Matter*, **21**, 395502 (2009).

# Index

- 2D Data Display, 114  
ABINIT, 139  
ALBA, 2, 135  
Alchemy, 2  
AMCSD, 131  
American Mineralogist Crystal Structure Database 131  
anisotropic atomic displacement, 2  
anisotropic atomic displacement parameter, 47  
asse, 131  
atomic form factor, 111  
axial vector, 64  
axis setting, 103  
ball-and-stick model, 4, 21, 27–29, 74, 79, 83, 102  
best plane, 3  
BMP, 142  
Bohr radius, 10, 50, 91, 116, 137  
bond angle, 9, 74, 79  
bond angle variance, 9, 76  
bond valence parameter, 9  
bond valence sum, 9, 77  
Cartesian coordinate, 134  
CASTEP, 137  
centrosymmetric space group, 104  
CG, 104  
charge distribution, 9, 76  
charge-flipping method, 137  
Chem3D, 131, 140  
CHG, 138  
CHGCAR, 138, 139  
CIF, 13, 77, 131, 140  
CNX, 137  
coherent-scattering length, 111  
complex lattice, 34, 42  
CONTCAR, 138  
contour line, 93, 118, 123  
coordination polyhedron, 75  
Crystallographic Information File, 131  
CrystalMaker, 131  
CSD, 132  
CSSR, 132  
Cut3D, 139  
cutoff plane, 70  
Debye–Waller factor, 111  
depth-cueing, 99  
diffraction index, 111  
dihedral angle, 9, 74, 79  
dispersion correction, 111  
displacement ellipsoid, 4, 8, 28, 29, 45, 59, 75, 84, 85  
distortion index, 9, 75  
DL\_POLY, 132, 140  
dot surface, 21, 22, 27, 30  
DV-X $\alpha$ , 134  
DVSCAT, 50  
dynamic displacement, 63  
Dysnomia, 2, 135  
effective coordination number, 9, 76  
electronic kinetic-energy density, 115, 135  
electronic potential-energy density, 115, 135  
electronic-energy density, 115, 135  
electrostatic site potential, 45  
electrostatic site potentials, 106  
ELFCAR, 138  
Elk FP-LAPW Code, 132  
encapsulated PostScript, 143  
Energy Band, 135  
ENIGMA, 135  
EPS, 142, 143  
equivalent isotropic atomic displacement parameter, 47  
FDAT, 132  
FEFF, 132  
FHI-aims, 132  
FindIt, 132  
formal charge, 45  
Fourier map, 136, 137  
fractional coordinate, 9, 103, 104, 111

GAMESS, 138  
gamma, 105  
Gaussian, 138  
general equivalent position, 22, 37, 101  
general grid, 128  
general position diagram, 86  
general volumetric data, 141  
general volumetric-data format, 141  
GLUI, 2  
GLUT, 2  
gnuplot, 108, 114  
Graphic Area, 102  
GSAS, 132, 135, 136  
GULP, 135  
  
hexagonal lattice, 104  
  
ICSD, 13, 77, 104, 132  
ICSD-CRYSTIN, 132  
Igor Pro, 108, 114  
interatomic distance, 9  
interfacial angle, 81  
inversion center, 103, 104  
isotropic atomic displacement parameter, 47  
  
JPEG, 142  
JPEG 2000, 142  
  
Laplacian, 115  
Laplacian of electron density, 115, 135  
lattice parameter, 36, 104  
lattice plane, 66  
lattice-plane spacing, 47  
LAZY PULVERIX, 103, 104, 109  
Line Profile, 114  
Linux, 4, 16–18, 20, 117  
LOCROT, 138  
  
MacMolPlt, 138  
macOS, 4, 16, 21, 23  
MADEL, 22, 106, 141  
Madelung energy, 45, 106  
magnetic moment, 4, 63  
maximum-entropy method, 1  
maximum-entropy Patterson method, 2  
MDL Molfile, 132  
mean square displacement, 2, 47  
MEED, 135  
MEM-based pattern fitting, 1  
MEND, 135  
metric tensor, 39, 40, 47  
  
MINCRYST, 132, 133  
MOLDA, 133  
MS-DOS, 132  
MXDORTO, 135  
MXDTRICL, 135  
  
neutron diffraction, 111  
Niggli-reduced cell, 105  
nuclear Thomson scattering, 111  
  
occupancy, 46, 74, 111  
opacity, 4, 9, 30, 88, 90, 91, 93  
OpenGL, 2, 15–17, 99  
ORFFE, 102, 140  
ORTEP-III, 60  
OUTCAR, 139  
oxidation state, 13, 77  
  
PARCHG, 138, 139  
Patterson function, 9, 135  
Patterson-function density, 2  
PDB, 13, 133, 140  
PDF, 143  
peak search, 115  
periodic grid, 128  
periodic volumetric-data format, 141  
PNG, 142  
polar vector, 64  
polyhedra, 74  
polyhedral model, 4, 21, 28, 29, 61  
polyhedral volume ratio, 75  
portable document format, 143  
POSCAR, 138, 140  
POTCAR, 139  
powder diffraction pattern, 22, 108, 125, 130  
PowderPlot, 109  
PPN, 142  
PRIMA, 2, 135  
primitive lattice, 42  
primitive translation vector, 39  
principal axis, 2  
protein data bank, 133  
PS, 143  
  
quadratic elongation, 9, 76  
  
RAW, 142  
reciprocal basis vector, 39  
reciprocal-lattice, 47, 71, 72  
redo, 3  
RETRIEVE, 132

RGB (SGI), 142  
rhombohedral lattice, 103  
RIETAN-2000, 133, 140  
RIETAN-FP, 13, 22, 81, 102, 108, 109, 125, 130, 133, 134, 140  
RietPlot, 108  
rotation matrix, 37, 38  
  
SCAT, 134, 136, 144  
SHELX-97, 112, 131  
shift of the origin, 39  
shininess, 67, 83, 88, 98  
space-filling model, 4, 6, 21, 27, 28, 83  
specular, 67, 83  
standard setting, 104, 105  
standardization of crystal data, 103  
standardization parameter, 104  
static displacement, 63  
stick model, 4, 21, 27–29, 87  
STRUCTURE TIDY, 104, 105, 110  
substructure, 42  
Superflip, 137  
superstructure, 42  
surface coloring, 9, 22, 30, 49, 91, 139  
SVG, 143  
symmetry operation, 9, 37, 38, 40, 41, 74, 75, 79, 80, 101  
  
temperature factor, 46  
TGA, 142  
TIFF, 142  
transformation matrix, 38, 40  
translation vector, 74  
  
undo, 3  
unit-cell volume, 38  
  
VASP, 138, 140  
VEND, 1, 2, 144  
VENUS, 1, 134, 137, 139  
VICS, 1, 2, 130, 144  
VICS-II, 2, 144  
Voronoi tessellation, 2  
voxel, 4, 128  
VRML, 141  
  
WIEN2k, 9, 134, 135, 137  
Windows, 4, 15, 16, 19, 20, 117, 132  
WinGX, 131, 137  
WinPLOTTR, 108, 114  
wireframe model, 4, 21, 22, 27–29

wxWidgets, 2, 14  
X-PLOR, 137  
XAFS, 132  
XANES, 132  
XCrySDen, 139  
XMol XYZ, 134, 141  
XSF format, 139  
XTL format, 135



# USER'S MANUAL FOR MADEL

## 1. WHAT IS MADEL?

MADEL is a FORTRAN 77 program to calculate electrostatic site potentials,  $\phi_i$ , and Madelung energies,  $E_M$ , of ionic crystals by the Fourier method. It was programmed by Dr. Katsuo Kato, National Institute for Research in Inorganic Materials (NIRIM), 1-1 Namiki, Tsukuba, Ibaraki 305, Japan.

This manual was translated from Japanese into English with some modifications and additions by Dr. Fujio Izumi of NIRIM during his short stay at the Argonne National Laboratory in March, 1991.

## 2. HOW TO COMPILE MADEL

This program should be compiled using an automatic double-precision option of a FORTRAN 77 compiler. If the compiler of your computer, unfortunately, does not support such a convenient feature, declare IMPLICIT DOUBLE PRECISION (A–H, O–Z) in the main program and all the subprograms of MADEL.

## 3. CREATING AN INPUT FILE FOR MADEL

Line 1. Title (A72)

Line 2. Radius of an ionic sphere and Fourier-summation range (2F6.2)

RADIUS: radius of an ionic sphere,  $s$ , in Å. The charge-density distribution,  $r$ , is given by

$$\rho(r) = \rho_0 [1 - 6(r/s)^2 + 8(r/s)^3 - 3(r/s)^4],$$

where  $r$  is the distance from the center of the ionic sphere ( $r < s$  and  $\rho(r) = 0$  for  $r \geq s$ ). When Lines 7 are not given, set RADIUS at a value that is large enough but less than the smallest interatomic distance (not half of it!).

REGION: reciprocal-space range (in Å<sup>-1</sup>) within which Fourier coefficients are summed up. MADEL sums up the Fourier coefficients with respect to all  $hkl$ 's within a sphere having a radius equal to RADIUS. Choose an appropriate value within the range 2.0–4.0 Å<sup>-1</sup> according to the desired precision of calculation. Also, check whether or not a curve for Madelung energy versus REGION is nearly flat around the selected value of REGION.

Line 3. Three integers related with the crystal structure (3I3)

NS: number of symmetry operations. Inverted positions ( $-x$ ,  $-y$ ,  $-z$ ) in a centrosymmetric cell are not required, whereas translated positions in a complex lattice must be input.

NA: number of atoms contained in the asymmetric unit.

I<sub>Z</sub>: = 0, non-centrosymmetric cell.

= 1, centrosymmetric cell.

Line 4. Lattice constants (3F9.4, 3F9.3)

A(1):  $a$  ( $\text{\AA}$ ) or  $a^*$  ( $\text{\AA}^{-1}$ ).

A(2):  $b$  ( $\text{\AA}$ ) or  $b^*$  ( $\text{\AA}^{-1}$ ).

A(3):  $c$  ( $\text{\AA}$ ) or  $c^*$  ( $\text{\AA}^{-1}$ ).

A(4):  $\alpha$  (degree) or  $\cos\alpha$ .

A(5):  $\beta$  (degree) or  $\cos\beta$ .

A(6):  $\gamma$  (degree) or  $\cos\gamma$ .

Lines 5. Symmetry operations (F11.6, 2I2, F11.6, 2I2, F11.6, 2I2)

Input NS lines ( $j = 1$ , NS).

Column

1 - 11: translational part of  $x_j$  or blank.

12 - 13: 1, 2, 3, -1, -2, -3, or blank for  $x$ ,  $y$ ,  $z$ ,  $-x$ ,  $-y$ ,  $-z$ , or blank, respectively, as used in the expression for the transformed  $x_j$ .

14 - 15: 1, 2, 3, -1, -2, -3, or blank for  $x$ ,  $y$ ,  $z$ ,  $-x$ ,  $-y$ ,  $-z$ , or blank, respectively, as used in the expression for the transformed  $x_j$ . Columns 12 and 13 are exactly equivalent to Columns 14 and 15. Also, note that an expression such as  $x_j = 2x$  must be treated as  $x_j = x + x$ .

16 - 26: translational part of  $y_j$  or blank.

27 - 30: integers representing plus or minus  $x$ ,  $y$ , or  $z$  in the expression for transformed  $y_j$  as described above.

31 - 41: translational part of  $z_j$  or blank.

42 - 45: integers representing plus or minus  $x$ ,  $y$ , or  $z$  in the expression for transformed  $z_j$  as described above.

These lines have the same format as those in ORFLS (least-squares structure-refinement program) and ORFFE (program to calculate interatomic distances, bond angles, *etc.*) developed at the Oak Ridge National Laboratory. Therefore, they can be copied easily from input files for these two programs.

Lines 6. Sites in the asymmetric unit (A8, 1X, 5F9.4)

Input NA lines ( $I = 1, NA$ ).

ATOM( $I$ ): name of an atom occupying the  $i$ th site.

Z( $I$ ): valence (oxidation state) of the atom. Input a positive value for a cation and a negative one for an anion. In case this site is partially occupied, Z( $I$ ) must be multiplied by its occupation factor (occupation probability).

W( $I$ ): (occupation factor for the  $i$ th site)  $\times$  (number of equivalent positions for the  $i$ th site) / (number of general equivalent positions).

X(1, $I$ ): fractional coordinate,  $x_i$ .

X(2, $I$ ): fractional coordinate,  $y_i$ .

X(3, $I$ ): fractional coordinate,  $z_i$ .

Lines 7. Fractional coordinates of vacant sites whose potentials are to be calculated (3F9.6)

Input lines as many as you like ( $I = NA+1, NA+2, \dots$ ). These lines are optional.

X(1, $I$ ): fractional coordinate,  $x_i$ .

X(2, $I$ ): fractional coordinate,  $y_i$ .

X(3, $I$ ): fractional coordinate,  $z_i$ .

In addition to the occupied sites input in Lines 6, electrostatic potentials containing no contribution from each site input in Lines 7 can be calculated automatically. In such a case, RADIUS should be set in such a way as not to overlap with each other: less than half the smallest interatomic distance in the whole structure.

#### 4. OUTPUT

The output of MADEL is described in German in the present version. The unit of the electrostatic site potential,  $\phi_i$ , for the  $i$ th site is  $e/\text{\AA}$  ( $1 e/\text{\AA} = 14.399652 \text{ V}$ ), where  $e$  is the elementary charge ( $= 1.6021773 \times 10^{-19} \text{ C}$ ). The precision of results obtained using MADEL is limited to 3 or 4 digits.

When the site input in Lines 7 is located within an ionic sphere, MADEL prints out a potential (POBBA) excluding contribution of the sphere and, in addition, a potential (PMBBA) calculated by substituting an original point charge for the sphere. If the site is not contained in any ionic sphere, a potential in which contribution of the nearest neighbor (either one if two or more nearest neighbors are present) is subtracted is output as POBBA.

The Madelung energy for the asymmetric unit,  $E_M$ , is calculated by using the formula

$$E_M = \frac{1}{2} \sum_i \phi_i Z_i W_i$$

where  $Z_i$  is the valence (oxidation state) of the  $i$ th site in the unit of  $e$ , and  $W_i$  is  $W(I)$ .  $E_M$  must be multiplied by the number of general equivalent positions to obtain the Madelung energy for the unit cell.

## How to use contrd and makec04d

contrd は DVSCAT で出力したバイナリーファイル f09 と f39 から三次元の電子密度、静電ポテンシャル、波動関数をテキストファイルに出力するための Fortran プログラム（コンソール・アプリケーション）です。contr の 3 次元版として作成しました。

makec04d は contrd の入力ファイル c04d のひな形を作成するためのユーティリティです。

いずれも Open Watcom Fortran Compiler (<http://www.openwatcom.org/>) でビルドしたため、Windows Vista 互換となっています。

### 1. 概要

contrd は SCAT がインストールされている PC 上で実行しなければなりません。すなわち、ユーザー環境変数あるいはシステム環境変数として dvdir が指定されており、かつ各種バッチファイルを収めたフォルダ DVXA\$EXEC にコマンド検索パスが設定されている必要があります。

contrd は三つのファイル f09, f39, c04d（下記）を読み込みます。球棒模型などを作成する際には、MAKEF05 用入力ファイル f01 を VESTA が入力します。

構造模型と等値面を重ね合わせて表示する場合は、両イメージの大きさを一致させるために f01 と c04d を同一フォルダに置き、両者を VESTA で読み込まなければなりません。f01 には直方体の大きさ（下記）が書かれていません。c04d が同一フォルダに存在する場合に限り、VESTA は f01 を読み込む際に c04d も同時に読み込みます。

テキスト・ファイル f01、バイナリー・ファイル f09（固有ベクトルの値）と f39（全変数配列の値）については、次の書籍を参照してください：

小和田善之、田中 功、中松博英、水野正隆、 “はじめての電子状態計算” 足立裕彦監修、三共出版（1998）。

contrd の実行形式ファイルは、上記の本に付属する CD-ROM に収録されている DVSCAT が output した f09 と f39 をコマンドプロンプトを用いて処理することを前提としています。

Windows 以外の OS（たとえば Mac OS X, UNIX）で DVSCAT を実行して得た f09 と f39 は、バイナリー・データのフォーマットが Windows 用 DVSCAT を用いたときと異なるため、Windows 用 contrd では読み込めません。その場合は、contrd のソースプログラムを当該 OS 上でビルドするか、Windows 用 DVSCAT

で f09 と f39 を出力し直してください。テキスト・ファイルである f01 は、行末だけ CR+LF に変更すれば大丈夫です。

## 2. contrd 用入力ファイル (c04d)

c04d では次のデータを入力します：

1 行目	(3I5)	x, y, z 方向のピクセル数
2 行目	(3F10. 5)	x, y, z 方向の長さ (単位: bohr, $a_0$ . $a_0 = 0.529177 \text{ \AA}$ )
3 行目	(3F10. 5)	中心座標 (単位: $a_0$ )
4 行目	(16I5)	ファイルに出力する波動関数の数と波動関数の番号
5 行目	(X5, 16I5)	波動関数の спинの向き (1: up, 2: down)

1 行目から 3 行目において、3D データを出力する領域を直方体で指定します。f01 に座標が記録されているすべての原子がこの直方体内に入っているなければなりません。VESTA はこの直方体があたかも単位胞であるかのようにみなします。直方体の外側に位置する原子が存在すると、VESTA は並進操作によって直方体の内側に不必要的「同価」原子を発生させてしまいます。

直方体中の全ピクセル数には、上限があります。合計 17 576 000 ピクセル（各方向あたり 260 ピクセルに相当）を越すと、「Number of pixels out of range」というエラー・メッセージが出力され、contrd が停止します。

中心座標の位置が直方体の中心、すなわち分率座標で (1/2, 1/2, 1/2) に置かれます。たとえば、f05 中のある原子の座標を中心座標に設定すると、その原子が直方体の中心に位置することになります。

電子密度と静電ポテンシャルは常に出力されます。静電ポテンシャル POT はマーデルング・ポテンシャル APOT を考慮して計算します：

$$\text{POT} = \text{CPOT} + \text{XPOT} + \text{APOT}$$

ただし CPOT は核引力項とクーロン項の和、XPOT は交換ポテンシャルを表しています。

波動関数を出力したい場合は 4 行目で指定します。最大 10 個まで出力できます。

5 行目はスピンの向きを指定する場合のみ追加します。

入力ファイル例を次に示します：

```
91   91   91  
20.00000 20.00000 20.00000  
0.00000 0.00000 0.00000  
2   37  385
```

この場合、f05における原点を中心とし、大きさ  $20a_0 \times 20a_0 \times 20a_0$  の直方体中の  $91 \times 91 \times 91$  個の三次元データを出力します。

出力する波動関数の数は 2 で、37 番と 385 番の波動関数が出力されます。

波動関数の番号については「はじめての電子状態計算」の 109 ページ、"波動関数・電子密度などの等高線の作図をする" を参照してください。

スピン計算の場合は、波動関数の番号の直下に up と down を識別する番号を追加します：

```
41   41   41  
20.00000 20.00000 20.00000  
0.00000 0.00000 0.00000  
2   37  385  
     1   2
```

この場合、37 番は up スピン、385 番は down スピンの波動関数が出力されます。

なお VESTA で結晶構造を表示する際、f01 だけでなく c04d 中の "格子定数" と中心座標も読み込まれます。この場合、f01 と c04d が同一フォルダに含まれていないと、エラーが発生しますので、ご注意ください。

なお、contrd が同時に open できるファイルの数は最大 106、波動関数の数は最大 100 です。

### 3. makec04d

自動的に c04d のひな形を作成するコマンド makec04d も利用できます。DVXA¥EXEC フォルダに置かれているバッチファイル makec04d.bat を使って makec04d を実行します。

f09, f39, c04d を収めたフォルダをカレント・ディレクトリーとしてから

```
makec04d
```

とコマンドラインで入力します。引数は不要です。

```
>Number of atoms to be analized (0:all atoms)
```

という問い合わせには、通常“0”を入力します。

必要に応じて、c04d 中の x, y, z 方向のピクセル数を適当な値に変更してください。

#### 4. 出力テキストファイル

contrd が output するテキストファイルは以下の通りです：

CHG3D.scat	電子密度
CHG3D_U.scat	Up スピンの電子密度（スピン版実行の場合のみ）
CHG3D_D.scat	Down スピンの電子密度（スpin版実行の場合のみ）
POT3D.scat	静電ポテンシャル
WXXX-3D.scat	XXX 番の波動関数
WXXXU-3D.scat	スピン計算の場合の up スピンの波動関数
WXXXD-3D.scat	スピン計算の場合の down スpinの波動関数

拡張子 scat は sca と同等です。

VESTA では、File メニューの下の Open... を選び、ファイル・フォーマット SCAT を指定して \*.scat を読み込み、等値曲面を 3D 表示させます。VESTA には、結晶模型に関する情報を保存した \*.vesta を読み込み、等値曲面と重ね合わせ表示させる機能があります。さらに、電子密度の等値曲面を静電ポテンシャルの値に応じて彩色することもできます。詳しくは VESTA\_Manual.pdf の 10.5 Isosurfaces をお読みください。

#### 5. contrd の実行方法

DVXA\$EXEC フォルダに置かれているバッチファイル contrd.bat を使って contrd を実行します。f09, f39, c04d を収めたフォルダをカレント・ディレクトリーとしてから

```
contrd
```

とコマンドラインで入力します。引数は不要です。

## 6. 出力ファイル形式

1 行目 (3I5, 3F10.5) メッシュ数と各辺の長さ  
2 行目以降 (E14. 6)  $y$  行  $x$  列の 2 次元データ ( $z$  組)

$x$  方向のメッシュ数が 72 以上の場合、1 行につき 10 列のデータが (10E14. 6) のフォーマットで出力されます。

出力されるデータの単位については、VESTA\_Manual.pdf 中の 15.4.2 Volumetric data を参照してください。

2002. 09. 30 水野正隆

2008. 03. 14 泉 富士夫 加筆・修正